CHAPTER 1

INTRODUCTION

1.1 Overview

Plant-derived compounds have always been an important source of medicines for various diseases and have received considerable attention in recent years due to their diverse pharmacological properties including cytotoxicity and cancer preventive effects (Gonzales and Valerio, 2006). Recently there is considerable scientific and commercial interest in the continuing discovery of novel anticancer agents of plant origin (Cragg and Newman, 2005) and such investigations targeting plant products have recently regained prominence with the increasing understanding of their biological significance and increasing recognition of the origin and function of their structural diversity (Conforti *et al*., 2008).

Cancer is the second leading cause of death and its incidence has increased dramatically worldwide (Madhusudan and Middleton, 2005). Cancer is the uncontrolled growth and spread of abnormal cells, associated with dysregulatin of apoptosis, a programmed cell death. Most of the current anticancer drugs are derived from plant sources, which act through different pathways converging ultimately into activation of apoptosis in cancer cells leading to cell cytotoxicity.

The plant *Swetenia macrophylla* (Family: Meliaceae), commonly known as “sky fruit”, because its fruits seem to point upwards to the sky, is a beautiful, lofty, evergreen large tree usually 30-40m in height and 3-4m in girth. This tropical timber tree grows natively throughout the tropical region of the America, especially in Central America, Mexico and Bolivia. In Malaysia, the seeds are used traditionally to treat diabetes, hypertension and also to relieve pain.

The seeds of *S. macrophylla* have been previously reported to have**,** anti-inflammatory, anti-mutagenecity and antitumor activity (Guevera *et al*., 1996), anti-malaria (Soediro *et al*., 1990), anti-microbial (Maiti *et al*., 2007), *in vivo* anti-diarrheal activity (Maiti *et al*., 2007), and antinociceptive activity (Das *et al*, 2009). The seeds have been used commercially in healthcare products to improve blood circulation and skin condition.

Phytochemical investigation has identified limonoids and it derivatives as the major constituents of this plant (Chen *et al*., 2010). The limonoid compounds that have been isolated are swietenine, swietenolide (Guha & Chakraborty, 1951), diacetylswietenolide, 6-Oacetylswietonolide (Goh *et al*., 2010a, 2010b) swietemahonin, khayasin, andirobin, augustineolide, 7- deacetoxy-7- oxogedunin, proceranolide, and 3β,6-dihydroxydihydrocarapin (Mootoo *et al.*, 1999). These limonoids were claimed to be responsible for its bioactivities.

However, the effect of *S. macrophylla* seeds on human cancer cell lines *in vitro* has hitherto not been reported. Thus, study was designed to investigate the cytotoxic properties of extract and factions of *S. macrophlla* seeds followed by elucidation of bioactive compound(s) which responsible for the activation of apoptosis mechanisms and the specific objectives of the study were listed as below:

1. To investigate the *in vitro* cytotoxic activity of the crude extract and fractions of *Swietenia macrophylla* King seeds against selected cancer lines (Ca Ski, MCF 7, KB, HEP G2 and HCT 116) using MTT assay.
2. To isolate, purify and elucidate the structures of the compounds responsible for the detected cytotoxic activity by fractionation using different chromatography, nuclear magnetic resonance spectroscopy (NMR) and mass spectrometry (MS).

3. To enhance the cytotoxic activity of swietenine through chemical modification.
4. To evaluate the modulation of the intracellular oxidative homeostasis exerted by SMEAF and swietenine acetate in HCT116 cells by detection of intracellular ROS and glutathione level.
5. To investigate the apoptosis inducing effects of SMEAF and swietenine acetate assessed by using Hoechst/PI staining and flow cytometric analysis by TUNEL, Annexin-V and JC-1 binding.
6. To determine the Bax and Bcl-2 expression level by SMEAF and swietenine acetate on HCT 116 in relation to mitochondrial-mediated apoptosis accompanied by a concomitant activation of down stream caspases.
7. To investigate the effects of SMEAF and swietenine acetate on cell cycle progression by flow cytometry analysis of PI binding and the expression level of core regulatory proteins including p53, p21 and cyclic dependent kinases.

1.2 Literature review

1.2.1 Cancer

The term ‘cancer’, which means “crab” in Latin, was described by Hippocrates in the fifth century BC to describe a family of diseases in which tissues grow and spread uncontrollably throughout the body, eventually lead to death (Lewis, 2006). There are different categories of cancer depending on the origin of cells, namely carcinomas, sarcomas, lymphomas and leukemia. Cancer cells can grow and divide autonomously leading to a progressive increase in the number of dividing cells. Tumor or neoplasm is referred to a resultant mass of growing tissue. The replication rate of tumor cells is not neccessarily faster than normal cells, but rather the crucial issues rely on the balance between cell division and cell differentiation (Becker, 2009).

Cancer development or carcinogenesis is a complex multi-sequence process that leads a cell from health stage to a precancerous state and finally followed by the entry into an early cancer stage. In general there are three stages of carcinogenesis which started with initiation followed by promotion and progression. Initiation stage involves DNA mutation which is a non-lethal form that subsequently produces an altered cell. As an example, initiation can proceed through oxidative stress. The increase of free radicals induced change in intracellular Ca (II) level. The high level of Ca (II) may cause unspecific activation of calcium-dependent endonucleases and lead to miss-cleaving of the DNA backbone (Wiseman *et al*., 1995) and give rise to mutated cells. Besides, an initiating genetic alteration may have been introduced by a long list of factors, including exposure to radiation or certain chemicals, insertion of retrovirus, generation of random mutations during replication, random DNA amplication or random loss of a DNA segment. In certain cases, the initial changes may also be inherited. Genetic predisposition accounted for about 5% of total cancer cases (Wolfe, 1993).

Promotion stage involves induction of cell proliferation and results in the formation of identifiable focal lesion. During this stage, there is a need for a continuous supply of the tumor promotion stimulus to maintain or bring the mutated cell to progression stage and therefore it is a reversible process. Additional gene conversion to oncogenic form can also occur at this stage. Further alteration to the initial and succeeding gene activation also occurs at this stage. For an example, initial conversion of a proto-oncogene to an oncogene by translocation may be compounded at successive steps by sequential changes and amplification. As the first change may have induced an increase in the rate of DNA replication and cell division, opportunities for additional changes are likely to come more frequently as progression advances (Wolfe, 1993). There are wide varieties of promoting agents and not all tumor promoters are foreign substances. Even the growth factors or hormones can act as tumor promoter if they exert the proliferation effect on a cell that has already sustained an initiating mutation (Becker, 2009).

Progression is known as the third or final stage in carcinogenesis. During this stage, tumor gradually gains aberrant characteristics and become more aggressive. The characteristics include, increased growth rate, invasiveness, ability to survive in blood stream, immune killing resistance, drug resistance, apoptosis evasion etc. In general, cell entry into progression stage is believed to be irreversible. Long term accumulation of genetic changes can lead the cell to go through the transition stage, from benign to malignant. Transformation includes, cell surface molecule alteration, connection break between neighbourigng cells or molecules on malignant cells are normally associated with metastasis. The acquired traits enable tumor cells to break loose from the tumor, evaded immune attack and eventually will lodge and grow in new locations of the body (Wolfe, 1993).

1.2.1.1 Hallmarks of Cancer

Evidences showed that changes in normal cell in terms of various combinations of mutations and epigenetic changes involving tumor suppressor genes and oncogenes can lead to cancer; however there is a need in common principles that would help simplify the picture. In year of 2000 Douglas Hanahan and Robert Weinberg (Hanahan and Weinberg, 2000) have proposed a series of six required traits in the development of cancer.

1. Self-sufficient in growth signals

   Generally, it is believed that normal cells proliferate under stimulation of appropriate growth factors. Apparently, cancer cells are less dependent on exogenous growth stimulation. Studies have shown that through the action of oncogenes that produce excessive quantities or mutant version of proteins enable the cancer cells to self-sustain on prolonged stimulation (Slamon, 1987; Yarden and Ullrich, 1988).

2. Insensitivity to anti-growth signals

   The existence of growth-inhibiting mechanisms is necessary in preventing excessive cell proliferation in normal tissues. Cancer cells must evade or acquire anti-growth signal mechanisms to continue proliferating. As an example, Rb protein responsible in inhibiting cell proliferation at end of G1 phase. Mutation of RB gene made cells insensitive to TGFβ growth inhibitory (Dyson *et al*., 1989; Fynan and Reiss, 1993).

3. Evasion of apoptosis

   The programmed cell death or apoptosis plays a major role in cell attrition. Principle studies and observations accumulated over the past indicate that

apoptosis is present in latent form in virtually all cell types throughout the body (Hanahan and Weinberg, 2000). The impairment of p53 pathway enables the cells to evade apoptosis (Zusman, 1997). As an example, overexpression of Bcl-2 gene which encodes for an inhibitor of apoptosis known as Bcl-2 protein affects the ability of p53 pathway to trigger apoptosis (Apakama *et al*., 1996).

4. Limitless replicative potential

   The overall effect of the preceding three traits is to uncouple cancer cells from the mechanisms that maintain normal cell replication. However, this will not ensure unlimited proliferation as telomere sequences are gradually lost from the end of each chromosome during DNA replication. A few of the cancer cells are able to activate an alternative mechanism for maintaining telomere length above a critical threshold and thereby retain the ability to divide indefinitely (Bryan and Cech, 1999; Bryan *et al*., 1995; Shay and Bacchetti, 1997; Wright *et al*., 1989).

5. Sustained angiogenesis

   Blood supply is needed for tumors to survive or grow beyond a few milimeters in size. Thus, angiogenic activation is a must in a certain stage of tumor development. A common strategy involves the activation of genes coding for angiogenesis stimulators combined with the inhibition of genes coding for angiogenesis inhibitors. For example, p53 protein activates the gene coding for angiogenesis inhibitor thrombospondin; hence the loss function of p53 function will eventually cause thrombospondin levels to decrease (Dameron *et al*., 1994).

6. Tissue invasion and metastasis

   Invasion or metastasis by tumor has been categorized based on its ability to invade surrounding tissues and spread to distant sites. Three major traits possessed by this type of cancer cells include decreased cell-cell adhesion, increased motility and production of proteases that can degrade extracellular matrix and basal lamina. The mechanisms underlying these molecular changes differ among tumor types and tissue environments, but they commonly involve activation of genes normally intended for use in embryonic development or wound healing (Becker, 2009).

Apart from the six biological capabilities acquired during the multiple step development of human tumors, based on the observations made through the last decade (Hanahan and Weinberg, 2011), two high potential and promising hallmarks were added to this list.

7. Deregulation of cellular energetics

   The adjustments of energy metabolism occur in neoplastic disease in order to sustain cell growth and proliferation. An anomalous cancer cell energy metabolism known as “aerobic glycolysis” was firstly described by Otto Warburg (Warburg, 1956; Warburg *et al*., 1927). Observation of cancer energy metabolism resulting in counterintuitive situation, as cancer cells would prefer undergo glycolysis rather than mitochondrial oxidative phosphorylation although have to compensate for almost 18-fold lower efficiency in term of ATP production. In some cases, tumors contain two subpopulations differing in energy-generation pathways, as both of them evidently function symbiotically: the hypoxic cancer cells rely mainly on glucose for survival and secrete lactate as waste, whereas the better-oxygenated neighbour cells imported and

preferently used lactate as fuel (Feron, 2009; Kennedy and Dewhirst, 2010; Semenza, 2008, 2009), forming a lactate-secreting and lactate-ultilizing cells.

8. Avoiding immune destruction

   It is the fact that immune system plays a vital role in eradicating or resisting the formation and progression of cancer. Thus, is a must for tumor cells to evade immune surveillance through certain means to limit or prevent immunological killing. Immunological monitoring defects in immunocompromised individual have shown striking increase of certain cancers (Vajdic and Leeuwen, 2009). Besides, studies have shown that cancer cells that originated from immunodeficient mice are often inefficient at initiating secondary tumors in syngeneic immunocompetent hosts, whereas cancer cells from tumors arising in immunocompetent mice are equally efficient at initiating transplanted tumors in both types of hosts (Teng *et al*., 2008).

With this holistic clarity of mechanism, cancer prognosis and treatment will become a rational science. It will surely help to understand with precision, how and why treatment regimens and specific antitumor drugs succeed or fail eventually help to develop or use appropriate combinations of drugs to gain better outcomes in treatment.

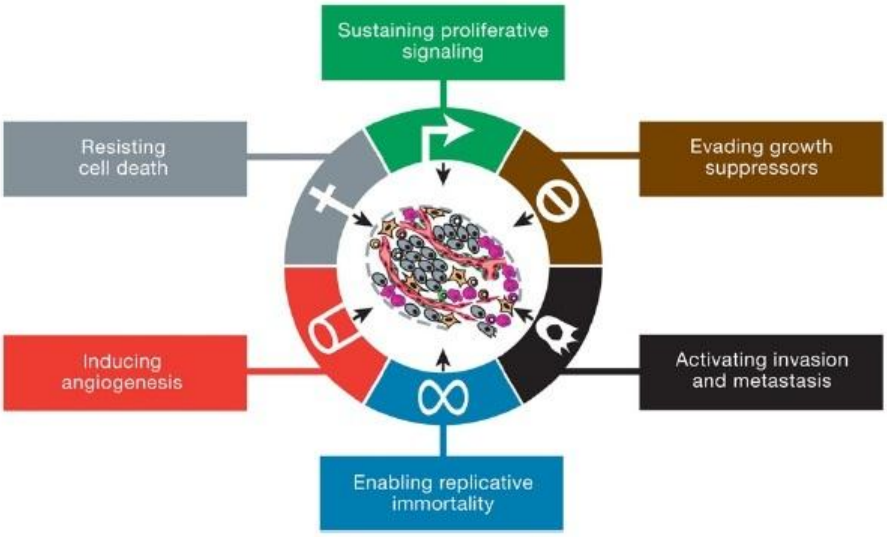

Adapted from (Hanahan and Weinberg, 2000)

Figure 1.1 Hallmarks of cancer.

1.2.1.2 Treatment of cancer

There are several treatment options available for patients diagnosed with cancer. Depending on both types and stage of the cancer, appropriate or combinatory treatment would be selected to suit the conditions. One of the most common approaches involves surgical removal of primary tumor followed by radiation or chemotherapy to destroy remaining cancer cells. The radiation therapy employs high-energy X-rays or other forms of ionizing radiation to kill cancer cells. The principle of this treatment relies on the ionizing radiation to destroy DNA content of cancer cells to the extent that the cells are unable to undergo mitosis or trigger apoptosis through p53 pathway and therefore die while trying to divide (Hamada *et al.*, 1996; Swisher *et al.*, 2003).

Chemotherapy is another mean to kill dividing cancer cells. Such drugs are subdivided into four major categories: 1. Antimetabolites that are able to inhibit metabolic pathways required for DNA synthesis. Example of this class of drug is fluorouracil (Peters *et al.*, 2000); 2. Alkylating agents that inhibit DNA function by chemically

crosslinking the DNA double helix. Example of a drug from this family is cisplatin (Comis, 1994; Gately and Howell, 1993); 3. Antibiotics where the substances made by microorganism that are able to bind to DNA or inhibit the topoisomerases activities in DNA replication. Example of an antibiotic is bleomycin produced by the bacteria *Streptomyces verticillus* (Blum *et al*., 1973; Umezawa *et al*., 1967); 4. Plant-derived drugs that either inhibit topoisomerases or disrupt formation or disintegration of mitotic spindle, for example, taxol (Schiff *et al.*, 1979; Schiff and Horwitz, 1980).

Other alternative treatments include immunotherapy that exploits the ability of the immune system to recognize cancer cells. For an example, the utilization of a special strain of *bacillus Calmette-Guerin* (BCG) bacteria to trigger localized immune response success in treating early stage of bladder cancer (Alexandroff *et al*., 1999; Lamm *et al.*, 1981). Anti-angiogenic treatment is another means of treatment (Boehm *et al*., 1997; Folkman, 1998a, 1998b). In 2004, Avastin was the first anti-angiogenic drugs approved for routine use in cancer patient.

1.2.2 Cell death

Cell death research has fascinated scientists of different disciplines for more than a century. The term "cell death" in general can be defined as an irreversible loss of plasma membrane integrity (G. Kroemer *et al*., 2005). Researchers have classified the cell death into three main types of cell death by distinguishing them through morphological features in mammalian cell. Type I cell death or commonly known as apoptosis, is defined by characteristic changes in nuclear morphology with DNA fragmentation (karyorrhexis) or chromatin condensation (pyknosis); cytoplasmic organelles changes; cell shrinkage followed by plasma membrane blebbing and

formation of apoptotic bodies that contain nuclear or cytoplasmic material. All named changes occur before plasma membrane integrity is lost.

Type II cell death is commonly characterized by a massive accumulation of two-membrane bounded autophagic vacuoles in the cytoplasm. Type III cell death or better known as necrosis is often defined in a negative manner as death lacking the characteristics of type I and type II processes, with only a classical definition based on morphological criteria: early rupture of plasma membrane, occurrence of cytoplasmic organelles dilation particularly mitochondria (Edinger and Thompson, 2004; Golstein and Kroemer, 2007; Kroemer *et al*., 2005).

The nomenclature of the cell death is important, as good distinct features between different types enable appropriate diagnostic and medical treatment can be done on the patients. As an example, occurrence of necrosis is quite common with association with unwarranted cell loss in human pathologies (Festjens *et al*., 2006; Yuan, 2006; Zong and Thompson, 2006), and can lead to local inflammation which required immediate proper treatment.

1.2.2.1 Autophagy

Autophagy, which has been proposed as a second mode of cell death, is a general term for the degradation of cytoplasmic components within lysosomes whereas require cells generate energy and metabolites by digesting their own organelles and macromolecules (Cuervo, 2004; Klionsky, 2007; Levine and Klionsky, 2004; Shintani and Klionsky, 2004). Autophagic process is mediated by a unique organelle called the autophagosome, a two-membrane vesicle containing cytoplasmic organelles or degenerating cytosol.

Autophagy is generally thought to be a non-selective degradation system, as autophagosomes can engulf a large portion of cytoplasm.

Autophagy is involved in numerous important processes in cell, one of the most typical role in cell allows a starving cell, or a cell that is deprived of growth factors, to survive. In this sense, lack of any type of essential nutrient can induce autophagy. For example, yeast undergoes nitrogen starvation can induce autophagy (Takeshige *et al*., 1992). Insufficient supply of nitrogen or carbon can also trigger autophagy in plant cells (Moriyasu and Ohsumi, 1996; Yoshimoto *et al*., 2004). In mammals, depletion of total amino acids can induces autophagy and it has been shown in many types of cultured cells. However the effects of individual amino acids differ, as it depends on cell type because the amino acid metabolism differs greatly among tissues (Lardeux and Mortimore, 1987).

Autophagy induction through starvation is greatly depending on the period of exposure. As a very short period of starvation, the cell would trigger ubiquitin-proteasome system rather than autophagy to maintain the amino acid pool (Vabulas and Hartl, 2005). Persistent starvation period up to several hours which acts as an adaptive response would eventually leading to up regulation of autophagy to occur in order to produce necessary amino acids to maintain the cells (Kuma *et al*., 2004; Onodera and Ohsumi, 2005). In general, autophagy allows a starving cell, or a cell that is deprived of growth factors, to survive. However, if the cells do not receive nutrients for extended periods ultimately digest all available substrates and die (autophagy-associated cell death) (Klionsky, 2007; Kroemer and Jaattela, 2005; Levine and Abrams, 2008; Levine and Deretic, 2007).

In addition to this role in the starvation response, autophagy has also been implicated in other physiological processes. Autophagy machinery may be used in recycle damaged organelles, thereby contributing to maintain cellular integrity. For example damaged mitochondria resulting from an incomplete apoptotic event are sequestered by autophagosomes to prevent cellular damage caused by uncontrolled release of reactive oxygen species (Xue *et al*., 2001).

1.2.2.2 Necrosis

Necrosis has been defined as a type of cell death that lacks the features of apoptosis and autophagy, and is usually considered to be uncontrolled. Morphological observation revealed necrosis occurred with the swelling of organelles, an increased cell volume, disruption of the plasma membrane followed by rupture of the plasma membrane with a consequent localized inflammatory response and damage to surrounding cells and tissues (Kroemer *et al*.,1998). It is originally thought as a "nonspecific" form of cell death or in other terms an accidental and unregulated cell death event. Recent research provided a mounting evidence that the execution of necrotic cell death is also regulated by a set of signalling pathways (Golstein and Kroemer, 2007; Vanlangenakker *et al*., 2008) this might facilitate a shift from the negative definition of necrosis to a more positive definition of this particular modality of cell death.

Studies showed necrosis can be induced through receptor induction. By utilizing L929 mouse fibrosarcoma cell line, necrosis can be induced by treated with TNFα. In this model, cells will eventually undergoes a complex multi-step signalling transduction in which Fas-associated death domain (FADD) is recruited to the TNF receptor 1 (TNF-R1) and induces necrosis, presumably through its death domain (Festjens *et al*., 2006). In addition, TNFα-induced necrosis is accompanied by a rapid increase of

mitochondrial ROS production that can be dampened by rotenone, an inhibitor of the respiratory chain complex I. The addition of rotenone (Schulze-Osthoff *et al*., 1993) and lipophilic antioxidants are shown be able to prevent necrotic cell death in this model (Sanchez-Alcazar *et al*., 2003). Besides, research have shown that the elevation level of Bcl-2 can eventually reduce TNFα induced necrosis (Denecker *et al*., 2001; Hennet *et al*., 1993). As there is no involvement early release of cytochrome c in necrosis (Denecker *et al*., 2001), Bcl-2 must exert its protective effect by another molecular mechanism. There are even more evidence supports a 'sequence' of events that characterize necrotic cell death at both the phenomenological and biochemical level, thereby reflecting a programmed course of events in the dying necrotic cell and contributing to a definition of necrotic cell death.

1.2.2.3 Apoptosis

Apoptosis or programmed cell death is an important component of the development and health of multicellular organisms that regulate and allows the wounded cell to commit suicide (Duprez *et al*., 2009; Hotchkiss *et al*., 2009; Wyllie, 2010). It is essential in granting the survival of multicellular organisms by selectively and orderly getting rid of old, mutated, damaged or infected cells that may interfere with normal function. There are two major well studied types of apoptosis pathways, extrinsic and intrinsic (Duprez *et al*., 2009).

i) Extrinsic pathway

Extrinsic pathway is always related to the triggers of cell surface receptors by extracellular ligands. Examples of death receptors mediated activities include Tumor Necrosis Factor receptors (TNFR) superfamily namely, TRAIL FAS and TNFR. Death receptors activation leads to the recruitment and activation of initiator caspases such as caspase -8 and -10 followed by

the assembly of the death inducing signaling complex (DISC). The initiation and activation of caspase-3 which is effector caspase followed after DISC formation (Pan *et al.*, 1997; Sheridan *et al.*, 1997).

ii) Intrinsic pathway

The cell autonomous or intrinsic pathway is largely centred around and/or regulated by the mitochondria (Brunelle and Letai, 2009; Galluzzi *et al*., 2010; Gupta *et al*., 2009). Well studied form of intrinsic apoptosis is initiated by the stress-mediated release of cytochrome c from the mitochondria that results in the formation of apoptosome. The apoptosome then activates the initiator caspase, typically caspase -9, which leads to the activation of the exercutioner caspase -3. Normally, the activation of intrinsic pathway is related to pro- and anti-apoptotic Bcl-2 family proteins. The ratio between the pro- and anti-apoptotic proteins in cell will eventually determine fate of cell's survival.

Even though the apoptotic pathways are well defined into two distinct pathways, namely, extrinsic and intrinsic pathway, the evidences have shown the greater complexity and diversity in apoptosis as it involves interconnection and cross-activation of two apoptotic pathways such as the extrinsic and intrinsic pathways or even together with necrotic sub-pathways activation (Wu *et al*., 2011).

1.2.3 Tumor suppressor p53 protein

Tumor suppressor protein p53 was firstly described in 1979 (DeLeo *et al*., 1979; Lane and Crawford, 1979; Linzer and Levine, 1979) and is encoded by TP53 gene (Isobe *et al*., 1986). It is probably the most popular molecule in the field of cellular biology as the

biological consequences of p53 activity include cell-cycle regulation, induction of apoptosis, development, differentiation, gene amplification, DNA recombination, chromosomal segregation, and cellular senescence (Oren and Rotter, 1999). As a tumor suppressor, p53 is essential for preventing inappropriate cell proliferation especially cells with damaged DNA and maintaining genome integrity following genotoxic stress (Vogelstein *et al*., 2000; Vousden and Lu, 2002). Various intracellular and extracellular stimuli can cause DNA damage (namely, ionizing radiation, UV radiation and virus infection), heat shock, hypoxia and oncogene over-expression, wild-type p53 is activated and emerges as a pivotal regulatory protein which triggers diverse biological responses, both at the level of a single cell as well as in the whole organism (Vousden and Lu, 2002; Levine, 1997; Vogelstein *et al*., 2000).

Since the discovery of the p53 tumor suppressor gene has been found to be mutated in more than 40% of human cancers (Cheah and Looi, 2001; Hernandez *et al*., 1999). Mutation at TP53 gene will eventually disrupted the function of translated p53 tumor suppressor protein activities by various mechanisms, including activation of DNA damage check point and p53-mediated apoptosis pathway consequently formation of cancer (Bartkova *et al*., 2005; Kastan and Bartek, 2004). Example, the patients with the Li–Fraumeni syndrome, who have an inherited germline mutation in one of the two p53 alleles, are at very high risk of developing cancer throughout their lifetimes (Srivastava *et al*., 1990; Malkin *et al*., 1990).

In many cancer cases, p53 is not functionally inactive but the function of p53 is impaired owing to mutations in proteins operating either upstream or downstream of p53 targets, such as MDM2 or the E6 protein of HPV, or deletion of key p53 co-activators such as the ARF gene (Hollstein *et al*., 1991; Sherr, 1998; Vogelstein *et al*.,

2000). The p53 inactivation without p53 mutation also leads to cancer development as functional p53 is not working as it is supposed to, this clearly demonstrated inactivation of p53 is a key event in carcinogenesis. An example of p53 inactivation is Burkitt's lymphoma, where the cells are under overexpression of MDM2 protein due to enhanced translation (Capoulade *et al*., 1998). As MDM2 is an ubiquitin ligase, it promotes ubiquitination of p53 (Meulmeester *et al*., 2003) for degradation, this would mean that if there is more MDM2 around, it would stimulate more p53 degradation and keep p53 levels low.

Evidence has shown that, this small 53-KDa tumor suppressor is a molecular node at the crossroads of an extensive and complex network of stress response pathways. This opened a new prospect in developing p53-based cancer therapy (Stoklsa and Golab, 2005), includes, gene therapy through reconstitution of wild-type p53 (Swisher *et al*., 2003) , or restoration of p53 function-targeting mutant p53 by using small molecules like styrylquinazoline that is capable to interfere with mutant p53 and restore wild type function (Foster *et al*., 1999) followed by mean of wild type p53-directed approaches like nutlins that can bind to p53 and prevent MDM2 targeting p53 degradation (Galimard *et al*., 2004).

1.2.4 BCL2 proteins family

There are at least 15 Bcl-2 family member proteins have been identified in mammalian cells (Gross *et al*., 1999).The Bcl2 family members responsible in controlling apoptosis process and are generally separated into pro-apoptotic (promote apoptosis) and anti-apoptotic (inhibit apoptosis) (Adams and Cory, 2007; Danial and Korsmeyer, 2004; Hotchkiss *et al*., 2009). The Bcl-2 family members have been classically been grouped into three classes. The first class inhibits apoptosis (Bcl-2, Bcl-XL, Bcl-W, Mcl1, Bcl-B or Bcl-2L10 and A1 or Bcl-2A1) whereas the second class promotes apoptosis (Bax,

Bak and Bok). The third class known as BH3-only protein (Bad, Bik, Bid, Hrk, Bim, Bmf, NOXA and PUMA) as they have a conserved BH3 domain that can bind and regulate the anti-apoptotic Bcl-2 proteins to promote apoptosis. The pro-apoptotic family members of Bcl-2 namely Bax and Bak are crucial in inducing permeabilization of the outer membrane of mitochondria. Subsequently release of apoptogenic molecules such as cytochrome c and SMAC which lead to caspase activation. Studies indicated that, the anti-apoptotic family members, such as Bcl-2 and Bcl-XL able to inhibit Bax and Bak while the BH3 only proteins de-repress Bax and Bak by direct binding and inhibit Bcl-2 and other anti-apoptotic family members (Willis *et al*., 2007; Youle and Strasser, 2008).

Overexpression Bcl-2 members family of pro-survival proteins is commonly associated with unfavourable pathogenesis in cancer (Chipuk *et al*., 2010). In colon, Bcl-2 protein is normally expressed only in the lower half of crypts of the colon, corresponding to the stem cell compartment, where Bcl-2 is believed to be responsible in protecting stem cells from apoptosis (Merritt *et al*., 1995). Most colonic adenomas express Bcl-2 protein at high levels throughout the neoplastic epithelium (Kinzler and Vogelstein, 1996; Nakamura *et al*., 1995; Baretton *et al*., 1996), while non-neoplastic polys have a normal pattern of Bcl-2 expression (Bronner *et al*., 1995; Flohil *et al*., 1996; Nakamura *et al*., 1995). Overexpression of Bcl-2 may therefore contribute to the transition between hyperplastic epithelium and adenomas. However, Bcl-2 is probably is not the only one of the genes that contributed to the colorectal neoplasms. Indeed, changes in the expression of other members of the Bcl-2 family have been shown during progression of colorectal tumors, such as the anti-apoptotic proteins Bcl-Xl, Mcl-1 and pro-apoptotic protein Bak, which may be more important than Bcl-2 (Krajewska *et al*., 1996).

1.2.5 Heat shock proteins (HSP)

The heat shock response was first discovered in 1962 by Ritossa (1962), who observed response pattern of Drosophila salivary gland chromosome puffs towards transiently elevated temperature. Since then, investigators have proved that the heat shock response is ubiquitous and highly conserved in all organisms. The importance of HSPs include acting as an defense mechanism to protect cells from different range of harmful exposure such as alcohols, heat shock, heavy metals, inhibitors of energy metabolim, oxidative stress, inflammation and fever (Lindquist, 1986; Morimoto, 1993).

Hsps have been classified into six major families according to their molecular size: Hsp 100, Hsp 90, Hsp 70, Hsp 60, Hsp 40 and small heat shock proteins. Within each gene family are members that are constitutively expressed, inducibly regulated, and/or targeted to different compartments. For example, Grp 94 performs an analogous function in endoplasmic reticulum, whereas Hsp 90 functions in both the cytosolic and nuclear compartments. Likewise, members of the Hsp 70 family exhibit complex patterns of growth-regulated and stress-induced gene expression and are targeted to different subcellular compartments.

Studies have shown that the stress response and apoptosis pathway are linked. Intensity and duration of heat shock responses resulting from stressful conditions and heat shock can also trigger apoptosis or necrosis (Barry *et al*., 1990). However, the exposure of cells to mild or little stress conditions that are sufficient to cause expression and accumulation of HSPs would eventually exert the protective effects on cell. This cell-protective process is known as thermotolerance or cytoprotection, (Parsell *et al*., 1993). Since survival and death correspond to opposing cellular events, there should be multiple checkpoints and points of regulatory cross-talk to ensure that cells sustaining reparable molecular damage survive and that cells damaged beyond repair undergo cell

death. There is increasing evidence that Hsps may function at multiple points in the apoptotic signalling pathway and exert their protective effects to apoptosis. For example, high level of Hsp 70 reduce or block caspase activation and supress mitochondrial damage, nuclear fragmentation (Buzzard *et al*., 1998; Mosser *et al*., 1997), prevent recruitment of procaspase 9 and 3, to the apoptosome formation (Beere *et al*., 2000). Meanwhile Hsp 27 has been shown to block apoptosis induced by heat, Fas ligand, H_2O_2, and anticancer drugs (Richards *et al*., 1996; Trautinger *et al*., 1997).

1.2.6 Characteristics of apoptosis

1.2.6.1 Ca^{2+} influx

Apoptotic cells acquired characteristic morphological and cytological changes while progressing through programmed cell death. The process of cellular suicide includes membrane modifications such as changes in membrane fluidity where involvement of Ca^{2+} influx. Whereas in studies conducted by Kim and coworkers indicated the Ca^{2+} occurs through the activation of voltage-sensitive Ca^{2+} permeable non-selective cation channels. (Kim *et al*., 2000). Marked elevation of Ca^{2+} activate hydrolytic enzymes, lead to exaggerated energy expenditure, impair energy production, initiate cytoskeletal degradation, and ultimately resulting in cell death (Nicotera and Orrenius, 1998).

1.2.6.2 Externalization of phosphatidylserine

Most of the cell would maintain the asymmetric distribution of phospholipids between their cytoplasmic and exoplasmic membrane leaflets (Bretscher, 1972). However, the phosphatidylserine which belongs to component of phospholipid would be externalized to the outer membrane when a cell undergoes apoptosis (Mirnikjoo *et al*., 2009) especially in the early phase of apoptosis (Castegna *et al*., 2004). Externalization of

phosphatidyserine will eventually will act as phagocytic recognition and attract the phagocytes uptake and kill the apoptotic cells (Hoffmann *et al.*, 2005).

1.2.6.3 Membrane Blebbing and formation of apoptotic bodies

Research showed that membrane blebbing may due to the level changes of cytoskeleton protein (Mills *et al*., 1998). In tumor cells which are lacking in the binding protein (ABP)[1] bleb extensively under normal conditions (Cunningham, 1992). Peroxide-induced blebbing is shown to be caused by the cleavage of actin binding proteins talin and α-actinin (Miyoshi *et al*., 1996). Membrane bledding can also occur when actin-binding cytoskeleton protein which known as fodrin being cleaved by caspases during apoptosis (Cryns *et al*., 1996; Vanags *et al*., 1996). F actin was shown to be necessary in formation of blebbing and eventually apoptotic bodies (Cotter *et al*., 1992), besides the concentration of F actin is showed to be correlated to bleb size (Cunningham, 1995). Several groups have suggested the cleavage of actin by activated caspases during apoptosis contribute to membrane blebbing (Kayalar *et al*., 1995; McCarthy *et al*., 1997). Other than actin, myosin was also shown to be involved in membrane blebbing formation (Mills *et al*., 1998).

1.2.6.4 Chromatin condensation and DNA fragmentation

During apoptosis, pro-apoptotic proteins such as AIF, endonuclease G and CAD are released from mitochondria. AIF would translocate to the nucleus and cause DNA fragmentation into ~50-300 kb pieces and condensation of peripheral nuclear chromatin (Joza *et al*., 2001). This early form of DNA condensation is referred to as “stage I” condensation (Susin *et al.*, 2000). Meanwhile, translocation of endonuclease G to nucleus will cause the cleavage of nuclear chromatin to produce oligonucleosomal DNA fragmentation (Li *et al*., 2001). Both AIF and endonuclease G functioning in caspase-

independent manner. The subsequent release of CAD protein from mitochondria during apoptosis would cleaved by activated caspase-3 and further translocate to nucleus where subsequently leads to oligonucleasomal DNA fragmentation or a more pronounced and advanced chromatin condensation (Enari *et al*., 1998). This later and more pronounced chromatin condensation is referred to as "stage II" condensation (Elmore, 2007; Susin *et al*., 2000).

1.2.7 Oxidative stress

Oxidative stress is generally defined as an imbalance that favours the production of ROS over antioxidant defences (Ott *et al.*, 2007). In humans, oxidative stress has been implicated in a wide variety of pathologies, including cancer, type II diabetes, arteriosclerosis, chronic inflammatory processes, ischemia/reperfusion injury, and various neurodegenerative diseases (Droge, 2002). In the cell, the major reactive oxygen species (ROS) is produced through mitochondrial respiration. The ROS would be countered by the intracellular antioxidant defense systems including the glutathione peroxidase (Gpx) (Han *et al*., 2003), SOD, catalase (Michiels *et al*., 1994) (Gus'kova *et al*., 1984), and most importantly tripeptide glutathione (GSH) molecules to prevent the interaction with various macromolecules in cells.

1.2.7.1 Consequences of oxidative stress

Damage to DNA

Increase of intracellular ROS level would cause the oxidative damage to the DNA content, especially through the modification of the purine and pyrimidine bases of the deoxyribose backbone. An important target of ROS is the mitochondrial DNA (mtDNA), which encodes polypeptides, transfer RNAs (tRNAs) and ribosomal RNAs (rRNAs) which are all essential for electron transport and ATP generation by oxidative

phosphorylation (Anderson et al., 1981). As the major locus for free radical generation is inside the mitochondria, mtDNA is very susceptible to the attack by ROS. For example, ROS can trigger the formation of 8-hydroxydeoxyguanosine which is a modified base in mtDNA and probably leads to the respiratiory dysfunction followed by cell death (Anderson *et al*., 1981; Ott *et al*., 2007).

Damage to proteins

An important mechanism of O_2^- toxicity is directly causing oxidation and inactivation of iron-sulfur (Fe-S) proteins, such as aconitases (Fridovich, 1997). The existence of aconitase in mitochondria plays a key role in the Krebs cycle, as it is responsible in catalysing the conversion of citrate to isocitrate. Partial or full inhibition of aconitase could result in Krebs cycle dysfunction and would cause an impact on energy production subsequently affecting the viability of the cell (Chen *et al*., 2005).

Damage to lipids

High level of ROS formation can stimulate lipid peroxidation in mitochondria and lead to suppression of mitochondrial metabolism. Mitochondrial functions such as respiration and oxidative phospholrylation, inner membrane barrier properties, maintenance of mitochondrial membrane potential ($\Delta\psi$), and mitochondrial Ca^{2+} buffering capacity would be affected by lipid peroxides (Zhang *et al*., 1990; Albano *et al*., 1991; Bacon *et al*., 1993). The deleterious effect on mitochondrial Ca^{2+} permeability plays the key role in the activation modes of cell death (Chen *et al*., 1995).

1.2.8 Caspases

Caspases or cysteine-dependent aspartate-specific proteases, are a family of cysteine proteases that play essential roles in apoptosis, necrosis and inflammation (Alnemri *et*

al., 1996). In human, twelve caspases belonging to apoptotic and inflammatory subfamilies of caspases have been described. Apoptosis caspases can be further subdivided into initiator (caspase-2, -8, -9, -10) and executioner (caspase-3, -6, -7) caspases. Available crystal structures demonstrate that caspase zymogens are single-chain proteins, with N-terminal prodomains preceding the conserved catalytic domains as shown in Figure 1.2. They occur either as monomers or dimers, a crucial property that defines their activation mechanism. During activation and/or maturation, the catalytic domain is cleaved to a large (α) and a small (β) subunit that interact intimately with each other. The active form of a caspase is a dimer of catalytic domain of α β β'α' symmetry, with two active sites per molecule (Denault *et al*., 2006; Pop and Salvesen, 2009).

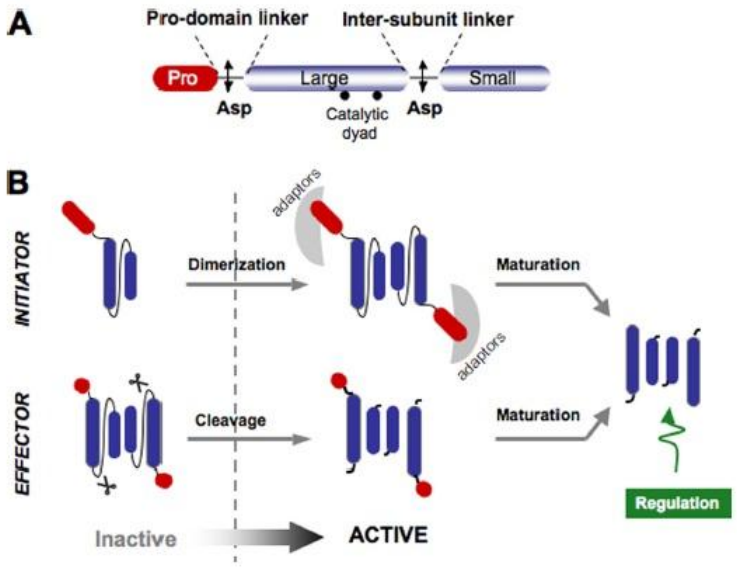

Adapted from (Pop and Salvesen, 2009)

Figure 1.2 [A] caspase organization. A prodomain precedes the catalytic domain, composed of two covalently linked subunits. Sites for (auto) proteolysis at Asp residues are indicated. [B] activation mechanisms. Initiators are monomers that activate by prodomain-mediated dimerization. Executioners are dimers that activate by cleavage of intersubunit linkers. Following activation, additional proteolytic events mature the caspases to more stable forms, prone to regulation.

1.2.8.1 Types of caspases

Initiator caspases, present in the cell as inactive or inert monomers. Its activation is by dimerization process where those monomers recruited to platform molecules via these protein-protein interaction domains and are subsequently activated by oligorization and proximity-induced autoproteolysis. Short prodomain caspases exist as preformed dimers in the cell and their enzymatic activity requires proteolytic maturation by the action of upstream caspases (Salvesen and Riedl, 2008).

Executioner caspases or downstream caspase group are thought to be responsible for the actual destruction of the cell. This group of caspases occur as inactive dimers that require cleavage of catalytic domain to become active (Figure 1.2). When compared to initiator caspases, the first step of activation namely dimerization has already occurred shortly after their synthesis. The large and small subunits of catalytic domain are restrained by a short linker. The crystal structure of the zymogen form of caspase-7 revealed clearly the molecular details of the catalytic groove formation upon activation (Chai *et al*., 2001; Chai *et al*., 2001). Proteolytic processing of the linker allows rearrangement of mobile loops equivalent to the initiator caspases, favouring formation of the catalytic site (Prior and Salvesen, 2004).

Generally, there are two pathways in which the caspase family proteases can be activated, namely, extrinsic or death receptor-mediated pathway and also intrinsic mitochondrial-mediated pathway. Commonly, the death receptor-dependent procaspase-activattion pathway involved caspase-8 and caspase-10. Whereas the activation of the death receptor by Fas ligand (FasL) and tumor necrosis factor (TNF)-2 signaling molecules occurs at outer plasma membrane of cell (Lu *et al*., 2003; Wang *et al*., 2005).

1.2.8.2 Caspase activation in extrinsic and intrinsic apoptotic pathway

The binding of the signalling molecules will eventually activate the death receptor. The binding of Fas to Fas associated death domain (FADD) (or TNFR-associated death domain, TRADD) will cause FADD aggregation followed by the emergence of death effector domains (DEDs). Interaction of DEDs with prodomain of procaspase-8 induces the oligorization of procaspase-8 followed by formation of a massive molecule complex known as the death-inducing signal complex (DISC). In DISC, two linear subunits of procaspase-8 are compacted together followed by procaspase-8 autoactivation to caspase-8 (Wang *et al*., 2005).

The following downstream effects of caspase-8 can be divided into two types. The first type involves direct vigorous activation of the procaspase-3 by caspase-8. It can be found in certain types of the lymphoid cell lines. Opposed to first type, the activated caspase-8 can be either mildly activated or totally unable to activate procaspase-3 directly. However, it can activate the mitochondrion-mediated pathway by truncating Bid (a pro-apoptotic Bcl-2 family member) in cytosol of cell and activated it to become tBid which can trigger the activation of the mitochondrion pathway (Arnoult *et al*., 2003).

The activation pathway mediated by procaspase-10, with a DED-containing prodomain, is similar to that mediated by procaspase-8. It can function independently of caspase-8 in initiating Fas- and TNF-related apoptosis. Moreover, Fas crosslinking in primary human T cells leads to the recruitment and activation of procaspase-10. Although caspase-8 and caspase-10 both interact with the DED of FADD in death receptor signalling, they may have different apoptosis substrates and therefore potentially function distinctly in death receptor signalling or other cellular process (Wang, 2001).

The intrinsic apoptosis pathway involves mitochondrion-mediated procaspase-activation of caspase-9. The activation of the mitochondrion-mediated pathway normally occurs when cell is under stress (e.g. DNA damage) which in turn will cause the activation of the proapoptotic protein in cytosol. Next, it induces the opening of mitochondrion permeability transition pores (MPTPs). As a result, cytochrome c that is localized in the mitochondria will be released to the cytosol.

The presence of the cytosolic dATP (deoxyadenosine triphosphate) or ATP, cytochrome c, apoptotic protease activation factor (Apaf-1) oligomerizes together with cytosolic procaspase-9 can result in the formation of a massive complex known as apoptosome. The N-terminal of Apaf-1 and the prodomain of procaspase-9 both have caspase recruitment domains (CARDs) and form a complex in the proportion of 1:1 (Arnoult *et al*., 2003; Fan *et al*., 2001). Activated caspase-9 can in turn activate procaspase-3 and procaspase-7. The activated caspase-3 will then activate procaspase-9 and form a positive feedback activation pathway to further enhance the apoptotic effects (Fan *et al*., 2005). Figure 1.3 and 1.4 summarized the caspase-8 and caspase-10 activation and downstream of executioner caspases activities mentioned above.

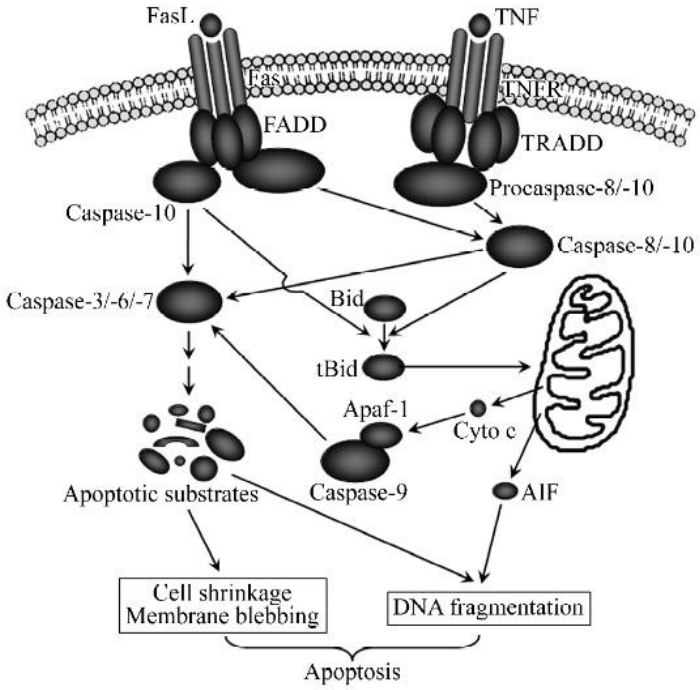

Adapted from (Fan *et al*., 2005)

Figure 1.3 Caspase -8/caspase -10 dependent procaspase-activation

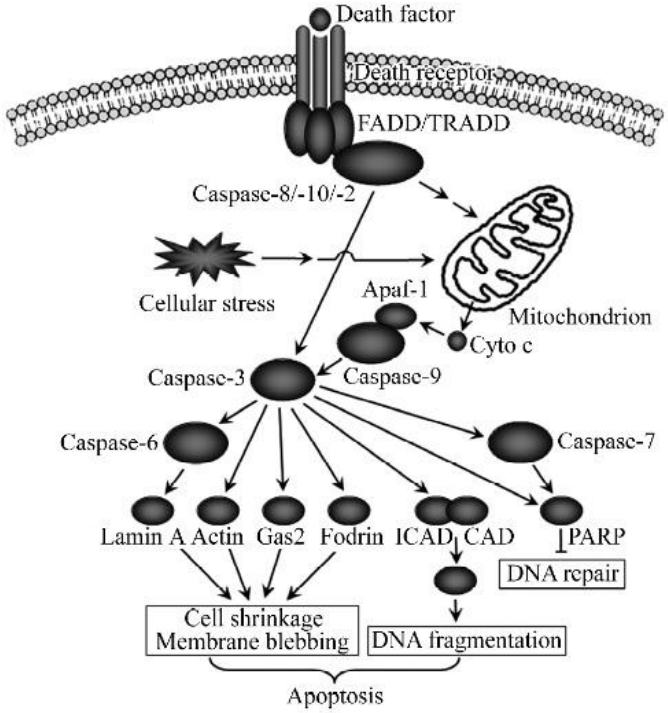

Adapted from (Fan *et al*., 2005)

Figure 1.4 Downstream substrates of apoptosis executioner caspases.

1.2.9 Possible intervention of apoptosis and chemoprevention in cancer

Of all the forms of cell death, apoptosis is the best characterized and its highly regulated nature makes it an attractive target for therapeutic intervention. Apoptosis is highly conserved throughout evolution (Lockshin and Zakeri, 2007; Samali *et al*., 1996) and plays a major physiological role in both embryonic development and aging (Lockshin and Zakeri, 2007; Samali *et al*., 1996). Thus, the therapies designed to stimulate apoptosis in target cells play an increasing central role in the prevention and treatment of both hereditary and non-hereditary types of cancer (Hawk *et al*., 1999). Chemoprevention in colorectal cancer is defined as the use of pharmacological agents to prevent or reverse the development of adenomatous polyps and subsequent progression to colorectal cancer (Plummer *et al*., 2001; Sharma *et al*., 2001).

Among these agents, curcumin (diferuloylmethane) a naturally occuring yellow phenolic chemical substance derived from the root of plant *Curcuma longa* is currently widely used as chemopreventive agent (Cheng *et al*., 2001; Rao *et al*., 1995). This major pigment in turmeric, possesses both anti-inflammatory (Srimal and Dhawan, 1973) and antioxidant properties (Motterlini *et al*., 2000; Sharma, 1976) and studies have shown that curcumin inhibits growth of cultured colon HCT-15 and HT-29 human cancer cell lines (Hanif *et al*., 1997), and also prevents the development of skin cancer in *in vivo* models (Huang *et al*., 1992). There are even more reports (Skommer *et al*., 2007; Yang *et al*., 2012; Yang *et al*., 2012) showing curcumin-induced apoptosis in numerous types of cancer cell lines, one of the apoptotic pathways is through generation of reactive oxygen species, down regulation of Bcl-XL and IAP followed with release of cytochrome c and inhibition of AKT (Woo *et al*., 2003).

As an important and common food coloring and flavouring agent (Kawamori *et al*., 1999), dietary administration of curcumin significantly suppresses development of chemically induced forestomach, duodenal and colon tumors in mice model (Huang *et al*., 1994). Reduction in formation of focal areas of dysplasia and aberrant crypt foci in the colon that are early preneoplastic lesions in rodents was detected with curcumin administration (Huang *et al*., 1992; Rao *et al*., 1993). Report (Pereira *et al*., 1996) has shown that, continuous administration of 0.8% and 1.6% curcumin during initiation and postinitiation phase significantly inhibited development of colonic adenomas in rats. Moreover, phase I clinical trial studies conducted by Cheng *et al*. (2001) in patients with high-risk or pre-maglinant lesions demonstrated that curcumin possesses chemoprevention activities. Results supported that curcumin is not only able to exert its effect in early stage of cancer-initiation stage, but also either in cancer promotion or may be progression stage. In addition, a high dose of curcumin up to 8 g/day could be administrated orally on daily mode to patients with premalignant lesion for 3 months without overt toxicity (Cheng *et al*., 2001).

A critical issue in chemoprevention is in the relative sensitivity of cells at different stages of neoplastic progression (Koornstra *et al.*, 2003). It is generally believed that, the apoptotic inducers that can directly induce apoptosis may provide less opportunity for cancer cells to acquire drug resistance traits and decrease mutagenesis and reduce toxicity on normal cells. It is for these reasons that researchers have a general interest in identifying compounds that possess apoptosis-inducing capabilities (Essack *et al*., 2011). As discussed earlier, curcumin is definitely a good example of plant-derived compound that complies to all necessary criteria and features mentioned. In the coming years, it seems likely that rational strategies to manipulate apoptotic mechanisms will produce new therapies that are less toxic than current chemoprevention strategies.

1.2.10 Cell Cycle

The cell cycle is a series of events that take place in a cell leading to its replication. There are two important phases in cell cycle where S phase is the chromosome duplication (synthesis) phase and M phase stands for mitotic phase, in which the cell's chromosomes are divided between two daughter cells. These two important phases are separated by G1 phase and G2 phase (interphase) making up the sequence M-G1-S-G2 as shown in Figure 1.5 (Kathleen, 1997). Regulation of the cell division cycle is an essential process by which the cell monitors its fidelity of cell division through several cell cycle checkpoints. The main function for the existence of checkpoints is to assess DNA damage and make sure the correct replication of DNA sequences. Scientists have identified several checkpoints along the cell cycle namely G1 checkpoint (located in G1 phase), G2 checkpoint (located in G2 phase) and so on (Anne, 2006; Julie and Jane, 2005).

Generally, the cell cycle progression relies on cyclin dependent kinases (cdks) and their inhibitors. If there are any DNA damages on the chromosomes, it will cause the absence or presence of certain regulators that can stop the cells from passing through their checkpoint and subsequently leading to cell cycle arrest or apoptosis (Alberson *et al*., 2005).

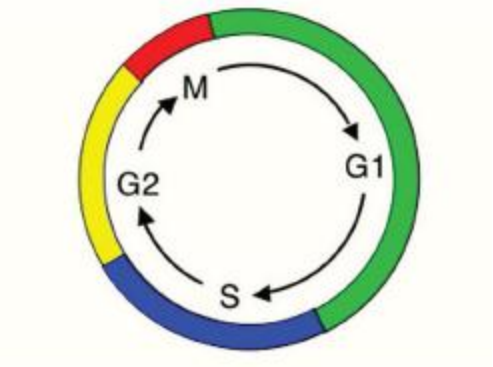

Figure 1.5 The different phases in cell cycle.

1.2.10.1 Early cell cycle progression: G1/S-phase

Cell cycle progression involves expression and/or activation of numerous regulatory proteins. The regulatory proteins include cyclin-dependent kinases (Cdk's) and holo-enzymes formed from complex of cyclins and the cyclin. Accumulation of D-type cyclins (D1, D2, and D3), Cdk's (Cdk4 and Cdk6) and proliferating cell nuclear antigen (PCNA) that occur during the early entry of G1-phase would promote DNA-polymerase activity (Stillman, 1994). PCNA is capable of forming complexes with cyclin D/Cdk4 complexes to regulate the cell cycle progression (Sherr, 1994). In fact, increased levels of the cyclin-dependent kinase inhibitor (CKI) typically $p27^{Kip1}$ will prevent the cell cycle entry into mitogen deprived (G0) phase (Sherr and Roberts, 1995) as $p27^{Kip1}$ is able to bind and cause deactivation of G1-phase cyclin/Cdk complexes. It is counter-balanced by increased level of activated D/Cdk4/PCNA complexes, as high level of D/Cdk4/PCNA compared to $p27^{Kip1}$ will allow an enzymatic activation of Cdk2. In late G1-phase, expressed cyclins E and A will form complexes with the activated Cdk2 together assisting in progression of cell through the cell cycle phase.

Retinoblastoma gene product (Rb) which is responsible as a timer of transcriptional events will be activated through phosphorylation process by activated G1-phase Cdk complexes (Weinberg, 1995). Hyper- or hypo-phosphorylated Rb would either inhibit or release different isoforms of E2F in late G1-phase. The primary isoform of E2F, E2F-1 regulates number of genes which are required for progression of cells in different phases including, S, G2 and M. The genes under regulation by E2F1 include PCNA, dihydrofolate reductase, cyclin E, Cdk1 and cyclin A (Gregori *et al.*, 1995).

Regulation of early phases of cell cycle also involves a 21-KD protein, $p21^{Cip1}$. As another CKI, $p21^{Cip1}$ is thought to act as a cyclin-Cdk assembly and a regulatory factor

(Sherr and Roberts, 1995). The importance of $p21^{Cip1}$ can be seen where a single $p21^{Cip1}$ molecule may be required for Cdk activation, whereas complexes are inactivated if bounded by multiple $p21^{Cip1}$ subunits. $p21^{Cip1}$ protein levels remained low in G0-phase cell, but an upsurge of this protein can be observed in late G1-phase. The increased level of this Cdk inhibitor is important as it can regulate or counterbalance the increased accumulation and enzymatic activity of cyclin/Cdk complexes (Sherr and Roberts, 1995).

Protein 53 (p53) or known as "the guardian of the genome" is a vital transcription factor that regulates the expression of a number of important genes. This protein has also been shown to be involved in cell cycle regulation (Levine, 1997). One example of the involvement of p53 in the cell cycle is through the response to DNA damage that leads to an arrest in G1-phase. It serves to provide the primary mechanism of the antiproliferative effect on cells that suffer from irradiation by stimulating the accumulation of $p21^{Cip1}$ (Deiry *et al*., 1993; Levine, 1997). Accumulation of $p21^{Cip1}$ will thereby directly block the ability of PCNA and suppress the processing ability of DNA polymerase. Consequently, it can cause the arrest of DNA replication and thus allows DNA repair to take part (Waga *et al*., 1994). In fact, besides acting as a transcription factor, p53 can also act through direct protein-protein interactions with E2F1 as an alternative preventive measure to promote apoptosis on the damaged DNA cells (Lowe *et al*., 1993). Indeed, studies have suggested that p53 plays a role in regulating the transition of G0-G1-S and also completion of G2/M-phase in cell cycle progression (Cross *et al*., 1995; Del Sal *et al*., 1995).

1.2.10.2 Late cell cycle progression: G2/M-phase

DNA replication process is completed at G1 phase and the cell is expected to progress further through the G2-phase with marked increase of cyclin B protein. The complex known as "mitosis-promoting factor" (MPF) would be formed when cyclin B protein interacts with Cdk1 with the presence of cell division cycle 2 (Cdc 2) kinase. Phosphorylation of Cdk1 on a threonine residue (Thr161) by Cdc25 phosphatase activates MPF (King *et al*., 1994). The activated MPF will then be able to induce the ubiquitin proteasome pathway that subsequently causes cyclin B degradation and the initiation of anaphase (King *et al*., 1996). Eventually, the reset of cell cycle clock is through dephosphorylation of Cdk 1 at Thr161.

Besides that, proto-oncogenes especially c-fos is believed to play a significant role in the completion of progression through the cell cycle. As it has been suggested c-fos is required for all phases of cell cycle (Pai and Bird, 1994). *C-myc* is able to increase Cdk activity, resulting in upregulation of cyclin level and further induces Cdc25 phosphatase activation in which it causes a rapid hyperphosphorylation of pRb at G1/S (Galaktionov *et al*., 1996). *C-myc* can also cooperate with activated H-*ras* to upregulate the Cdk1 protein level, an interaction that is further correlated with its ability to promote progression into M-phase (Born *et al*., 1994). Meanwhile, C-myb regulates the transcription level of Cdk1 (Ku *et al*., 1993) and increases the expression of IGF-1 (Travali *et al*., 1991), indicating a bidirectional regulation of prooncogene and growth factor expressions in cell (Pardee, 1989). Figure 1.6 summarized the regulatory proteins involved in cell cycle regulation.

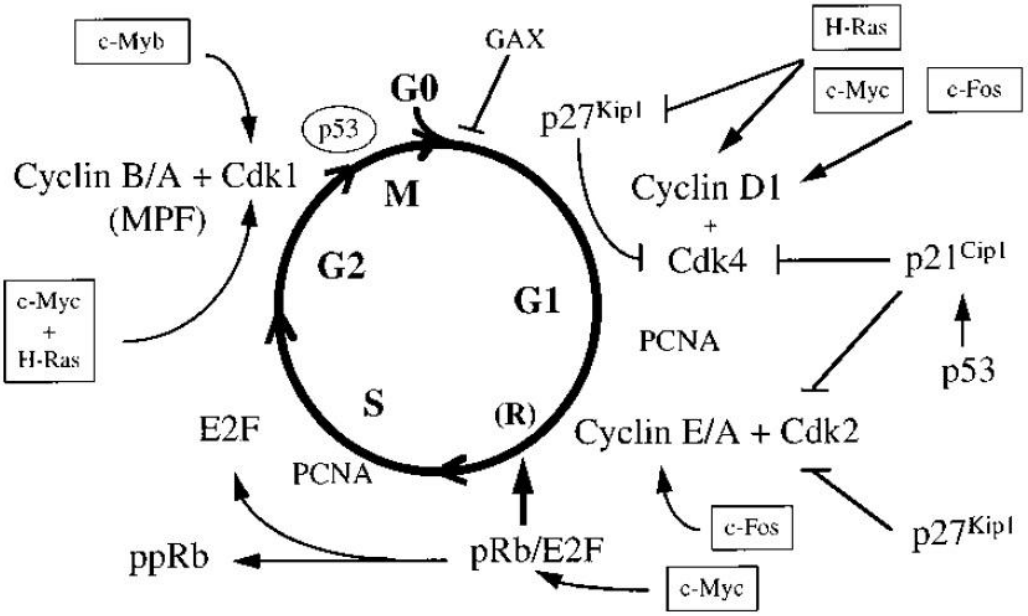

Figure 1.6 Involvement of cell cycle regulatory proteins in cell cycle regulation.

1.2.11 Cancer and Natural Products

In recent years, oriental medicinal herbs have aroused scientific interest as complementary or alternative medicines (Lee, 2000). The utilization of modern analytical and chemical purification techniques has resulted in the discovery of novel natural compounds from herbs, a step further and easier than before. Intensive scientific studies are being conducted in search for new drugs or chemicals from natural sources as there are 250,000 species of plant in the world and most of them are in wait to be discovered (Cragg and Newman, 1999; Cragg *et al.*, 1997). Furthermore, the uniqueness and diversity of chemical compounds in natural products intensify the identification and mechanistic investigation in natural product field. These lead to the discovery of novel lead compounds acting on newly discovered therapeutic targets (Harvey, 1999). Besides, the synthetic analogs of natural products as potential cancer chemopreventive agents has also become an important issue in current public health-related research (Steele *et al.*, 1998; Alberts *et al.*, 1995).

Today, naturally derived products play an important role as a source of medicine and many pharmaceutical agents have been discovered (Harvey, 1999). Several important chemotherapeutic drugs derived from plants have been discovered, such as podophyllotoxin, vinblastine, camptothecin and Taxol, and are widely used in tumor medical treatment (Raskin *et al*., 2002). One of the most noteworthy examples of the plant-derived anticancer agent is the vinca alkaloids vincristine isolated from periwinkle *Catharanthusroseus*, which is endemic in Madagascar rain forests. Plant-derived vincristine is known as mitotic inhibitor which is commonly used in cancer chemotherapy. It acts through binding to tubulin and depolymerize the microtubules (Okouneva *et al*., 2003), leading to cell cycle arrest in mitosis especially in the metaphase (Gidding *et al*., 1999). Besides the interaction with tubulins, its efficacy toward cancer cells is also due to other mechanisms such as membrane-bound drug efflux transporters, signal transduction pathways and programmed cell death.

1.2.12 Limonoids

Limonoids are found most abundant in Meliaceae and Rutaceae Families. Natural occurring citrus limonoids contain a furan ring attached to the D-ring, at C-17. The oxygen containing functional groups occur at C-3, C-4, C-7, C-16 and C-17 of the structure of citrus limonoids. On the other hand, the structural variations of limonoids found in Rutaceae are lesser compared to Meliaceae as there are generally due to limitation of the modification at ring A and B. Limonoids found in the family of Meliaceae are far more complex as their structures have higher number of oxygen molecules and far more types of rearrangement are exhibited in the parent limonoid structure (Roy and Saraf, 2006).

Due to commercial reasons, limonoids were discovered way back when researchers started looking for the factor responsible for the bitterness in citrus as it created a negative impact on the fruit and juice industry. The ability of some limonoids to produce an extremely bitter taste in these products has provided much impetus to the study of their structural makeup and characteristics. Eventually limonin was the first tetranortriterpenoid to be discovered from citrus which is responsible for its bitterness, consequently contributed to the derivation of the term limonoids (Roy and Saraf, 2006). Scientific studies of this group of compounds have been shown to exhibit a wide range of biological activities including antifungal, antibacterial, antimalaria, anticancer, antiviral and also a number of pharmacological activities on humans (Saraf, 2006).

1.2.12.1 Structure-related activities

According to studies conducted by Govindachari and coworkers (1999) limonoids namely, swietenine, 3-tigloylswietenolide and 6-acetylswietenine were evaluated for antifungal activity and the results have revealed that the double bond position in these compounds at 8, 30 and 8, 14 did not play a role in the antifungal activity. However, it was proposed that functional group substitutions at C-6 may be important in increasing the antifungal effect as the 3-tigloylswietenolide and 6-acetylswietenine compounds with acetoxy group at C-6 possessed stronger bioactivity. This concluded the C-6 substitution is crucial for antifungal activity.

Comparison between 3,6-Di-O-acetylswietenolide and swietenolide has resulted in the conclusion that C-3 substitution with a tigloyl group possessed the strongest activity followed by hydroxyl and acetyl group. Meanwhile, mexicanolide derivatives such as 2,3 dihydroxymexicanolide, 3-hydroxymexicanolide and 3-acetoxymexicanolide with carbonyl group substitution at C-3 and 2α-hydroxymexicanolide (A-hydroxyl substitution at C-2 and a carbonyl functional group at C-3) showed limited activity .

1.2.13 *Swietenia macrophylla*

[A]

[B] [C]

Figure 1.7 The view of [A] whole tree, [B] Fruit and [C] seeds of *Swietenia macrophylla* King.

The existing study is to focus on the seeds of *Swietenia macrophylla* as shown in Figure 1.7. The details of this plant are listed as below.

A) Scientific classification of *Swietenia macrophylla*.

Kingdom : Plantae

Order: Sapindales

Family: Meliaceae

Genus: Swietenia

Species: *S. macrophylla*

B) Common name:

Sky fruit, Coaba (throughout Latin America), Acajou (French-speaking areas), Tunjuk Langit (Malay).

C) Physical Characteristic:

They are medium-sized to large trees growing to 20-45 m tall, and up to 2 m trunk diameter. The leaves are 10-30 cm long, pinnate, with 3-6 pairs of leaflets, the terminal leaflet absent; each leaflet is 5-15cm long. The leaves are deciduous to semi-evergreen, failing shortly before the new foliage grows. The flowers are produced in loose fluorescence, each flower small, with five white to greenish-yellowish petals. The fruit is a pear-shaped five-valved capsule 8-20 cm long, containing numerous winged seeds about 5-9 cm long (Brown *et al*., 2003).

D) Traditional usage

The seeds of *Swietenia macrophylla* are used in traditional medicine to improve blood circulation or hypertension, diabetes, skin condition (Tan *et al*., 2009) and as antimalarial (Munoz *et al*., 2000).

E) Previous works on *Swietenia macrophylla*

i) Phytochemicals

Previous phytochemical investigations have revealed the present of limonoids such as swietenin, swietenolide, 8,30-epoxyswietenine acetate, swietenine acetate, swietenolide diacetate, swietenolide tiglate, augustineolide and 3β, 6-dihydroxydihydrocarapin in the seeds (Anne, 1983; Chakravarty, and Chatterjee , 1955; Chakravarty *et al*., 1957; Chan *et al*., 1976; Connolly, 1964; Mootoo *et al*., 1999). On the other hand, its leaves have been reported to yield essential oils which contain himachalene, germacrene D, germacrene A, cadina-1,4-diene, hexadecanoic acid, and ethyl hexadecanoate (Soares, 2010). Besides that, the most recent finding reported that four new phragmalin-type limonoids were successfully isolated out, named swietephragmin H-J and swietemacrophine from dichloromethane extract of *Swietenia* leaves (Tan *et al*., 2009).

ii) Bioactivity

Several bioactivities works have been done by scientists around the world on this particular plant. The limonoids of this tree have been shown to exhibit antimalarial (Soediro *et al*., 1990) insect anti-feedant (Nsiama, 2008), anti-inflammatory (Chen *et al*., 2010), antimicrobial (Maiti *et al*, 2007), oral hypoglycemic (in vivo) (Dewanjee *et al*., 2009a) and antioxidant activities (Tan *et al*., 2009) and the essential oil of *S. macrophylla* have been shown able to induce electrophysiological responses to Zeller (Soares *et al*., 2003).

CHAPTER 2

MATERIAL AND METHODS

2.1 Material

2.1.1 Solvents

Acetone, chloroform, ethanol (95%), absolute ethanol, ethyl acetate, hexane, methanol and sulphuric acid were purchased from Merck.

2.1.2 Cell lines

The cell lines namely Ca Ski (Human Caucasoid cervical carcinoma cells, CRL1150), KB (Human Negroid cervical carcinoma cells, HeLa derivative, CCL-17), MCF-7 (Human breast carcinoma cell, HTB-22), Hep G2 (Human hepatocellular carcinoma cell, HB-8065), HCT116 (Human colorectal carcinoma cell , CCL-247) and MRC-5 (Human fibroblast cell, CCL-17) were procured from American Type Culture Collection.

2.1.3 Growth medium

The growth medium namely EMEM (Eagle's Minimum Essential Medium), DMEM (Dulbecco's Modified Eagle's Medium), Medium 199 and RMPI (Roswell Park Memorial Institute) 1640 were purchased from Sigma.

2.1.4 Drugs, chemicals and reagents

The following purchased items are listed according to manufacturer:

Sigma: Bovine Serum Albumin (BSA), HEPES, Hoechts 33342, camphothecin (CPT), dimethyl sulfoxide (DMSO), ethylene diamine tetrachloroacetic acid (EDTA.4Na.4H_2O), paraformaldehyde (PFA), PBS, propidium Iodide, RNase A, sodium azide, trypan blue, DCFH-DA (6-carboxy-2', 7'-dichlorodihydrofluorescein

diacetate), Copper sulphate, N,N'-Methylethylenediamine (TEMED), ammonium persulfate, acrylamide and sodium dodecyl sulphate.

Merck: Thin Layer Chromatography (TLC) plate silica gel 60 F_{254}, Silica gel F254 (0.063-0.200 mm), Trixon X-100, sodium carbonate, potassium sodium tartarate, hydrochloric acid, Folin-Ciocalteu reagent, bromophenol blue, Tris (hydroxymethyl)-aminomethane, glycerol, glycin and acetic acid.

PAA Lab: Amphotericin B, Fetal bovine serum and penicillin-streptomycin (liquid).

BD-Bioscience: Annexin V FITC, Annexin V binding buffer and Cytofix/Cytoperm.

Innovative Cell Technologies: Accutase

Bio-Rad: Coomassie brilliant blue R-250.

2.1.5 Kits

The following purchased kits are listed according to manufacturer:

Immunochemistry technologies, LLC: FAM-FLICA Caspase 3/7, FAM-FLICA Caspase 8, FAM-FLICA Caspase 9 and FAM-FLICA Caspase 10.

Qiagen: QIAamp RNA Blood Mini Kit, Qiagen SA Biosciences PCR array and First Strand kit.

Stratagene: Mitochondrial membrane potential detection kit.

Ambion: RNAqueous-4PCR kit.

Quantace: SensiMix One-Step Kit.

2.1.6 Oligonucleotides

Table 2.1: The different primers used in this study are listed as below.

Target Genes	Function	Sequence
Bcl-2	Forward primer	5'-TTGGCCCCCGTTGCTT-3'
	Reverse primer	5'-CGGTTATCGTACCCCGTTCTC-3'
Bax	Forward primer	5'-GTCGCCCTTTTCTACTTTGCCAG-3'
	Reverse primer	5'-TCCAGCCCAACAGCCGCTCC-3'
PBGD	Forward primer	5'-ACCATCGGAGCCATCTGCAAG-3'
	Reverse primer	5'-CCCACCACACTCTTCTCTGGCA-3'
PCNA	Forward primer	5'-GCCTGCTGGGATATTAGCTC–3'
	Reverse primer	5'-CATACTGGTGAGGTTCACGC–3'
GADPH	Forward primer	5'-CCAGGGCTGCTTTTAACTCTG–3'
	Reverse primer	5'-CGTTCTCAGCCTTGACGGTG–3'

2.1.7 Instrumentation/ Equipment

Instruments and equipment used including Nanodrop (Thermo Scientific), Centrifuge (Eppendorf), CO_2 incubator (RS biotech), Microplate reader Asys UVM 340 (Biochrom Ltd), Flow Cytometer (FACSCalibur) and CellQuest software (Becton Dickinson), Leica Fluorescent microscope (Leica),Liquid nitrogen storage Dewar (MVE), pH meter (Jenway), RotorGene-6000 System (Qiagen), Rotary evaporator with vacuum & water bath (Buchi), NMR Spectrometer 400MHz (JEOL), LC-MS (Fisher Scientific), LC-MS/MS-TOF (Agilent), SDS-PAGE system (Bio-Rad), BD-C6 Accury Flow cytometer (Becton Dickinson) and High performance liquid chromatography (Shimadzu).

2.1.8 Miscellaneous

Items listed according to manufacturer:

Orange Scientific: cell culture flasks (25 and 75 cm^2), cell culture dishes (60 mm) and cell culture multiwall plate (96 well, flat bottom).

DB Biosciences: conical centrifuge tubes (15 and 50ml).

Nalge Nune International: Cryovials.

Becton Dickinson: falcon round bottom tubes (5ml).

Pyrex Co.: glassware.

Fisher Scientific: glass slides and cover glass slips and haemocytometer and cover slips.

Sartorius: sterile syringe and syringe filters (0.2 μm).

2.2 Methods

2.2.1 Plant material

The dried seeds of *Swietenia macrophylla* (600 g) were purchased from local market and were identified by Professor Dr. Ong Hean Chooi, a botanist from Institute of Biological Sciences, Faculty of Science, University of Malaya, Malaysia. A voucher specimen (No. KLU46901) is on deposit at Herbarium of Institute of Biological Sciences, Faculty of Science, University of Malaya, Malaysia.

2.2.2 Extraction and Fractionation of *S. macrophylla*

Seeds of *S. macrophylla* were extracted to obtain the crude ethanolic extract 66.6 g out of 600 g of sample (11.1 g per 100g of dry weight) and further fractionation to yield fractions with different polarities.

2.2.2.1 Solvent extraction

The dried, ground seeds powder was then soaked for 3 days in ethanol at room temperature. The extract was then filtered from the residue by using filter paper and the residue was re-extracted with ethanol again for two times. By using a rotary evaporator, the ethanol solvent was evaporated under reduced pressure at a temperature of 45 ℃ to give a dark yellow crude ethanolic extract.

2.2.2.2 Solvent-solvent partitioning of the crude extract

A solvent-solvent partitioning step was employed to separate the extract based on polarities (Figure 2.1). The use of solvents with varying polarities ensures that a wide polarity range of compounds could be extracted in the process. 30 g of the ethanolic extract was partitioned with hexane to yield a 4.28 g hexane soluble fraction. The resultant hexane-insoluble residue was further partitioned with ethyl acetate and water (1:1) in a separating funnel. The bottom aquoeus layer was collected and concentrated by evaporation under vacuum and freeze-dried to yield a water fraction of 2.48g. The upper ethyl acetate layer was evaporated under pressure to give an ethyl acetate fraction of 23.1g. This afforded another three fractions from the crude plant extract, namely, *S. macrophylla* ethanol extract (SMEE) , *S. macrophylla* hexane fraction (SMHF), *S. macrophylla* ethyl acetate fraction (SMEAF) and *S. macrophylla* water fraction (SMWF).

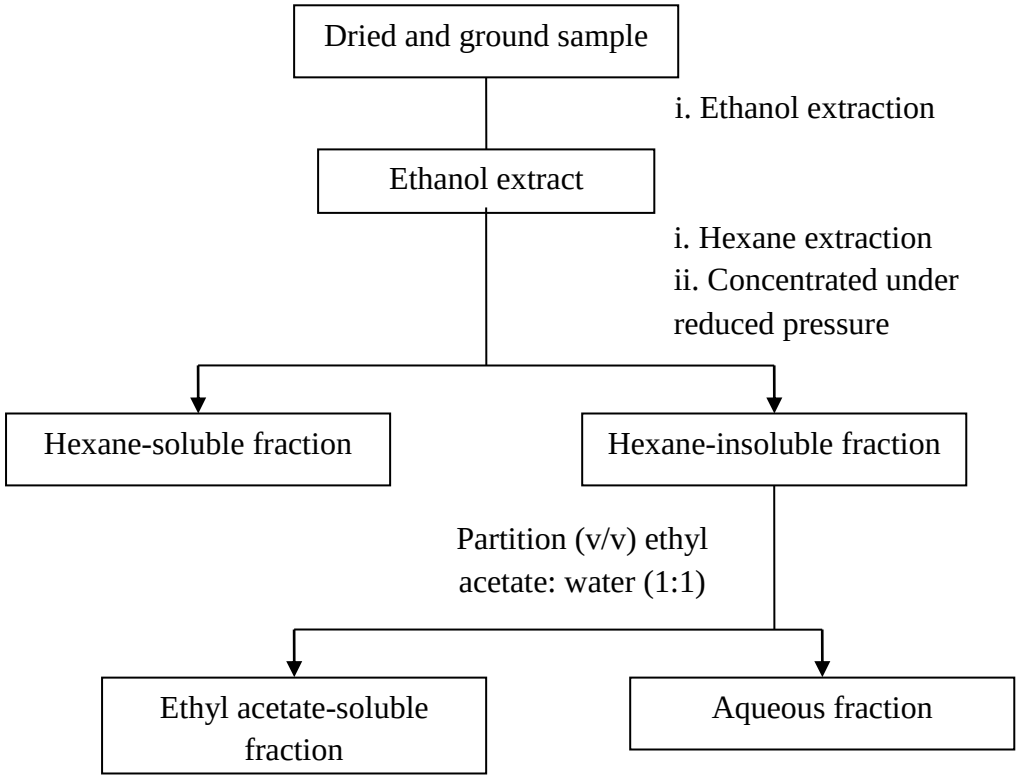

Figure 2.1 Extraction and fractionation procedures.

2.2.3 Cell culture

2.2.3.1 Maintenance of cells

HCT116, Ca Ski, MCF-7, KB, Hep G2 cells were cultured in RPMI (Roswell Park Memorial Institute) 1640 Medium. The MRC-5 cells were cultured in MEM medium which supplemented with sodium pyruvate. Both type of medium were further supplemented with 10% (v/v) heat-deactivated fetal bovine serum, 100 µg/ml streptomycin, 100 unit/ml penicillin and 50 µg/ml amphotericin B. All the media were filter-sterilized by using a membrane filter with pore size of 0.22 µm. the cells were cultured as monolayers and maintained in 5% CO_2 incubator at 37 ℃ in a humidified atmosphere.

2.2.3.2 Cryopreservation of cells

For cryopreservation, the cells were first viewed using an inverted microscope to assess the degree of cell density and confirm the absence of contamination. The confluent cells were harvested and centrifuged at 1000 rpm for 5 min and the cell pellet was washed 3 times with PBS and resuspended at a concentration of 1 x 10^6 cells per ml in a freezing medium. Since the formation of ice crystals during the freezing process could rupture the cells, a special feezing medium consisting of 70% of respective culture medium, 20% of FBS and 10% of DMSO was used. Then 1 ml aliquot of the cell suspension was transferred into sterile cryovial and labelled with the cell-line name, date, passage number and user name. To ensure successful cryopreservation, gentle freezing method was used whereby the temperature was decreased gradually. The vials were first frozen at -20 ℃ for 6 h and then transferred to -80 ℃ for 2 h before placed in the vapour phase of liquid nitrogen storage vessel for long-term storage.

2.2.3.3 Reviving of cells

For resuscitation of cells, cryovials were removed from the liquid nitrogen storage and quickly defrosted by immersed in a 37 ℃ water bath and gently shaken until thawed. Once fully thawed, the cells were pipetted into 15 ml conical centrifuge tube containing warmed medium. After centrifugation at 1000 rpm for 5 min, the supernatant was removed and the pellet was resuspended in fresh warm medium. The cells were then pipetted into 25 cm^2 cell culture flask and incubated inside CO^2 incubator overnight to allow cells to adhere. The medium was removed the next day to remove traces of DMSO and replaced with fresh medium. The cells were culture for at least 3 passage before use for any experiment.

2.2.3.4 Subculturing the cells

When the cell growth reached confluency, the cells were subcultured/ passaged in order to prevent the cells from dying by providing spaces for continuous growth and supply of fresh nutrients. To subculture the cells, the medium was removed and the cells were washed twice with phosphate buffer saline (PBS) by gently swirling the flask. After discarding the PBS, 2ml of Accutase solution was added to cover the adhering monolayer cells and the flask was returned to the incubator and left for 3~8 min. During the incubation period, the flask was examined under an inverted microscope to ensure that all the cells were detached and floating. The bottom of the flask was gently tapped to dislodge any remaining attached cells. When the cells were rounded up and detached from the surface, medium was added into the flask. The cell suspension was transferred into a 15ml conical centrifuge tube and centrifuged at 1000 rpm for 5min. After discarding the supernatant, the pellet was resuspended in the medium and diluted to appropriate concentration before transferred to new flasks for further incubation.

2.2.3.5 Counting the cells

A trypan blue exclusion assay was performed to count the viable cells using a haemocytometer. Trypan blue is a dye that excludes viable cells but selectively stains dead cells with damaged plasma membrane. To count the cells, adherent cells were harvested and resuspended in a volume of medium. Then 100 µl of 4% (w/v) trypan blue solution was added (dilution factor=2). The cells were mixed and left for 2 min at room temperature. Then 20 µl aliquots of cell mixtures were pipetted into each of the two haemocytometer chambers covered with a coverslip and the chamber was filled by capillary action. The haemaocytometer was viewed under an inverted phase contrast microscope using 10x or 20x magnifications to focus on the grid lines of the chamber. The number of viable cells were counted in the five large squares. Non-viable cells (stained blue) were not included in the cell counts. The number of viable cells per ml was calculated by the equation: total number of viable cells/ml = the average count per square x dilution factor x 10^4, where the dilution factor = 2 (if volume of cell suspension and trypan blue = 1:1) and 10^4 = correction factor (supplied by haemocytometer manufacturer). To obtain the total viable cell number in the original suspension, the viable cell number/ml was multiplied by the total volume (ml) in the original suspension.

2.2.3.6 Treatment of cells

Stock solution (20mg/ml) of the plant extract/ fractions and isolated pure compounds were prepared by dissolving them in DMSO. These solutions were filter-sterilized and stored in lightly sealed dark glass container in at -20 ℃. For the experimental procedures, the stock solutions were serially diluted by using medium and added to the cells. Exponentially growing cells were then treated with the vehicle DMSO. The final concentration of DMSO was 0.5% (v/v). Cells were harvested at the appropriate time points, and were then subjected to various processing procedures accordingly.

2.2.4 Evaluation of cytotoxic effect of extract and fraction of *S. macrophylla*

The crude ethanolic extract and fractions from *S. macrophylla* were evaluated their cytotoxic effect using MTT cell viability assay.

2.2.4.1 MTT cell viability assay

3-(4,5-dimethylthiazol-2yl)-2,5-diphenyltetrazolium bromide or known as MTT assay has been routinely used to assess cell growth/ inhibition and cell viability and compared well with other available assays (Alley *et al*., 1988; Hansen *et al*., 1989; Mosmann, 1983; Rubinstein *et al*., 1990). The assay is based on the reduction of yellow water soluble tetrazolium MTT by mitochondrial dehydrogenase to a purple water insoluble formazan cystal. the reduction takes place only in metabolically active cells and therefore, the generated formazan product is proportional to the number of viable cells (Liu *et al*., 1997). The amount of MTT formazan produced can be dissolved in a suitable solvent and determined spectrophotometrically. The reaction is shown in Figure 2.2.

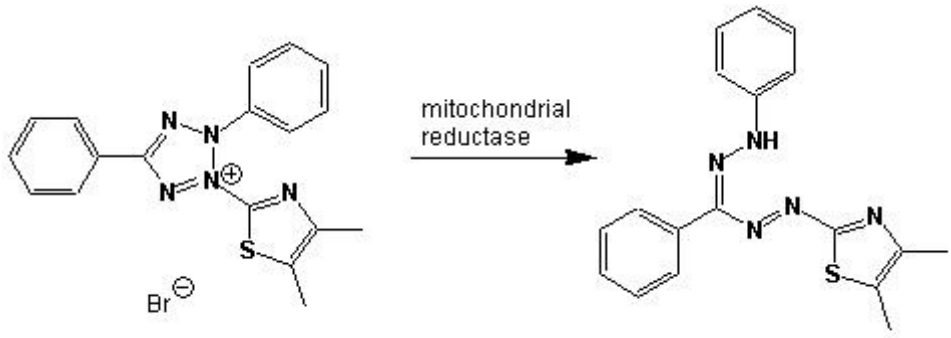

Figure 2.2 Principle of MTT chemical reaction.

The effect of *Swietenia macrrophylla* extracts on cell viability was assessed using the 3-(4,5-dimethylthiazol-2yl)-2,5-diphenyltetrazolium bromide (MTT) assay according to Mosmann (1983) with some modifications. A total of 5 x 10^3 cells were seeded at a density of 5 X 10^3 cells/well into a sterile flat bottom 96-well plate and allowed to adhere overnight. After 24 h, 20 µl of the appropriate extract solution in the

concentration range of 10 to 200 µg/ml was added. For untreated cells (control), vehicle DMSO was added instead of the sample. The cells were then incubated at 37 ℃ in a humid atmosphere with 5% CO_2, 95% air for 24, 48 or 72h. After the indicated period of exposure, 20 µl of MTT solution (5mg/ml, in PBS) was pipetted into each well of the plate. The plates were protected from light and further incubated for another 4h at 37 ℃. Following 4 h of incubation, the medium was removed by gentle aspiration and the crystal formazan formed was dissolved in 150 µl of DMSO. The amount of formazan product was measured at 570 nm against the reference wavelength of 650 nm using a microplate reader. The effect of various treatments on cell growth was expressed as percentage of cell viability of the treated cells compared to that of the untreated control cells set at 100%. Cell viability (%) = (absorbance of treated cells/ absorbance of untreated cells) x 100%. The results obtained from MTT assay were presented as dose-response curves (percentage of cell viability vs the concentration of the sample in µg/ml) for each cell line. The 50% inhibitory concentration (IC_{50}) is the concentration that reduces cell viability to 50% and is obtained from dose-response curves.

2.2.4.2 Total Cell Count

Briefly, $1x10^6$ of cells were plated into 60 mm dish and incubated 24 hours to let the cells to adhere. After 24 hours, the medium of the cell were replaced with the fresh medium containing different concentrations of extract ranging from 50µg/ml to 1mg/ml. The cells were further incubated either for 24, 48 or 72 hours. After incubation period, the cells were detached by accutase and pelleted for 5 minutes at 1000rpm centrifugation. The cell pellets were diluted with the desired dilution factor in 0.4% of trypan blue solution and the viable cells were counted by using a haematocytometer. Figure 2.3 shown distribution quadrants of haematocytometer and the formula used for cells count.

A	B	C
D	E	F
G	H	I

Figure 2.3 Major quadrates view of haematocytometer under light microscope.

The cell number of treated samples was counted by using formula as below: (A+C+E+G+I) / 5 x Dilution factor x 10^4.

2.2.5 Evaluation of apoptotic effect of the most active fraction of *S. macrophylla*

Based on the MTT assay, the most active fraction of *S. macrophylla* was determined. The apoptotic-inducing effects were further evaluated using the following methods and elucidation of the apoptotic pathways.

2.2.5.1 Hoechst-propidium iodide staining and morphological observation

Hoechst 33342 (2'-[4-ethoxyphenyl]-5-[4-methyl-1-piperazinyl]-2,5'-bi-1H-benzimidazole trihydrochloride trihydrate) is a cell-permeable DNA stain that is excited by ultraviolet light and emits blue fluorescence at 460-490nm. Hoechst 33342 binds preferentially to adenne-thyymine (A-T) regions of DNA. Combination of Hoechst 33342/PI stains provides a rapid and convenient assay for apoptosis based upon fluorescent detection for the compacted stage of the chromatin in apoptotic cells. As Hoechst33342 (Figure 2.4) is a vital blue fluorescing DNA stain that is

membrane permeable, it brightly stains the condensed chromatin of apoptotic cells, whereas nuclei of live cells exhibit lower fluorescence. The red propidium iodide (Figure 2.5) is another DNA staining dye that only stains nuclei of cells with compromised plasma membrane and thus does not stain normal cells (Vanderlaag *et al*., 2006). The morphological signs of apoptosis in HCT 116 cells were evaluated by monitoring the nuclear changes using the named assay. The cells were grown in 60 mm culture dish and after 24 h of incubation and the cells were treated with 50 µg/ml of the active fraction for different time periods. After treatment, the cells were subjected to analysis using inverted microscope (Leica, Germany) and photographs of the cells were captured using camera (Leica, Germany).

The cells were then rinsed with PBS and harvested by using accutase. The suspension of the cells was collected by centrifugation and stained with Hoechst 33342 (10 µM) and propidium iodide (10 µM) for approximately 10 min while protected from light.

Observation was made by using inverted fluorescent microscope and photographs were taken using camera.

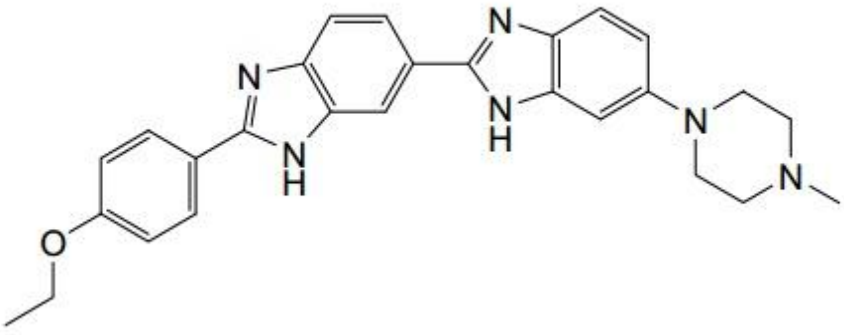

Figure 2.4 Chemical structure of Hoechst 33342.

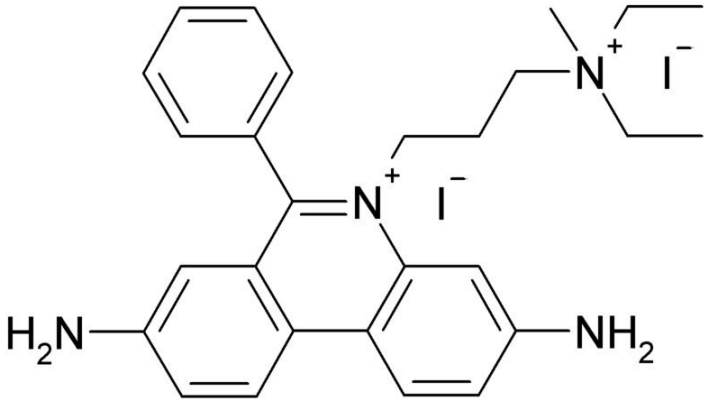

Figure 2.5 Chemical structure of propidium iodide (PI).

2.2.5.2 Examination of intracellular reactive oxygen species (ROS)

Various techniques can be used to determine ROS production including chemiluminescense (Briheim, 1989), fluorescence (Rest, 1994) or even cytochrome c reduction (Smith and Weidemann, 1993). The use of DCFH-DA as a fluorometric assay was first described for hydrogen peroxide detection (Keston, 1965), since then the use of dichlorofluorescin (DCFH) became popular as a probe to evaluate intracellular hydrogen peroxide formation by flow cytometry (Wang and Joseph, 1999). The principle for the experiment using DCFH-DA is that nonfluorescent fluorescin emitted fluorescence that is directly proportional to the concentration of hydrogen peroxide. However, when applied to intact cells, the non-ionic, non-polar DCFH-DA can cross cell membranes and is hydrolysed enzymatically by intracellular esterases into nonfluorescent DCFH. The presence of ROS would oxidize DCFH into highly fluorescent dichlorofluorescein (DCF) (LeBel *et al*., 1992). Therefore, the intracellular DCF fluorescence can be used to determine the oxidative stress condition in cells.

In this experiment, $1x10^6$ of HCT116 cells were grown on $23cm^3$ dishes and allowed to attach overnight and subsequently treated with 0.05mg/ml of SMEAF or DMSO for 4h. After the incubation period the cells were washed twice with PBS and 100 µM of DCF-

DA dye was added to each of the samples and incubated for 1h in darkness. The cells were harvested by using accutase and washed with ice-cold PBS. Florescence intensity was monitored using BD Accuri C6 flow cytometer. The mean of DCFH florescence was obtained from 10, 000 cells with excitation wavelength of 488 nm and emission wavelength of 525 nm.

2.2.5.3 Measurement of intracellular total glutathione (GSH) content

Glutathione (GSH) is a tripeptide (γ-gluyamylcysteinglycine) and major thiol antioxidant. Glutathione is a multifunctional intracellular non-enzymatic antioxidant. It is highly abundant in the cytosol, nuclei and mitochondria and is the major soluble antioxidant in these cell compartments. The reduced form of glutathione is GSH (glutathione) and the oxidized form is GSSG (glutathione disulphide) (Strużyńska *et al.*, 2005). Generally the antioxidant capacity of thiol compounds is due to the sulfur atom which can easily accommodate the loss of a single electron (Karoui *et al*., 1996). Reaction with radicals oxidized glutathione, but the reduced form is regenerated in a redox cycle involving glutathione reductase and the electron acceptor NADPH.

The presence of intracellular GSH provides protection for damage induced by antineoplastic agents, free radicals, reactive oxidant species (ROS) and other stress-induced conditions (Arrick and Nathan, 1984; Sies, 1999). It has been reported that intacellular level of GSH offered protective effect against apoptotic cell death and depletion of GSH was found in pre-apoptotic cells (Fernandes and Cotter, 1994; Macho *et al.*, 1997a). The experiment is based on the reaction between GSH and 5,5'-dithio-bis (2-nitrobenzoic acid or TNB) (DTNB, Ellman's reagent) to produce a yellow colored 2-nitro-5-thiobenzoic acid (TNB). The generated glutathione disulphide (GSSG) is reduced by glutathione reductase (GR) to GSH in the presence of coenzyme

nicotinamide adenine dinucleotide phosphate (NADPH). Since GR was used in this assay, total glutathione (GSH and GSSG) was measured in this assay (Figure 2.6) (Baker *et al*., 1990; Eyer and Podhradsky, 1986; Griffith, 1980).

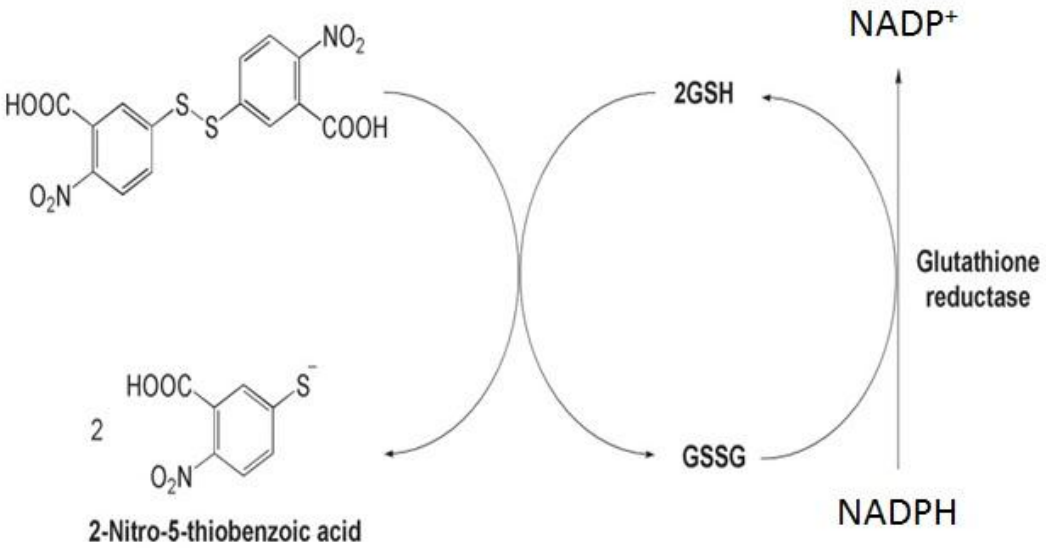

Figure 2.6 Principle of total glutathione assay.

The assay was started by seeding 1 x 10^6 of HCT116 cells in 60 mm dishes and after 24 h of incubation; the cells were harvested, collected by centrifugation (1000 rpm, 5min) and washed with ice-cold PBS. The cells were adjusted to 1 x 10^6 cells per sample. Samples were mixed with 250 µl, 5% 5-sulfosalicylic acids (SSA) and vortexed. The samples were further subjected to freeze and thaw process for 3 times and proceeded to centrifugation at 10,000 rpm, 4 ℃ for 15 min. The supernatant was collected and glutathione assay was performed in a 96-well plate. Each well consisted of GSH standards, DTNB and NADPH in phosphate buffer and the reaction was initiated by addition of glutathione reductase (GR). The final concentrations were 0.031 mg/ml DTNB, 0.038 mg/ml (48 µM) NADPH, 95 mM potassium phosphate buffer (pH 7.0), 0.95 mM EDTA, 0.115 units/ml GR and 0.24% SSA. The absorbance was read at 405 nm and measurements were taken every 1min interval for 10 min. For each sample, the rate of TNB production (change in absorbance/min) was calculated and the total GSH

concentration was determined based on a linear regression curve obtained from the GSH standard curve.

2.2.5.4 Analysis of cell cycle distribution

The HCT 116 cells were seeded in 60 mm culture dishes (1×10^6) and left for 24 h for attachment. The cells were then treated without or with desired concentration of sample and incubated for indicated time period in CO_2 incubator. The cells were harvested and rinsed with ice-cold PBS. After centrifugation at 1000 rpm for 5 min, the supernatant was removed and the cell pellets were resuspended in 100 µl of ice-cold PBS. Cells were fixed by adding dropwise into 1 ml of 70 % (v/v) ethanol (in PBS) while vortexing the cells. Cells were gently mixed to prevent clumping of cells. The fixed cells were stored at -20 ℃ for 24 h, followed by centrifugation (15000 rpm, 5 min) to discard the ethanol. Fixed cells were washed with PBS thoroughly to discard the ethanol. After washing and centrifugation, cells were resuspended in 500 µl of hypotonic staining solution containing 50 µg/ml PI, 0.1 % (w/v) sodium citrate, 0.1 % (v/v) Triton-X-100 and 100 µg/ml RNase A. After incubation for 1 h in the dark at room temperature, the cells were immediately subjected to analysis by flow cytometer at excitation 488 nm and emission 620 nm. 10,000 cells were analysed and the cell-cycle distribution was calculated by using CellQuest software.

2.2.5.5 Assessment of DNA fragmentation using TUNEL assay

During apoptosis, the DNA strands are cleaved or nicked by endonucleases, generating DNA fragments with abundance of exposed 3'-OH ends. These DNA strand breaks (DSBs) induced by apoptosis can be detected using terminal deoxynucleotidyl transferase (TdT) dUTP nick end labelling (TUNEL) assay (Darzynkiewicz *et al.*, 2008a; Darzynkiewicz *et al.*, 2006; Jiang *et al.*, 1995; Li *et al.*, 1995). A TUNEL assay

kit (Apo-BRDU, Sigma) was used for this purpose according to the manufacturer protocol. The assay relies on the incorporation of bromo-deoxyuridine triphosphate (Br-dUTP) into fragmented DNA at the 3'-OH ends, catalysed by Tdt. FITC-conjugated anti BrdU antibody then binds to the incorporated Br-dUTP residues and labelling the apoptotic cells. The principle of TUNEL assay is illustrated in Figure 2.7.

A total of 1 x 10^6 of HCT116 cells were seeded in 60 mm culture dishes and after 24 h of incubation, the attached cells were treated with 500 µg/ml of the active faction for 24 h. After designated treatment hours, cells were harvested, washed with PBS and centrifuged at 1000 rpm for 5 min. After resuspending the pellets in 500 µl of PBS, the cell suspensions were added into 5 ml of 1% (w/v) paraformaldehyde in PBS and incubated on ice for 15 min. This was followed by washing twice with PBS and the pellets were fixed in 5 ml of ice-cold 70% (v/v) ethanol at -20 ℃ for 24 h. The ethanol-fixed cells were centrifuged at 1800 rpm for 5 min to pellet the cells and the ethanol was discarded. The washed cell pellets were then incubated in 50 µl of buffer containing TdT enzyme and Br-dUTP at 37 ℃. After 60 min of incubation, the cells were then added to 400 µl of PBS and the FITC signal was detected and analysed by FACSCalibur flow cytometer using CellQuest software.

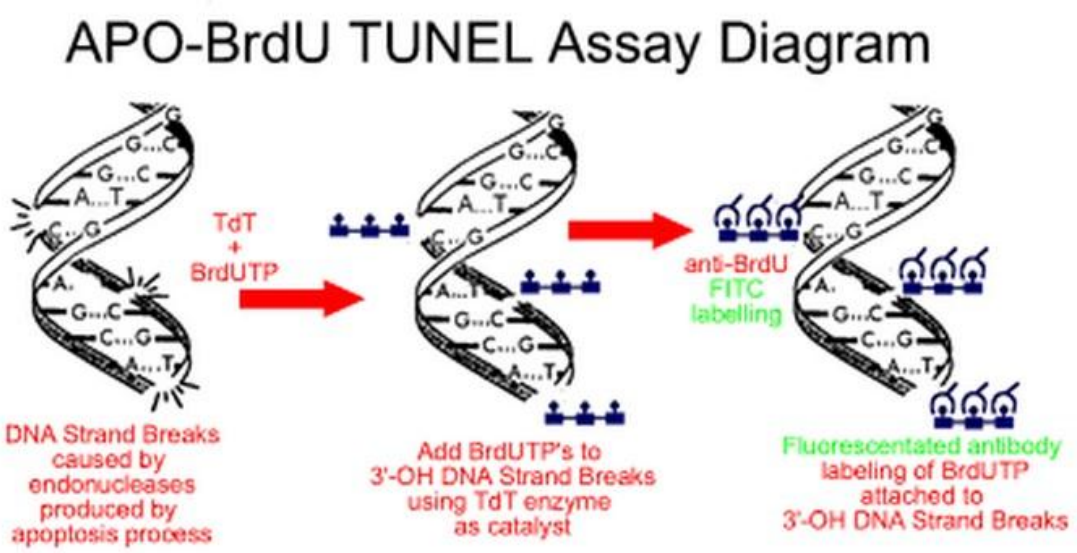

Figure 2.7 Principle of TUNEL assay.

2.2.5.6 Measurement of mitochondrial membrane potential using JC-1

Mitochondrial dysfunction during apoptotic process is often associated with loss of the mitochondrial membrane potential (Δψm), which is one of the characteristics of apoptosis (Green and Reed, 1998). This event can be monitored by using a liphophilic cationic fluorochrome, 5,5',6,6'-tetrachloro-1,1',3,3' tetraethylbenzimidazolyl-carbocyanine iodide (strans for 1st J-aggregate-forming cationic dye, JC-1) (Smiley *et al*., 1991). The JC-1 (Figure 2.8) is commonly used to detect mitochondrial depolarization that occurs during early apoptosis (Cossarizza *et al*., 1993; Reers *et al*., 1995). In healthy cells, JC-1 accumulates in the mitochondria as JC-1 aggregates (which fluoresce red) and also in the cytoplasm as JC-1 monomers (which fluorescence green). In apoptotic cells, the Δψm collapses. Consequently, JC-1 aggregates cannot accumulate within the mitochondria and dissipate into JC-1 monomers leading to loss of red fluorescence. Therefore, Δψm collapse is signified by the decrease of the red to green ratio fluorescence indicating the loss of mitochondrial membrane potential (Cossarizza *et al*., 1993; Reers *et al*., 1995).

This assay started by seeding1 x 10^6 of HCT116 cells in 60 mm dishes and treated with desired sample concentration and incubated in CO_2 incubator for indicated exposure periods. After exposure to the sample and centrifugation, the cell pellets were resuspended in JC-1 solution and further incubated at 37 ℃ in the CO_2 incubator for 15 min. Cells were then washed twice and resuspended in fresh medium. Analysis was carried out using a FACSCalibur flow cytometer and CellQuest software. 10,000 events were examined for each sample. The JC-1 aggregates (red fluorescence) were detected in the FL-2 (620 nm) channel, while the JC-1 monomers (green fluorescence) were detected in FL-1 (520 nm) channel.

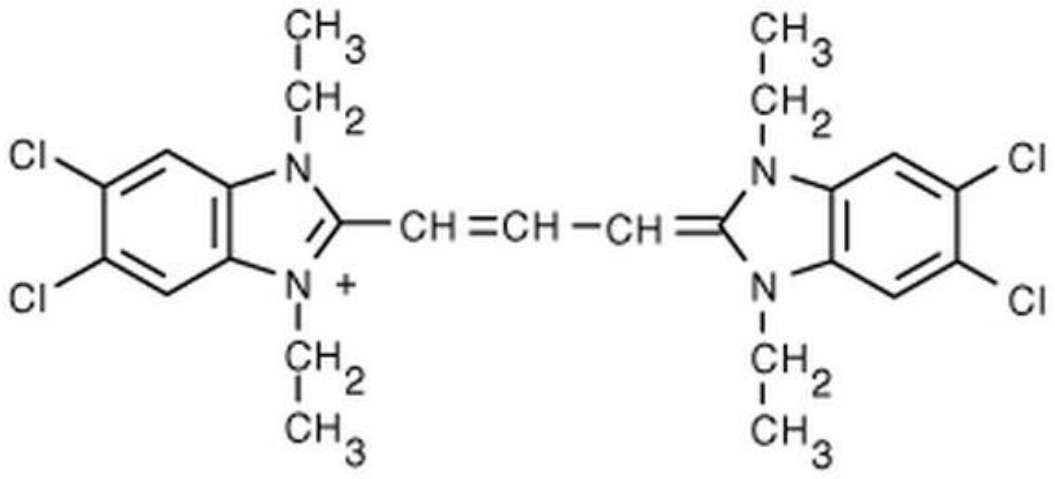

Figure 2.8 Chemical structure of JC-1 dye.

2.2.5.7 Detection of phosphatidylserine using Annexin V-FITC/ PI staining

Multiple alterations of the plasma membrane occur during apoptosis (Morris *et al*., 1984). This includes the loss of membrane asymmetry, where phosphatidylserine (PS) is externalized to the outer leaflet of the membrane (Martin *et al*., 1995). The mechanism that underlies the loss of membrane asymmetry remains unclear. Some studies suggested the involvement of downregulation of an ATP-dependent aminophospholipid translocase and upregulation of 'flippase' in this event (Bratton *et al*., 1997; Savill,

1997). Annexin V/ PI assay was performed using flow cytometry to measure the externalization of PS during early apoptosis (Koopman *et al*., 1994; Olie *et al*., 1996; Vermes *et al*., 1995). The assay relies on the fact that annexin V binds to exposed PS in early and late apoptotic cells, while PI is excluded from cells with intact and uncompromised plasma membrane such as the viable and early apoptotic cells. As a result, viable cells (with no stain), early apoptotic cells (with annexin V stain only) and late late apoptotic (with both annexin V and PI stain) or necrotic cells or deadscells (with PI only) can be discriminated by quantitatively estimate the relative amounts of the annexin V/ PI-stained cells in population.

In this assay 1 x 10^6 of HCT 116 cells were plated in 60 mm dishes and were allowed to attach to the surface. After 24 h of incubation, the cells were exposed to the bioactive fractions for different range of concentrations for indicated time periods. After treatment, both floating and attached cells were collected into 15 ml centrifuge tubes and washed with PBS. After centrifugation at 1000 rpm for 5 min, the pellets were resuspended in 1 ml of annexin V binding buffer (10 mM HEPES, 140 mM NaCl, 5mM $CaCl_2$, pH 7.4). This was followed by the transfer of 100 µl of the cell suspensions into 5 ml falcon round bottom tubes. The cells were added with 5 µl of FITC-conjugated annexin V and 10 µl of PI (50 µg/ml). The cells were gently mixed by pipetting, and incubated for 30 min in the dark at room temperature. Afer staining, 400 µl of binding buffer was added to the tubes and mixed again by gentle pipetting. The cells were then analysed by FACSCalibur flow cytometer and CellQuest software whereby 10,000 events were acquired for each analysis. After excitation at 488 nm, the green fluorescent intensity of annexin V-FITC was measured at 520 nm in the FL-1 channel while the red fluorescent intensity of PI was measured at 620 nm in FL-2 channel. The results were represented as quadrants in the bivariate PI versus annexin V-FITC fluorescence plot.

2.2.5.8 RNA isolation and real-time PCR (Q-PCR)

In this study, we applied real-time quantitative polymerase chain reaction (Q-PCR) analysis to investigate the effect of sample on gene expression of PCNA (proliferating cell nuclear antigen), Bcl-2 (B-cell CLL/ lymphoma 2) and Bax (BCL-2 associated X protein). HCT 116 cells were plated into 60 mm dishes at a density of 1 x 10^6 cells/ dish. After 24 h of incubation for attachment, exponentially growing cells were treated with samples for indicated time frames. After designated exposure times, cells were harvested and total RNA was extracted using a commercial kit, QIAamp RNA Blood Mini Kit (Qiagen).The procedures were according to manufacturer guidelines. In brief, the cells were lysed by vortexing the pellets in 600 µl of RLT buffer. The lysate was transferred directly into a QIAshredder spin column in a 2ml collection tube (provided), centrifuged and homogenized for 2 min at maximum speed. The spin column was discarded. 600 µl of 70% ethanol was added into the lysate and homogenized by gentle pipetting. The sample was carefully pipetted into a new QIAamp spin column in a 2 ml collection tube without moistening the rim. After centrifugation for 15 s at 10, 000 rpm, the flow-through was discarded. On-column DNase digestion treatment was conducted according to the kit. RW1 buffer (350 µl) was added to QIAampspin column and centrifuged for 15 s at 10,000 rpm to wash the spin column membrane. The flow through was then discarded. 80 µl of DNase (10 µl DNase plus 70 µl RDD buffer) was added on the membrane of the spin column and left for 15 min. 350 µl of buffer RW1 was added to the spin column, centrifuged and the flow through was discarded. The spin column was then transferred to a new 2 ml collection tube. The procedures were followed with washing twice with 500 µl of buffer RPE each time. Approximately 30 µl of RNase-free waster was directly added on the QIAamp membrane and centrifuged for 1 min at 10,000 rpm to elute out the RNA. The quantity and quality of the RNA was measured at 260 nm and 280 nm using Nanodrop and bioanalyzer.

The target genes (PCNA, Bax and Bcl-2) expression was assessed using one-step SYBR Green relative Q-PCR protocol performed on RotorGene 600 real-time amplification instrument. The gene expression of PCNA was normalized to GADPH (Glyceraldehyde 3- phosphate dehydrogenase) reference gene, while Bax and Bcl-2 were normalized to PBGD (porphobilinogen deaminase) reference gene. The primer sequences were based on literature (Kralovcova *et al.*, 2008; Truong *et al.*, 2007) and were shown in Table 2.1.

Real-time Q-PCR was performed in (0.2 ml flat-cap microcentrifuge tubes. For each sample, a PCR mixture was prepared using SensiMix SYBR One-Step kit. A total volume of 25 µ reaction mixture were created with the following reagents (Table 2.2). The tubes were then transferred to the Rotor-Gene 6000 (36-well rotor) and cycling conditions for real-time QPCR experiment are shown in Table 2.3. At the end of the reaction, the cycle threshold (Ct) values were determined using Rotor-Gene software and the $\Delta Ct = Ct_{\text{target gene}} - Ct_{\text{reference gene}}$. The expression of target gene in the treated cells relative to untreated cells was quantitated using the formula $2^{-\Delta\Delta CT}$ (Livak and Schmittgen, 2001), by calculating the $\Delta\Delta C_T$ ($\Delta\Delta C_T = \Delta C_{T\ \text{sample}} - \Delta C_{T\ \text{untreated}}$).

Table 2.2: The reaction mixtures of Q-PCR.

Reagents	1 reaction (total volume 25 µl)	Final concentration
Water (H_2O)	4.5 µl	-
Sensimix SYBR One-Step	12.5 µl	1x
SYBR green	0.5 µl	1x
$MgCl_2$	-	3mM
Forward primer	1 µl	200 nM
Reverse primer	1 µl	200 nM
RNase inhibitor	0.5 µl	10units
RNA	5 µl	20 ng/ml

Table 2.3 The cycling conditions for real-time Q-PCR.

Target gene	Reference gene	Denaturation	Annealing	Extension
PCNA	GAPDH	95 ℃ 45 seconds	56 ℃ 45 seconds, 30 cycles	72 ℃ 120 seconds
Bax	PBGD	95 ℃ 20 seconds	60 ℃ 40 seconds, 45 cycles	72 ℃ 10 seconds
Bcl-2	PBGD	95 ℃ 20 seconds	42 ℃ 40 seconds, 45 cycles	72 ℃ 10 seconds

2.2.5.9 Flow cytometric immunofluorescence staining of Bax and Bcl-2

The expression level of protein Bax and Bcl-2 were determined by immunofluorescence staining using flow cytometry. This method was based on Roussi et al (Roussi *et al*., 2007) with some modifications. Following the sample treatment, the cells were harvested and washed twice in PBS and the fixed and permeabilized using Cytofix/ Cytoperm^{TM} kit (BD Biosciences). The kit consisted of two solution: Cytofix/Cytoperm solution (1x) and perm/Wash buffer solution (10x). The Cyto/Perm solution was used for fixation and permeabiliztion of the cells before staining with antibody. The Perm/Wash buffer solution was used to permeabilize the cells before staining, antibodies dilution and also used as washing buffer. A total of 1x 10^6 cells were resuspended in 500 µl of fixation/ permeabilization solution and incubated for 20 min at 4 ℃. The cells were washed twice with Perm/Wash buffer and incubated for 15min in 1ml of Perm/Wash^{TM} buffer to detect Bax or Bcl-2. The fixed and permeabilized cells were incubated with 100 µl of Perm/ Wash^{TM} buffer containing antibodies. For Bcl-2 protein, the cells were stained directly for 30 min with 20 µl FITC-conjugated mouse anti-human Bcl-2 monoclonal antibody (clone 124) or IgG1 isotype control (BD Biosciences) at 4 ℃. For indirect Bax staining, the cells were incubated for 30 min with

either rabbit anti-human Bax polyclonal antibody or IgG1 isotype control (BD Biosciences) at 4℃. After washing, the cells were further incubated for 30 min with FITC-conjugated goat anti-rabbit F(ab')2 polyclonal secondary antibody (Abcam) at 4℃. The cells were then washed with Perm/WashTM buffer and analyzed using BD Accuri C6 flow cytometer.

2.2.5.10 Determination of Caspase -3/7 and -9 activities

This assay was performed using the protocol recommended by the manufacturer (Immunochemistry technologies, LLC). The HCT 116 cells were seeded in 60 mm dishes and treated with the desired concentration of samples. After the indicated treatment periods, the cells were harvested and counted using haemocytometer. The cell suspension in 290 µl (~5 x 10^5 cells per 100 µl) was suspended in a new 1.5 ml centrifuge tube, 10 µl of 30X FAM-DEVD-FMK (Caspase -3/7), FAM-LETD-FMK (Caspase -8), FAM-LEHD-FMK (Caspase -9) or FAM-AEVD-FMK (Caspase -10) solution was directly added into the cell suspension. After gentle tapping, followed by 1 hour incubation at 37℃ under 5% CO_2, the cells were washed twice by using 1X washing solution (provided) and further suspended in 400 µl of washing solution. The cells were analysed by using BD Accury C6 flow cytometer.

2.2.5.11 Protein extraction

The cells treated with sample for indicated treatment period were then harvested and appropriate amounts of Cytobuster containing protease inhibitors was added into the pellet of the cells. The mixture was then vortexed and stored for about 10 min before subjected to centrifugation at 12,000 x g for 10 min. The supernatant was transferred into a new tube and kept in -20 freezer for further processing.

2.2.5.12 Protein estimation

The protein concentration of the cell lysates was determined by using Bradford Kit (Biorad) BSA was used as the standard.

2.2.5.13 Protein array

Protein array was conducted according to the procedures recommended RayBio Human Apoptosis Antibody Array kit. After 24 hour exposure of SMEAF on HCT116, the cells were harvested and lysed using the lysis buffer (provided), priorly added with protease inhibitors. The protein content was determined as described in Materials and Methods (Section 2.2.5.12). After quantification, the working concentration of the sample protein was adjusted to 500 µg/ml. 100 ul of blocking buffer was added into each well of pre-assembled array and incubated at room temperature for 30 min. Then, the blocking buffer was discarded and 100 µl of each sample was added to the array wells. The arrays containing the sample were incubated overnight at 4 ℃.

After the incubation period, the samples were removed and washed 5 times with 150 µl of wash buffer I at room temperature with gentle shaking. The slides was then washed 2 times by using 150 µl of wash buffer II. Biotin-conjugated antibodies (70 µl) were added to each corresponding well and subjected to 2 hours incubation at room temperature. The wells were further washed 5 times and 2 times by using wash buffer I and wash buffer II, respectively. After the washing steps, 70 µl of HiLyte Plus-conjugated streptavidin was added into each well and incubated in the dark room for 2 hours. Finally, the array was washed twice using wash buffer I.

The array was disassembled from its incubation chamber and placed in a 50 ml centrifuge tube, followed by the addition of 45 ml of washing buffer I and gently shaken

for 10 min at room temperature. Washing buffer I was decanted and replaced with wash buffer II for 10 min incubation. After removal of wash buffer II the slide was rinsed using distilled water. The slides were centrifuged at 1,000 rpm for 3 min to remove any water droplets remaining on the slides. Images were captured using laser scanner Axon GenePi using cy3 channel and analysed by GenePixPro 6.1 software.

2.2.5.14 PCR array analysis

The RNA of HCT116 cells that treated with 0.05 mg/ml of SMEAF for 12 h was lysed and performed on PCR Array Kit (PAH-033, Human Cancer PathwayFinder PCR Array, Qiagen) and data analysis according to protocol provided.

2.2.6 Isolation and purification of chemicals

There are hundreds or even thousands of chemical compounds as a mixture in plant extracts (Hamburger and Hostettmann, 1991). In order to discover the bioactive compounds from *S. macrophylla*, a bioassay-guided isolation was employed, which is considered the most efficient method of searching for active plant-derived anticancer agents (Pezzuto, 1997). In this study, MTT cell viability assay was used to guide the isolation process and was performed as described in Section 2.2.4.1 The fractions and sub-fractions obtained from each separation step were tested at the final concentration of 6.25-200 µg/ml. In addition to the bioassay-guided procedures, further steps were taken to purify other chemicals constituents for characterization.

2.2.6.1 Analysis by Thin Layer Chromatography (TLC)

Thin layer chromatography (TLC) was normally used to detect and separate compounds. In this study, it was used to determine the suitable solvent system for the isolation of chemical compounds from the bioactive fraction. Silica gel 60 F_{254} TLC plates (plastic)

from Merck were chosen for TLC analysis. Generally, the soluble sample was spotted about 1.0 cm from the bottom of the TLC plate by using a fine capillary tube and allowed to dry. The TLC plate is then placed into a TLC developing tank filled with premixed solvent system. When the TLC plate was fully developed to the solvent front the plate was removed from the developing tank. The TLC plate was dried by using air blower and was viewed under both short (254 nm) and long (365 nm) ultra violet (UV) visible light. The TLC plate was then placed into an iodine vapour chamber to stain the separated chemical compounds.

2.2.6.2 Fractionation of Ethyl Acetate Fraction

The ethyl acetate fraction was subjected to column chromatography by using a glass column (60cm L X 6cm I.D.) and packed with stationary phase as Merk kieselgel 60 (0.063-0.200 mm). Briefly, the silica gel was made into slurry with solvent before it was packed into the column and was allowed to equilibrate for at least an hour before use. The fraction was then introduced on top of the silica surface. The column was generally eluted with combinations of different solvents; with stepwise increase in the solvent polarities until flushed with methanol. Fractions were monitored by TLC and appropriate fractions were combined, dried and stored at -20 ℃ until further investigations.

2.2.6.3 HPLC Analysis

Purification of the compounds was performed by using Shimadzu HPLC system equipped with diode array detector (DAD) on a Chromolith reversed phase C18 HPLC column (100.0 x 10.0 mm). The mobile phase used for analysis was water (A) and HPLC grade methanol (B) with flow rate of 4.7 ml/min. Each sample (50 µl) was injected into HPLC column and their separation was detected at the wavelengths of 214

and 254 nm. The mobile phase of each collected fraction was evaporated with rotary evaporator, weighed and analyse with TLC. Fractions that contained pure compound were then analysed with GC-MS and NMR to determine their chemical structures and molecular weight.

2.2.6.4 Structural elucidation

2.2.6.4.1 NMR analysis

For structural elucidation purposes, isolated compounds were subjected to Nuclear magnetic resonance (NMR) spectroscopy analysis at Chemistry Department, Faculty of Science, University of Malaya, Malaysia. The compounds were dissolved in deuterated chloroform ($CDCl_3$) solvent and subjected to proton (^1H), Carbon-13(^{13}C), distortionless enhancement by polarization transfer (DEPT), heteronuclear multiple-bond correlation spectroscopy (HMBC) and heteronuclear single quantum coherence spectroscopy (HSQC), NMR analysis. The NMR spectra were recorded on a JOEL 400 MHz spectrometer. The internal reference standard used was tetramethylsilane (TMS).

2.2.6.5 GC-MS Analysis

GC-MS analysis was performed using Agilent Technologies 6980N equiped with 5979 Mass Selective Detector, HP-5MS (5% phenyl methyl siloxane) capillary column of dimensions 30.0m x 250μm x 0.25 μm and used helium as carrier gas at 1 ml min^{-1}. The column temperature was programmed with the desired condition after several tries. MS was operating at 70 eV. The constituents were identified by comparison of their mass spectral data with those from NIST 05 Spectral Library. Only mass spectral fragmentation pattern that gave greater than 90% match were accepted particularly applicable for SMHF analysis. GCMS analysis provides the molecular weight (MW) data for confirmation of isolated compounds.

2.2.7 Chemical modification of Swietenine

The purified compound swietenine was subjected to acylation process as a solution to the solubility problem. A solution of swietenine (81mg, 0.55 mmol) was stirred, cooled (0–5 ◦C)in dry DMF (20 ml), sodium hydride (45 mg, mmol) and acetic anhydride (0.2938ml, mmol) was added into the reaction flask. The ice bath was then removed and the mixture was allowed to stir overnight at room temperature. Saturated ammonium chloride was added to the reaction mixture followed by extraction with ethyl acetate. The combined ethyl acetate extracts were then washed with distilled water to remove DMF. The solution was then filtered and dried over anhydrous sodium sulfate. The crude product obtained after evaporation under reduced pressure, was purified by column chromatography to yield the purified product in yellowish solid form.

The structure elucidation of the modified compound was further subjected to NMR analysis as described in earlier section. The compound isolated was further subjected to additional correlation spectroscopy (COSY) and nucler overhauser effect spectroscopy (NOESY) NMR analysis. LC-MS/MS analysis was performed as well to obtain high resolution mass spectrometry (HRMS) data.

2.2.8 Evaluation of the cytotoxic effect of swietenine derivative

2.2.8.1 MTT cell viability assay

The MTT cell viability assay was carried out as described in section 2.2.4.1. The pure compounds was tested at different final concentration for 72 h incubation period.

2.2.9 Evaluation of apoptotic effect of swietenine derivative

After MTT assay, the swietenine derivative was further subjected to the bioassays as described earlier. The final concentration of the modified compound was 50 μM and subjected to different exposure times in HCT116.

2.2.9.1 Hoechst-propidium iodide staining and morphological observation

The analysis was performed as described in section 2.2.5.1 except that the cells were treated with 50 μM of the modified compound for 48.

2.2.9.2 Determination of intracellular reactive oxygen species (ROS)

The analysis was performed as described in section 2.2.5.2 except that the cells were treated with 50 μM of the modified compound.

2.2.9.3 Measurement of intracellular total glutathione (GSH) content

The analysis was performed as described in section 2.2.5.3 except that the cells were treated with 50 μM of modified compound for 24-72 h.

2.2.9.4 Analysis of cell cycle distribution

The analysis was performed as described in section 2.2.5.4 except that the cells were treated with 50 μM of modified compound for 24-72 h.

2.2.9.5 Measurement of mitochondrial membrane potential using JC-1

The analysis was performed as described in section 2.2.5.6 except that the cells were treated with 50 μM of modified compound for 24-72 h.

2.2.9.6 Detection of phosphatidylserine using Annexin V-FITC/ PI staining

The analysis was performed as described in section 2.2.5.7 except that the cells were treated with 50 µM of modified compound for 24-72 h.

2.2.9.7 RNA isolation and real-time PCR (Q-PCR)

The analysis was performed as described in section 2.2.5.8 except that the cells were treated with 50 µM of modified compound for 6-24 h.

2.2.9.8 Flow cytometric immunofluorescence staining of Bax and Bcl-2

The analysis was performed as described in section 2.2.5.9 except that the cells were treated with 50 µM of modified compound.

2.2.9.9 Determination of Caspase -3/7, -8, -9 and -10 activities

The analysis was performed as described in section 2.2.5.10 except that the cells were treated with 50 µM of modified compound for 3-24 h.

2.2.9.10 PCR array analysis

The analysis was performed as described in section 2.2.5.14 except that the cells were treated with 50 µM of modified compound for 24 h.

2.2.9.11 Sodium dodecyl sulphate polyacrylamide gel electrophoresis

The extracted crude protein was checked on 10% (w/v) polyacrylamide gel using tri-glycin buffer containing 0.025 M tris and 0.192 M glycin, pH 8.3. Following solutions were used to prepare both stacking and resolving gels.

Solution A:

29.2% (w/v) Acrylamide and 0.8% (w/v) N,N'- methylenebisacrylamide

Solution B:

1.5 M Tris-HCl buffer, pH 8.8 and 0.4 % (w/v) SDS

Solution C:

10% (w/v) Ammonium persulfate

Solution D:

0.5 M Tris-HCl buffer, pH 8.8, 0.4% SDS (w/v)

Sample buffer:

62 mM Tris-HCl buffer, pH 6.8 containing 2.3% (w/v) SDS, 5% mercaptoethanol, 10% (v/v) glycerol and 0.01% (w/v) bromophenol blue.

Electrophoresis buffer:

Tris-glycin bufeer containing 0.025 M tris, 0.1% SDS and 0.192 M glycin, pH 8.3

Fixing solution:

40% (v/v) Methanol and 10% (v/v) acetic acid in water

Staining solution:

0.2% (w/v) Coomassie brilliant blue R-250 in fixing solution

Destaining solution:

7% (v/v) Acetic acid and 5% (v/v) methanol in water.

Resolving gel was prepared by sequential mixing of 6.0 ml of solution A, 6.0 ml of solution B, 6.0 ml of water, 0.1 ml of solution C and 10 µl of TEMED. This solution was poured gently into the space between the glass plates assembled in the gel casting unit up to $3/4^{th}$ of their height. Subsequently, a layer of water was added on top of the resolving gel solution and the gel was allowed to polymerize at room temperature for 40 minutes. Meanwhile, stacking gel was prepared by mixing 1.4 ml of solution A, 2.5 ml

of solution D, 6.1 ml of water, 0.2 ml of solution C and 10 µl of TEMED. After polymerization of the resolving gel, water layer from its top was removed with the help of filter paper strips. Then stacking gel solution was poured gently at the top of the resolving gel up to a height of 2.0 cm with the help of a micropipette. A comb was inserted into it and left for 1 hour at room temperature for polymerization. After 1 hour, the comb was removed from the stacking gel and the newly-formed wells were rinsed three times with electrophoresis buffer. The glass plates with the polymerized gel were then fitted into the electrophoresis apparatus half-filled with the electrophoresis buffer. About 50 µg of crude protein dissolved in 50 µl of the sample buffer and 20 µl (10 µg) of each preparation was loaded into different wells. The remaining space of each well and the tank was filled with the electrophoresis buffer followed by covering of the tank with the lid containing electrode. The whole apparatus was connected to a power supply and a current of 60 V (6 V per well) was passed initially till all the protein bands had entered into the resolving gel. The voltage was increased to 120 V (12 V per well) and electrophoresis was continued for 1.5 hours till dye front reached near the bottom of the gel. Upon completion of the electrophoresis, the current was stopped; gel was gently removed from the glass plates and placed in the fixing solution overnight. It was stained with the staining solution for 2 hours and destained repeatedly with the destaining solution until the background was clear.

2.2.9.12 LCMS protein analysis

Protein samples were trysin digested and peptide extracted. Peptides were analysed by electrospray ionization mass spectrometry using the Ultimate 3000 nano HPLC system [Dionex] coupled to a 4000 Q TRAP mass spectrometer [Applied Biosystems]. Tryptic peptides were loaded onto C18 PepMap100, 3µm [LC Packings] and separated with a linear gradient of water/acetonitrile/0.1% formic acid (v/v). Spectra were analysed to

identify proteins using Mascot sequence matching software [Matrix Science] with taxonomy set to Homo sapiens (human).

2.2.9.13 Protein array analysis

The analysis was performed as described in section 2.2.5.13 except that the cells were treated with 50 μM of compound for 6-24 h.

2.2.10 Statistical analysis

All values are expressed as mean ± standard deviation (S.D.) or means ± standard error (S.E.) of three independent experiments. Statistical analyst were performed by Student's *t*-test to compare the difference between untreated and treated group and considered significant when $p < 0.05$.

CHAPTER 3

RESULTS

3.1 Biological evaluation of extract and fractions of *S. macrophylla*

The extraction and fractionation of *S. macrophylla* yielded crude ethanolic extract (SMCE) and different polarity fractions, namely hexane (SMHF), ethyl acetate fraction (SMEAF) and water fraction (SMWF). All of the extract and fractions were subjected to cytotoxic screening to determine their cytotoxic effects on different cancer cell lines.

3.1.1 MTT cell viability assay of extract and fractions of *S. macrophylla*

The crude ethanol extract of *Swietenia macrophylla* demonstrated cytotoxic effect when screened against KB, CasKi, HCT 116, Hep G2 and MCF-7 cancer cell lines, especially HCT 116 cells (IC_{50} = 48.273 ± 1.649 µg/ml). Thus, the crude extract was further fractionated to yield hexane, ethyl acetate and aqueous fractions for further screening.

Results are shown in Figure 3.1 (A-E) where the effect of cytotoxicity screening of the ethanol extract and fractions against five different human cancer cell lines (HCT 116, Ca Ski, KB, MCF-7 and Hep G2) with increasing extract concentrations in the range of 10 to 200 µg/ml. The IC_{50} values of *S. macrophylla* against KB, CasKi, HCT 116, Hep G2 and MCF-7 cancer cell lines are shown in Table 3.1. Among the five cancer cell lines, *S. macrophylla* ethyl acetate fraction (SMEAF) showed selective cytotoxic effect against HCT116 cells with lowest IC_{50} value recorded among all cell lines which is 35.35 µg/ml at 72 h of incubation period. The effect of SMEAF on cell viability was further evaluated at 24 and 48 h by determining the percentage of MTT reduction upon incubation of HCT116 cells and the results are shown in Figure 3.1 (F). The values of IC_{50} decreased from 156.30 ± 10.25, 64.05 ± 7.45 to 35.35 ± 0.50 µg/ml after incubation for 24, 48 and 72 h, respectively. Results showed that ethyl acetate fraction significantly reduced the cell viability in time- and dose-dependent manner.

In order to evaluate whether the SMEAF would causing any toxic effect on human normal cell line, MRC-5 cells were utilized for the experiment. A 72 h exposure of SMEAF with concentrations 6.25-200 µg/ml on MRC-5 was performed. The results showing the SMEAF was less cytotoxic to the normal cells, as revealed by the relative higher IC_{50} value on MRC-5 cell line screening (187.82 ± 3.42 µg/ml). By dividing the IC_{50} value of MRC-5 cell line with the IC_{50} value of HCT116 cell line we obtained the selective index (SI) value of SMEAF (Wong *et al.*, 2011). SMEAF was about 5 times more cytotoxic to HCT116 cells compared to MRC-5, indicated the specificity and a higher potency of inhibition effect on cancer cell line.

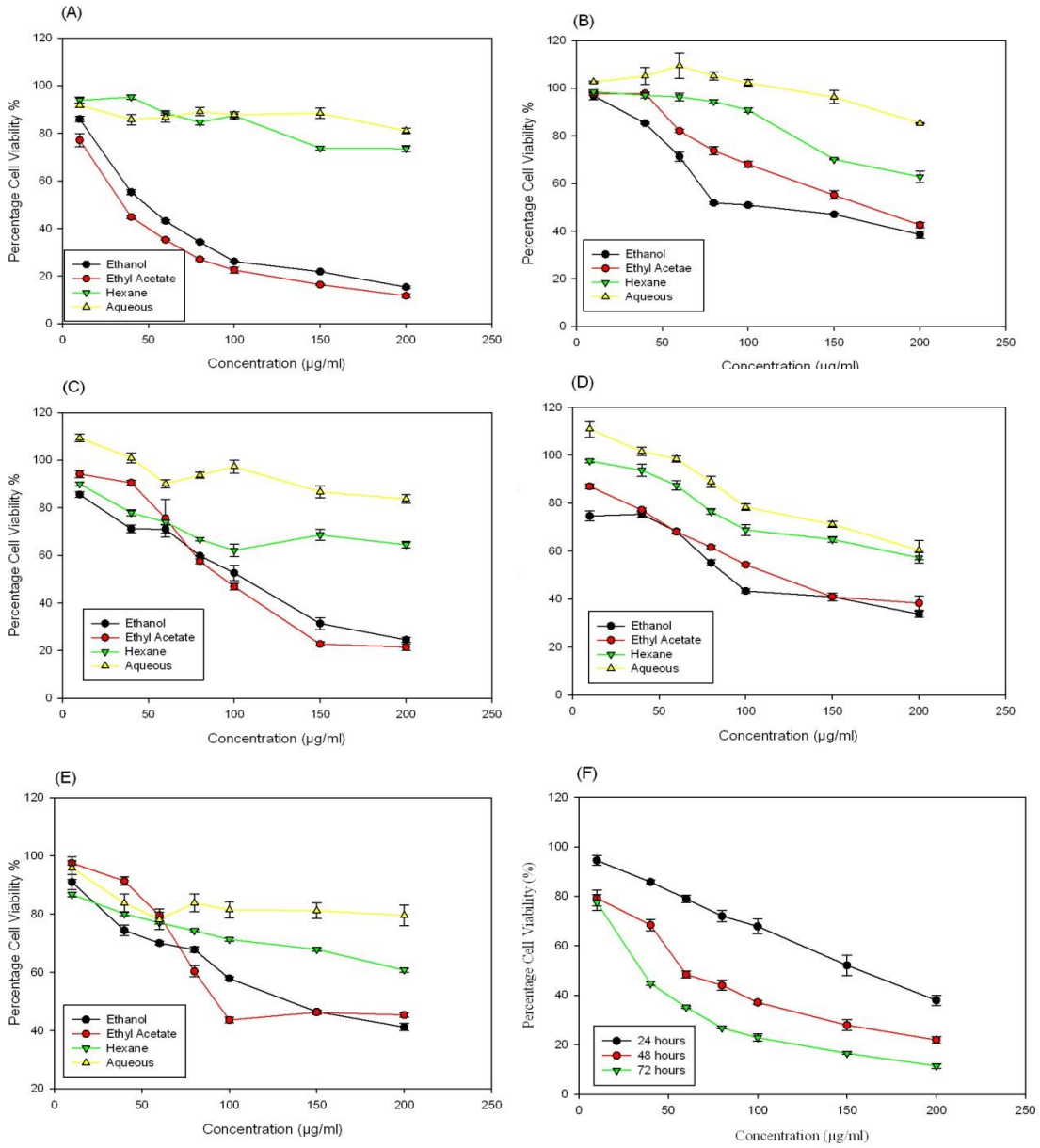

Figure 3.1 The cytotoxicity effect of *S. macrophylla* ethanol extract and fractions against various cancer cell lines at 72h incubation time. The measurements were taken using MTT cell viability assay. The graphs in 16(A) – 16(E) represent the cytotoxicity effects against HCT 116, Ca Ski, KB, MCF-7 and Hep G2, respectively. Graph 16(F) represents the cytotoxic effect of *S. macrophylla* ethyl acetate fraction on HCT116 at 24h, 48h and 72h of incubation period. The data represent mean ± S.E. of three independent experiments (n=9).

Table 3.1: IC_{50}values (μg/ml) of extract and fractions from *S.macrophylla* seeds against different cell lines, calculated after 72 h exposure.

Cell Lines	IC_{50}(μg/ml)			
	Ethanol	Hexane	Ethyl acetate	Aqueous
MCF-7	88.43 ± 1.17	>200	116.43 ± 3.18	>200
KB	106.72 ± 6.9	>200	94.29 ± 2.18	>200
HepG2	135.49 ± 4.01	>200	92.52 ± 0.53	>200
CasKi	115.89 ± 4.51	>200	170.08 ± 6.96	>200
HCT116	48.27 ± 1.65	>200	35.35 ± 0.50	>200
MRC-5	N.A.	N.A.	187.82 ± 3.42	N.A.

The data represent mean ± S.E. of three independent experiments (n=9).

3.1.2 Trypan blue exclusion (TBE) assay

The SMEAF was added to the cells as described above and its anti-proliferative effect was determined by using trypan blue exclusion assay. The 24 hour exposure of HCT116 cells to various concentrations of SMEAF resulted in a marked increase in percentage inhibition of proliferation. The results are shown in Figure 3.2 A and B. This was evident when the degree of inhibition of proliferation was reduced with increasing concentrations of SMEAF. This provided evidences that SMEAF possessed dose-dependent growth inhibitory effect on HCT116 cells.

[A] [B]

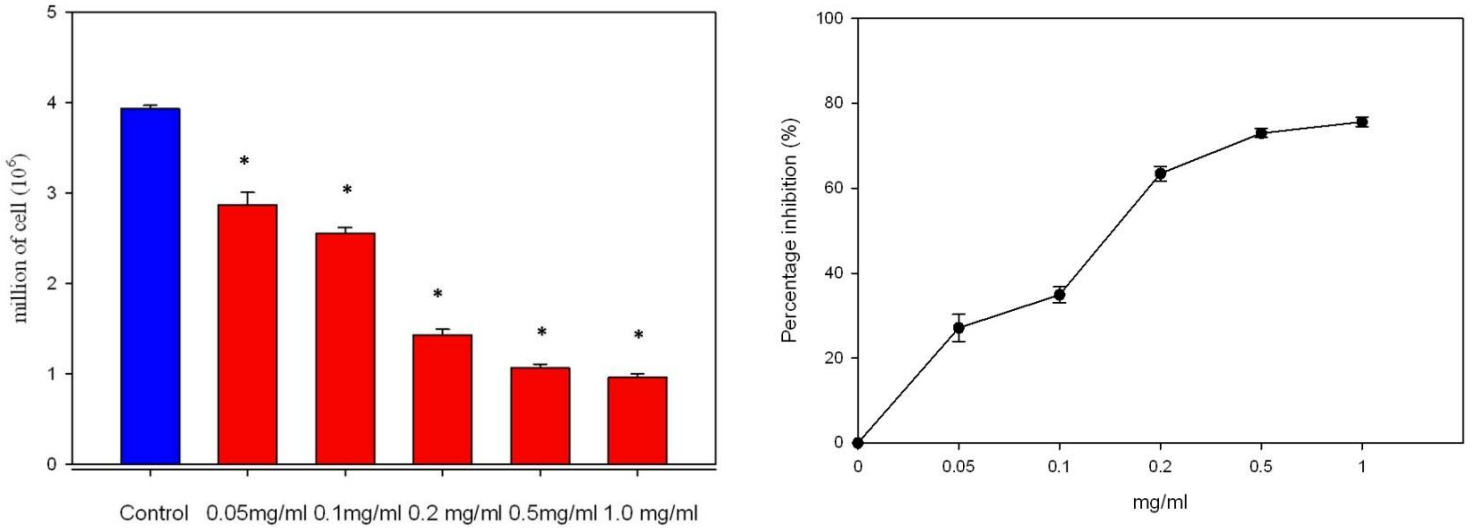

Figure 3.2 [A] Effect of SMEAF on the viable cell count at different concentration of SMEAF treated HCT116 cells. [B] Percentage inhibition (%) on HCT116 cells after treatment with different concentration of SMEAF. Cells were treated without or with different concentration (0.05-1.0 mg/ml) of SMEAF for 24h. The numbers of viable cells were counted using a hemocytometer as described in TBE assay in the methods. Each bar represents means ± S.E. from three experiments. Asterisks indicate a significant difference between untreated and treated cells (*P < 0.05).

3.2 Evaluation of apoptotic effect of SMEAF on HCT116 cells

3.2.1 Morphological study

A single dose of 0.05 mg/ml of SMEAF on HCT116 was evaluated at different time periods of 6, 12, 24, 48 and 72h. The nuclear changes of the cells exposed to SMEAF appeared to be shrunk with condensed chromatin which can be detected as early as 6h and 12h of SMEAF treatment which provide the morphological hallmark of apoptotic nuclei. Besides, the prolonged period of SMEAF exposed HCT116 cells tend to have higher number of the detached cells and membrane blebbing are clearly seen.

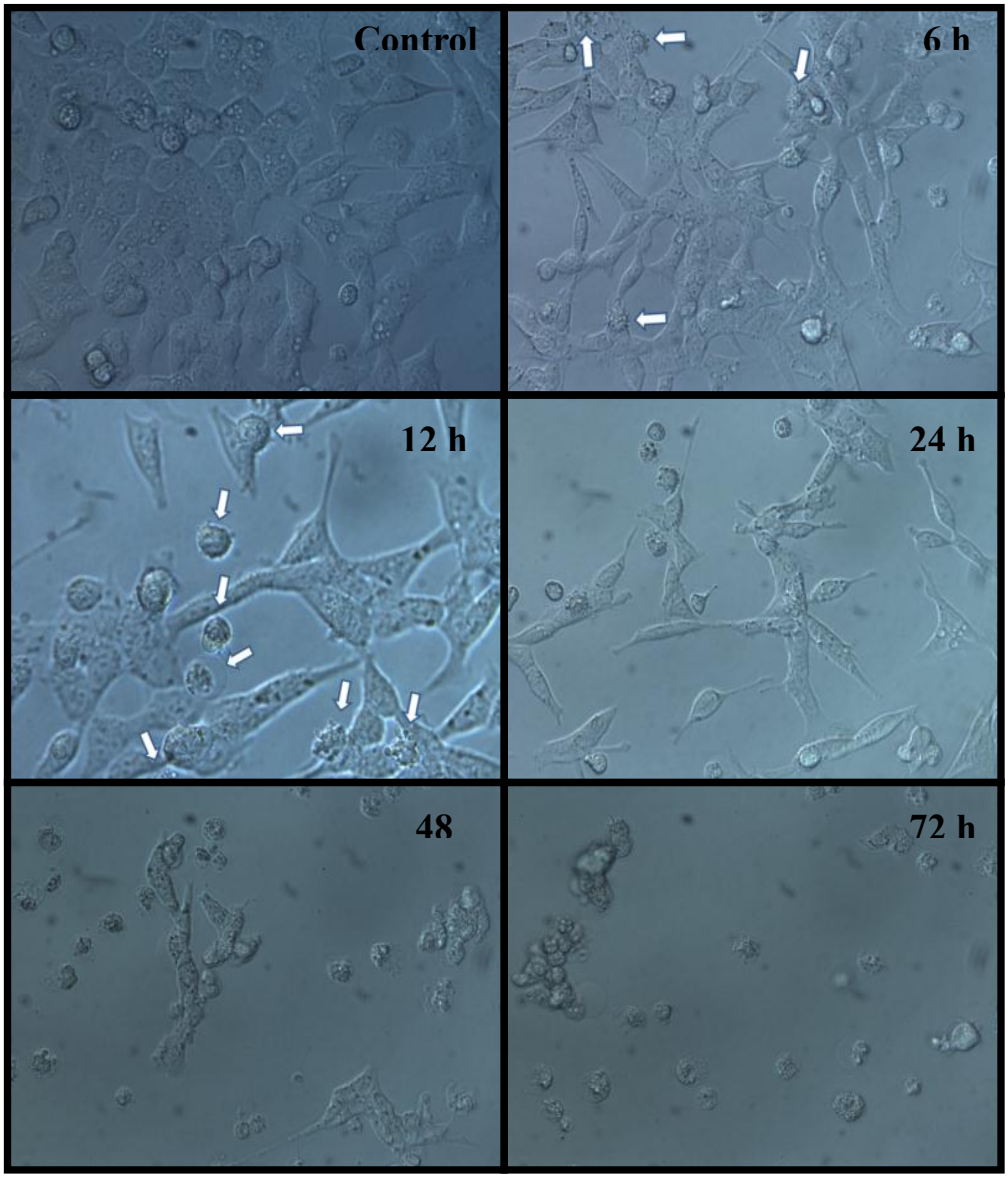

Figure 3.3 Effect of SMEAF on the morphological changes of HCT116 cells.

3.2.2 Hoechst-propidium iodide staining

To gain further insight on the effect of SMEAF on nuclear and membrane alteration, treated cells were stained with Hoechst-propidium iodide stains. As showed in Figure 3.4, the cells underwent remarkable nuclear changes upon treatment. In the control untreated cells, the cells were uniformly stained with blue fluorescence Hoechst stain and not stained with red-fluorescence propidium iodide indicating the nuclei of cells and membrane of the cells were intact. However, after exposed to SMEAF, there was an increase of intensity captured on blue and red fluorescence signals where the cells manifested two apoptotic morphological changes, namely nuclear condensation and also alteration of cell membrane integrity.

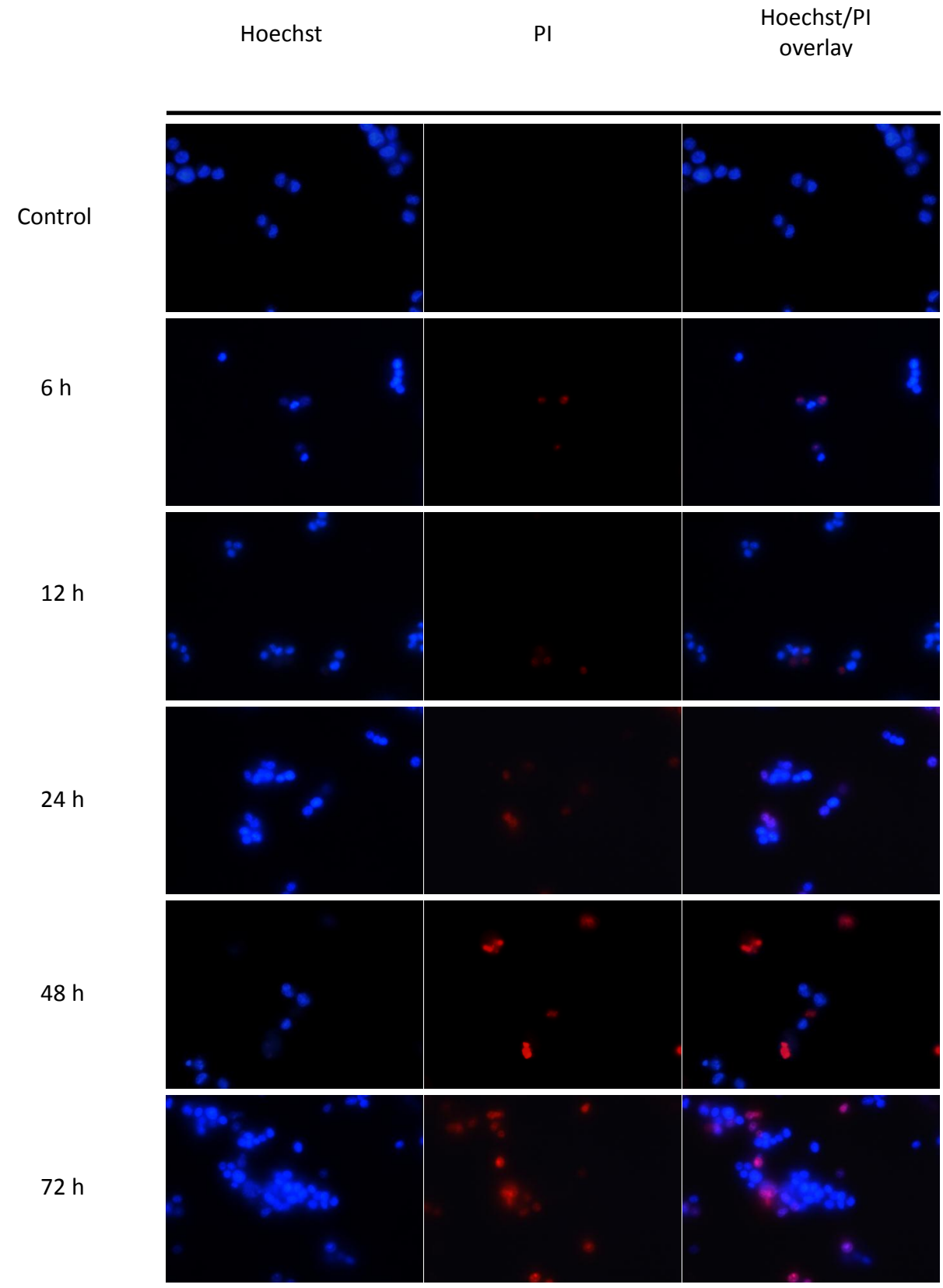

Figure 3.4 Effect of SMEAF on HCT116 cells. Cells were incubated without or with 0.05 mg/ml of SMEAF for different times and the cells were harvested and stained with Hoechst and Propidium iodide and visualized by fluorescence microscope.

3.2.3 Reactive Oxygen Species (ROS) production is one of the mediators of SMEAF-induced apoptosis.

Endogenous and exogenous agents may cause formation of ROS such as hydrogen peroxide, hydroxyl radical, singlet oxygen peroxyl radical and superoxide anion inside the cells (Halliwell and Gutteridge, 1989). Elevation in the intracellular ROS levels was able to induce apoptosis in cells (Lu *et al*., 2011). The sensitive probe DCFH-DA was utilized to determine whether the ROS were involved in apoptotic inducing effects of SMEAF treated HCT116 cancer cells. Intracellular ROS levels increased (a shift of the histogram to right hand side) after SMEAF treatment for 4h (Figure 3.5). Further analysis revealed the SMEAF caused up to 259 ± 2.7 fold ROS level increase in treated cancer cells compared to control cells. The data suggested that the SMEAF exposed cells generated an increase intracellular ROS level which is a sign of cells undergoing oxidative stress.

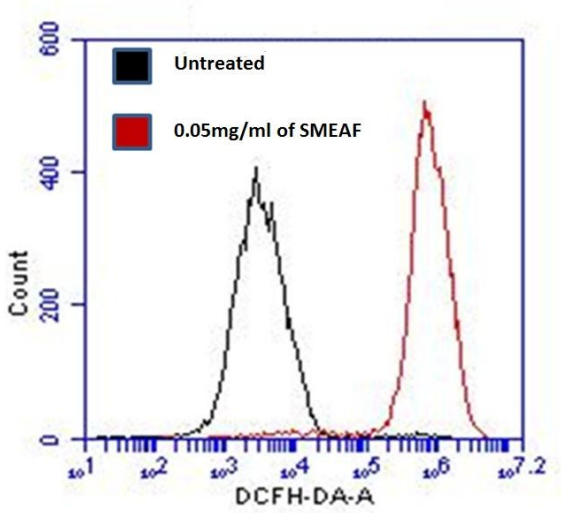

Figure 3.5 Effect of SMEAF on intracellular ROS level in HCT116 cells. After treatment with 0.05mg/ml of SMEAF for 4 h, the cells were harvested and intracellular levels of ROS were determined as described in methods. Representative overlay of histrograms showing ROS-associated fluorescence intensity.

3.2.4 Externalization of Phosphatidylserine

Apoptosis is an active form of programmed cell death with several biochemical features (Jacobson *et al*., 1997; Nagata, 1997) and membrane-bound apoptotic bodies (Kidd, 1998). Transverse redistribution of plasma membrane phosphatidylserine (PS) occurs during early apoptosis; thus, the annexin V binding assay was performed to detect the surface exposure of PS. Figure 3.6 [A] shows the FACS histograms with dual parameters including V-FITC and PI for different concentration of treatment (24h); Figure 3.6 [B] shows different hours of incubation period of 24, 48 and 72h for 0.05mg/ml of ethyl acetate fraction.

The dual parametric dot plots combining annexin V-FITC and PI fluorescence showed the viable cell population in the lower left quadrant (annexin V-negative/PI-negative), the early apoptotic cells in the lower right quadrant (annexin V-positive/PI-negative), and the late apoptotic cells in the upper right quadrant (annexin V-positive/ PI-positive). In untreated HCT116 cells, 3.23% of the cells were in the early apoptotic cells while 6.20% were late apoptotic cells. The early and late apoptotic cells increased to 4.95% and 18.96%, respectively, after being treated with 1.0mg/ml of ethyl acetate fraction 24h. Figure 3.6 (B) shows significant increase in the percentage of late apoptotic and dead cells throughout the increasing incubation period, with decreasing percentage of early apoptotic cells.

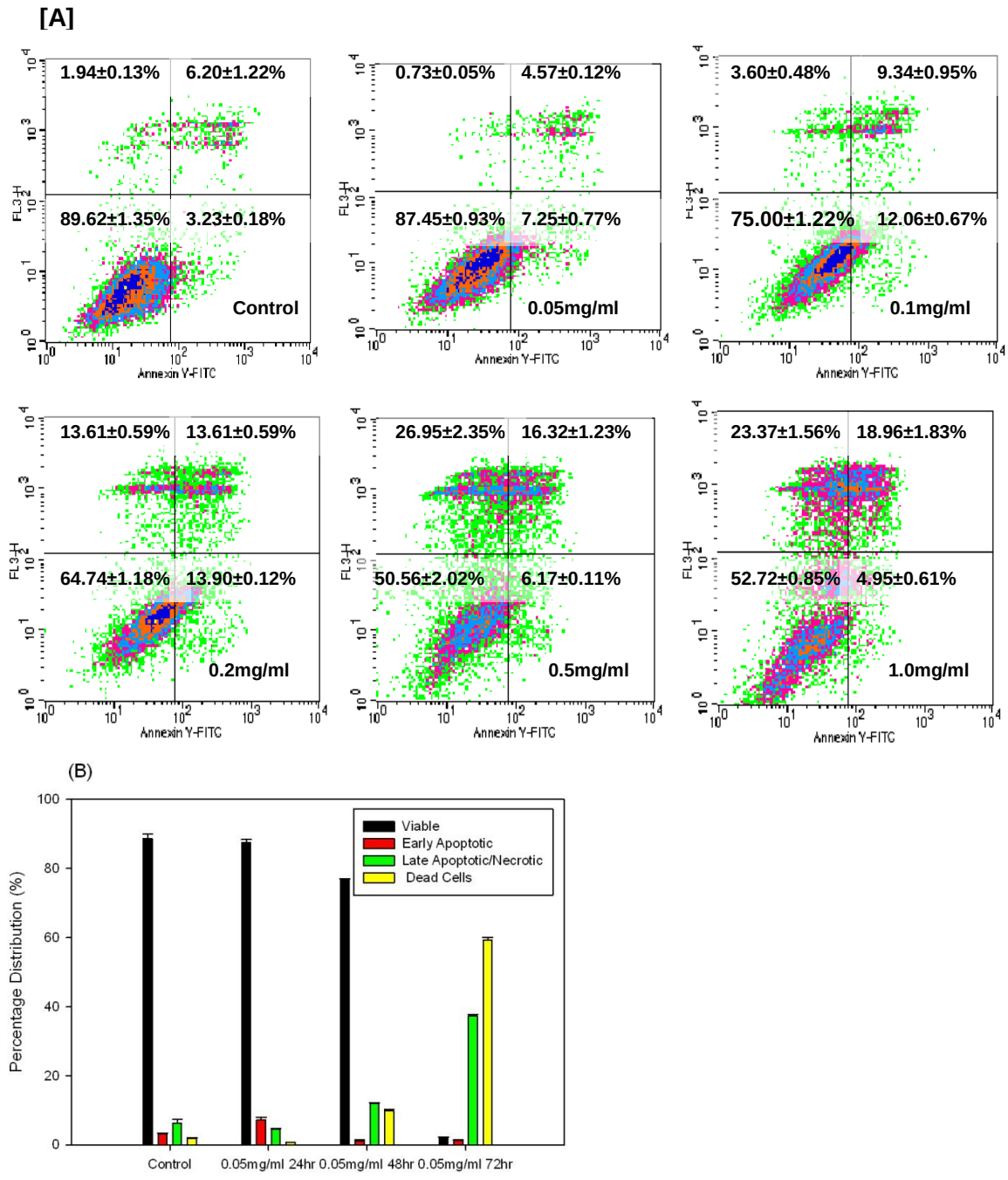

Figure 3.6 Effect of *S. macrophylla* ethyl acetate fraction on the induction of phosphatidylserine externalization and cell membrane integrity in HCT116 cells undergoing apoptosis, measured using flow cytometry analysis. Histogram in [A] shows induction with dual parameters including V-FITC and PI for different concentrations of treatment at 24h; Histogram in [B] shows induction at different incubation periods of 24, 48 and 72h for 0.05mg/ml of ethyl acetate fraction. The data represent mean±S.D. of three replicates. (n=3).

3.2.5 Induction of DNA fragmentation detected by TUNEL assay

The induction of apoptosis was further studied and quantified by performing Terminal deoxynucleotidyl transferase-mediated d-UTP Nick End Labelling, utilizing APO-BRDU kit. DNA breakage that occurred during late apoptosis was observed in Figure 3.7 after treatment of ethyl acetate fraction. The apoptotic index was 0.12% in control cells, and it increased to 0.39%, 0.85%, 2.33%, 3.71% and 12.90% in cells treated with increasing concentrations ranging of *S. macrophylla* ethyl acetate fraction from 0.05mg/ml to 1.0mg/ml.

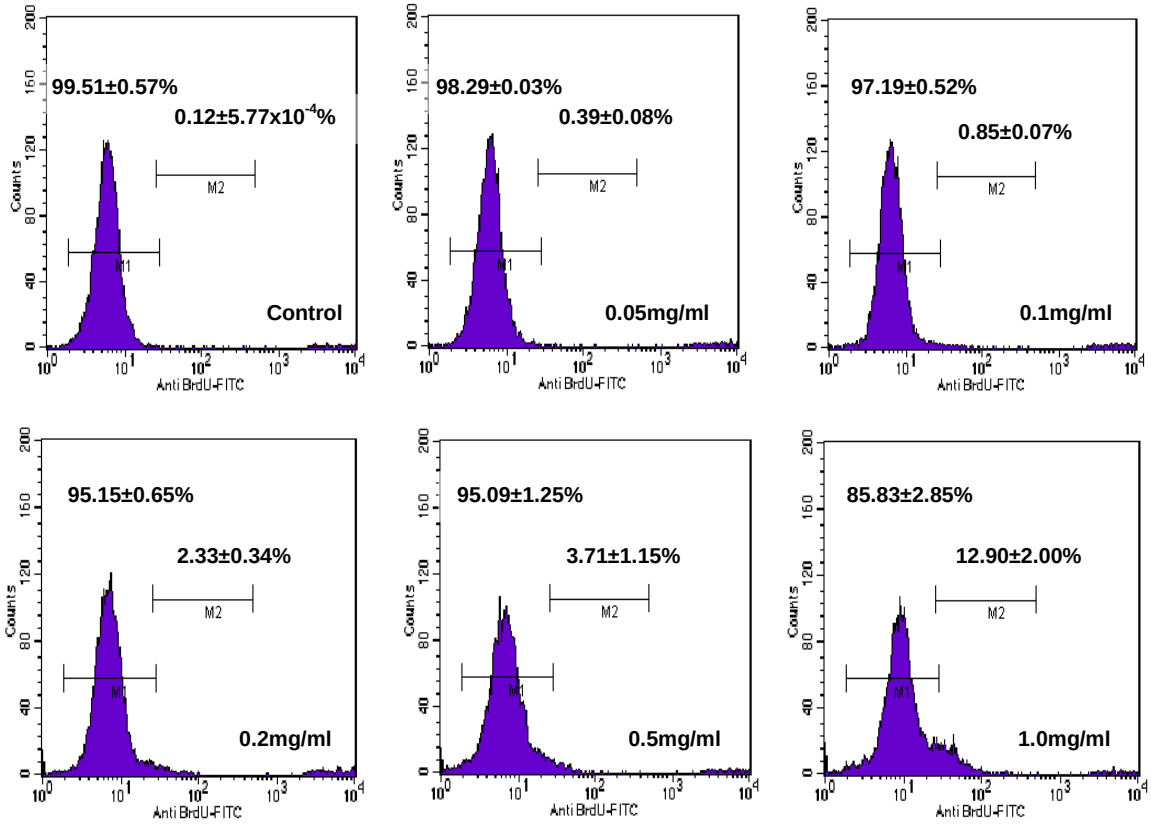

Figure 3.7 Effect of *S.macrophylla* ethyl acetate fraction on DNA fragmentation of HCT116 cells, measured by TUNEL assay using flow cytometry analysis, at increasing concentrations ranging from 0.05mg/ml to 1mg/ml, 24h following treatment. The data represent mean ± S.D. of three replicates (n=3).

3.2.6 Alteration of intracellular total glutathione (GSH) level

Impairment of mitochondrial function may lead to a decrease in cytosolic glutathione, as GSH synthesis required ATP and deficiency of energy supplied by mitochondria is likely to affect cellular turnover of GSH (Mithöfer *et al*., 1992). Eventually, changes in the level of glutathione in cells might eventually lead to apoptosis (Ratan *et al*., 1994). The results showed a significant dose-dependency in the drop of GSH level corresponding to the increase in ethyl acetate fraction concentrations (Figure 3.8). The lowest GSH level was established at 9.56±0.50nmoles when treated with 1.0mg/ml of ethyl acetate fraction.

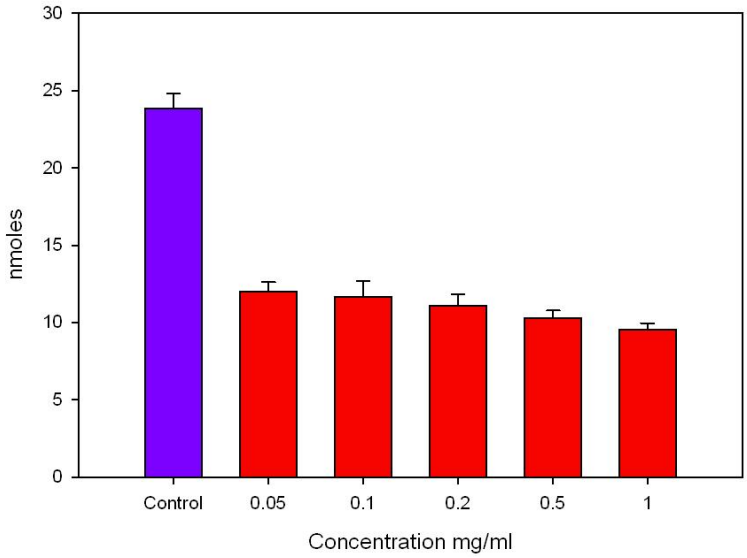

Figure 3.8 Effect of *S.macrophylla* ethyl acetate fraction on intracellular total glutathione level of HCT116 cells at 24 hours following treatment. The data represent mean ± S.E. of three independent experiments (n=9).

3.2.7 Disruption of mitochondrial membrane potential (ΔΨm)

Mitochondria play an important role in the apoptotic cascade by serving as a convergent center of apoptotic signals originating from both the extrinsic and intrinsic pathways (Kim *et al*., 2006). Depletion of ΔΨm caused the opening of the mitochondria permeability transition pore, eventually leading to apoptosis (Narita *et al*., 1998). The changes in mitochondrial membrane potential in HCT116 cell line with ethyl acetate fraction were measured by JC-1 dye. Results in Figure 3.9 showed that most of the JC-1 fluorescence in the upper right quadrant of control untreated cells moved to the lower right quadrant after the treatment. The results indicated that the treatment has caused the depletion of ΔΨm in a dose-dependent manner.

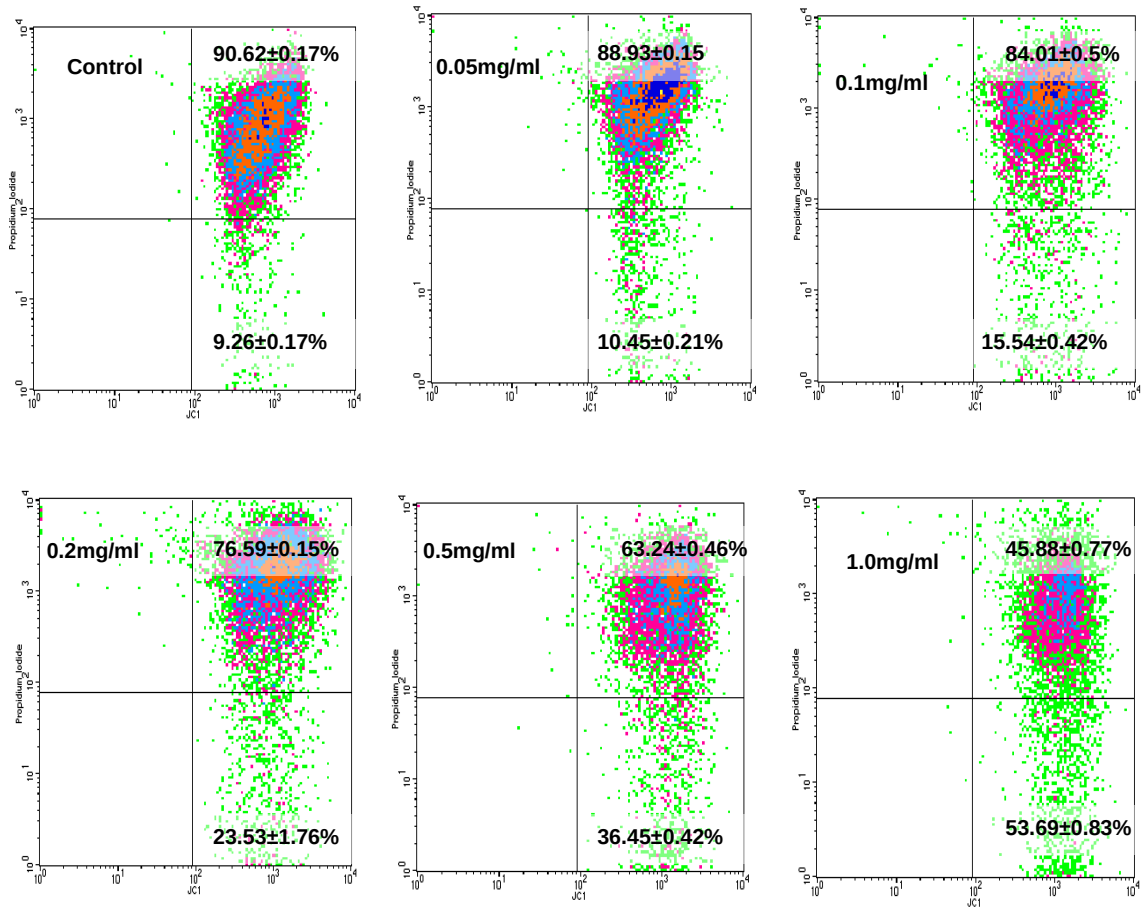

Figure 3.9 Effect of *S.macrophylla* ethyl acetate fraction on the mitochondrial membrane depolarization of HCT116 cells at various concentrations ranging from 0.05mg/ml to 1.0mg/ml. JC-1 intensity was measured using flow cytometry fluorescence pattern analysis. The data represent mean ± S.D. of three replicates (n=3).

3.2.8 Cell cycle distribution analysis

To determine whether the HCT116 cells treated with SMEAF undergo the apoptosis accompanied by alteration in the cell cycle, the distribution index was examined by PI staining. The increasing accumulation of G1 phase of cell distribution was observed as low as concentration of 0.05mg/ml, and increased toward 1.0mg/ml at 24h incubation period (Figure 3.10 [A]). This was accompanied by an increase in sub-G1 population and concurrent decrease in G2/M phase cells with increasing hours of incubation at 0.05mg/ml as shown in Figure 3.10[B].

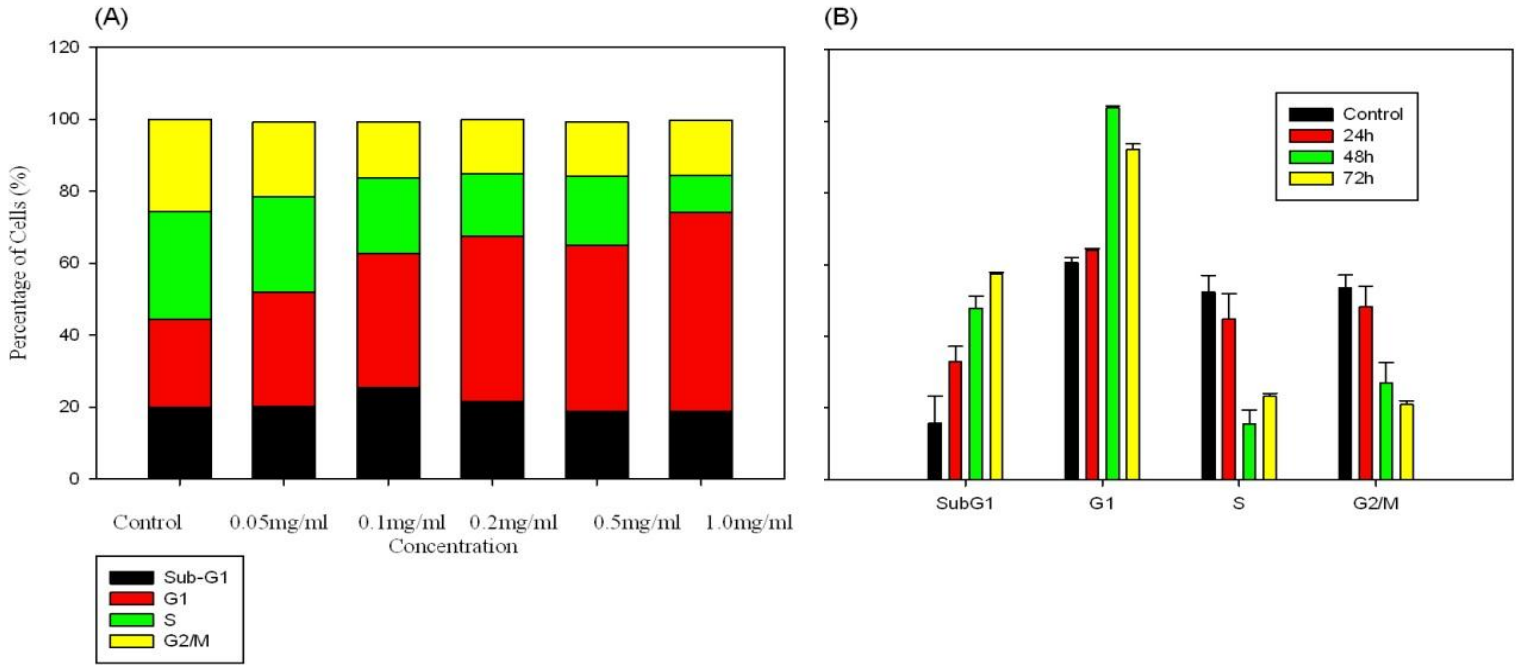

Figure 3.10 Effect of *S.macrophylla* ethyl acetate fraction on DNA distribution patterns of HCT116 cells. Propidium iodide (PI) fluorescent intensity was measured using flow cytometry. (A) DNA distribution in different phases of cells following treatments ranging from 0.05mg/ml to 1.0mg/ml for 24-hour incubation period. (B) DNA distribution in different phases of cells following treatment of 0.05mg/ml at 24h, 48h and 72h incubation periods. The data represent mean ± S.D. of three replicates (n=3).

3.2.9 SMEAF-induced change in Bax and Bcl-2 ratio and inhibit the proliferation of HCT116

Bax and Bcl-2 proteins are known to be involved in cell death mechanism. Specifically, increasing level of Bcl-2 was shown to promote cellular survival (Dohlman *et al*., 1988) and in contrast, the anti-apoptotic activity of Bcl-2 appears to be opposed by Bax (Oltval *et al*., 1993). It is generally thought that the ratio of Bcl-2 and Bax in a cell may determine the survival fate of the cell (Dohlman *et al*., 1988; Oltval *et al*., 1993). Since SMEAF is capable to induce apoptosis, therefore the investigation of gene expression level of Bax and Bcl-2 was performed by using Q-PCR. As depicted in Figure 3.11 [B], there is a slight decrease in Bcl-2 gene expression level and a significant concomitant increase of Bax expression detected after 6h and 12h of SMEAF treatment (Figure 3.11 [A]). Taken together, the increase in Bax and decrease in Bcl-2 expression significantly elevated the Bax/Bcl-2 expression ratio (Figure 3.11 [C]). These results suggested that an increase level of Bax/Bcl-2 may sensitize the cells towards apoptotic stimuli.

Further confirmation of the expression level of Bax and Bcl-2 was determined by using cytometric immunofluorescence staining method. As depicted in Figure 3.12, when compared to the untreated cells, the SMEAF-treated cell profiles shifted to the right in Bax histograms while there was no drastic shift in Bcl-2 histograms. This showed that the Bax protein level was increased after the treatment but no changes in Bcl-2 protein level was detected. This was consistent with the q-PCR results where no significant changes in Bcl-2 level was observed while increasing number of cells exhibited higher level of Bax expression upon the SMEAF treatment. Thus, these results supported the notion that SMEAF-induced apoptosis in HCT116 cells was mediated through the up regulation of Bax/Bcl-2 expression ratio.

Though the effect of apoptotic sensitizing effect was confirmed above, further investigation was focused on PCNA gene in determining the anti-proliferation effect of SMEAF. PCNA involves in vast number of cellular activities including cell cycle regulation, DNA synthesis and DNA repair and it is greatly expressed in most of the proliferating cancer cells (P. K. Chan et al., 1983). Thus PCNA is a well known marker for proliferating cells. Involvement of PCNA in SMEAF inhibitory effect was confirmed using Q-PCR showed Figure 3.13 the expression level of PCNA on SMEAF exposed cells gradually decreased throughout the treatment period. Reflecting the proliferation of the cells was halted upon the treatment.

[A] [B] [C]

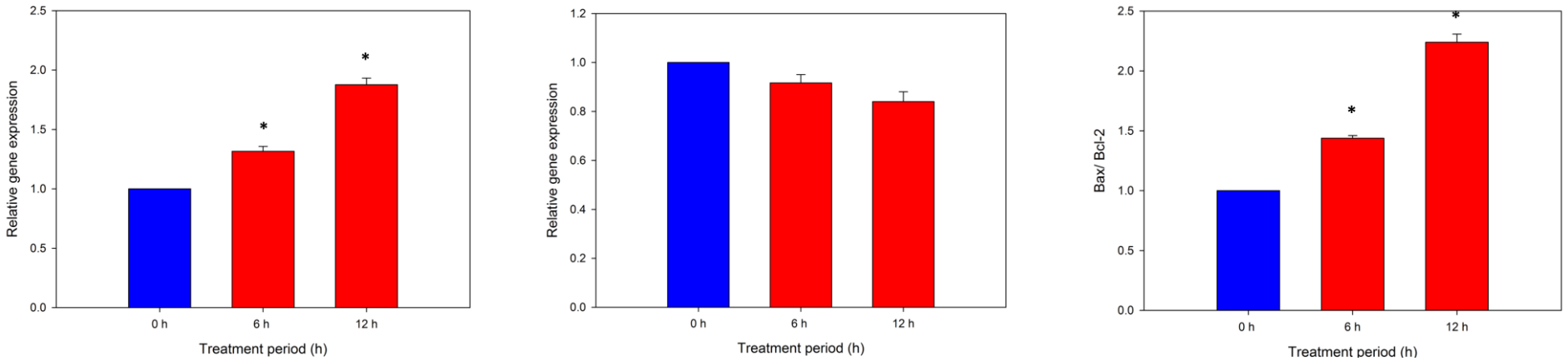

Figure 3.11 Effect of SMEAF on gene expression level of Bax and Bcl-2 in HCT116 cells. Cells were treated with 0.05mg/ml of SMEAF for different times. After designed exposure times, cells were harvested and the total RNA was extracted. The RNA was subjected to q-PCR analysis as described in methods. [A] The relative gene expression level of Bax was compared to control, [B]The relative gene expression level of Bcl-2 was compared to control which were normalized against PBGD expression using the formula $2^{-\Delta\Delta CT}$. [C] Values are mean ± S.E. of three experiments. Asterisks indicate a significant difference between untreated and treated cells (*$P < 0.05$).

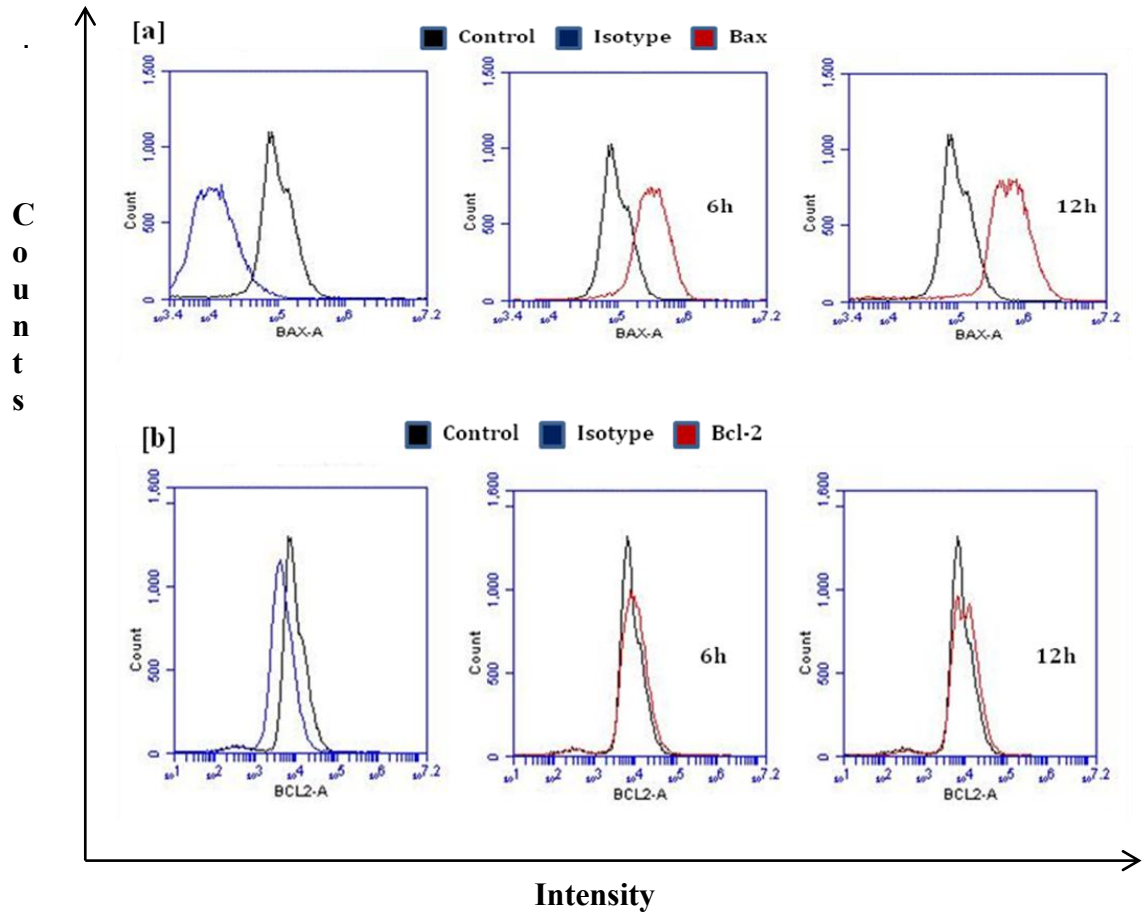

Figure 3.12 Effect of SMEAF on protein expression level of Bax and Bcl-2 in HCH116 cells. After treatment with 0.05mg/ml of SMEAF for different time periods, the cells were harvested and intracellular levels of Bax and Bcl-2 were determined as described in methods. Representative overlay of histrograms [a] showing Bax-associated immunofluorescence, while [b] showing Bcl-2-assiociated immunofluorescence.

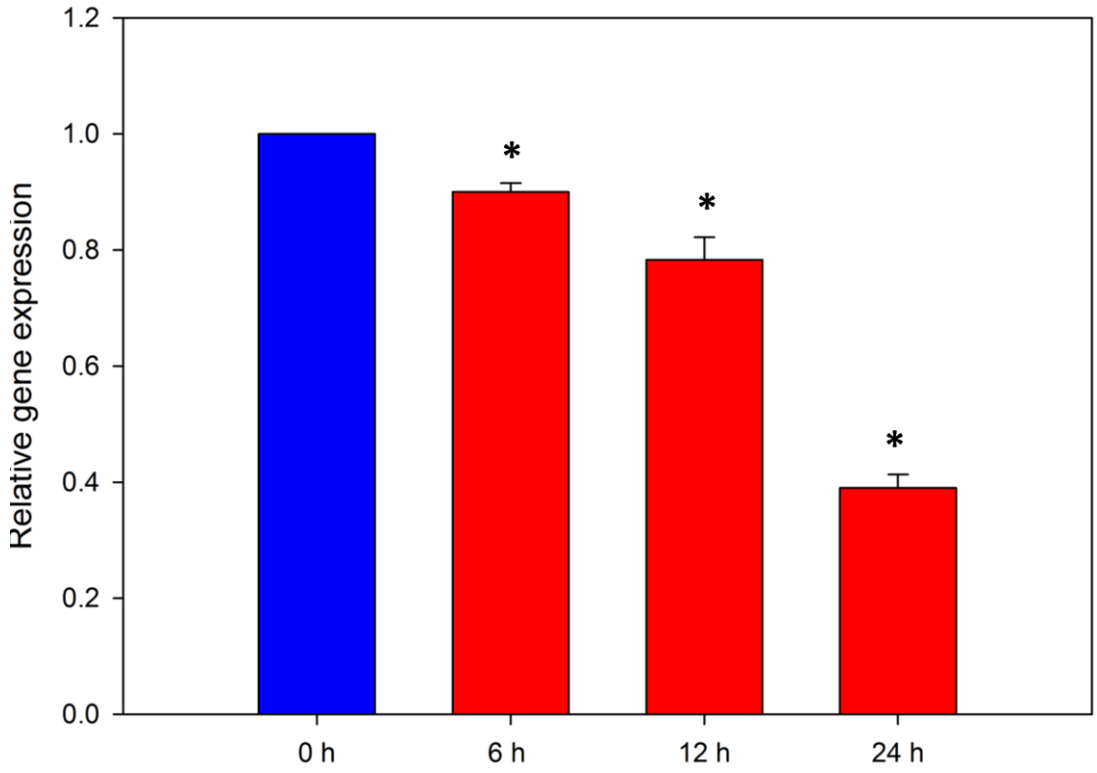

Figure 3.13 Effect of SMEAF on gene expression level of PCNA in HCT116 cells. Cells were treated with 0.05mg/ml of SMEAF for different times. After designated exposure times, cells were harvested and the total RNA was extracted. The RNA was subjected to q-PCR analysis as described in methods. The relative gene expresion level of PCNA expression was compared to control, which were normalized against GADPH expression using the formula $2^{-\Delta\Delta CT}$. Values are mean ± S.E. of three experiments. Asterisks indicate a significant difference between untreated and treated cells (*P < 0.05).

3.2.10 Caspase -3/7 and -9 involved in SMEAF induced apoptosis

Executioner Caspase -3/7 and initiator Caspase -9 were evaluated. The ability of SMEAF to activate the caspases was studied using fluorescence linked inhibitor of caspase -3/7 and -9. HCT116 were incubated with 0.05 mg/ml of SMEAF for 3, 6, 12 and 24 hours followed by addition of the fluorescent inhibitor and results of flow cytometer analysis were showed in Figure 3.14 From the histograms (Figure 3.14 [A]), the intensity of fluorescence signal of caspase -3/7 increased after 3hours of incubation period and slight decrease was detected on 12h of incubation and resume higher level on 24h. This may due to the nature different of cells reaction toward stimuli. Meanwhile, evaluation of initiator caspase -9 activity was showed of Figure 3.14 [B]. There were slight increase of activity of caspase -9 on 3 and 6h followed by bigger argument on 12 and 24h of incubation period. Therefore, the results suggested SMEAF able to induce apoptosis through execution by caspase cascade process especially through caspase -3/7 and -9.

[A]

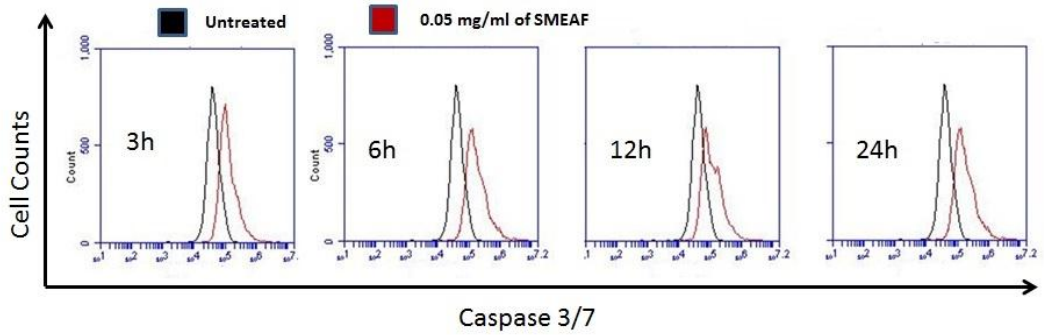

[B]

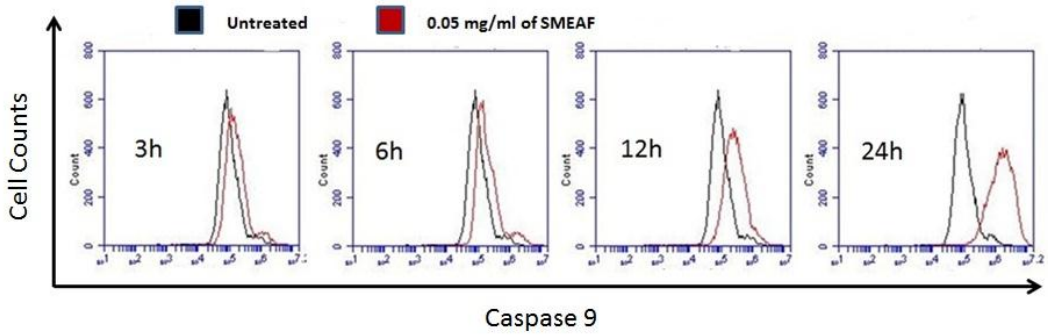

Figure 3.14 [A] Effect of SMEAF on caspase 3/7 and [B] caspase 9 activity level in HCH116 cells. After treated with 0.05mg/ml of SMEAF for different times, the cells were harvested and intracellular levels of caspase 3/7 were determined as described in methods.

3.2.11 SMEAF induced changes in cell cycle regulatory genes

PCNA down regulation may exert its effect on cell cycle regulatory pathway, in effort to gain further insight into the molecular mechanisms affected by SMEAF in HCT116 cells, we profiled the expression of key pathways involved in cell cycle using human cancer pathway finder PCR array with SMEAF treated cells and control cells. This PCR array contains 84 genes in different cancer related pathways (cell cycle, apoptosis, adhesion, angiogenesis, invasion and metastasis, signal transduction molecules and transcriptional factors (gene details on SABiosciences website, catalog PAH-033)). Numerous key genes involved in cell regulatory pathways were altered in its expression level, specifically CCNE1, CDC25A, CDK2, CDK4 and E2F1 were down regulated to identified and proved by real-time PCR as shown in Figure 3.15 In addition, the Q-PCR study showed the gene that encoded p21 and p53 protein which known as CDKN1A and TP53 respectively were up regulated. Besides, SMEAF exposure causing the down regulation of MDM2 gene which encoding the negative regulator of p53 was detected after the SMEAF treatment. The data indicating SMEAF may cause the p53-p21 activation and subsequently leading to cell cycle arrest in HCT116 and apoptosis.

[A] [B]

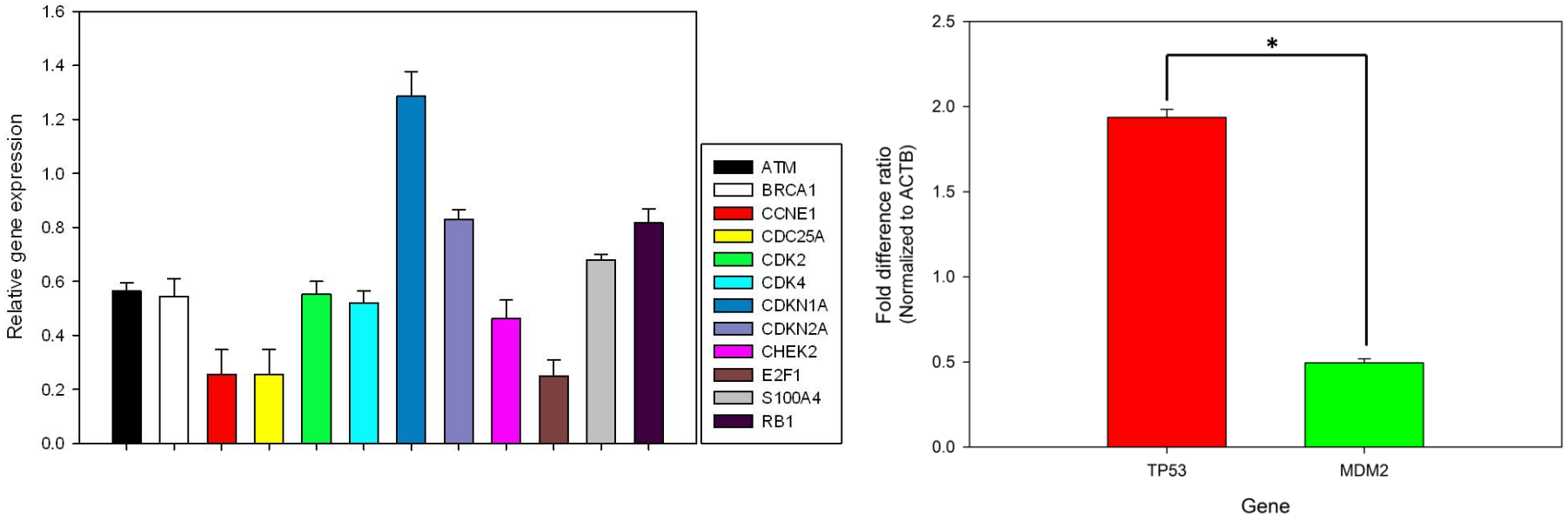

Figure 3.15 The cells were treated with 0.05 mg/ml of SMEAF, harvested after 12 h incubation and the total RNA was extracted. The RNA was subjected to Q-PCR analysis by using PCR array as described in methods. Analysis was done by using RT^2 Profiler Data Analysis Excel platform. The genes expression was normalized against ACTB expression values. Values are mean ± S.D. of three experiments. [A] Effects of SMEAF treatment on cell cycle regulatory genes of HCT116 after 24h incubation period. [B] Effects of SMEAF on expression level of TP53 and MDM2 after 24h exposure period. Asterisks indicate a significant difference between expression level of TP53 and MDM2 of treated cells (*$P < 0.05$).

3.2.12 p53 and p21 proteins expression level detection by using protein array

Proteins p53 and p21 play important roles in regulating the cell cycle progression. Protein array analysis was utilized in determination of protein expression of p21 and p53 proteins in HCT116 cells treated with SMEAF. Figure 3.16 [A] and Figure 3.17 [A], indicate the duplicates of experiments conducted on 0h (control) and 24 h exposure of SMEAF particularly on HCT116. The photographs clearly shown the treatment of SMEAF for 24 h caused the increase of p53 and p21 proteins level indicating by the sharper fluorescence signal. The fluorescent signal of each of the sample was subtracted with background fluorescent signal and further normalized against pre-coated positive control probes in arrays. Figure 3.16 [B] and Figure 3.17 [B] show mean fluorescent signals of its duplicates. The 0 h or control samples fluorescence intensity at 39.60 while the treated group at 138.95 which indicating more than three folds increase in p21 protein level.

[A] [B]

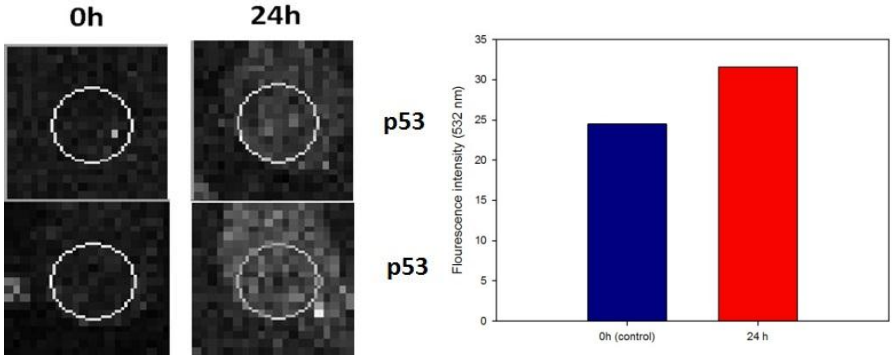

Figure 3.16 Protein expression level of p53 on 0h (control) and 24h exposure of SMEAF on HCT116 cell line. [A] RayBiotech protein array analysis on control and treated cells photographed by GenePix 4000B. [B] Means fluorescence of p21 of control (0h) and 24h SMEAF treated cells after subtracted with background and normalized against pre-coated positive control probes using Acuity 4.0 analysis software.

[A] [B]

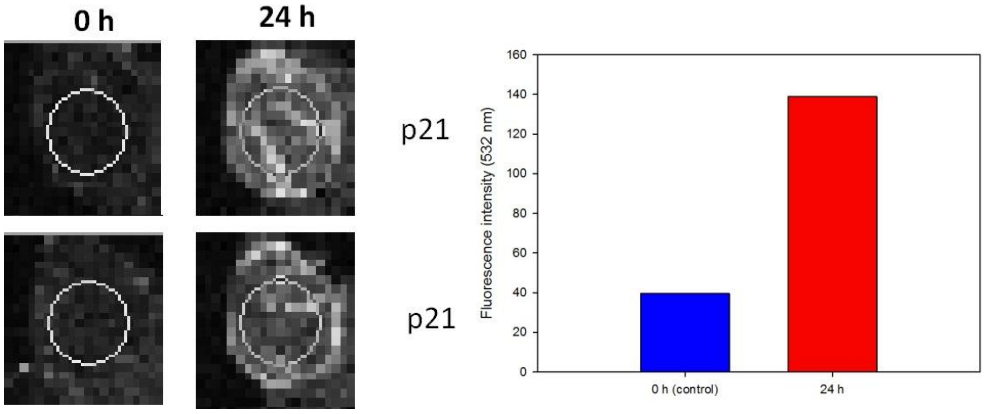

Figure 3.17 Protein expression level of p21 on 0h (control) and 24h exposure of SMEAF on HCT116 cell line. [A] RayBiotech protein array analysis on control and treated cells photographed by GenePix 4000B. [B] Means fluorescence of p21 of control (0h) and 24h SMEAF treated cells after subtracted with background and normalized against pre-coated positive control probes using Acuity 4.0 analysis software.

3.3 Chemicals purification and identification of SMEAF

3.3.1 Cell viability evaluation of SMEAF chromatographed frations

The previous results demonstred SMEAF possessed apoptotic inducing effects in HCT116 cells, therefore 3g of SMEAF was subjected for isolation of bioactive compounds through column chromatography. The isolation procedures were guided by MTT cell viability assay. As depicited in Figure 3.19 there are 11 fractions after chromatographed using mixture of solvents started with n-hexane followed by increasing proportions of chloform. Eleven fractions were obtained and all of them were subjected to biological screening against HCT 116 cells using MTT assay. The results show that, only five out of the eleven fractions were able to give IC_{50} with the range of screening concentration up to 200 µg/ml. The fractions were, EA 4 , EA 5, EA 7, EA 8 and EA 11 with IC_{50} values 141.03 $\pm$ 2.16, 152.82 $\pm$ 3.19, 58.32 $\pm$ 5.02, 194.05 $\pm$ 4.44 and 89.78 $\pm$ 4.72 µg/ml respectively (Figure 3.18).

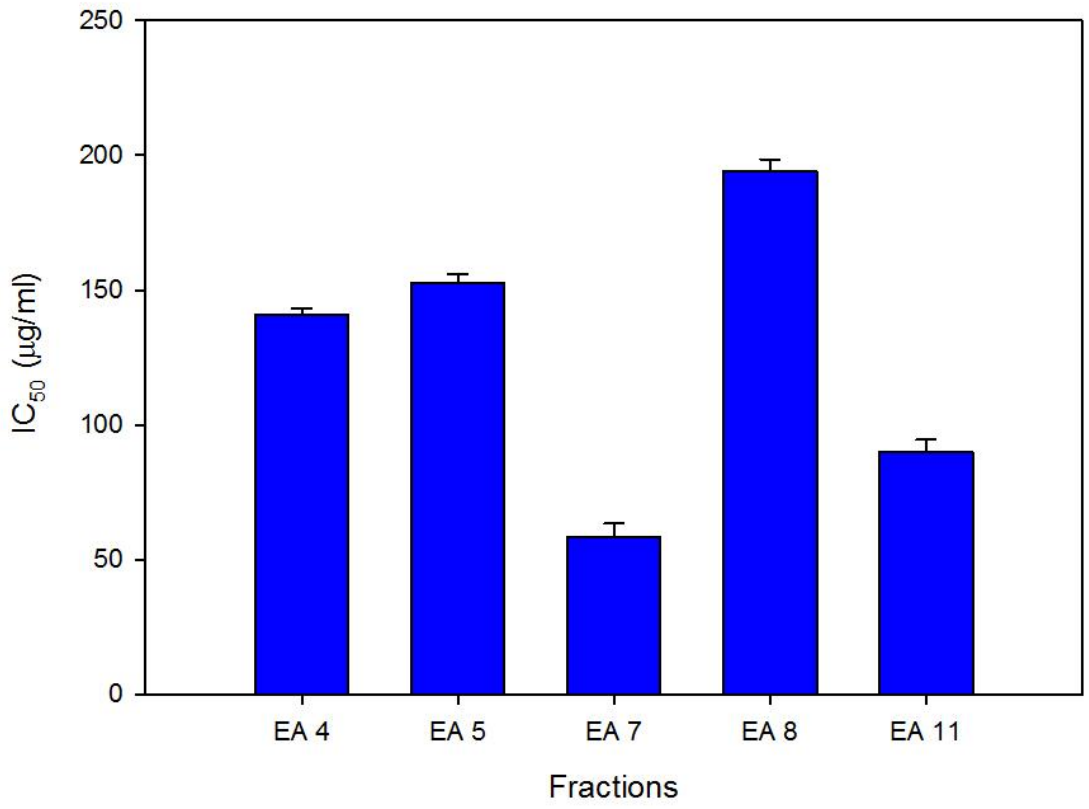

Figure 3.18 MTT cell viability assay evaluation on different fractions of SMEAF after chromatograpy. The data represent mean ± S.E. of three independent experiments (n=9).

3.3.2 Identification of chemical constituents of EA 1, EA 2, EA 3 and EA 4 Fraction using GC-MS

The named fractions were subjected to GC-MS anlysis and the results obtained are shown in Table 3.2, 3.3, 3.4 and 3.5 respectively.

Table 3.2: Chemical constituents of EA 1 identified by GC-MS.

Compounds Name	Retention time	Percentage (%)
Pentadecanoic acid, metyl ester	19.526	5.97
Hexadecanoic acid, ethyl ester	21.127	26.96
Octadecanoic acid, methyl ester	23.861	4.76
(E)-9-Octadecanoic acid, ethyl ester	24.648	1.79
Octadecanoic acid, ethyl ester	25.181	22.52
Eicosanoic acid, ethyl ester	27.551	4.07
Heptadecanoic acid, ethyl ester	28.671	2.07
Stigmasterol	35.383	3.03
Gamma-sitosterol	37.253	8.03
Total Identified Amount: 79.20%		

Table 3.3: Chemical constituents of EA 2 identified by GC-MS.

Compounds Name	Retention time	Percentage (%)
Pentadecanoic acid, metyl ester	19.519	1.12
Ethyl 9-hexadecenoate	20.614	0.57
Hexadecanoic acid, ethyl ester	21.121	5.82
9,12-Octadecadienoic acid, methyl ester	23.254	9.16
9-Octadecanoic acid (z), methyl ester	23.385	8.22
Octadecanoic acid, methyl ester	23.867	0.35
Linoleic acid methyl ester	24.693	38.84
Ethyl oleate	24.824	33.38
Octadecanoic acid, ethyl ester	25.180	2.28
Total Identified Amount: 99.74%		

Table 3.4: Chemical constituents of EA 3 identified by GC-MS.

Compounds Name	Retention time	Percentage (%)
Oxacycloheptadecan-2-one	19.726	0.29
Tridecanoic acid	20.426	0.21
9,12-Octadecadienoic acid, methyl ester	23.216	1.28
912,15-Octadecatrienoic acid, methyl ester (z,z,z)	23.354	3.11
9,12-Octadecadienoic acid (z,z)-	24.298	5.42
Linoleic acid ethyl ester	24.573	5.74
9,12,15-Octadecatrienoic acid, ethyl ester, (z,z,z)	24.730	12.44
Decanedioic acid, bis(2-ethylhexyl) ester	34.939	0.14
9,19-cyclolanost-24-en-3-ol, (3.beta.)-	42.432	0.52
Total Identified Amount: 29.15%		

Table 3.5: Chemicals constituent of EA 4 identified by GC-MS.

Compounds Name	Retention time	Percentage (%)
n-Hexadecanoic acid	20.477	0.73
9,17-Octadecadienal, (z)-	24.505	41.97
2-Methyl-z,z-3,13-octadecadienol	25.706	6.65
12-Methyl-E,E-2,13-octadecadien-1-ol	27.045	1.22
9,12-Octadecadienoic acid (z,z)-	27.345	0.59
2-Methyl-z,z-3, 13-octadecadienol	27.564	1.36
2-Methyl-z,z-3,13-octadecadienol	27.864	0.96
Cis-7, cis-11-Hexadecadienol-1-yl acetate	31.273	0.08
2-methyl-z,z-3,13-octadecadienol	33.494	0.22
.gamma.-Tocopherol	38.279	0.32
.gamma.-Sitosterol	41.864	7.10
Total Identified Amount: 61.20%		

3.3.3 Purification and identification of compound from EA 4

EA 4 was subjected to another column chromatography, initially eluting with n-hexane and later with acetone to give twelve fractions. The sixth fraction [EA 4 (6)] was subjected to preparative thin layer chromatography yielding compound swietenolide (4). The eighth fraction [EA 4 (8)] was dissolved in methanol and stored in a refrigerator. A white solid was obtained after two days (1) and a second crop (2) was obtained after another two days. Recrystalization of the first (1) and second crop (2) from chloroform yielded colorless crystals namely diacetylswietenolide or 3,6-*O*,*O*-diacetylswietenolide (1) and swietenine (2). The ninth fraction [EA 4 (9)] was also dissolved in methanol and stored in refrigerator for three days until formation of white solid. Recystalization of crop from chloroform yielded 6-O-acetylswietenolide (8). The flow chart of purification procedure is show in Figure 3.19.

The chemical structure of purified compounds were confirmed by comparison of obtained NMR data with published data as in tables listed below.The molecular weight of compounds was further confirmed by using GC-MS and fragmentation ions of compounds were shown in Table 3.20.

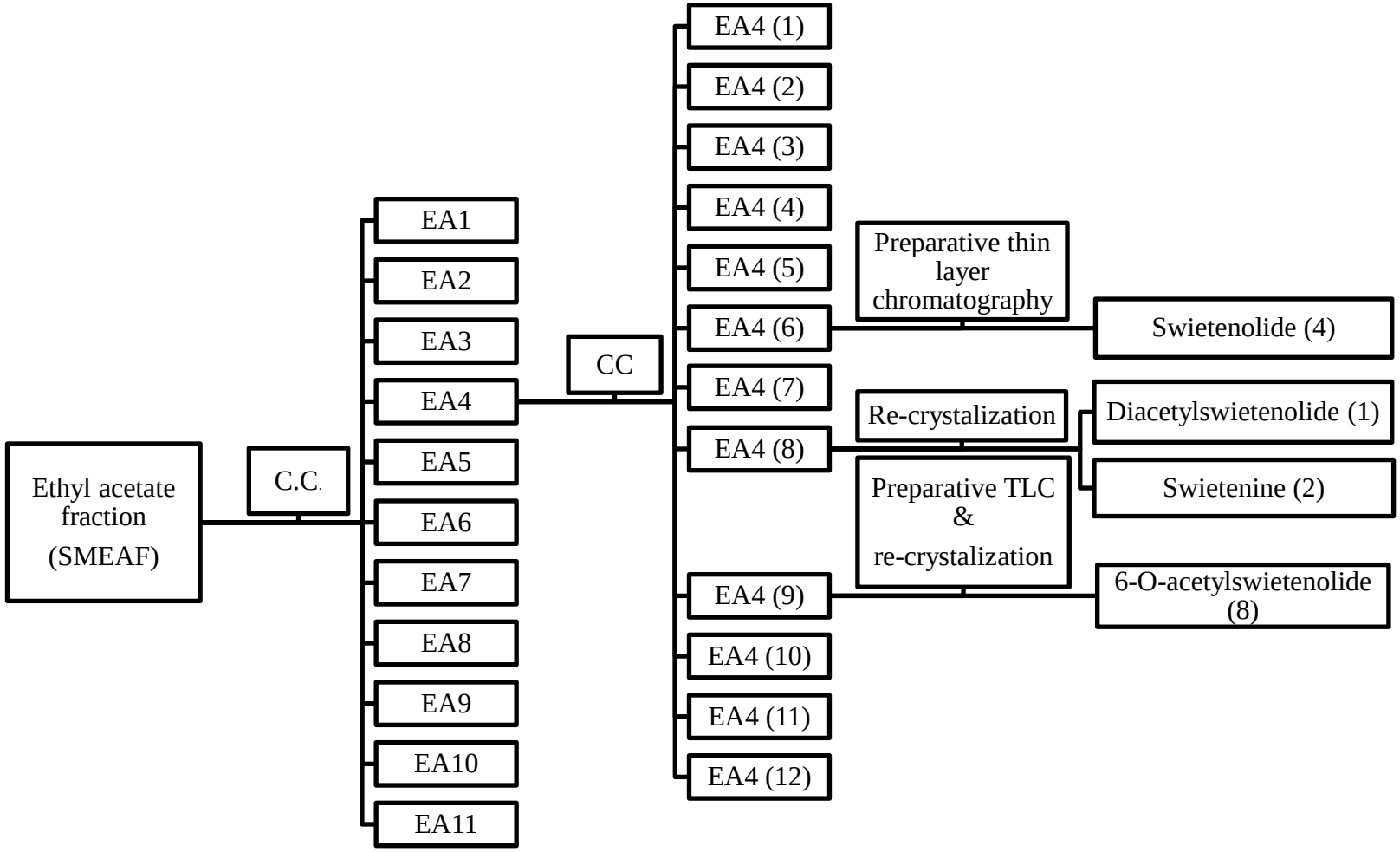

Figure 3.19 Flow chart of column chromatography isolation of compounds 1, 2, 4 and 8.

3.3.4 Purification and identification of compound from EA 5

The EA 5 was subjected to preparative HPLC using 45% methanol: 55% water as the mobile phase and the compound known as 3-*O*-tigloylswietenolide (3) was obtained (Figure 3.20). The structures were confirmed by comparison of obtained NMR data with published literature data in Table 3.8 and 3.15. The structures were further confirmed using GC-MS Table 3.20.

3.3.5 Purification and identification of compound from EA 7

The EA 7 fraction of SMEAF was further fractionated using column chromatography, initially eluting with n-hexane and later with chloroform and finally increasing the mobile phase polarity using acetone until flushed out by using methanol. This gives six fractions. After evaluation using MTT assay for their cytotoxic activity, the most potent fraction EA 7(2) was subjected to preparative TLC (Figure 3.21 & Figure 3.22). This afforded the compound named hexadecanoic acid (5).

3.3.6 Purification and identification of compounds from EA 8

The EA 8 faction of SMEAF was subjected to column chromatography with hexane as initial eluting solvent and step-wise increasing polarities using acetone until flushed out using methanol. The column chromatography afforded us a total of ten fractions (Figure 3.23) and all of them were evaluated for their cytotoxic activities. The IC_{50} of fractions EA 8 (1-10) were shown in Figure 3.24. The most potent faction was then subjected to preparative TLC and afforded compound Khayasin T (7).

3.3.7 Purification and identification of compound from EA 9

The EA 9 fraction was separated using TLC (Figure 3.25). With the assistance of UV ray (254nm) we managed to purify out the compound known as proceranolide (6). The data of NMR spectra and GC-MS data were shown Table 3.10, 3.17 and 3.20.

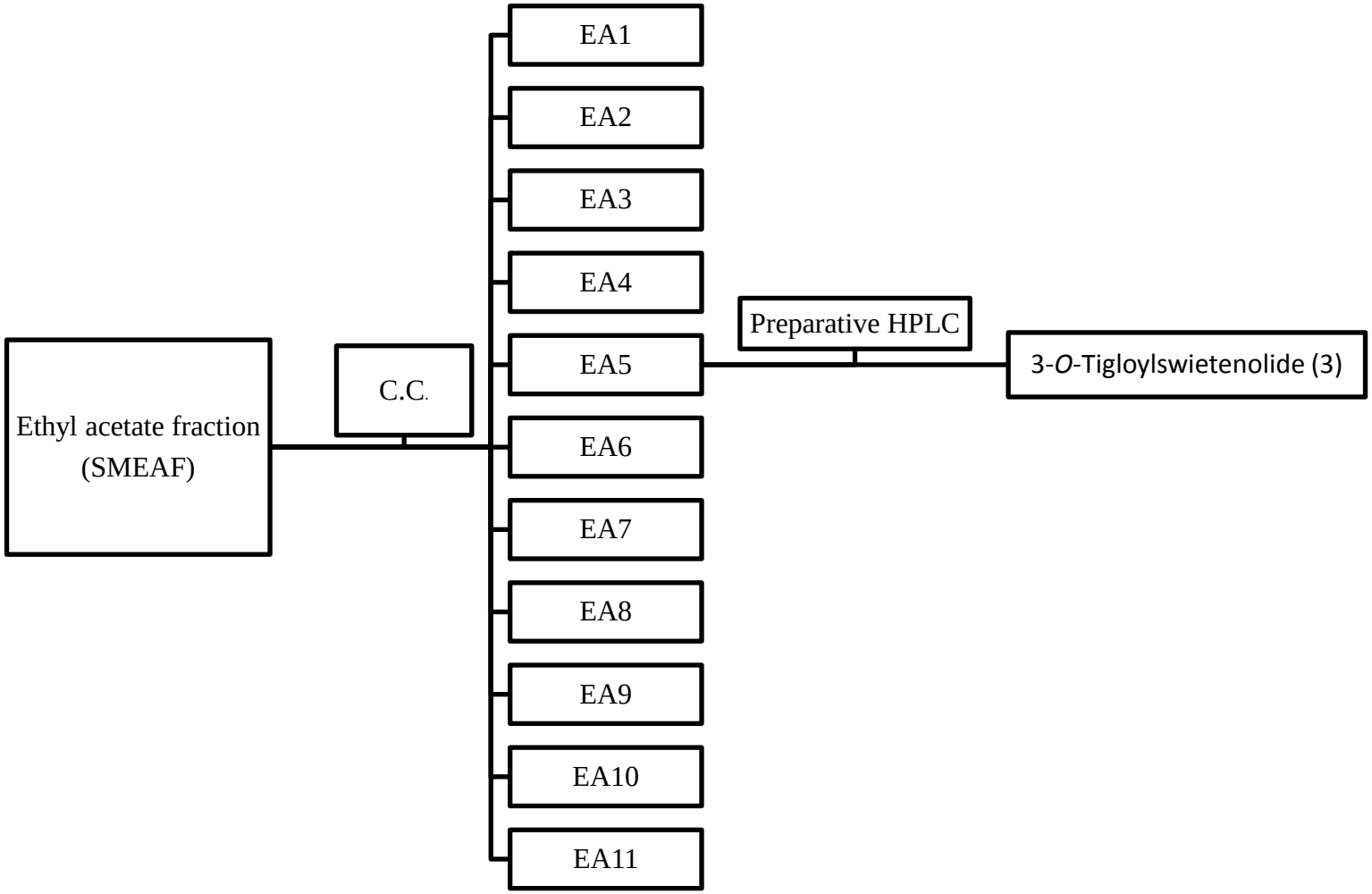

Figure 3.20 Flow chart of column chromatography isolation of compound 3.

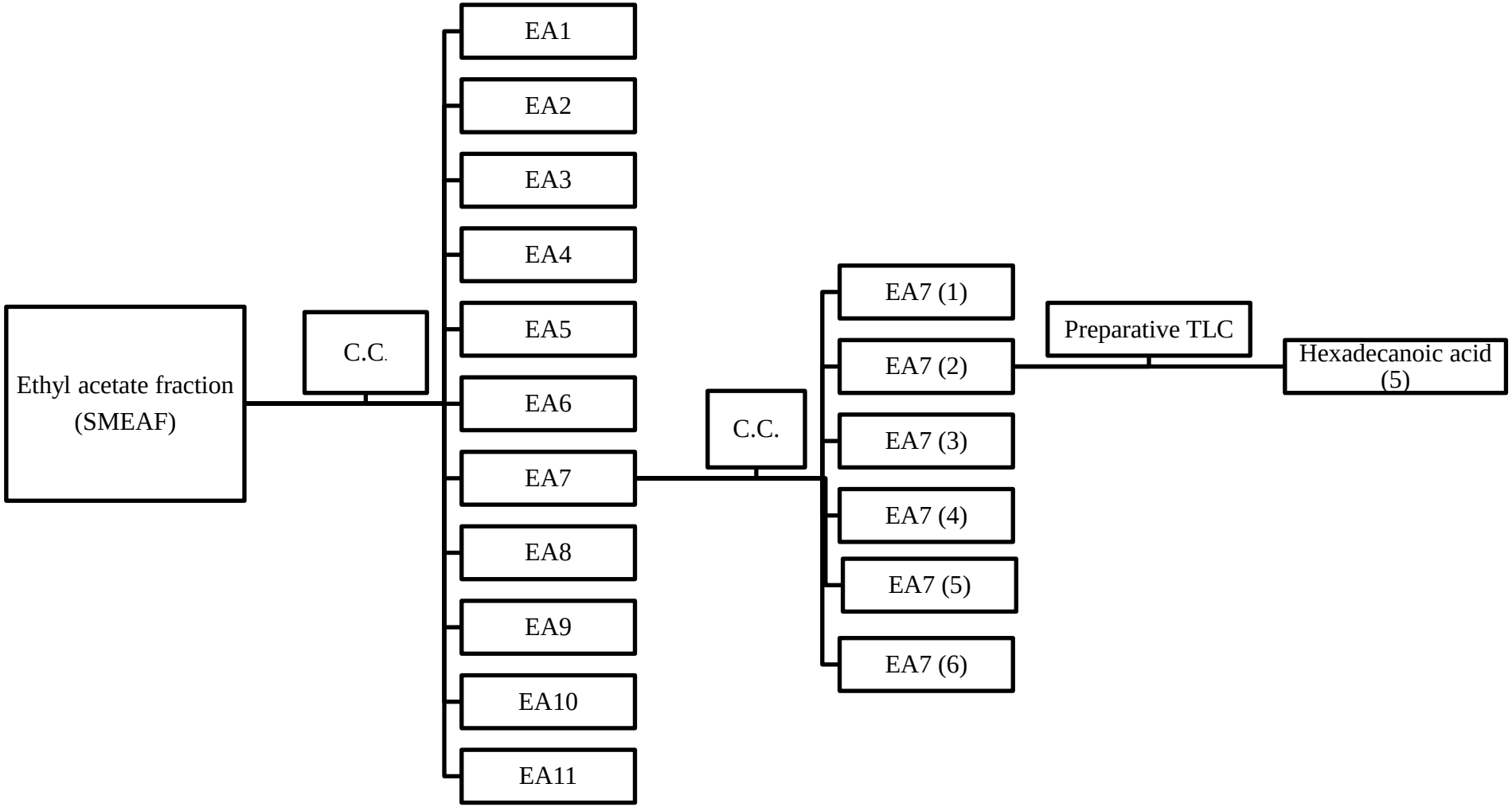

Figure 3.21 Flow chart of column chromatography isolation of compound 5.

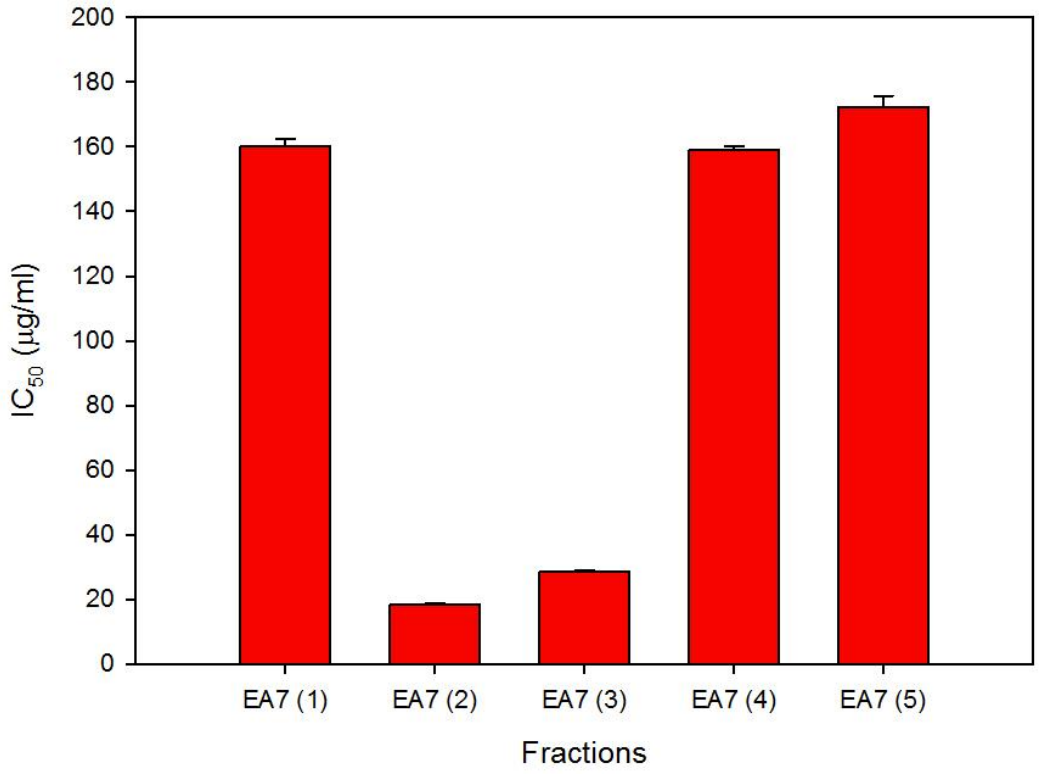

Figure 3.22 MTT cell viability assay evaluation on different fractions of EA 7 after chromatographed. The data represent mean ± S.E. of three independent experiments (n=9).

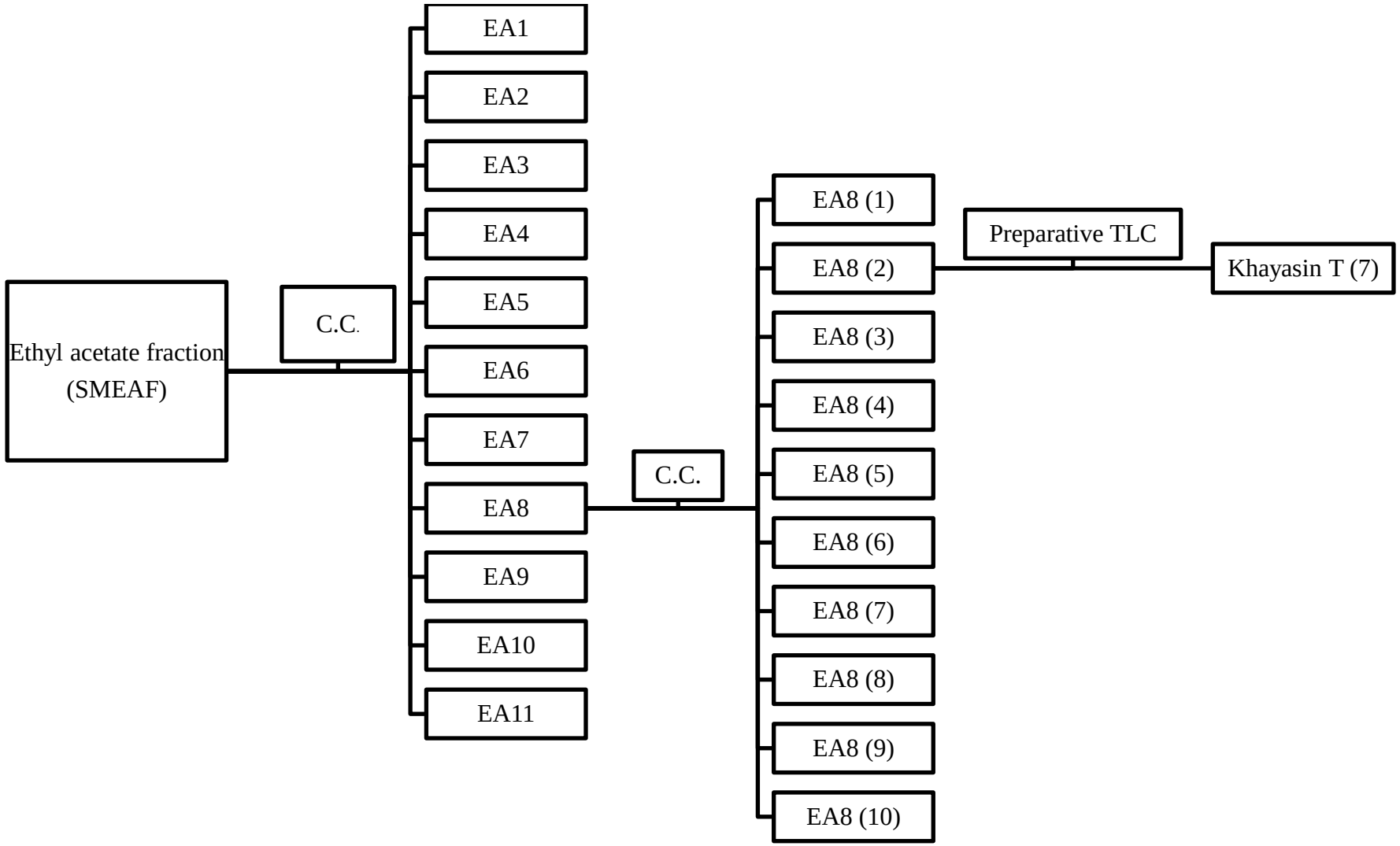

Figure 3.23 Flow chart of column chromatography isolation of compound 7.

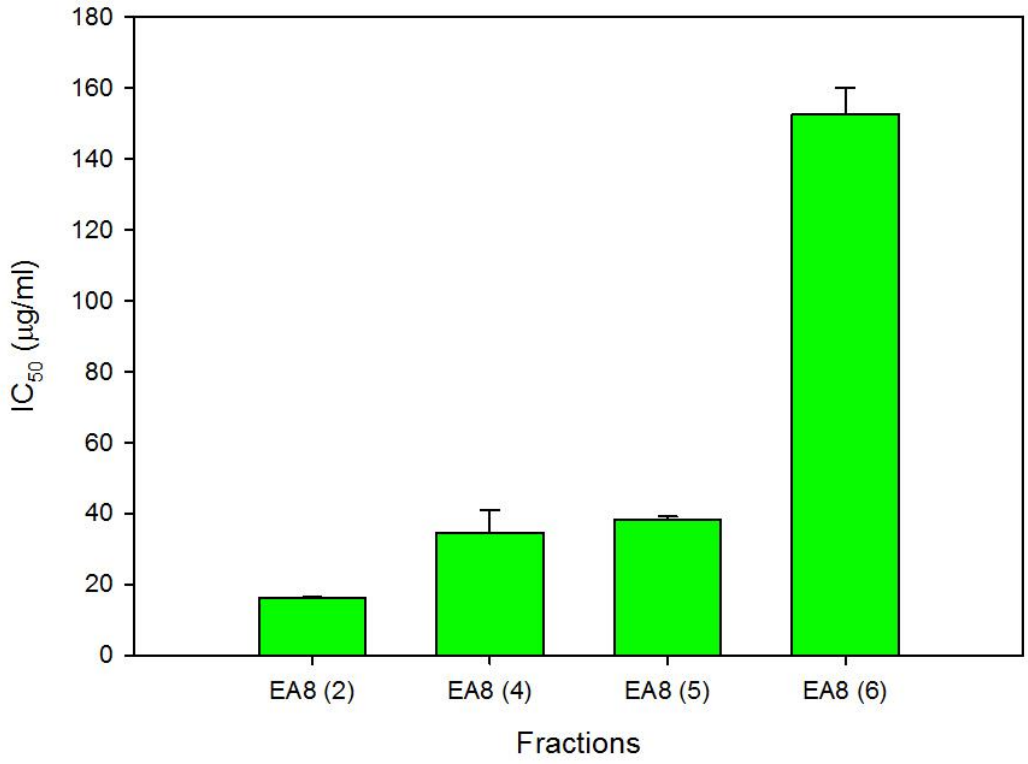

Figure 3.24 MTT cell viability assay evaluation on different fractions of EA 8 after chromatographed. The data represent mean ± S.E. of three independent experiments (n=9).

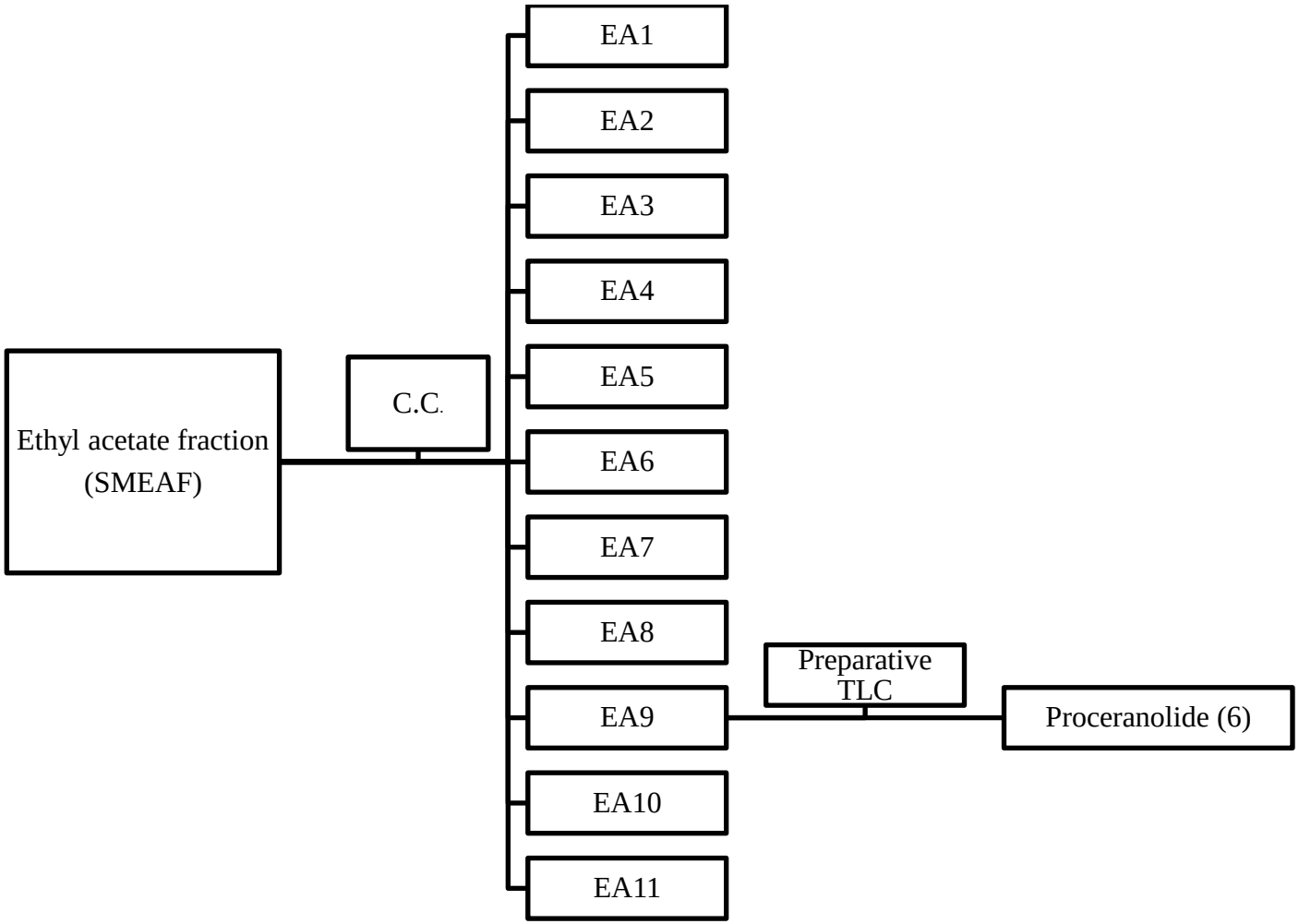

Figure 3.25 Flow chart of column chromatography isolation of compound 6.

3.3.8 Chemicals structures of purified compounds

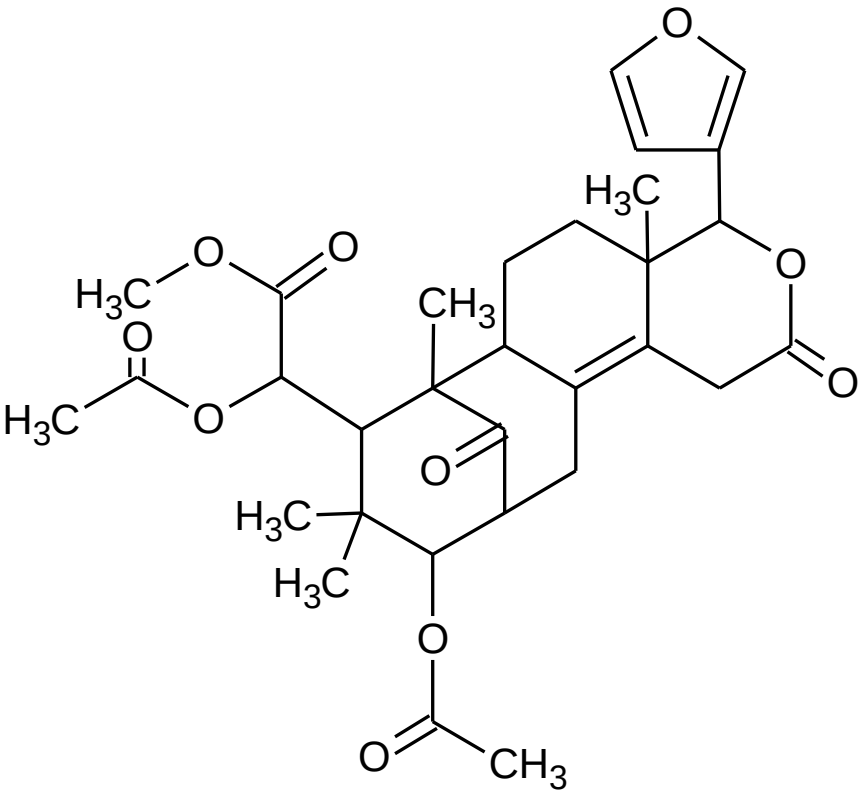

Figure 3.26 Chemical structure of 3,6-*O*,*O*-Diacetylswietenolide (1).

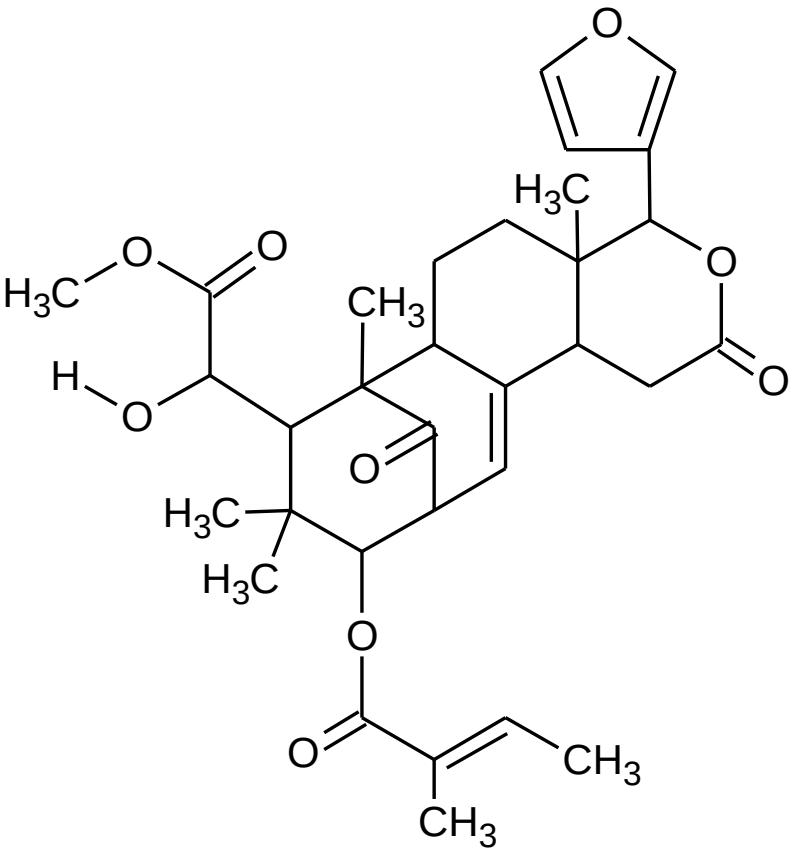

Figure 3.27 Chemical structure of Swietenine (2).

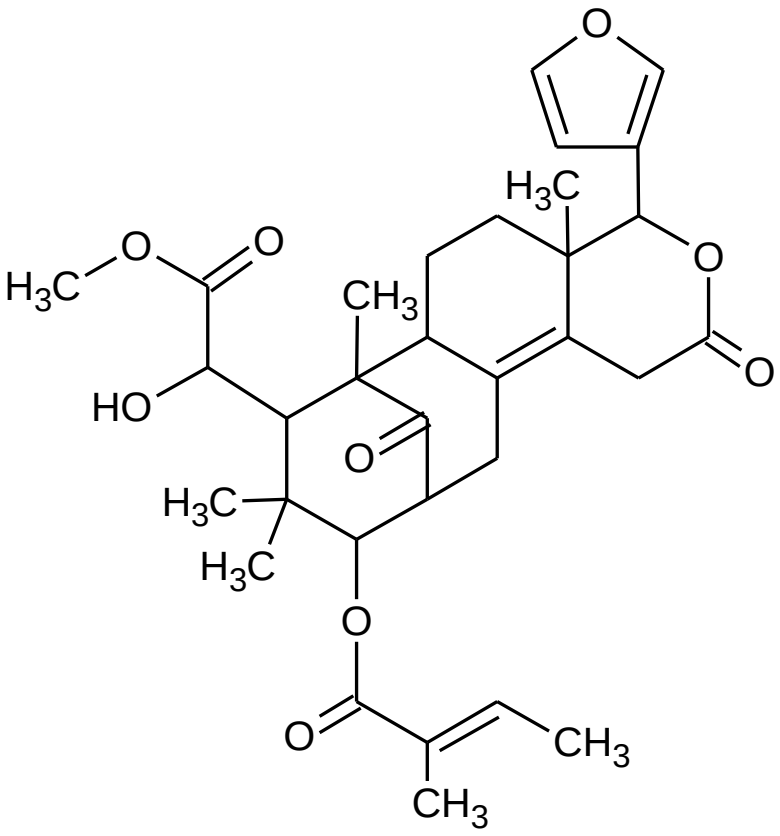

Figure 3.28 Chemical structure of 3-*O*-Tigloylswietenolide (3).

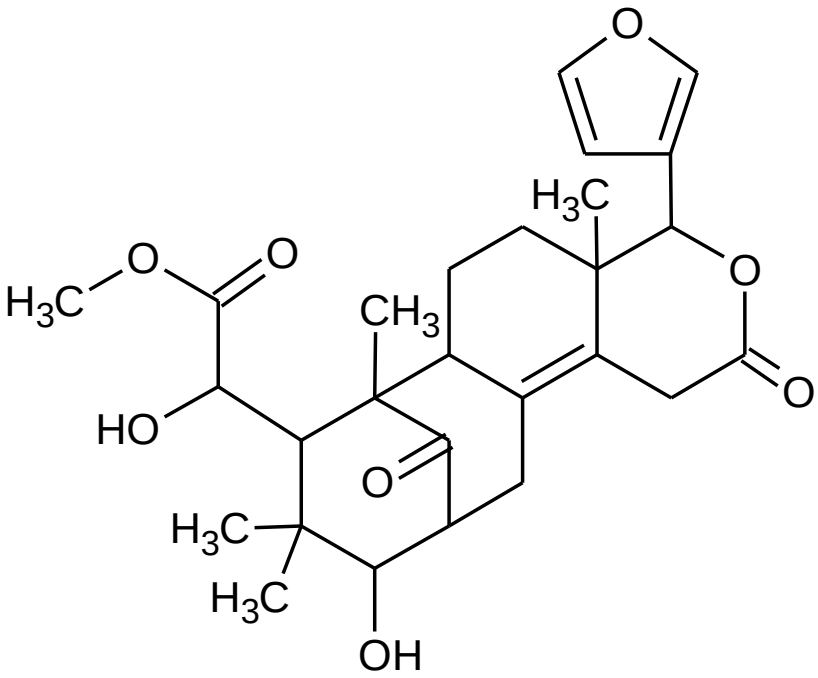

Figure 3.29 Chemical structure of swietenolide (4).

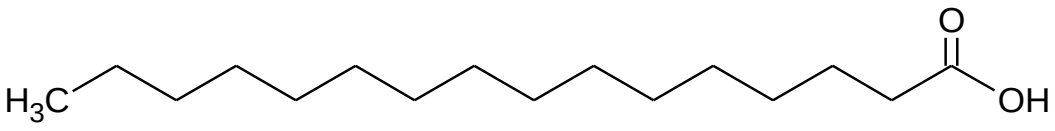

Figure 3.30 Chemical structure of hexadecanoic acid (5).

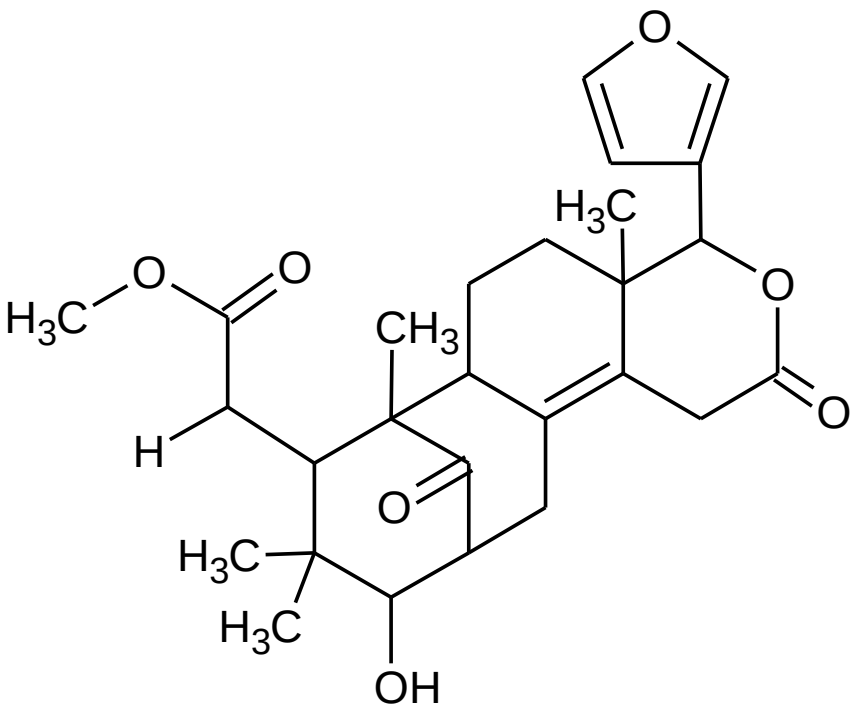

Figure 3.31 Chemical structure of proceranolide (6).

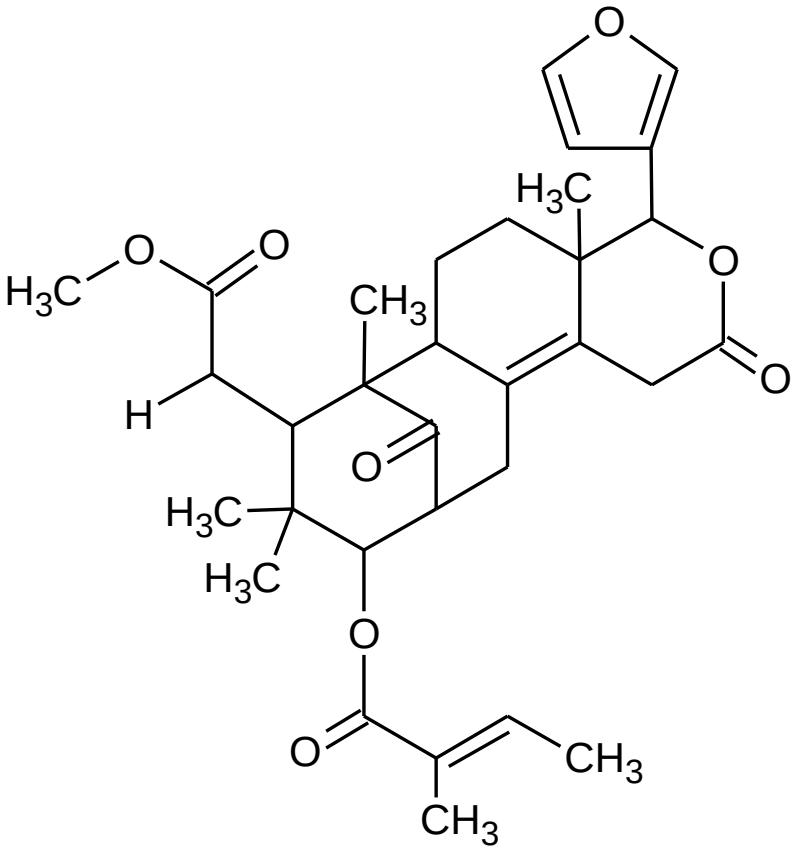

Figure 3.32 Chemical structure of khayasin T (7).

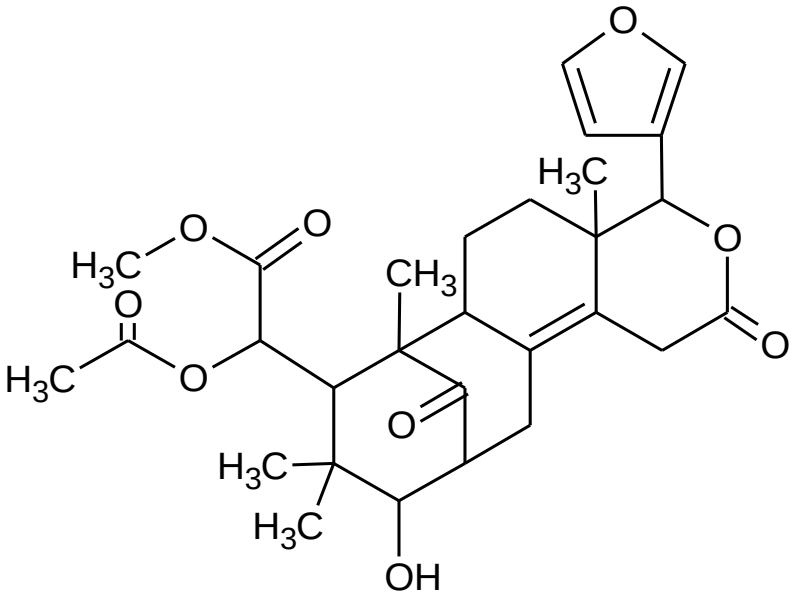

Figure 3.33 Chemical structure of 6-O-acetylswietenolide (8).

3.3.9 Spectral data of purified compounds

Table 3.6: ^{1}H-NMR spectral data for diacetyl swietenolide (1).

Position/type	Chemical shift δ, ppm (400MHz, $CDCl_3$)	Literature[a] δ, ppm (400MHz, $CDCl_3$)
H2, C<u>H</u>	3.13 (m)	3.14 (ddd)
H3, C<u>H</u>OCOCH$_3$	4.85 (d)	4.86 (d)
H5, C<u>H</u>	3.38 (s)	3.40 (s)
H6, C<u>H</u>OCOCH$_3$	5.44 (s)	5.46 (s)
H9, C<u>H</u>	2.08 (m)	2.08 (m)
H11, C<u>H</u>$_2$	1.74 (m) 1.85 (m)	1.16 (m) 1.81 (m)
H12, C<u>H</u>$_2$	1.16 (m) 1.80 (m)	1.76 (m) 1.89 (m)
H15, C<u>H</u>$_2$	3.43 (dt) 3.66 (d)	3.44 (dt) 3.68 (d)
H17, CH	5.58 (s)	5.60 (s)
H18, C<u>H</u>$_3$	1.02 (s)	1.04 (s)
H19, C<u>H</u>$_3$	1.13 (s)	1.15 (s)
H21, olefinic C<u>H</u>	7.50 (s)	7.52 (dd) (1.8, 1.0)
H22, olefinic C<u>H</u>	6.43 (d)	6.45 (dd)
H23, olefinic CH	7.40 (s)	7.43 (t)
H28, C<u>H</u>$_3$	1.05 (s)	1.07 (s)
H29, C<u>H</u>$_3$	0.83 (s)	0.85 (s)
H30, C<u>H</u>$_2$	2.08 (m) 2.77 (dd)	2.13(ddd) 2.79 (dd)
COOC<u>H</u>$_3$	3.73 (s)	3.74 (s)
6-OCOC<u>H</u>$_3$	2.15 (s)	2.16 (s)
H2', COC<u>H</u>$_3$	2.13 (s)	2.15 (s)

Table 3.7: ^{1}H-NMR spectral data for swietenine (2).

Position/type	Chemical shift δ, ppm (400MHz, $CDCl_3$)	Literature[a] δ, ppm (400MHz, $CDCl_3$)
H2, C<u>H</u>	3.53 (dd)	3.52 (ddd)
H3, CO<u>H</u>	4.64 (d)	4.64 (d)
H5, C<u>H</u>	3.50 (br s)	3.50 (br s)
H6, C<u>H</u>OC_2H_3=C_2H_4	4.56 (br s)	4.56 (br s)
H9, C<u>H</u>	2.30 (dd)	2.30 (ddd)
H11, C<u>H_2</u>	1.81 (m) 2.05 (dddd)	1.81 (m) 2.05 (qd)
H12, C<u>H_2</u>	1.45 (m) 1.74 (m)	1.46 (ddd) 1.77 (m)
H14, C<u>H</u>	2.22 (d)	2.23 (ddd)
H15, C<u>H_2</u>	2.85 (dd) 2.79 (dd)	2.83 (dd) 2.76 (dd)
H17, C<u>H</u>	5.55 (s)	5.54 (s)
H18, C<u>H_3</u>	0.97 (s)	0.97 (s)
H19, C<u>H_3</u>	1.45 (s)	1.45 (s)
H21, olefinic C<u>H</u>	7.55 (s)	7.56 (dd)
H22, olefinic C<u>H</u>	6.38 (d)	6.38 (dd)
H23, C<u>H_3</u>	7.45 (t)	7.45 (t)
H28, C<u>H_3</u>	1.12 (s)	1.12 (s)
H29, C<u>H_3</u>	0.89 (s)	0.89 (s)
H30, olefinic C<u>H</u>	5.34 (dt)	5.34 (dt)
COOC<u>H_3</u>	3.76 (s)	3.76 (s)
H2'-CH_3, 2'-C<u>H_3</u>	1.81 (br d)	1.82 (br s)
H3', olefinic C<u>H</u>	6.87 (dddd)	6.87 (qq)
H3'-CH_3, 3'H-C<u>H_3</u>	1.74 (br dd)	1.74 (br d)

Table 3.8: ^{1}H-NMR spectral data for 3-*O*-tigloylswietenolide (3).

Position/type	**Chemical shift δ, ppm (400MHz, $CDCl_3$)**	**Literature[a] δ, ppm (400MHz, $CDCl_3$)**
H2, C<u>H</u>	3.22 (m)	3.21 (ddd)
H3, C<u>H</u>	4.71 (d)	4.71 (d)
H5, C<u>H</u>	3.38 (s)	3.38 (br s)
H6, C<u>H</u>	4.56 (s)	4.56 (br s)
H9, C<u>H</u>	2.12 (m)	2.11 (m)
H11, C<u>H</u>$_2$	1.74 (m) 1.88 (m)	1.76 (m) 1.88 (m)
H12, C<u>H</u>$_2$	1.19 (m) 1.74 (m)	1.17 (m) 1.74 (m)
H15, C<u>H</u>$_2$	3.28 (t) 3.54 (d)	3.25 (dt) 3.54 (dt)
H17, C<u>H</u>	5.43 (s)	5.43 (s)
H18, C<u>H</u>$_3$	0.99 (s)	0.99 (s)
H19, C<u>H</u>$_3$	1.43 (s)	1.43 (s)
H21, olefinic C<u>H</u>	7.49 (s)	7.48 (dd)
H22, olefinic C<u>H</u>	6.43 (t)	6.40 (dd)
H23, olefinic CH	7.44 (s)	7.43 (s)
H28, C<u>H</u>$_3$	1.10 (s)	1.10 (s)
H29, C<u>H</u>$_3$	0.86 (s)	0.86 (s)
H30, C<u>H</u>$_2$	2.12 (m) 2.68 (d)	2.12 (m)
COOC<u>H</u>$_3$	3.86 (s)	3.86 (s)
H2'-CH_3, 2'-C<u>H</u>$_3$	1.88 (s)	1.89 (t) (1)
H3', olefinic C<u>H</u>	6.93 (dd)	6.93 (qq)
H3'-CH_3, 3'-C<u>H</u>$_3$	1.83 (d)	1.83 (dd)

Table 3.9: ^{1}H-NMR spectral data for swietenolide (4).

Position/type	Chemical shift δ, ppm (400MHz, $CDCl_3$)	Literature[a] δ, ppm (400MHz, $CDCl_3$)
H2, C<u>H</u>	3.02 (m)	3.04 (ddd)
H3, C<u>H</u>OH	3.56 (d)	3.58 (d)
H5, C<u>H</u>	3.23 (s)	3.25 (br s)
H6, C<u>H</u>OH	4.51 (s)	4.54 (br s)
H9,C<u>H</u>	2.04 (br d)	2.07 (br s)
H11, C<u>H</u>$_2$	1.73 (m) 1.99 (m)	1.14 (m) 1.73 (m)
H12, C<u>H</u>$_2$	1.12 (dd) 1.73 (m)	1.78 (ddd) 1.86 (ddd)
H15, C<u>H</u>$_2$	3.43 (dt) 4.00 (d)	3.46 (dt) 4.03 (dt)
H17, C<u>H</u>	5.45 (s)	5.47 (s)
H18, C<u>H</u>$_3$	0.97 (s)	0.99 (s)
H19, C<u>H</u>$_3$	1.38 (s)	1.40 (s)
H21, olefinic C<u>H</u>	7.46 (s)	7.48 (dd)
H22, olefinic C<u>H</u>	6.38 (d)	6.40 (dd)
H23, olefinic C<u>H</u>	7.39 (s)	7.41 (t)
H28, C<u>H</u>$_3$	0.97 (s)	1.00 (s)
H29, C<u>H</u>$_3$	0.86 (s)	0.88 (s)
H30,C<u>H</u>$_2$	1.99 (dd) 3.16 (dd)	2.01 (ddd) 3.19 (dd)
COOC<u>H</u>$_3$	3.81 (s)	3.82 (s)

Table 3.10: ^{1}H-NMR spectral data for proceranolide (6).

Position/type	Chemical shift δ, ppm (400MHz, $CDCl_3$)	Literature[a] δ, ppm (400MHz, $CDCl_3$)
H2, C<u>H</u>	3.03 (ddd)	3.04 (ddd)
H3, C<u>H</u>OH	3.72 (d)	3.74 (d)
H5, CH	3.23 (dd)	3.24 (dd)
H6,C<u>H</u>$_2$	2.34 (d) 2.41 (d)	2.34 (dd) 2.40 (dd)
H9, C<u>H</u>	1.98 (m)	1.98 (m)
H11, C<u>H</u>$_2$	1.70 (m) 1.77 (m)	1.72 (m) 1.80 (m)
H12,C<u>H</u>$_2$	1.04 (m) 1.80 (m)	1.03 (m) 1.79 (m)
H15, C<u>H</u>$_2$	3.48 (dt) 4.10 (dt)	3.46 (dt) 4.08 (dt)
H17, C<u>H</u>	5.59 (s)	5.59 (s)
H18, C<u>H</u>$_3$	1.02 (s)	1.03 (s)
H19, C<u>H</u>$_3$	1.12 (s)	1.13 (s)
H21, olefinic C<u>H</u>	7.49 (dd)	7.57 (dd)
H22,olefinic CH	6.46 (dd)	6.49 (dd)
H23, olefinic CH	7.37 (t)	7.39 (t)
H28, C<u>H</u>$_3$	0.72 (s)	0.72 (s)
H29,C<u>H</u>$_3$	0.80 (s)	0.81 (s)
H30, C<u>H</u>$_2$	1.95 (m) 3.17 (dd)	1.97 (m) 3.19 (dd)
COOC<u>H</u>$_3$	3.69 (s)	3.70 (s)

Table 3.11: ^{1}H-NMR spectral data for khayasin T (7).

Position/type	Chemical shift δ, ppm (400MHz, $CDCl_3$)	Literature[a] δ, ppm (400MHz, $CDCl_3$)
H2, C<u>H</u>	3.23 (m)	3.23 (ddd)
H3, C<u>H</u>O	4.83 (d)	4.85 (d)
H5, C<u>H</u>	3.35 (dd)	3.37 (dd)
H6, C<u>H</u>$_2$	2.34 (m) 3.38 (dd)	2.37 (dd) 2.42 (dd)
H9, C<u>H</u>	2.01 (m)	2.01 (m)
H11, C<u>H</u>$_2$	1.74 (m)	1.73 (m) 1.84 (m)
H12, C<u>H</u>$_2$	1.11 (m) 1.82 (m)	1.10 (m) 1.83 (m)
H15, C<u>H</u>$_2$	3.23 (m) 3.59 (br d)	3.23 (dt) 3.61 (dt)
H17, C<u>H</u>	5.54 (s)	5.55 (s)
H18, C<u>H</u>$_3$	1.01 (s)	1.03 (s)
H19, C<u>H</u>$_3$	1.15 (s)	1.17 (s)
H21, olefinic C<u>H</u>	7.56 (s)	7.57 (dd)
H22, olefinic C<u>H</u>	6.45 (dd)	6.48 (dd)
H23, olefinic C<u>H</u>	7.40 (t)	7.42 (t)
H28, C<u>H</u>$_3$	0.80 (s)	0.82 (s)
H29, C<u>H</u>$_3$	0.76 (s)	0.77 (s)
H30, C<u>H</u>$_2$	2.07 (m) 2.64 (dd)	2.08 (ddd) 2.66 (dd)
COOC<u>H</u>$_3$	3.71 (s)	3.74 (s)
H2'-C<u>H</u>$_3$, 2'-C<u>H</u>$_3$	1.88 (s)	1.89 (d)
H3', olefinic C<u>H</u>	6.95 (qq)	6.96 (qq)
H3'-C<u>H</u>$_3$, 3'-C<u>H</u>$_3$	1.82 (dd)	1.83 (dd)

Table 3.12: ^{1}H-NMR spectral 6-O-acetylswietenolide (8).

Position/type	**Chemical shift δ, ppm (400MHz, $CDCl_3$)**	**Literature[a] δ, ppm (400MHz, $CDCl_3$)**
H2, C<u>H</u>	3.04 (m)	3.05 (ddd)
H3, C<u>H</u>OH	3.60 (d)	3.62 (d)
H5, C<u>H</u>	3.46 (s)	3.45 (br s)
H6, C<u>H</u>	5.43 (s)	5.45 (br s)
H9, C<u>H</u>	2.03 (m)	2.02 (m)
H11, C<u>H</u>$_2$	1.77 (m) 1.88 (m)	1.76 (m) 1.89 (m)
H12,C<u>H</u>$_2$	1.13 (m) 1.84 (m)	1.15 (m) 1.84 (m)
H15, C<u>H</u>$_2$	3.59 (d) 4.01 (d)	3.45 (dt) 4.01 (dt)
H17,C<u>H</u>	5.51 (s)	5.53 (s)
H18, C<u>H</u>$_3$	0.99 (s)	1.01 (s)
H19, C<u>H</u>$_3$	1.13 (s)	1.15 (s)
H21, olefinic C<u>H</u>	7.51 (d)	7.54 (dd)
H22, olefinic C<u>H</u>	6.45 (dd)	6.47 (dd)
H23, olefinic C<u>H</u>	7.39 (t)	7.41 (t)
H28, C<u>H</u>$_3$	0.97 (s)	0.99 (s)
H29, C<u>H</u>$_3$	0.91 (s)	0.94 (s)
H30, C<u>H</u>$_2$	2.02 (m) 3.13 (dd)	2.00 (m) 3.17 (dd)
COOC<u>H</u>$_3$	3.73 (s)	3.74 (s)
6-OCOC<u>H</u>$_3$	2.15 (s)	2.17 (s)

Table 3.13: ^{13}C NMR spectral of diacetyl swietenolide (1).

Position/type	Chemical shift δ, ppm (400MHz, $CDCl_3$)	Literature[a] δ, ppm
C1, C=O	217.08	216.86
C2, CH	47.91	47.86
C3, $\underline{C}HOCOCH_3$	79.52	79.49
C4, C quaternary	38.90	38.84
C5, CH	44.43	44.40
C6, CH	73.09	73.05
C7, 6-$\underline{C}OOCH_3$	171.33	171.26
C8, C olefinic	127.66	127.61
C9, CH	53.13	53.55
C10, C quaternary	53.43	53.43
C11, CH_2	18.74	18.94
C12, CH_2	29.40	29.79
C13, C quaternary	38.21	38.13
C14, C olefinic	132.35	131.61
C15, CH_2	33.51	33.16
C16, C=O	169.72	169.23
C17, CH	80.91	81.11
C18, $\underline{CH_3}$	18.06	18.04
C19, $\underline{CH_3}$	16.81	16.71
C20, C olefinic	120.56	120.53
C21, C olefinic, CH	141.64	141.57
C22, C olefinic,CH	109.94	109.88
C23, C olefinic, CH	143.08	143.00
C28, $\underline{CH_3}$	23.43	23.36
C29, $\underline{CH_3}$	23.07	23.02
C30, $\underline{CH_2}$	33.77	33.71
$COO\underline{C}H_3$	52.25	53.35
6-$O\underline{C}OCH_3$	169.85	169.71
6-$OCOO\underline{CH_3}$	21.08	20.93
C1', 3-$O\underline{C}OCH_3$	170.23	170.23
C2', 3-$OCO\underline{CH_3}$	21.33	21.20

Table 3.14: ^{13}C NMR spectral of swietenine (2).

Position/type	Chemical shift δ, ppm (400MHz, $CDCl_3$)	Literature[a] δ, ppm
C1, C=O	216.61	216.53
C2, CH	48.93	48.95
C3, COH	78.38	78.41
C4, C quaternary	39.01	39.04
C5, CH	45.43	45.47
C6, $\underline{C}HOC_2H_3{=}C_2H_4$	72.84	72.87
C7,6- $\underline{C}OOCH_3$	175.96	175.97
C8, C olefinic	138.27	138.28
C9, CH	57.52	57.56
C10, C quaternary	50.36	50.39
C11, CH_2	21.24	21.28
C12, CH_2	34.60	34.64
C13, C quaternary	36.69	36.73
C14, CH	45.04	45.09
C15, CH_2	29.54	29.57
C16, C=O	168.48	168.45
C17, CH	76.71	76.71
C18, $\underline{CH_3}$	21.24	21.28
C19, $\underline{CH_3}$	16.52	16.53
C20, C olefinic	121.33	121.38
C21, C olefinic, CH	140.51	140.54
C22, C olefinic, CH	109.21	109.24
C23, C olefinic, CH	143.19	143.20
C28, $\underline{CH_3}$	22.77	22.80
C29, $\underline{CH_3}$	23.02	23.05
C30, C olefinic, CH	123.60	123.66
$COO\underline{C}H_3$	53.29	53.28
C1', CH	166.91	166.92
C2', C olefinic	127.73	127.77
C3', C olefinic, CH	139.02	139.02
C2'-$\underline{C}H_3$	11.72	11.75
C3'-$\underline{C}H_3$	14.63	14.64

Table 3.15: ^{13}C NMR spectral of 3-*O*-tigloylswietenolide (3).

Position/type	Chemical shift δ, ppm (400MHz, $CDCl_3$)	Literature[a] δ, ppm
C1, C=O	218.01	217.95
C2, CH	48.13	48.14
C3, CH	80.55	80.57
C4, C quaternary	39.16	39.17
C5, CH	45.06	45.08
C6, CH_2O	73.33	73.36
C7, 6-$\underline{C}OOCH_3$	175.63	175.63
C8, C olefinic	128.48	128.52
C9, CH	53.52	53.55
C10, C quaternary	53.43	53.43
C11, CH_2	18.91	18.94
C12, CH_2	29.76	29.79
C13, C quaternary	38.10	38.13
C14, C olefinic	131.59	131.61
C15, CH_2	33.19	33.16
C16, C=O	169.27	169.23
C17, CH	81.11	81.11
C18, $\underline{CH_3}$	17.64	17.79
C19, $\underline{CH_3}$	17.64	17.65
C20, C olefinic	120.84	120.87
C21, C olefinic, CH	141.05	141.06
C22, C olefinic,CH	109.74	109.76
C23, C olefinic, CH	143.11	143.12
C28, $\underline{CH_3}$	23.09	23.11
C29, $\underline{CH_3}$	23.73	23.75
C30, $\underline{CH_2}$	34.05	34.07
$COO\underline{C}H_3$	53.13	53.14
C1', CH	167.22	167.21
C2', C olefinic	129.03	129.06
C3', C olefinic, CH	138.99	138.98
C2'-$\underline{C}H_3$	12.29	12.31
C3'-$\underline{C}H_3$	14.59	14.60

Table 3.16: ^{13}C NMR spectral of switenolide (4).

Position/type	Chemical shift δ, ppm (400MHz, $CDCl_3$)	Literature[a] δ, ppm
C1, C=O	219.8114	219.80
C2, CH	50.0386	49.99
C3, CHOH	78.6455	78.50
C4, C quaternary	39.7590	39.66
C5, CH	44.0701	44.00
C6, CHOH	73.6637	73.57
C7, 6-$COOCH_3$	175.9240	175.83
C8, C olefinic	129.1337	129.05
C9, CH	53.0564	52.96
C10, C quaternary	54.0720	53.99
C11, CH_2	18.8356	29.08
C12, CH_2	29.1919	18.71
C13, C quaternary	37.9195	37.81
C14, C olefinic	130.8695	130.75
C15, CH_2	33.8767	33.15
C16, C=O	171.4308	171.43
C17, CH	80.5903	80.51
C18, CH_3	17.9925	17.91
C19, CH_3	17.9925	17.91
C20, C olefinic	120.9043	120.81
C21, C olefinic, CH	141.1475	141.06
C22, C olefinic,CH	109.9060	109.80
C23, C olefinic, CH	142.9869	142.88
C28, CH_3	23.3000	23.22
C29, CH_3	23.7119	23.63
C30, CH_2	33.2539	33.80
$COOCH_3$	53.3726	53.23

Table 3.17: ^{13}C NMR spectral of proceranolide (6).

Position/type	Chemical shift δ, ppm (400MHz, $CDCl_3$)	Literature[a] δ, ppm
C1, C=O	220.06	220.08
C2, CH	50.13	50.15
C3, CHOH	77.30	77.23
C4, C quaternary	39.38	39.30
C5, CH	39.38	39.30
C6, CH_2	33.63	33.54
C7, 6-$COOCH_3$	174.46	174.39
C8, C olefinic	128.30	128.27
C9, CH	51.90	51.76
C10, C quaternary	53.69	53.61
C11, CH_2	18.83	18.74
C12, CH_2	28.69	28.56
C13, C quaternary	38.01	37.88
C14, C olefinic	131.43	131.20
C15, CH_2	33.17	33.06
C16, C=O	171.60	171.73
C17, CH	80.32	80.25
C18, CH_3	17.65	17.54
C19, CH_3	16.99	16.92
C20, C olefinic	120.88	120.78
C21, C olefinic, CH	141.80	141.71
C22, C olefinic,CH	110.18	110.09
C23, C olefinic, CH	142.72	142.62
C28, CH_3	20.25	20.17
C29, CH_3	23.92	23.90
C30, CH_2	33.39	33.33
$COOCH_3$	52.08	51.97

Table 3.18: ^{13}C NMR spectral of Khayasin T (7).

Position/type	Chemical shift δ, ppm (400MHz, $CDCl_3$)	Literature[a] δ, ppm
C1, C=O	218.56	218.41
C2, CH	48.30	48.30
C3, CHO	79.35	79.28
C4, C quaternary	38.80	38.73
C5, CH	40.57	40.51
C6, CH_2	33.48	33.42
C7, 6-$COOCH_3$	174.36	174.28
C8, C olefinic	127.87	127.80
C9, CH	52.29	52.23
C10, C quaternary	53.27	53.18
C11, CH_2	18.83	18.77
C12, CH_2	29.20	29.16
C13, C quaternary	38.18	38.11
C14, C olefinic	131.97	131.93
C15, CH_2	33.00	32.95
C16, C=O	169.88	169.74
C17, CH	81.00	80.92
C18, CH_3	17.34	17.29
C19, CH_3	16.79	16.72
C20, C olefinic	120.86	120.81
C21, C olefinic, CH	141.76	141.69
C22, C olefinic,CH	110.05	109.98
C23, C olefinic, CH	142.91	142.83
C28, CH_3	20.34	20.28
C29, CH_3	23.91	23.86
C30, CH_2	33.69	33.63
$COOCH_3$	52.18	52.09
C1', C quaternary	167.49	167.41
C2', C olefinic	128.97	128.91
C3', C olefinic, CH	139.51	139.42
C2'-CH_3	12.46	12.40
C3'-CH_3	14.73	14.66

Table 3.19: ^{13}C NMR spectral of 6-O-acetylswietenolide (8).

Position/type	Chemical shift δ, ppm (400MHz, $CDCl_3$)	Literature[a] δ, ppm
C1, C=O	219.00	218.83
C2, CH	49.98	49.95
C3, CHOH	77.31	78.37
C4, C quaternary	40.08	39.84
C5, CH	43.10	43.09
C6, $CHOCOCH_3$	73.62	73.60
C7, 6-$COOCH_3$	171.45	171.35
C8, C olefinic	128.08	128.15
C9, CH	52.67	52.68
C10, C quaternary	54.38	54.11
C11, CH_2	18.65	18.62
C12, CH_2	28.84	28.85
C13, C quaternary	34.08	37.96
C14, C olefinic	130.55	131.77
C15, CH_2	33.21	33.16
C16, C=O	171.45	171.35
C17, CH	80.41	80.37
C18, CH_3	17.72	17.74
C19, CH_3	17.12	17.04
C20, C olefinic	120.98	120.81
C21, C olefinic, CH	141.60	141.54
C22, C olefinic,CH	110.10	110.03
C23, C olefinic, CH	142.88	142.82
C28, CH_3	23.23	23.21
C29, CH_3	23.63	23.60
C30, CH_2	33.69	33.65
$COOCH_3$	53.17	53.05
6-$OCOCH_3$	170.90	170.26
6-$OCOCH_3$	21.10	20.99

Table 3.20: Mass spectrum fragmentation of purified compounds.

Compound (1) 3,6-*O,O*-Diacetylswietenolide: Colourless needles. EIMS *m/z* 570 (M^+), 510, 474, 446 (base peak), 439, 414, 386, 354, 326, 301, 283, 255, 207, 173, 137, 119, 95.

Compound (2) Swietenine: Colorless needle. EIMS *m/z*: 568 (M^+), 550 (M^+-H_20), 535 (M^+-H_2O-H), 468, 451, 419, 283, 253, 207, 155 and 83 ($C_4H_7CO^+$, base peak).

Compound (3) 3-*O*-Tigloylswietenolide: Colorless needle. EIMS *m/z*: 568 (M^+), 550 (M^+-H_20), 535 (M^+-H_2O-H), 479, 444, 426, 355, 283, 255, 207, 119 and 83 ($C_4H_7CO^+$, base peak).

Compound (4) Swietenolide: Pale yellowish oil. EIMS *m/z*: 568 (M^+), 550 (M^+-H_20), 535 (M^+-H_2O-H), 468, 451, 419, 283, 253, 207, 155 and 83 ($C_4H_7CO^+$, base peak).

Compound (5) Hexadecanoic acid ($C_{16:0}$). White coloured crystalline powder. MS *m/z*: 256 (M^+), 213, 185, 171, 157, 129, 115, 97, 83, 73 and 60.

Compound (6) Proceranolide. Colorless needles. EISM *m/z*: 470 (M^+), 452, 374, 346, 318, 273, 246, 210, 189, 173, 149, 137, 119, 105 and 91.

Compound (7) Khayasin T. EIMS *m/z*: 552 (M^+), 456, 428, 356, 328, 313, 281, 256, 207, 149, 119 and 83 ($C_4H_7CO^+$, base peak).

Compound (8) 6-O-acetylswietenolide. Colorless needles. EIMS *m/z*: 528 (M^+), 528 (M^+), 468, 432, 404, 372, 344, 326, 301, 255, 207, 137, 119 and 95.

3.4 Evaluation of cytotoxic effects of compounds purified from SMEAF

The purified compounds isolated from SMEAF were evaluated their cytotoxic effect on selected cancer cells using MTT assay. A 72h exposure to colon cancer cells HCT116 particularly by 3-*O*-tigloylswietenolide (3), hexadecanoic acid (5), proceranolide (6) and khayasin T (7) led to significant reduction of cell viability. As shown in Table 3.21, the IC_{50} values of corresponding compounds were 40.06 ± 0.71 µg/ml, 21.34 ± 0.27 µg/ml, 80.41 ± 1.79 µg/ml and 82.29 ± 3.67 µg/ml. This indicated the present of bioactive compounds in SMEAF that able to cause cytotoxic effect on HCT116 cell line.

Moreover, those isolated compounds were also tested for their cytotoxic effects on HT-29, KB, CasKi and MCF-7 cell lines. As indicated at Table 3.21, only hexadecanoic acid (5) and proceranolide (6) were active against all screened cell lines. Compound 3-*O*-tigloylswietenolide (3) the strongest puried limonoid in this experiment on HCT116 showed no effect on other cell lines except Caski where the IC_{50} value stand at 93.81 ± 0.43 µg/ml. The four limonoids namely diacetylswietenolide (1), swietenine (2), swietenolide (4) and 6-O-acetylswietenolide (8) showed no cytotoxic effect at concentration up to 100 µg/ml.

Table 3.21: IC_{50} values (μg/ml) of purified compounds from SMEAF against different cell lines, calculated after 72 h exposure.

Compounds	Cell lines				
	HCT 116	HT-29	KB	CasKi	MCF-7
Diacetylswietenoldie (1)	>100	>100	>100	>100	>100
Swietenine (2)	> 100	>100	>100	>100	>100
3-*O*-Tigloylswietenolide (3)	40.06±0.71	>100	>100	93.81±0.43	>100
Swietenolide (4)	>100	>100	>100	>100	>100
Hexadecanoic acid (5)	21.34±0.27	18.86±0.28	18.08±0.30	41.06±1.42	30.61±3.51
Proceranolide (6)	80.41±1.79	67.63±1.39	38.69±1.18	70.85±0.96	61.85±2.04
Khayasin T (7)	82.29±3.67	>100	19.08±4.04	>100	>100
6-O-acetylswietenolide (8)	>100	>100	>100	>100	>100

The data represent mean ± S.E. of three independent experiments (n=9).

3.5 Swietenine derivative

The chemical modification of swietenine into its derivative as described in section 2.2.7 in methods was initiated with 81 mg starting material. After the reaction, the purification of the swietenine derivative was conducted using column chromatography with a constant gradient solvent system with 10% ethyl acetate increment in hexane was eluted. The fractionation of the chemical composition was determined by TLC. After concentrated under reduced pressure, pure form of swietenine derivative (60.2 mg) was obtained which represented 74.32% of total conversion. The NMR spectrum data of swietenine derivative are shown on Table 3.22. As compared to the literature the swietenine derivative is known as swietenine acetate, which can be found in seeds of *S. macrophylla* (Taylor and Taylor, 1983b).

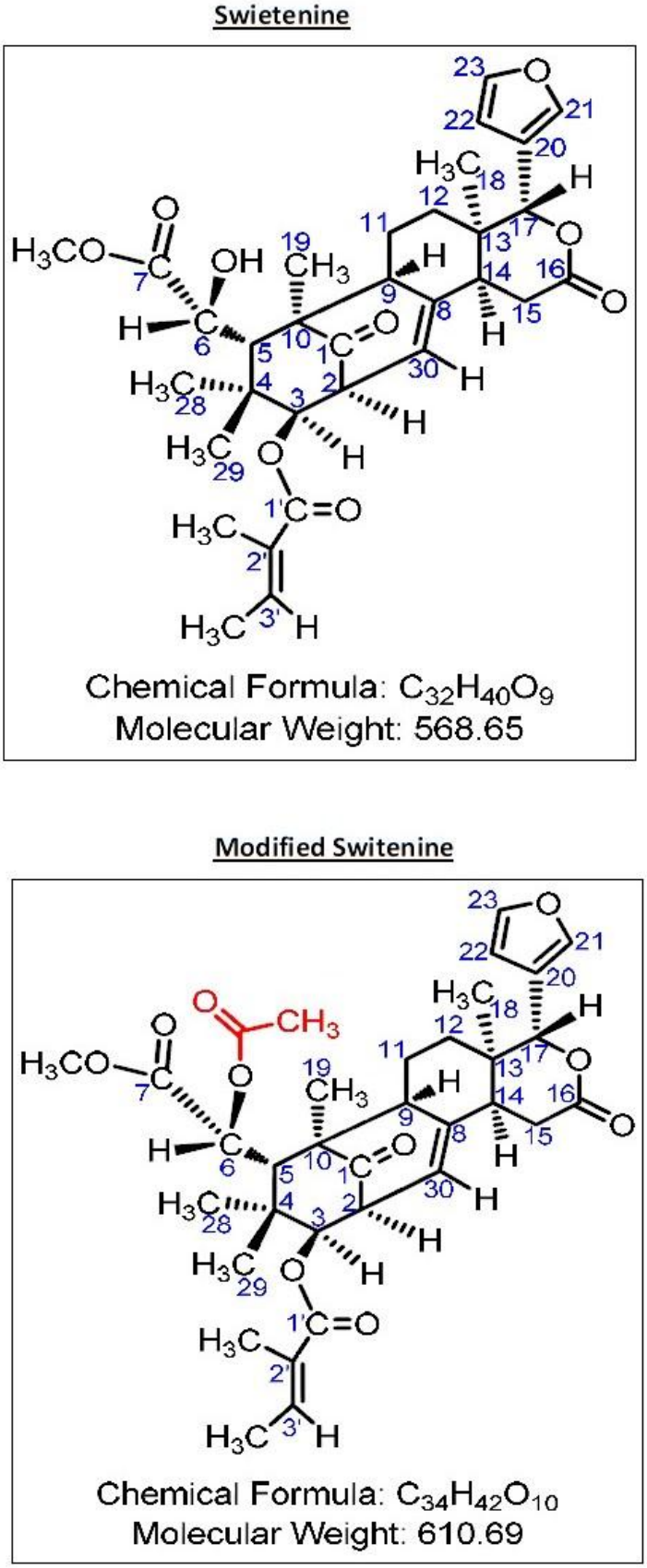

Figure 3.34 The structure of swietenine and its chemical-modified derivative or which known as swietenine acetate.

Table 3.22: The comparison of ^{1}H and ^{13}C NMR spectral of swietenine and its modified swietenine derivative (swietenine acetate).

No.	1H		13C	
	Switenine δH (ppm)	Modified δH (ppm)	Switenine δC (ppm)	Modified δC (ppm)
1	-	-	216.53	216.14
2	3.52 ddd (9,8,1.5)	3.48 t (9)	48.95	48.83
3	4.64 d (9)	4.64 d (9.6)	78.41	77.95
4	-	-	39.04	39.03
5	3.50 brs	3.67 s	45.47	44.56
6	4.56 brs	5.53 s	72.87	72.81
7	-	-	175.97	171.22
8	-	-	138.28	138.55
9	2.30 ddd (13,4,1.5)	2.21 ddd (13,4,2)	57.56	57.51
10	-	-	50.39	50.19
11	1.81 m	1.76 m	21.28	21.06
	2.05 qd (13,4)	2.13 m		
12	1.46 ddd (17,11,4)	1.40 ddd (15,14,4)	34.64	34.51
	1.77 m	1.76 m		
13	-	-	36.73	36.83
14	2.23 ddd (5,2,1.5)	2.17 m	45.09	45.18
15	2.83 dd (18,5)	2.82 dd (19,6)	29.57	29.60
	2.76 dd (18,2)	2.76 d (18)		
16	-	-	168.45	168.76
17	5.54 s	5.51 s	76.71	76.76
18	0.97 s	0.98 s	21.28	21.17
19	1.45 s	1.14 s	16.53	15.74
20	-	-	121.38	120.97
21	7.56 dd (1.8,1)	7.65 s	140.54	141.30
22	6.38 dd (1.8, 1)	6.39 d (0.9)	109.24	109.53
23	7.45 t (1.8)	7.40 t (1.8)	143.20	143.21
24	-	-	-	-
25	-	-	-	-
26	-	-	-	-
27	-	-	-	-
28	1.12 s	1.06 s	22.80	22.80
29	0.89 s	0.92 s	23.05	22.94
30	5.34 dt (8,1.5)	5.27 d (7)	123.66	123.18
$COOCH_3$	3.76 s	3.69 s	$COO\underline{C}H_3$ 53.28	53.25
1'	-	-	166.92	166.98
2'	-	-	127.77	127.58
3'	6.87 qq (7,1.5)	6.87 qq (7,1.4)	139.02	139.54
2'-CH_3	1.82 brs	1.76 brs	2'-$\underline{C}H_3$ 11.75	11.79
3'-CH_3	1.74 brd (7)	1.68 m	3'-$\underline{C}H_3$ 14.64	14.73
$COCH_3$	-	2.16 s	$CO\underline{C}H_3$	21.52
C=O	-	-	C=O	169.83

3.6 Cytotoxic effect of swietenine acetate on HCT116 cell line

Evaluation of the cytotoxic properties of swietnine acetate on HCT116 cell line was performed using MTT assay. Concentrations ranging from 3.125- 50 µg/ml of the named compound were applied to cancer cells and the level of formed formazan was determined after 72 h of incubation period. As shown in Figure 3.35 the increasing concentrations of treatment compound caused dose-dependent decrease in cell viability. The treatment of cells with 3.125 µg/ml of swietenine acetate caused the viability of cells to reduce to 94.03 ± 0.30%. Further increase in the concentrations of 6.25, 12.5, 25 and 50 µg/ml resulted in the prominent decrease of viability percentage to 87.42 ± 0.90, 77.43 ±1.05, 65.36 ±2.24 and 56.31 ±0.98 % respectively. This indicated the cell proliferation or growth was hindered when incubated with the presence of swietenine acetate.

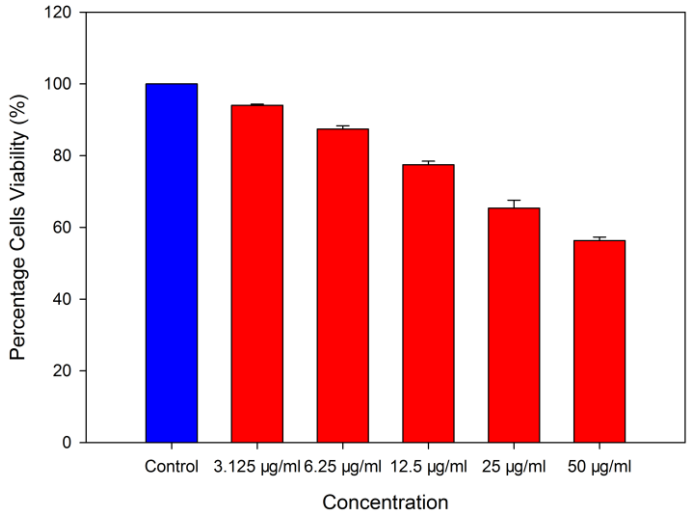

Figure 3.35 Effect of swietenine acetate on the viability of HCT 116 cells. HCT 116 cells were treated with vehicle DMSO (control) or with increasing concentration (3.125-50 µg/ml) of swietenine acetate for 72 h and then followed by measurement of cell viability using MTT assay. Results were expressed as mean percentage of cell viability (ratio of absorbance in treated cells to control cells) ± S.E. of three experiments.

3.7 Evaluation of apoptotic effect of swietenine derivative in HCT16 cells

3.7.1 Morphological analysis of swietenine acetate treatment on HCT116 cancer cell line

Swietenine, one of the purified limonoids from SMEAF has been shown to pose solubility problem as it crystalized shortly after treatment. As indicated in Figure 3.36 swietenine formed crystal structure after treatment on HCT116. There were no changes in the morphological appearances of the treated cells, reflecting the high possibility of null cytotoxic effects was due to the lack of contact between the compound and cells.

A single dose 50 μM of swietenine acetate or derivative of swietenine treatment on HCT116 was evaluated. The nuclear changes of the cells exposed to swietnine acetate appeared to be shrinkage and condensed chromatin as evidence of the morphological hallmark of apoptotic nuclei. As compared to the switenine, swietenine acetate dissolved completely in aqueous solution and thereby exerting its effects on HCT116 cells.

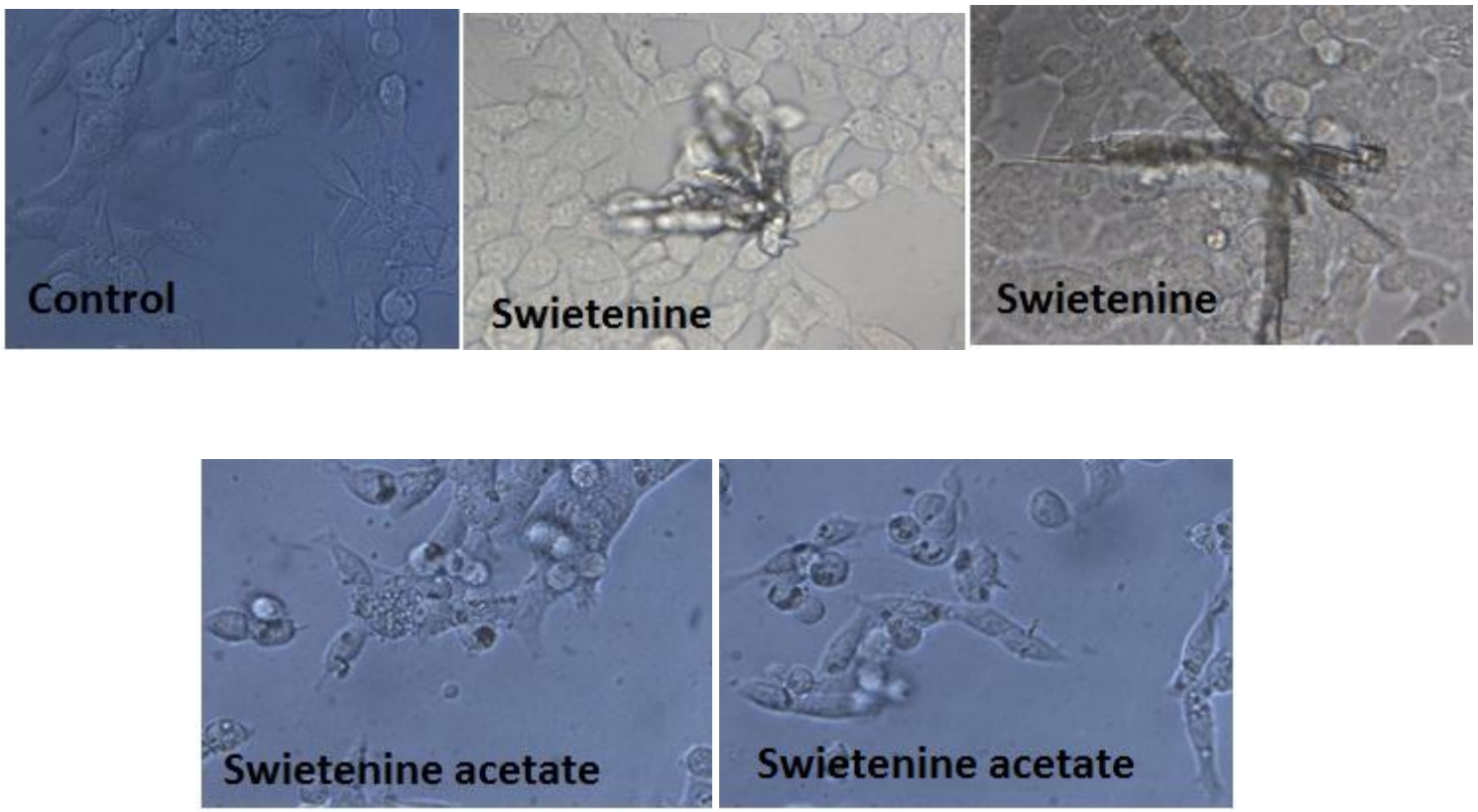

Figure 3.36 Effect of swietenine and its derivative (swietenine acetate) on morphological changes of HCT 116 cells. The figures showed cells were either treated with 25 µg/ml of swietenine or 50 µM of swietenine acetate for 48 h. the untreated cells represents HCT116 cells without treatment at 0 h. The cells were visualized under light microcope and photographed. Magnification: 200X

3.7.2 Hoechst-propidium iodide staining

To gain further insight into the effect of swietenine acetate on nuclear and membrane alteration, treated cells were stained with Hoechst-propidium iodide stains. As shown in Figure 3.37, the cells underwent remarkable nuclear changes upon treatment. Control or untreated cells were uniformly stained with blue fluorescence Hoechts stain and were not stained with red-fluorescence propidium iodide indicating that the nuclei of cells and membrane of the cells were intact. When exposed to swietenine acetate HCT116 cells showed an increase in intensity captured on blue and red fluorescence signals where the cells manifested two apoptotic morphological changes, namely nuclear condensation and alteration of cell membrane integrity.

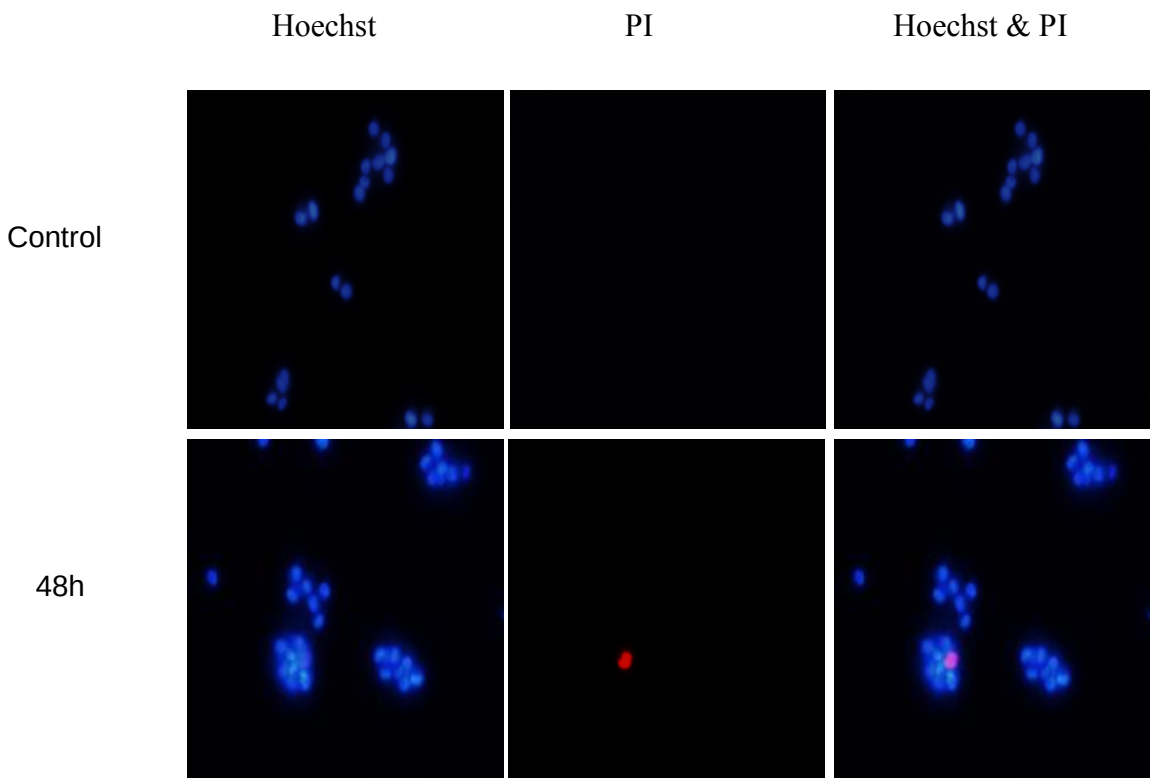

Figure 3.37 Effect of swietenine acetate on HCT116 cells stained with Hoechst and Propidium iodide. Cells were incubated without or with 50 µM of swietneine acetate for 48 h. At the indicated time, the cells were harvested and stained with Hoechst and Propidium iodide and visualized by fluorescence microscope and photographed. An intense blue and red fluorescence signals captured on SMEAF treated cells indicating condensation of cell nuclei and disruption of cell membrane integrity.

3.7.3 Detection of Reactive Oxygen Species (ROS) production induced by swietenine acetate

ROS is known to play an important role in apoptosis induction (Simon *et al*., 2000). The formation of the intracellular ROS level upon the treatment of swietenine acetate was evaluated utilizing the sensitive probe known as DCFH-DA according to the method described earlier in Section 2.2.9.2. Intracellular ROS level was found to increase after swietenine acetate treatment for 4 h. Further analysis revealed the swietenine acetate caused up to 152.6 ± 6.7 fold ROS level increase in treated cancer cells compared to control cells. This indicated that swietenine acetate may cause treated HCT116 cells to undergo oxidative stress.

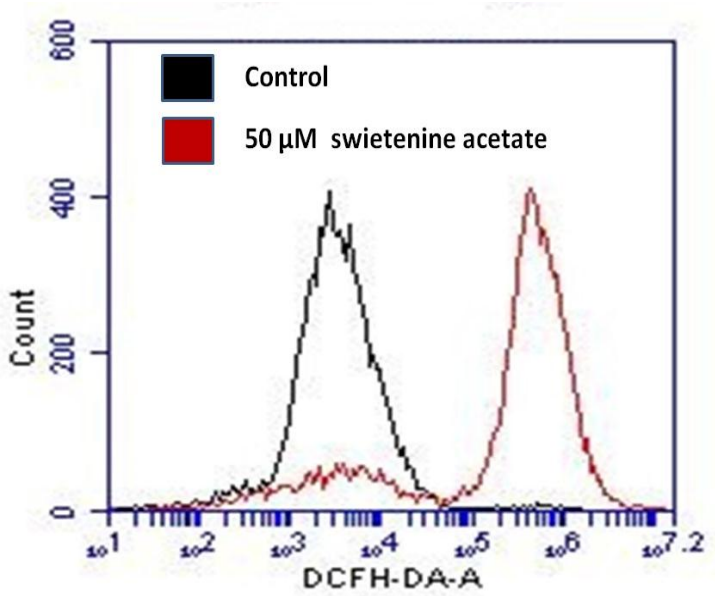

Figure 3.38 Effect of swietenine acetate on intracellular ROS production in HCT 116 cells. DCF-DA fluorescence probe was employed as described in material and methods. The black histogram represents the control, treated with vehicle (0.5 %, DMSO) and red histogram represents the treated HCT 116 cells with 50 µM of swietenine acetate.

3.7.4 Swietenine acetate depleted intracellular total glutahione (GSH) level

The measurement of intracellular total GSH content was conducted by using a colorimetric quantitative method. As depicted in Figure 3.39, treatment of HCT116 cells with swietenine acetate exhibited a time-dependent attenuation in the level of GSH. Compared to the control cells, a significant reduction in the intracellular GSH level in the treated cells was observed at all indicated time periods. Thus, treatment of HCT116 cells with swietenine acetate caused the decrease of intracellular GSH from 27.4±2.14 nmoles (control) to 13.38±1.55 nmoles (24h) 13.2±1.20 nmoles (48h) and finally, 12.42 ±1.34 nmoles (72h).

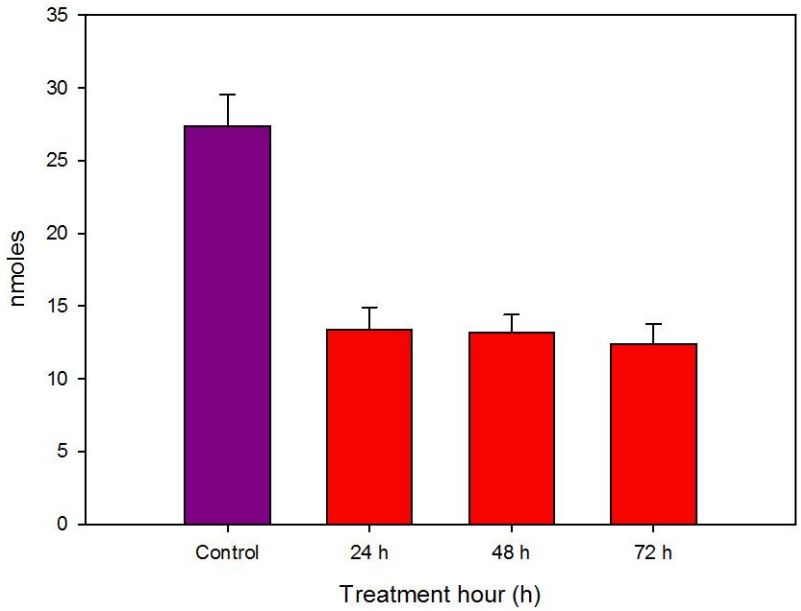

Figure 3.39 Effect of swietenine acetate on intracellular total glutathione level of HCT116 cells at 24, 48 and 72 hours following treatment. The data represent mean ± S.E. of three independent experiments (n=9).

3.7.5 Swietenine acetate dissipated mitochondrial membrane potential

In an attempt to gain further insight whether swietenine acetate exposure in HCT116 cells involved a change in mitochondrial membrane potential (Δψm), we measured the Δψm using the fluorescence probe JC-1. As shown in Figure 3.40 [A], most of the JC-1 fluorescence appeared in the upper quadrant in the control cells. However, after exposure to swietenine acetate, there was a shift of fluorescence signal resulting in the treated cells having lower red fluorescence than the control cells. Intriguingly, the loss of red fluorescence was found intensified in a time-dependent manner. Based on the JC-1 fluorescence ratio, swietenine acetate caused a substantial time-dependent reduction of red/green fluorescence (Figure 3.40 [C]).

[A] [B]

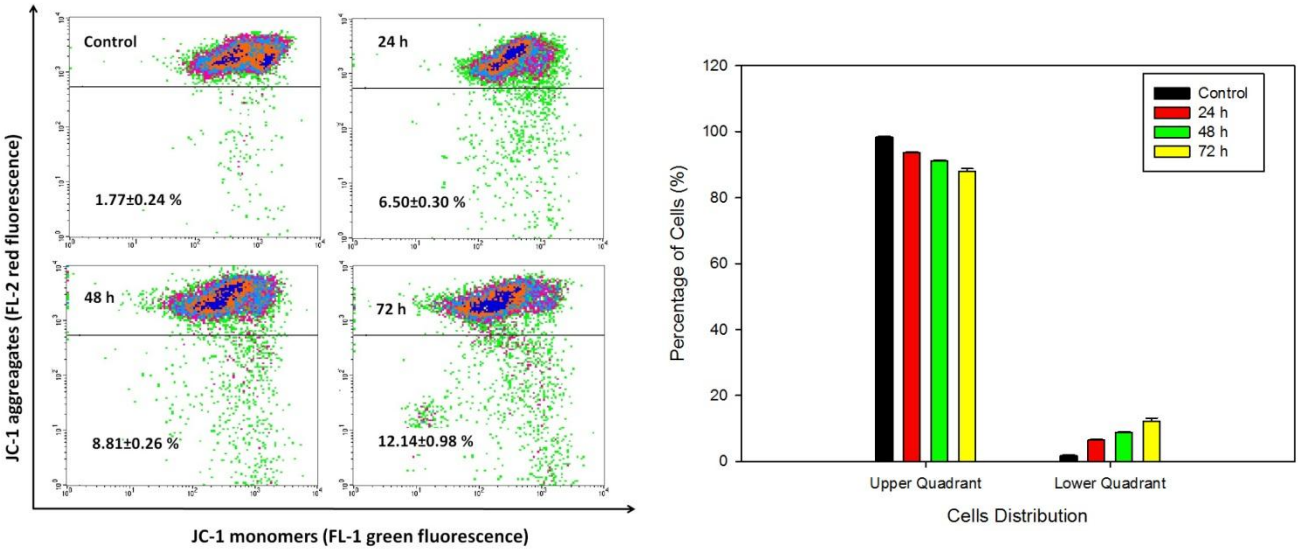

Figure 3.40 Effect of swietenine acetate on mitochondrial membrane potential (Δψm) of HCT 116 cells. HCT 116 cells were incubated in the absence (control) or 50 µM of swietenine acetate for 24 h, 48 h and 72 h. After treatment, the cells were stained with JC-1 and analysed with flow cytometer. Data presented are representative of means ± S.E. calculated from three individual experiments. [A] Flow cytometry, fluorescence patterns analysis of JC-1 staining. [B] Bar charts showed the percentage in the distribution of HCT 116 cells in the upper and lower quadrants of intensity plot.

[C]

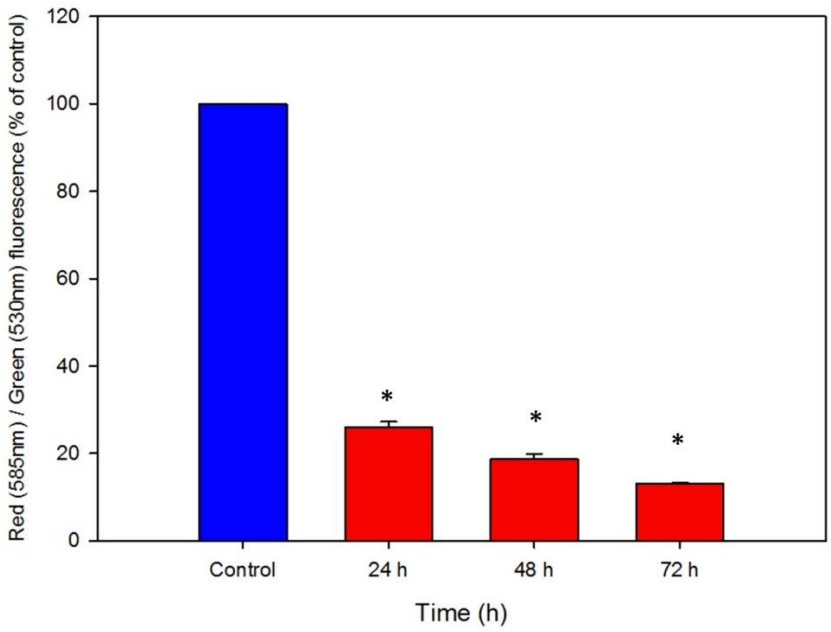

Figure 3.40, continued [C] Bar charts showed the quantitative presentation of the data as red (585nm) / green (530 nm) fluorescence, expressed as percentage of control, indicated ratio high / low Δψm. Data presented are representative of means ± S.E. calculated from three individual experiments. The asterisk (*) represented significantly difference from control (* $p < 0.05$).

3.7.6 Swietenine acetate increased the expression of Bax, decreased the expression of Bcl-2 and augmented the ratio of Bax/Bcl-2

The involvement of Bcl-2 family protein members in swietenine acetate induced apoptosis were examined using Q-PCR. As depicted in Figure 3.41, Bax expression increased slightly after 6 h and 12 h treatment. At 24 h, the expression level was found to be around 2 folds higher compared to control. Further investigation of the expression level of Bcl-2 revealed that swietenine acetate treatment eventually decreased the expression level of Bcl-2 significantly in time-dependent manner. The increase in Bax and decrease in Bcl-2 expression significantly elevated the Bax/Bcl-2 expression ratio, thus sensitizing the cells to apoptotic stimuli. Taken together, these results showed that swietenine acetate was able to induce apoptosis by altering the regulation of apoptotic genes particularly through up-regulation of Bax and down-regulation of Bcl-2.

[A] [B] [C]

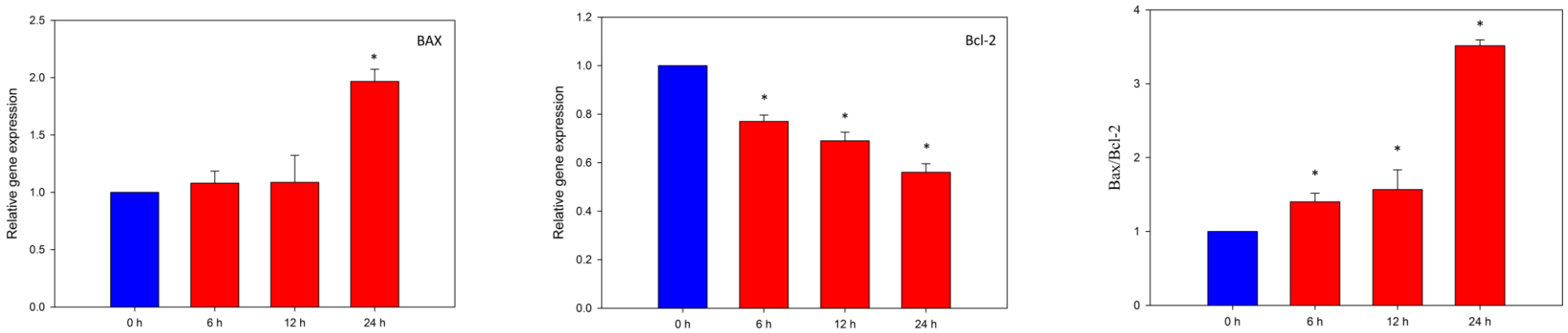

Figure 3.41 Effect of SMEAF on gene expression level of Bax and Bcl-2 in HCT116 cells. Cells were treated with 50 µM of swietenine acetate for different time periods. After designated exposure times, cells were harvested and the total RNA was extracted. The RNA was subjected to q-PCR analysis as described in methods. [A] The relative gene expression level of Bax was compared to control, [B] The relative gene expression level of Bcl-2 was compared to control which were normalized against PBGD expression using the formula $2^{-\Delta\Delta CT}$. [C] Values are means ± S.D. of three experiments. Asterisks indicate a significant difference between untreated and treated cells (*$P < 0.05$).

3.7.7 Bax and Bcl-2 proteins changes induced by swietenine acetate

The intracellular immunofluorescence staining method by flow cytometry was performed to confirm the expression of Bax and Bcl-2 in individual cells. As seen in Figure 3.42, the Bax histogram showed a shift to the right while there was no shift in the Bcl-2 histrogram. Respectively, this reflected an increase of Bax and no change of Bcl-2 associated immunofluorescence. The results for Bax were consistent with the Q-PCR results, however not in case of Bcl-2 where the Q-PCR expression was lower but not in its protein expression level. However, despite the null changes in Bcl-2, the high level of Bax expression is till noteworthy in delivering the notion that the swietenine acetate-induced apoptosis in HCT 116 cells was mediated through mitochondrial pathway.

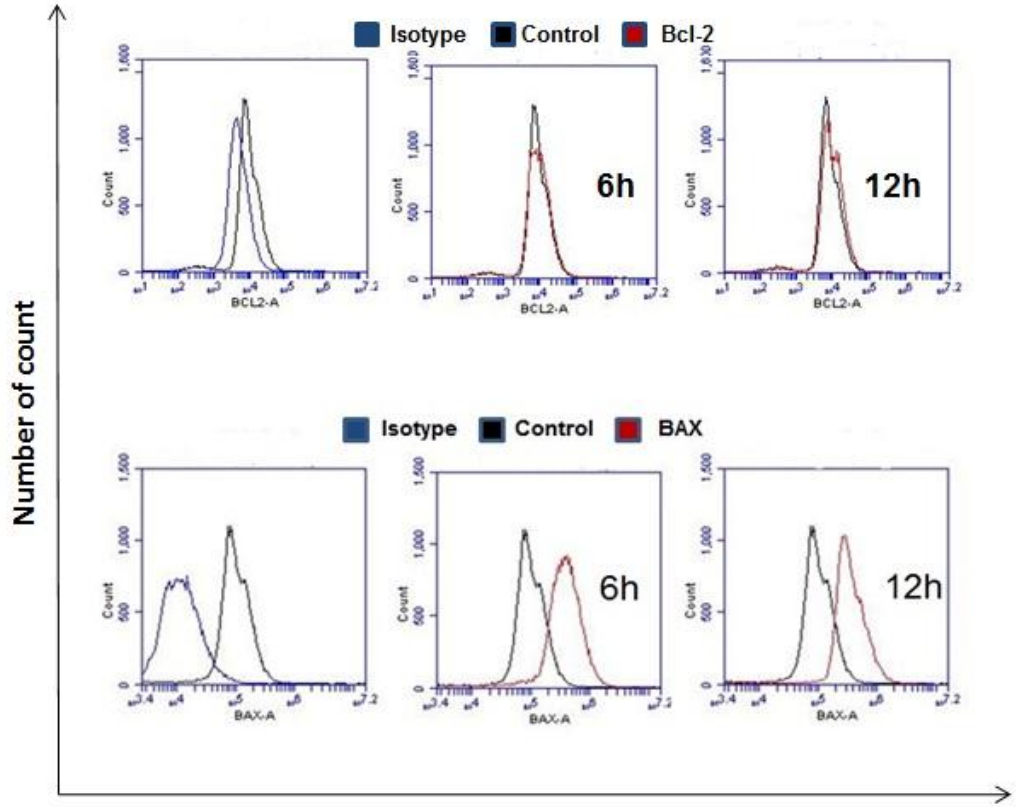

Figure 3.42 Effect of swietenine acetate on protein expression level of Bax and Bcl-2 in HCH116 cells. After treated with μM of swietenine acetate for different times, the cells were harvested and intracellular levels of Bax and Bcl-2 were determined as described in methods. Representative overlay of histrograms, showing Bax-associated immunofluorescence and Bcl-2-assiociated immunofluorescence.

3.7.8 SMAC protein elevated by treatment of swietenine acetate

SMAC or also referred as second mitochondria-derived activator of caspases is a mitochondrial protein that participates in apoptotic cell death by means of sequestering a number of members of inhibitors of apoptosis proteins (IAPs) (Velazquez *et al*., 2007). The release of SMAC by mitochondria into cytosol promotes cytochrome-c dependent activation of caspases in apoptosis (Vucic *et al*., 2002). Swietenine acetate treatment was found to cause increased expression level of SMAC protein in a time-dependent manner detected in protein array analysis (Figure 3.43). The level of SMAC protein was found to increase more than four folds as compared to control cells, indicating the down-stream event after the release of cytochrome c in mitochondrial-mediated apoptosis.

[A]

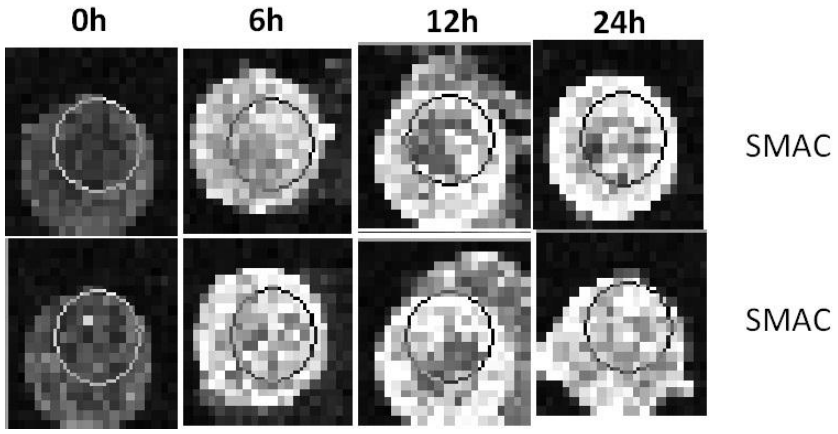

[B]

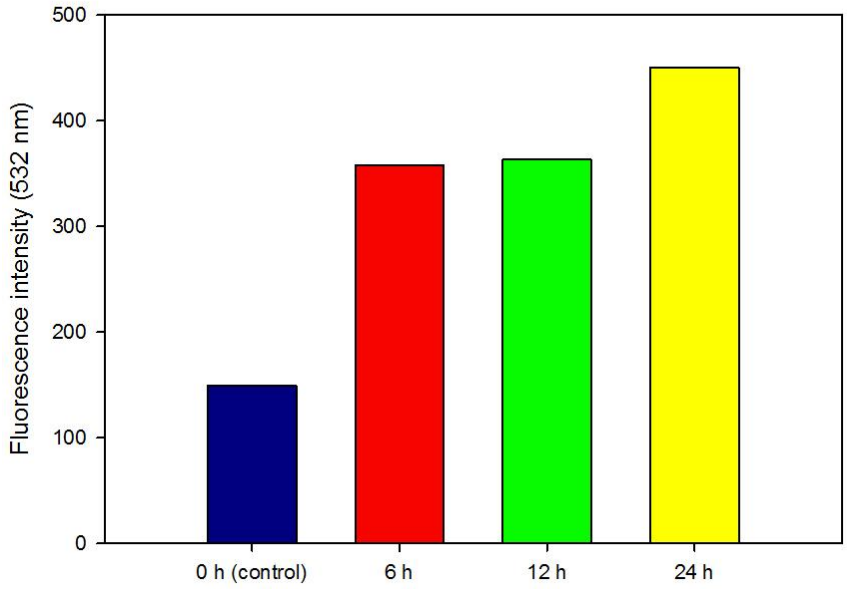

Figure 3.43 Protein expression level of SMAC at 0 h (control), 6, 12 and 24 h exposure to 50 µM of swietenine acetate in HCT116 cell line. [A] RayBiotech protein array analysis on control and treated cells photographed by GenePix 4000B. [B] Means of duplicates fluorescence signals of SMAC control (0 h), 6, 12 and 24 h swietenine acetate treated cells after subtracted with background and normalized against pre-coated positive control probes using Acuity 4.0 analysis software.

3.7.9 Caspase -3/7 and -9 involved in switenine acetate induced apoptosis

Involvement of executioner Caspase -3/7 and initiator Caspase -9 were evaluated. The ability of swietenine acetate to activate the caspases was studied using fluorescence linked inhibitor of caspase -3/7 and -9. The HCT116 cells were incubated with 50 µM of swietenine acetate for 3, 6, 12 and 24 hours followed by addition of the fluorescent inhibitor and results of flow cytometer analysis were showed in Figure 3.44[A]From the histograms, the intensity of fluorescence signals of caspase -3/7 was detected to be higher throughout the treatment period. Meanwhile, evaluation of initiator caspase -9 activity was shown in Figure 3.44[B]. There was a slight increase in caspase -9 activity at 3 and 6 h followed by a more pronounced augmentation at 12 and 24h of incubation periods. Therefore, the results suggested that swietenine acetate was able to induce apoptosis through execution by caspase cascade especially through caspase -3/7 and -9.

[A]

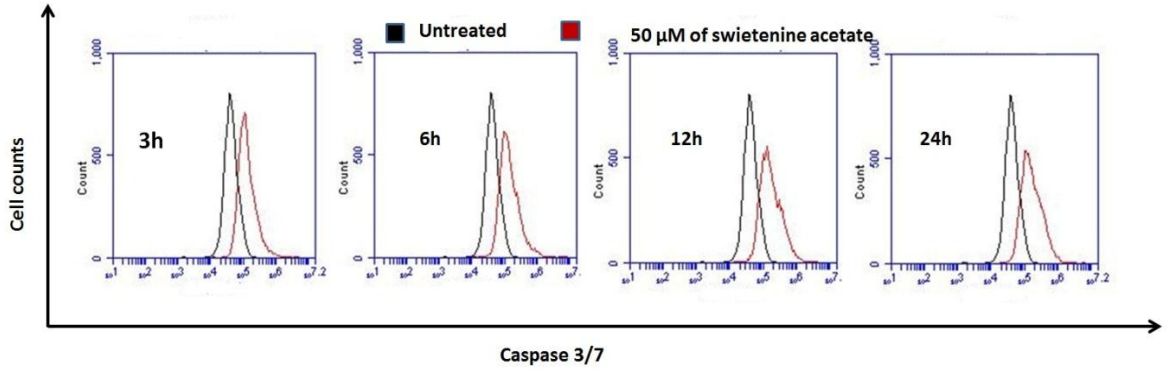

[B]

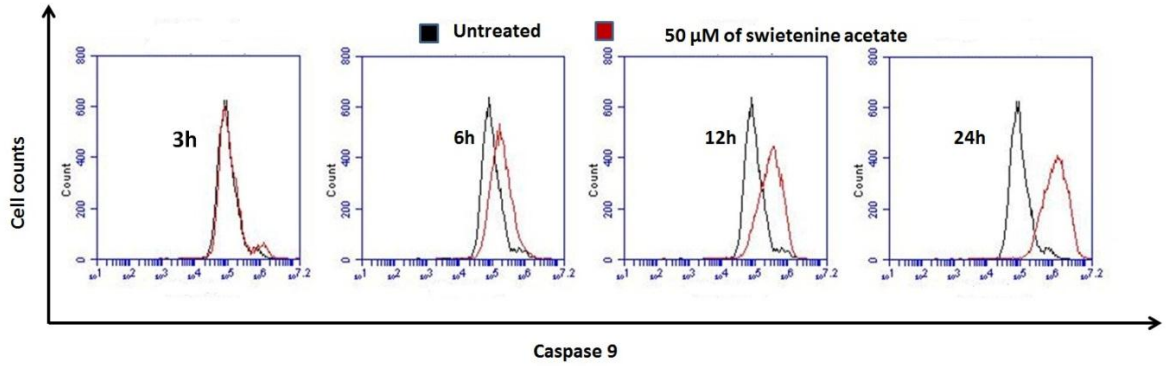

Figure 3.44 Effect of swietenine acetate on caspase level of HCT 116 cell. The HCT 116 cells were incubated in the absence (control) or 50 µM of swietenine acetate for 3 h, 6 h, 12 h and 24 h. After treatment, the cells were stained with FAM-DEVD-FMK (Caspase -3/7) or FAM-LEHD-FMK (Caspase -9) and analysed with flow cytometer. Representative overlay of histrograms [A] showing Caspase -3/7- associated fluorescence signal, while [B] showing Caspase -9-assiociated fluorescence signal.

3.7.10 Swietenine acetate arrested cells in G1-phase and increased Sub-G1 population

Meanwhile, cell cycle analysis on HCT116 also showed arrest of G1 phase by the swietenine acetate treatment. As depicted in Figure 3.45, the percentage of G1 phase cells was shown to increase from 64.13 ±0.86% to 70.52±0.41% in 24 h treatment period. The prolonged treatment with swietenine acetate for 48 h and 72 h showed an increase in Sub-G1 population up to 52.96 ±0.57% compared to control cells which was 1.57 ±0.16% indicating a shift in arrested cells towards Sub-G1 population which is known as apoptotic population. This population of cells possess sub-diploid DNA content which is indicative of DNA fragmentation occurring during apoptosis (Raveh *et al*., 2001).

[A]

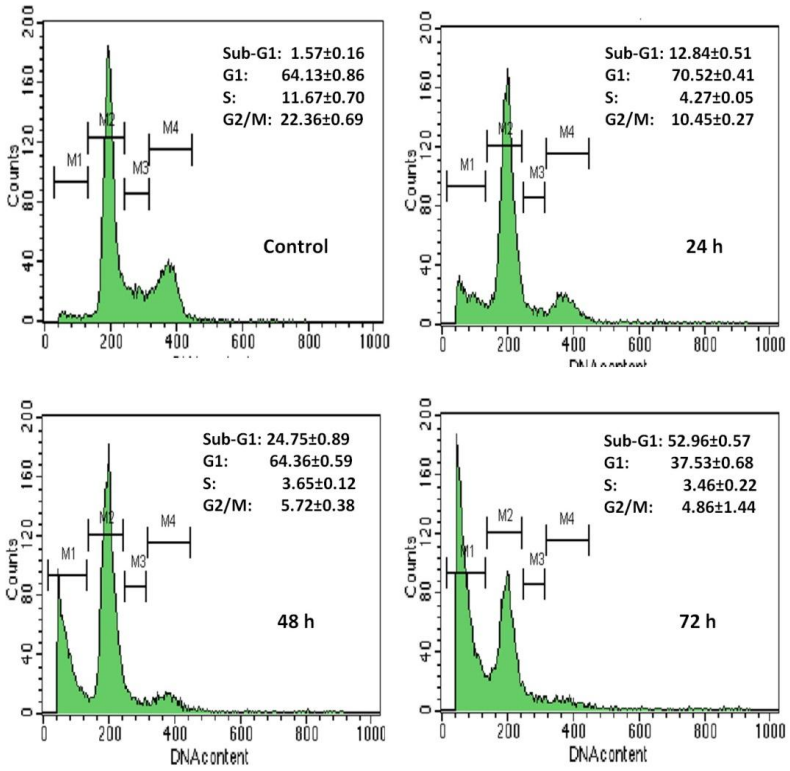

Figure 3.45 Effect of swietenine acetate on cell cycle and apoptosis of HCT 116 cells. The cells were treated with 50 µM of swietenine acetate for 24, 48 and 72 h.

[B]

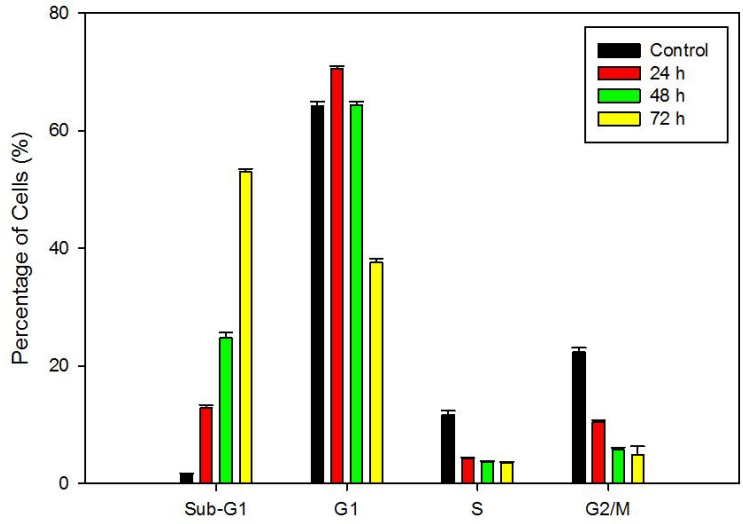

Figure 3.45, continued Effect of swietenine acetate on cell cycle and apoptosis of HCT 116 cells. The cells were treated with 50 μM of swietenine acetate for 24, 48 and 72 h. The untreated corresponded to cells without swietenine acetate treatment at 0 h and similar results were obtained at other incubation time periods. After treatment, cells were harvested, fixed, stained with PI and analysed by flow cytometry as described in the methods. [A] Representive histograms showed the cell cycle phase distribution. [B] Bar charts showed the percentage of cells in sub-G1, G1, S and G2/M phases of the cell. Results are mean value ± S.D. of three experiments.

3.7.11 Swietenine acetate induced changes in cell cycle regulatory genes

Cell cycle analysis revealed the alteration in distribution of phases of HCT116 cells after exposure to swietenine acetate. In an effort to gain further insight into the molecular mechanisms affected by swietenine acetate in HCT116 cells, we profiled the expression of key pathways involved in cell cycle using human cancer pathway finder PCR array in swietenine acetate treated cells and control cells. Numerous key genes involved in cell regulatory pathways were altered in their expression levels, specifically CCNE1, CDC25A, CDK2, CDK4 and E2F1 were down regulated and detected by real-time PCR as shown in Figure 3.46. In addition, the Q-PCR study conducted revealed the genes encoding p21 and p53 protein which are known as CDKN1A and TP53 respectively, were up regulated. Besides, swietenine acetate exposure caused the down regulation of MDM2 gene which encodes the negative regulator of p53 was detected after the SMEAF treatment. These data indicated that SMEAF may cause the p53-p21 activation and subsequently lead to cell cycle arrest in HCT116 cells and ultimately apoptosis.

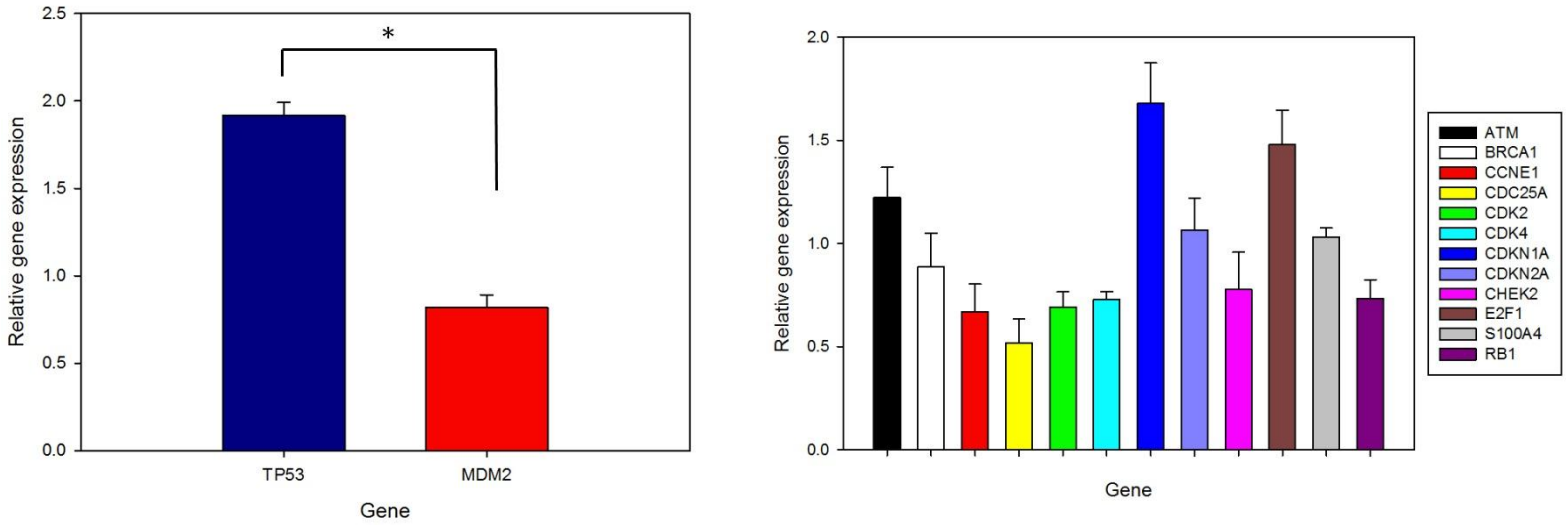

[A] [B]

Figure 3.46 The cells were treated with 50 µM of swietenine acetate, harvested after 24 h incubation and the total RNA was extracted. The RNA was subjected to q-PCR analysis by using PCR array as described in methods. Analysis was done by using RT^2 Profiler Data Analysis Excel platform. The gene expression was normalized against ACTB expression values. Values are mean ± S.D. of three experiments. [A] Effects of swietenine acetate treatment on cell cycle regulatory genes of HCT116 after 24h incubation period. [B] Effects of swietenine acetate on expression level of TP53 and MDM2 after 24h exposure period. Asterisks indicate a significant difference between expression level of TP53 and MDM2 of treated cells (*$P < 0.05$).

3.7.12 p53 and p21 protein expression level detection by using protein array

Protein array analysis was utilized in the determination of protein expression of p53 and p21 proteins in HCT116 cells treated with 50 μM of swietenine acetate. Figure 3.47[A] and Figure 3.48[A], indicated the duplicates of experiments conducted on 0 h (control), 6 h, 12 h and 24 h exposure to swietenine acetate particularly in HCT116. The photographs clearly showed that treatment with swietenine acetate at 6 h, 12h and 24 h caused an increase in the named protein levels as indicated by the sharper fluorescence signals. The fluorescent signals of each of the sample was subtracted with background fluorescent signal and further normalized against pre-coated positive control probes in arrays. Figure 3.47[B] and 3.48[B] showed the mean fluorescent signal of its duplicates. The 0 h or control samples fluorescence intensity for the p53 was shown to increase by ~ 2 folds after a 24 h of swietenine acetate exposure. Meanwhile, p21 protein was found to peak at 12 h of incubation, approximately 4 fold increase as compared to the control. Taken together, these results indicated the possible involvement of p53-p21 proteins in cell cycle regulatory mechanism that resulted in apoptosis.

[A]

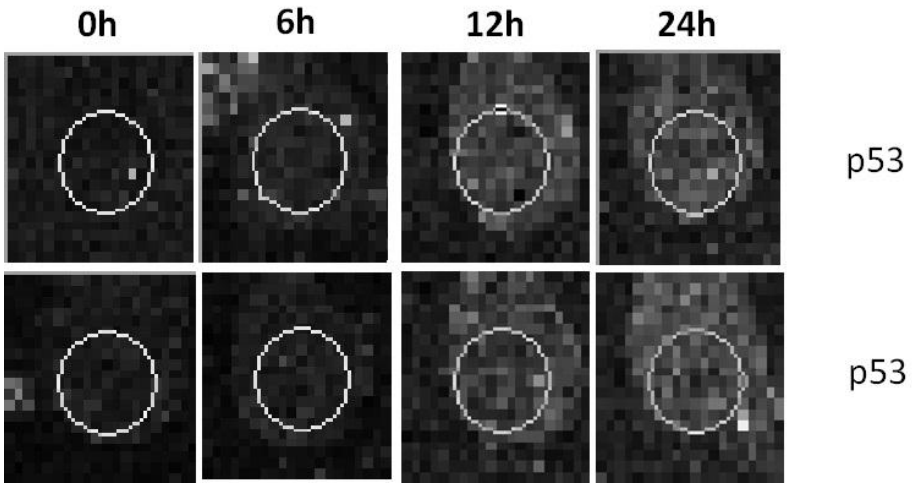

[B]

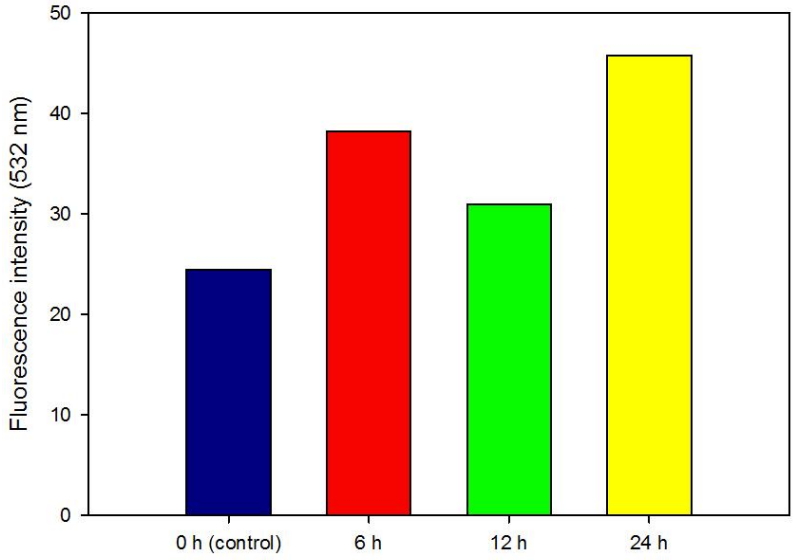

Figure 3.47 Protein expression level of p53 at 0 h (control), 6, 12 and 24 h exposure to 50 µM of swietenine acetate on HCT116 cell line. [A] RayBiotech protein array analysis on control and treated cells photographed by GenePix 4000B. [B] Means of duplicate fluorescence signals of p53 control (0 h), 6, 12 and 24 h in swietenine acetate treated cells after subtraction with background and normalized against pre-coated positive control probes using Acuity 4.0 analysis software.

[A]

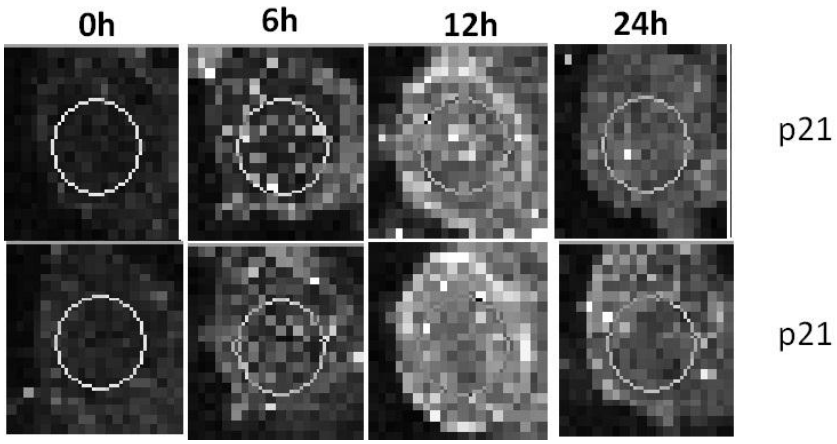

[B]

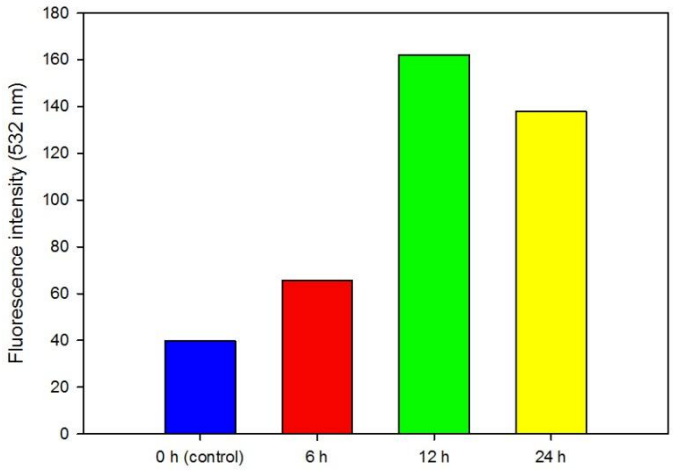

Figure 3.48 Protein expression level of p21 at 0 h (control), 6, 12 and 24 h exposure of 50 µM of swietenine acetate in HCT116 cell line. [A] RayBiotech protein array analysis on control and treated cells photographed by GenePix 4000B. [B] Means of duplicate fluorescence signals of p21 control (0 h), 6, 12 and 24 h in swietenine acetate treated cells after subtraction with background and normalized against pre-coated positive control probes using Acuity 4.0 analysis software.

3.7.13 Caspase -8 and -10 involved in swietenine acetate-induced apoptosis

To check whether swietenine acetate induced activation of initiator caspase -8 and -10 fluorescence analysis detection by using flow cytometry was utilized. The ability of switenine acetate to activate the named caspases were studied using fluorescence linked inhibitor of caspase -8 and -10. The HCT116 cells were incubated with 50 µM of swietenine acetate for 3, 6, 12 and 24 hours followed by addition of the fluorescent inhibitor and the results of flow cytometer analysis were shown in Figure 3.49. From the histograms, the intensity of fluorescence signals of caspase -8 was found to be constant at 3 h of incubation period, the level was then increased further at 6 , 12 and also 24 h. The evaluation of caspase -10 activity is shown in Figure 3.49[B]. There was no change in activity level at 3 h, 6 h and 12 h of treatment periods. However, there was a marked augmentation in activity at 24 h incubation period. Therefore, the increased activities of caspase -8 and -10 activities results suggested swietenine acetate may also exert its apoptotic effects through extrinsic pathway.

[A]

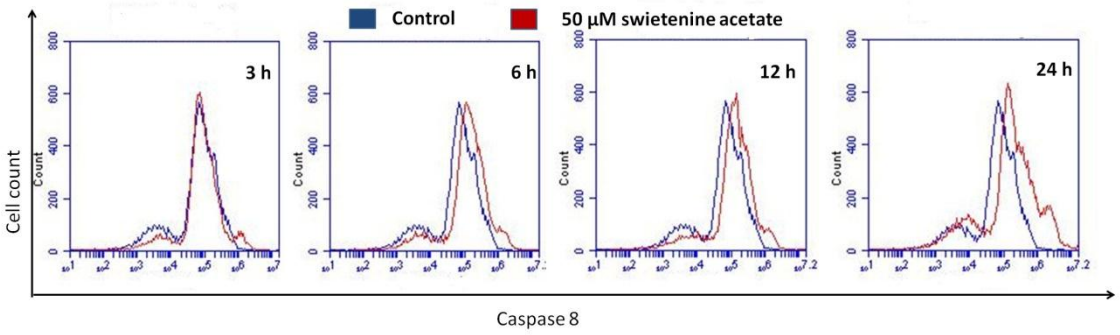

[B]

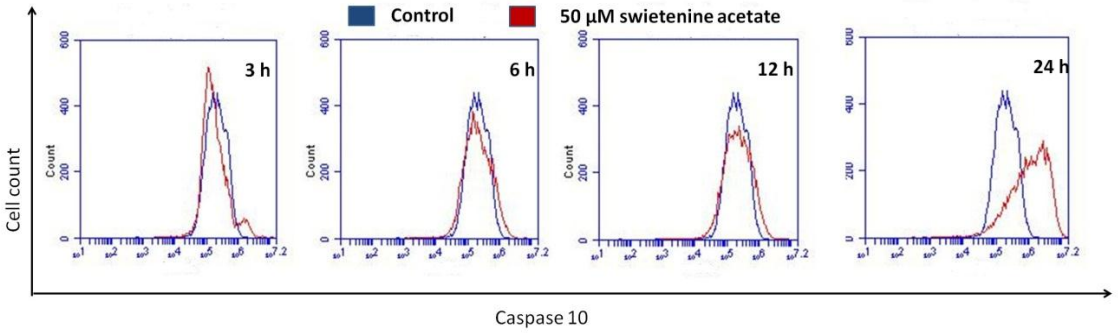

Figure 3.49 Effect of swietenine acetate on the caspase levels in HCT 116 cells. HCT 116 cells were incubated in the absence (control) or 50 µM of swietenine acetate for 3 h, 6 h, 12 h and 24 h. After treatment, the cells were stained with FAM-LETD-FMK (Caspase -8) or FAM-AEVD-FMK (Caspase -10) and analysed by flow cytometry. Representative overlay of histrograms [A] showed Caspase-8-associated fluorescence signal, while [B] showed caspase-10-associated fluorescence signal.

3.7.14 Alteration of extrinsic apoptotic regulatory genes by swietenine acetate

PCR array analysis also revealed alteration of numerous genes involved in extrinsic apoptotic pathway following treatment with swietenine acetate. The results showed that swietenine acetate exposure up-regulated genes encoding tumor necrosis factor receptor superfamily proteins such as TNFRSF1A, TNFRSF10B and also TNFRSF25. Besides, the CASP8 and FAS levels were up-regulated as well upon the treatment. These data suggested the role of swietenine acetate in modulating the expression of genes involved in extrinsic apoptotic pathway (Figure 3.50).

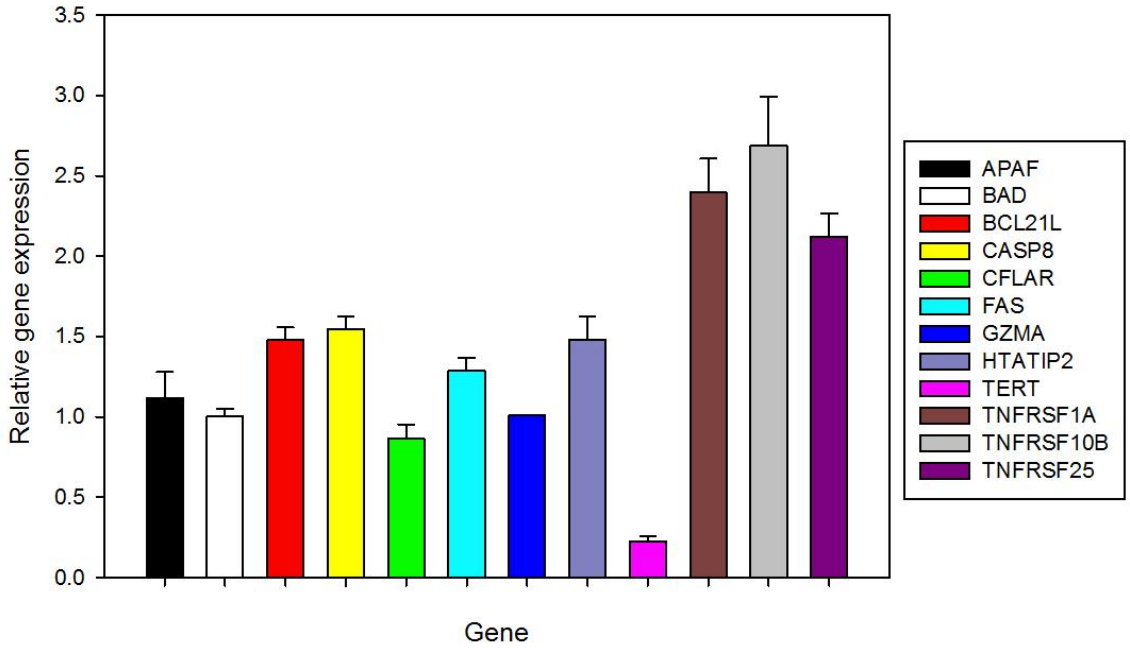

Figure 3.50 The HCT116 cells were treated with 50 µM of swietenine acetate, harvested after 24 h incubation and the total RNA was extracted. The RNA was subjected to q-PCR analysis by using PCR array as described in methods. Analysis was conducted by using RT^2 Profiler Data Analysis Excel platform. The gene expression was normalized against ACTB expression values. Values are means ± S.D. of three experiments.

3.7.15 Swietenine acetate provoked the externalization of phosphatidylserine of HCT116 cells

To further confirm the induction of apoptosis in HCT116 cells, the cancer cells were double stained with annexin V-FITC and PI and results were summarized in Figure 3.51 According to Figure 3.51[A], the control cells were predominantly found in lower left quadrant of the dot plot, indicating the viable cells. After treatment with 50 μM of swietenine acetate for 24 h, the cells were progressively detected in the lower and upper right quadrants. The early apoptotic cells (annexin V+/PI-) began to appear as early as 24 h of treatment, and were found to decrease from 18.57 ± 2.46% (24 h), 14.02 ±2.21% (48 h) and 7.05 ± 0.71% (72 h). On the other hand, the late apoptotic cells (annexin V+/PI+) were found to increase from 8.09 ±1.18% (24 h), 12.18 ±1.16% (48 h) and 16.25 ±0.49% (72 h). However, there was no marked decrease of viable cell population throughout the treatment period in the control untreated cells.

[A]

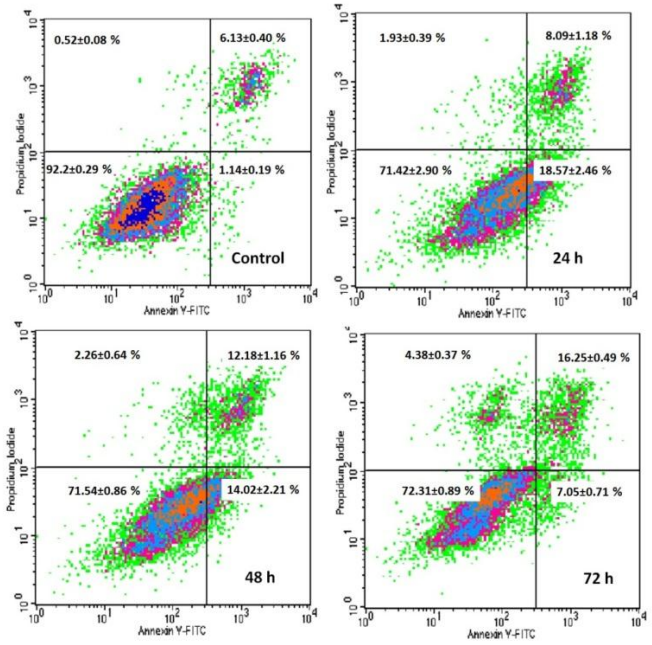

[B]

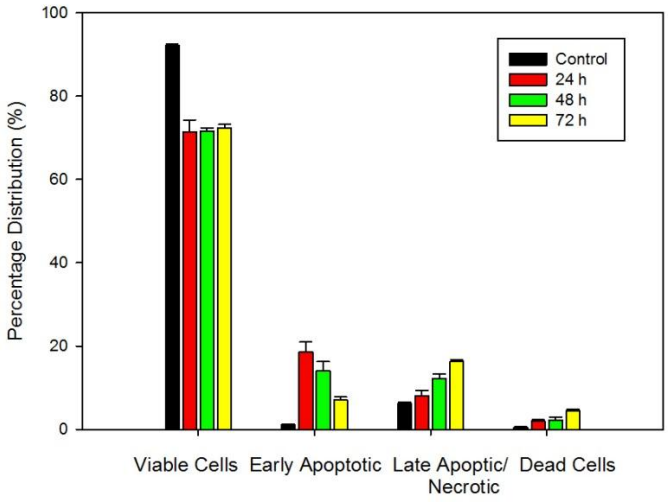

Figure 3.51 Effect of swietenine acetate (50 µM) on the induction of phosphatidylserine externalization and cell membrane integrity in HCT116 cells undergoing apoptosis, measured using flow cytometry analysis. Histogram in [A] shows induction with dual parameters including V-FITC and PI for treatment period, 24, 48 and 72 h; Histogram in [B] shows induction effects on HCT 116 cells at different stages of apoptosis. The data represent mean ± S.D. of three experiments. (n=3).

3.7.16 SDS-PAGE analysis of HCT116 cells lysate treated with swietenine acetate

The cells treated with swietenine acetate were lysed by using Cytobuster solution and separated by using SDS-PAGE. The gel stained with bromophenol blue revealed a sharper and thicker protein band at ~70 KDa observed with increasing treatment period. The mentioned band was marked in red rectangular box shown in Figure 3.52, as evident, the band started to thicken particularly by 48 h and 72 h.

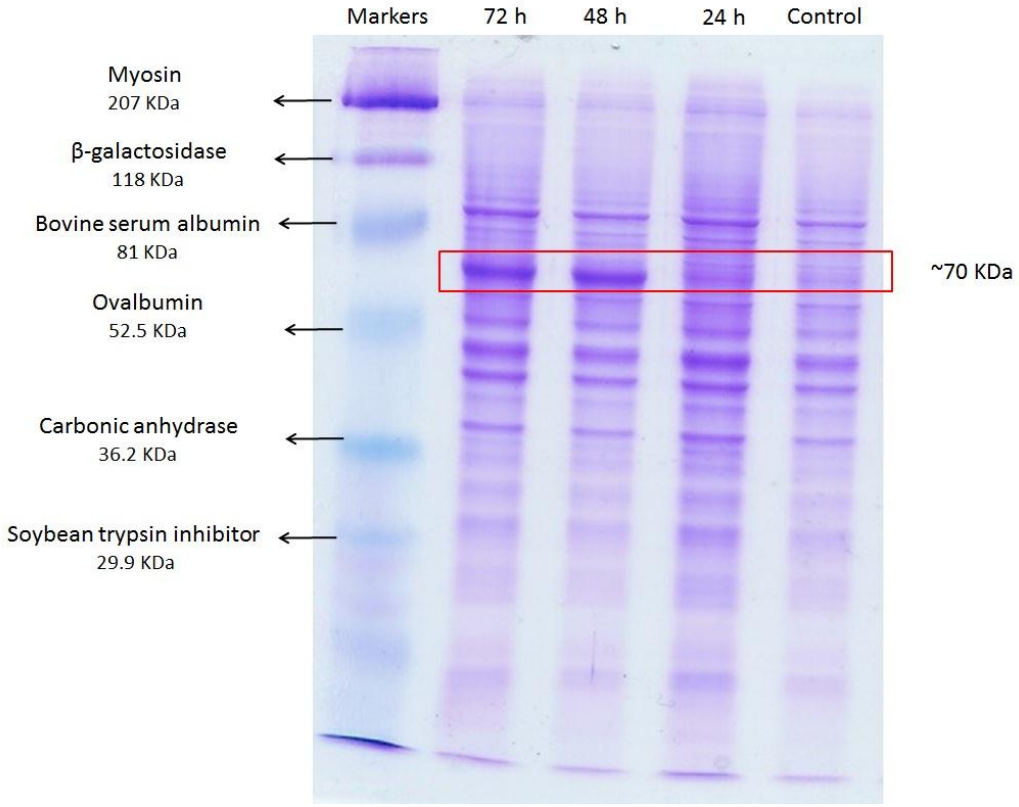

Figure 3.52 HCT116 cells treated with 50 µM of swietenine acetate for different time periods were harvested and lysed. The lysates were subjected to SDS-PAGE analysis. The red rectangular box showed the sharper protein band detected with bromophenol stain.

3.7.17 LC-MS analysis of excised protein band

LC-MS analysis was conducted in order to determine the protein presence in the band detected in the SDS-PAGE. As described in section 3.7.17, the excised protein band was treated and subjected to LCMS analysis. The result obtained are shown in the Table 3.23 The detected proteins including heat shock 70kDa protein 1A/1B, Transketolase and X-ray repair cross-complementing protein 6. Recently, studies have shown that HSPs are involved in apoptosis regulation and HSP 70 is known to be one of the determinants of cell death which acts as anti-apoptotic protein (Helmbrecht *et al*., 2000; Jolly and Morimoto, 2000; Myung *et al*., 2004). Thus, we postulate that protein HSP 70 may exert its anti-apoptotic effect in swietenine acetate-induced apoptosis in HCT116 cells.

Table 3.23: Data showed the proteins detected after excised protein band subjected to LC-MS analysis. Accession numbers are from MASCOT database (http:// www.matrixcience.com).

Protein name	Accession number	Theoretical mass (Da)	Theoretical *pI*	MASCOT score	Queries matched	Sequence coverage (%)
Heat Shock 70kDa protein 1A/1B	P08107	70 009	5.48	548	13	17
Transketolase	P29401	67 835	7.58	423	7	14
X-ray repair cross-complementing protein 6	P12956	69 799	6.23	237	3	8

3.7.18 HSP 70 protein detection by using protein array

The expression level of the HSP 70 was confirmed in protein array analysis. As depicted in Figure 3.53, the expression level of HSP 70 was up-regulated after treatment with swietenine acetate. The HSP 70 fluorescence signals elevated for more than 2 folds as early as 6 h of swietenine acetate incubation and the level remained high after 12 h and 24 h.

[A]

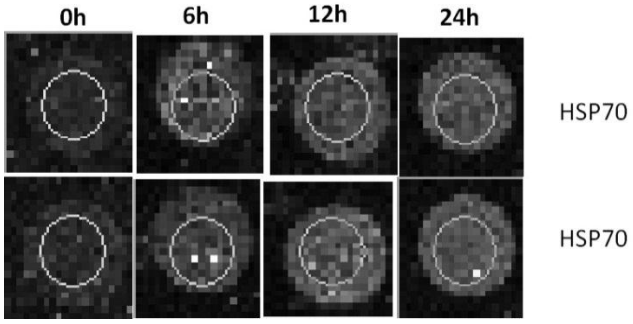

[B]

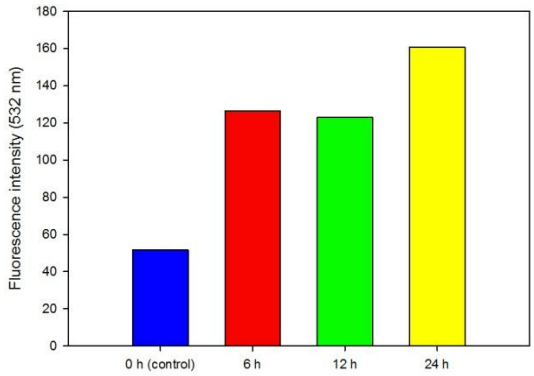

Figure 3.53 Protein expression level of HSP 70 at 0 h (control), 6, 12 and 24h exposure to 50 µM of swietenine acetate in HCT116 cell line. [A] RayBiotech protein array analysis on control and treated cells photographed by GenePix 4000B. [B] Means of duplicate fluorescence signals of HSP 70 in control (0 h) and 6, 12 and 24 h swietenine acetate treated cells after subtracted with background and normalized against pre-coated positive control probes using Acuity 4.0 analysis software.

CHAPTER 4

DISCUSSION

One major goal of anticancer potential of any drug/naturally-derived agent is the induction of apoptosis in cancer cells (Denicourt and Dowdy, 2004). Apoptosis or programmed cell death is one of the most important targets for cancer treatment. It is characterized by membrane blebbing, cytoplasmic condensation, formation of apoptotic bodies, DNA fragmentation, alteration in membrane symmetry, activation of caspase cascade and loss of mitochondrial membrane potential (Kang *et al*., 2007). In the present study, cytotoxic potential of SMEAF was assessed by MTT assay against selected cancer cell lines (HCT 116, KB, Ca Ski and MCF-7). The assay is based upon reduction of yellow tetrazolium salt (MTT) by the reductase enzyme in metabolically active cells to a dark blue formazan (Loosdrecht *et al*., 1994), which has been employed by many workers to measure cytotoxicity to cells.

Apart from preliminary screening on KB cells using the bark and leaf extracts (Camacho *et al*., 2003), to the best of our knowledge, this is the first study to show that *S. macrophylla* seeds were able to cause cytotoxicity towards cancer cells and induced apoptosis specifically in HCT-116 cells. The cytotoxicity effect of the crude ethanol extract of *S. macrophylla* seeds has demonstrated varying levels of cytotoxicity when screened against KB, CasKi, HCT 116, Hep G2 and MCF-7 cancer cell lines. Hence, the crude ethanol extract was further fractionated to yield hexane, ethyl acetate and aqueous fractions. The cytotoxicity effect was only observed in SMEAF treated cells and the lowest IC_{50} value was against HCT116. Hexane and aqueous fractions were found to have no effect on all cell lines (IC_{50} > 200µg/ml in all cases). SMEAF did show higher values of IC_{50} compared to ethanol extract especially on CasKi and MCF-7 but lower IC_{50} values were obtained on KB, Hep G2 and HCT-116 cells. Eventually, the

minimum IC_{50} value of 35.5µg/ml was obtained with the ethyl acetate fraction against HCT-116 cells. Thus, it can be concluded that ethyl acetate fraction was selectively toxic against HCT116 cells and hence further investigations were carried out using HCT116 cell line.

To investigate the mechanism of cell death induced by SMEAF in HCT116 cells, flow cytometric analysis by PI and annexin V-FITC labeling was conducted as a marker to confirm apoptosis (Kawamura and Kasai, 2007). During apoptosis, a number of changes occur in the cell surface markers that show affinity for PI and annexin V-FITC labelling (Vermes *et al.*, 1995). The results in the present study indicated apoptotic induction by the *S. macrophylla* ethanol extract in a dose-and time-dependent manner. This was inferred on the basis of flow cytometric evidences, which showed an increment of apoptotic cell percentage in dose- and time-dependent manner by using Annexin V/PI staining.

Another important characteristic of apoptosis induction is DNA fragmentation and measurement of DNA content makes it possible to identify apoptotic cells. TUNEL assay which measures DNA fragmentation or DNA strand breaks by the incorporation of Br-dUTP into the exposed 3'-OH DNA ends, followed by detection with fluorochrome-conjugated anti-BrdU antibody (Darzynkiewicz *et al.*, 2008b) was performed to further confirm the potential of SMEAF to induce apoptosis in HCT-116 cells. The results which showed increasing TUNEL positive cells at 24h, with increasing concentrations of SMEAF were found to be complementary with the results from Annexin V/PI. To recognize the cell cycle phase specificity and to quantify apoptosis, propidium iodide (PI) dye binds to DNA in cells at all stages of the cell cycle,

and the intensity with which a cell nucleus emits fluorescent light is directly proportional to its DNA content.

Cell cycle analysis on a 24 h SMEAF treatment showed a significant increase in the percentage of G1-phase from 24.33% (control) to 55.34% of cells at the highest concentration of 1.0mg/ml suggesting that SMEAF arrested the cells at G1-S transition in a dose-dependent manner. To further confirm the involvement of cell cycle arrest in apoptosis, cells were subjected to different periods of incubation of 24, 48 and 72h). As depicted in Figure 4(B), there was a gradual increase in the percentage of Sub-G1 cells during prolonged induction by 0.05mg/ml of SMEAF at 24 h, 48 h and 72 h incubation periods. These results seem to suggest that the apoptosis occurred through G1 arrest in HCT-116.

Generally, apoptosis is regulated through two distinct pathways: the cell surface death receptor and mitochondrial-mediated pathways (Darzynkiewicz *et al*., 2008b; Desagher and Martinou, 2000) and the $\Delta\Psi m$ loss of MMP appears to be a critical event in apoptotic process (Kroemer and Reed, 2000). In the present study, SMEAF treatment has induced $\Delta\Psi m$ loss in the period of 24h treatment performed by using JC-1 dye. The results demonstrated that concentration as low as 0.05mg/ml of SMEAF was able to induce disruption of mitochondrial membrane integrity of tested HCT-116 cells up to 10.45%, while at the highest concentration of 1.0mg/ml, 53.69% of cells were affected.

The investigation on intracellular total glutathione (GSH) level was performed to determine the involvement of oxidative stress in cell death. The depletion of GSH has been known to contribute to the onset of apoptosis, by rendering the cells more sensitive to apoptotic agents (Macho *et al*., 1997b). Heales and coworkers (1995) and Mitchofer

and coworkers (1992) have reported the importance of GSH in maintaining optimum mitochondrial functions and the role of ATP production in maintaining GSH level, indicating the correlation of GSH to MMP. Thus, the deficiency in the energy supplied by mitochondria is likely to affect the cellular turnover of GSH that protects the cells from oxidative stress and consequently apoptosis. Treatment with SMEAF at 0.05mg/ml significantly depleted the level of GSH by as much as 49.56% (12.02±0.59 nmoles) and showed ability in attenuating the GSH level in a dose-dependent manner. Based on these results, it is believed that SMEAF might cause cancer cells to undergo oxidative stress leading to the depletion of GSH and disruption of the mitochondrial membrane integrity and eventually leading to apoptosis.

ROS generation in several anti-cancer therapies has been reported to contribute to their anti-cancer activities. Manipulation of ROS generation in cancer cells has also been reported to be a potential therapeutic strategy to enhance the cytotoxicity of drugs (Renschler, 2004; Wang and Yi, 2008). In this study, we found that treatment with SMEAF greatly increased ROS production and cytotoxicity in HCT116 cells. The increased oxidative stress has been shown to cause DNA damage, followed by cell cycle arrest (Stadtman & Berlett, 1998; Wang and Yi, 2008). An imbalance between the production of ROS and the ability to readily detoxify the reactive moieties in a biological system is known as oxidative stress. Severe effects of oxidative stress have been known to be involved in activating apoptosis responses in affected cell (Lu *et al*., 2011). Intracellular glutathione level was shown to be decreased after treatment with SMEAF (Goh and Kadir, 2011) which was a sign of oxidative stress. These findings suggest the involvement of oxidative stress in SMEAF-induced cells with the detection of increment in intracellular ROS level.

Apoptosis is a gene-regulated phenomenon induced by many chemotherapeutic agents in cancer treatment (Gerl and Vaux, 2005; Ward *et al*., 2008) and well characterized by chromatin condensation, nuclear shrinkage, membrane blebbing, and oligonucleosomal DNA fragmentation (Green and Reed, 1998; Nesslany *et al*., 2009). Morphological observation of the SMEAF-treated HCT116 cells revealed that SMEAF induced cells to undergo apoptosis. As depicted in Figure 3.3, various morphological changes including, abnormal cell shape, nuclear condensation, cell detachment and membrane blebbing were observed and these characteristics implied the occurrence of apoptosis. Hoechst 33342/PI is commonly used in differentiating the apoptotic versus normal cells and our findings confirmed the occurrence of apoptosis in SMEAF induced-cells which exhibited DNA condensation and alteration of plasma membrane permeability characteristics. This study indicated that SMEAF induced apoptotic cell death in HCT116 cells.

This study addresses the induction of apoptosis and the underlying mechanisms of SMEAF-induced cell death in HCT116 cells. Apoptotic induction in tumor cells is considered to be very useful in the management, therapy, and prevention of cancer (Hu *et al*., 2007; Ram and Kumari, 2001). The present study revealed SMEAF-induced apoptosis in HCT116 cells in which the roles of caspase cascades, ROS production, and pathways involving Bcl-2 family, TP53 and MDM2 were to gain further insight into the molecular mechanisms of SMEAF in colon cancer. The present findings are consistent with earlier results in HCT116 cells, indicating that SMEAF possesses *in vitro* cytotoxic effect.

To gain further insight into the potential mechanisms underlying the cytotoxicity effect of SMEAF, the expression of pro- and antiapoptotic proteins was investigated in the

present study. The Bcl-2 family, such as proapoptotic (Bid, Bax and Bcl-2-xs) and antiapoptotic (Bcl-2 and Bcl-xl), proteins plays an important role in induction of apoptosis in cancer cells (Cai *et al*., 2009; Gavathiotis *et al*., 2008). These pro- and antiapoptotic proteins have emerged as critical regulators of mitochondria-mediated apoptosis. An increase in the levels of pro-apoptosis proteins and/or a decrease in anti-apoptosis proteins can lead to a decrease in mitochondrial membrane potential and an opening of mitochondrial permeability transition pores, leading to cytochrome *c* release from mitochondria into cytosol. In this study, we found that SMEAF increased the expression of the proapoptotic protein, Bax, and decreased the expression of anti-apoptotic protein, Bcl-2, thus the Bax/Bcl-2 ratio was significantly elevated. Previous reports have shown that the ratio of Bax/Bcl-2 determines, in part, the susceptibility of cells to death signals [30]. This alteration may be responsible for the concomitant execution phase of apoptosis through the activation of caspase -9, caspase -3 and ultimately cell death.

The level of Bax expression is an important determining index of apoptotic cell death, which also confirms that the mitochondrial signaling pathway is involved in SMEAF-induced apoptosis in HCT116 cells. Once activated, Bax is inserted into the mitochondrial membrane to cause the dysfunction of mitochondria to increase membrane permeability (Green and Chipuk, 2008; Green and Reed, 1998), leading to the formation of the mitochondrial permeability transition pore (Bernardi *et al*., 2006). These findings seem to correlate with our previous results mentioned earlier on the SMEAF-induced loss of MMP (Goh and Kadir, 2011). Disruption of MMP is always accompanied by release of apoptogenic factors such as cytochrome c that forms a multi-protein complex known as the apoptosome and initiates activation of caspase cascade effect by caspase-9 and which in turn cleaves and activates effector caspases such as

caspase-3 (Jin and Deiry, 2005). Thus detection of caspase activities was conducted using flow cytometric method, revealing the elevation of caspase -3/7 and -9 activities in HCT116 cells after exposure to SMEAF.

TP53-regulated apoptosis involves activating the mitochondrial-mediated pathway by elevating expression of proapoptotic genes and suppressing the expression of antiapoptotic genes in the Bcl-2 family (Fang *et al*., 2000; Green and Kroemer, 2004). Besides, the encoded p53 protein interacts with Bcl-2 family to enhance Bax-promoted outer-mitochondrial membrane permeabilization, and acts as a direct transcriptional activator of the Bax gene (Toshiyuki and Reed, 1995). TP53 has been reported to induce apoptosis in various systems, as an example, TP53 activation can serve as an upstream cellular event that leads to mitochondrial membrane potential dissipation and caspase-3/7 activation, and may be responsible in executing the downstream process of apoptosis (Chen *et al*., 2009; Jin and Deiry, 2005).

The MDM2 gene has been described as a negative regulator of TP53 as the amplification of MDM2 gene would lead to devoid of tumor-suppressor function of p53 protein. Thus, overexpression of the MDM2 is oncogenic and inhibits upstream apoptosis pathways. Hence under expression of MDM2 may lend support for the acceleration of apoptosis (Arden *et al*., 2007). Whereas the presence of caspase-3/7 and -9 indicates that mitochondrial release of cytochrome-c has taken place. In the current study, SMEAF was found to upregulate the expression of TP53 up to ~ 2 folds as compared to the control cells. Interestingly, a concomitant decrease of MDM2 expression was detected (~2 folds) in the SMEAF- treated cells. More interestingly, the upregulated expression of Bax and TP53 was accompanied by activation of caspase -3/7 and -9 in cells treated with SMEAF, while Bcl-2 and MDM2 expression was down-

regulated. Meanwhile, a marked increase in caspase-3/7 and -9 activities was detected when the HCT 116 cells were treated with SMEAF (Figure 3.14). These findings suggest that induction of apoptosis in SMEAF-treated HCT116 cells could be associated with a caspase-dependent cascade that involves the activation of the mitochondrial pathway through TP53 mediated, initiated by the suppression of Bcl-2 and the activation of Bax. This delivers the notion that inhibition of the p53-MDM2 interaction may be an important target in cancer therapy.

The existence of the cell cycle checkpoints in cells is important, as it determines the survival of the cells and decreases the defected heritable genetic changes following exposure to DNA damaging agents (Kastan *et al*., 1992). The p53 is known to be associated to cell cycle regulatory process (Kastan *et al*., 1991). The presence of the wild type p53 is important in determining the arrest of cells that exhibited DNA damage in G1 phase (Kastan *et al*., 1992). Earlier in this study, p53 encoding gene TP53 was shown to be up regulated following treatment with SMEAF. In contrast, the negative regulatory protein gene MDM2 was shown to be down regulated. The protein array analysis confirmed the above finding particularly the p53 expression level was up regulated. Based on the results obtained an assumption can be made that the apoptosis induction of HCT116 cells was linked to p53 pathway.

As indicated in the cell cycle analysis, SMEAF treated cells appeared to be arrested in G1 phase as the percentage of distribution increased in dose- and time-dependent manners. Extensive studies conducted on PCNA revealed a critical role in biological processes especially DNA metabolism whereby it serves as an accessory protein for DNA polymerases, required for chromosomal DNA synthesis and also shown to interact with cellular proteins involved in cell cycle regulation (Kelman, 1997). Thus,

expression of robust functioning PCNA encoded gene was evaluated using Q-PCR method. The analysis found that the expression level of PCNA gene decreased dramatically and significantly upon the SMEAF exposure. Therefore, these results suggested that the regulation and progression of the cell cycle might be affected by SMEAF in HCT116 cells.

Next, the regulatory genes involved in cell cycle progression were then assayed using PCR array. Previous studies reported the importance and necessary existence of CDK2 and CDK4 in permitting the transition of cells from G1 to S phase. Inhibition or down regulation of CDK2 and CDK4 were then shown to increase in cells arrested at G1 phase (Carlson *et al.*, 1996; Sherr, 1994). In the current study, Q-PCR analysis demonstrated reduction in expression level of CDK2 and CDK4. This may explain the observed G1 phase arrest in earlier analysis.

In most organisms, the cell cycle machinery was known to rely on multiple cyclin-CDKs (Roberts and Sherr, 2003). The CCNE1 or Cyclin-E1 was known to form a complex or worked as a regulatory subunit of CDK2 in G1/S transition state (Caldon and Musgrove, 2010); while rapid degradation of CDC25A or cell division cycle 25 homolog A was reported to have blocked the entry into the S phase and DNA replication resulting in cells remaining in the G1 phase (Mailand *et al*., 2000). Thus, in order to strengthen the claim of G1 phase arrest in HCT116 cells by SMEAF, CCNE1 and CDC25A expression was then assayed. The results indicated down regulation in the expression of both CCNE1 and CDC25A genes in HCT116 as a response to SMEAF exposure.

The gene CDKN1A encoded protein p21, a potent cyclin-dependent kinase inhibitor plays important roles in cell cycle progression and its expression is controlled by p53 protein. The presence of p21 would directly inhibit the activity of Cyclin E/CDK2 complexes and thus functions as a regulator of cell cycle process (Gartel and Radhakrishnan, 2005). In most of the cases, the arrest of cells by p21 was shown to be associated to p53 protein (Bunz *et al*., 1998; Waldman *et al*., 1995). Earlier analysis demonstrated tumor suppressor protein p53 expression was expressed in higher level as compared to control cells. In the current study, the gene and protein expression level of p21 was up regulated, thus this finding suggested that the arrest of cells may be sustained by p53-p21 dependent G1 arrest.

Taken together, these findings suggested that there is a presence of bioactive compounds in SMEAF which are able to alter the molecular expression level and eventually lead to cell growth inhibition by arresting at G1 phase and activation of cell death pathway particularly through mitochondrial mediated apoptotic pathway.

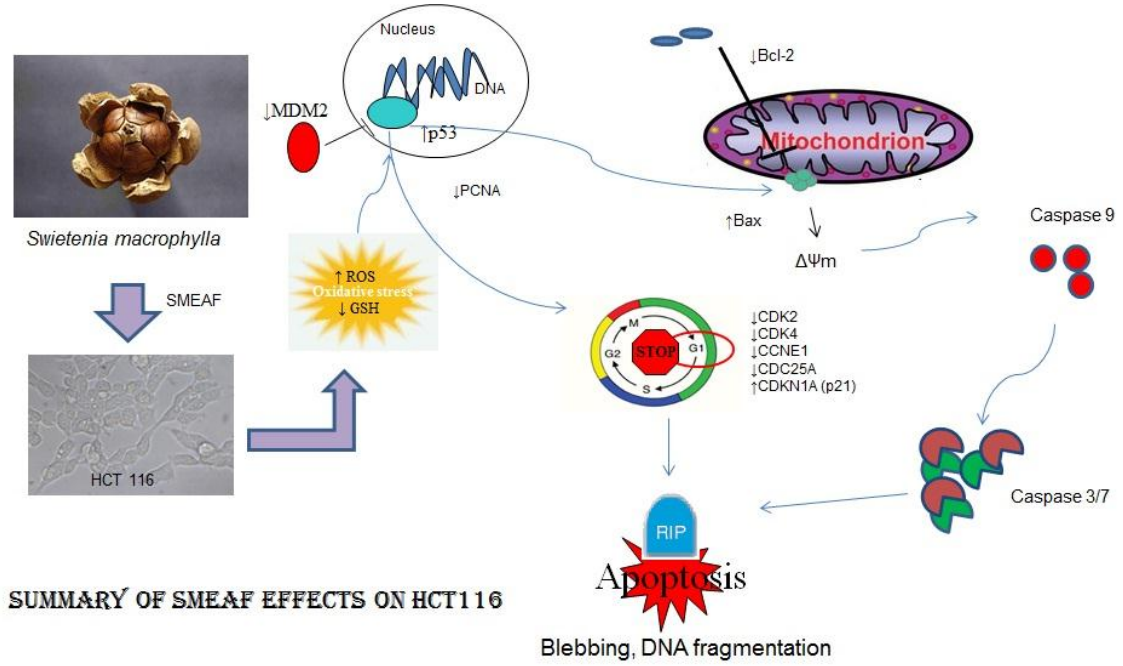

Figure 4.1 Summary of SMEAF apoptosis inducing effects on HCT116 cells.

Since time immemorial, exploration of nature by human in search of new drugs have resulted in the use of large number of medicinal plant in treating various diseases (Verpoorte, 1999). The advancement in modern scientific methods enables recent researchers to discover the bioactive chemicals and identify the secondary metabolites in plants that are responsible for their activities (Dong *et al*., 2011). Secondary metabolites are complex organic compounds that are produced by organisms and are not directly involved in the normal growth, development or reproduction of an organism (Fraenkel, 1959). The production of the secondary metabolites in plants was thought to be produced primarily as plant defense strategy against herbivores (Baldwin *et al*., 2001). Some of the metabolites are designed to attract creatures for pollination or seed distribution, as pigments to protect from sun's radiation so as regulatory hormone in response to environmental changes (Baldwin *et al*., 2001; Stepp, 2004).

As discussed earlier, the molecular and cellular responses exerted by SMEAF on HCT116 are so dramatic and thus is crucial to identify and determine the bioactive constituents present. This will play an important role in the safe and effective use of SMEAF for therapeutic purpose. Therefore, the isolation and identification of the bioactive compounds were performed accordingly.

Phytochemical investigation conducted previously on *S. macrophylla* have led to the isolation of structurally diverse secondary metabolites from the family of limonoids (Chen *et al*., 2010). Naming a few of them, swietenolide, proceranolide, augustineolide, 3β, 6-dihydroxydihydrocarapin, 7-deacetoxy-7-oxogedunin, andirobin, proceranolide, 6-O-acetylswietenolide, 3,6,-O,O-diacetylswietenolide, khayasin T, and swietemahonins E-G, 2-hydroxyswietenine, and 6-deoxyswietenine (Mootoo *et al.*,

1999), swietenine (Dewanjee *et al*., 2009a) and etc. The bioactivities possessed by *S. macrophylla* were associated to these limonoids as proven through numerous bioassays (Dewanjee *et al*., 2009b).

In the current study we managed to purify eight compounds from this plant and identified using different spectroscopic analysis with further confirmation by using GC-MS analysis. Cytotoxicity evaluation particularly on HCT 116 cells revealed the compounds namely, 3-O-tigloyswietenolide, hexadecanoic acid, proceranolide and khayasin T to possess cytotoxic effect (Table 3.21) particularly in HCT 116 cells. The results suggested that the purified compounds have a high probability of being the active principles that are responsible for the cytotoxicity and apoptosis inducing effects of SMEAF.

The comparison in term of IC_{50} values revealed the purified compounds exhibiting higher IC_{50} value compared to SMEAF except for hexadecanoic acid. This is understandable, as in the mixture form, compounds may act synergistically to each other resulting in the stronger biological effect which is the situation commonly seen to happen in many studies (Lee *et al.*, 2012; Lin *et al*., 2005; Yee *et al*., 2004). However, no significant or clear cytotoxicity effect observed on any cancer cell lines particularly by swietenine aroused curiosity. As swietenine is sharing similar backbone structure with 3-O-tigloyswietenolide except for the difference in the orientation of the double bond particularly at C-8, C-14 for swietenine and C-8, C-30 corresponds to 3-O-tigloyswietenolide. Previous study conducted particularly on antifungal activity concluded the position of this double bond did not affect its biological activity (Govindachari *et al*., 1999), but in the current cytotoxicity studies we postulated to be otherwise.

The observation on the swietenine treated cells found that the compound (Figure 3.36) was crystalized in the medium. Thus, an attempt was taken in re-analysing those purified limonoids especially diacetylswietenolide (1) and 6-O-acetylswietenolide (8). As expected those limonoids also presented similar condition, in which crystallization occurred in the medium (results not shown) when treated on cancer cells. Thus, it is believed that crystallization of the compounds would affect the results eventually, as there would not be direct contact between the cancer cells and the compounds. Low solubility of natural product in water poses considerable problems in drug discovery. This factor has resulted in the demise of a number of promising leads, such as bruceantin and maytansine in cancer chemotherapy (Pavlik *et al*., 1983). Different co-solvents, surfactants, emulsifiers such as ethanol (Sovova, 2001), acetone (Adams *et al.*, 1993), Tween 40 and 80 (O'Sullivan *et al*., 2004), polyethyl glycol 4000 (Honda and Magalhaesyô, 2004), Cremophor EL (Gelderblom *et al*., 2001) have been proven in previous studies to be capable in combating the solubility problems. However, all these previously stated methods were of no avail in encountering solubility problem with swietenine (2).

Derivatization procedures have been shown to be able to improve solubility of compounds (Govindachari *et al*., 1999; Julka and Regnier, 2004; Zhang and James, 2005). In the current study, acetylation procedure was performed on swietenine specifically aiming the 6-OH functional group on swietenine. The conversion efficacy was around 74% of the total amount of 81 mg obtained after purification of the end product from reaction mixture. Structural elucidation by utilizing numerous spectroscopy procedures revealed the derivative of swietenine known as swietenine acetate which is coincidently present in seeds of *S. macrophylla*. The spectral data are

also well correlated with the literatures (Narender *et al*., 2008; Taylor and Taylor, 1983a).

The cytotoxicity effect of swietenine acetate was conducted on HCT116 revealed that the compound was able to exert its proliferation inhibitory effect on the particular cell line. The microscopy observation showed that the compound did not experience solubility problems as what was experienced with swietenine (Figure 3.36). At concentration of 50 µM, swietenine acetate caused the cells to undergo apoptosis. In Figure 3.36 the cells treated with 50 µM of swietenine acetate demonstrated the apoptotic features such as detachment from the culture surface, cell shrinkage and membrane blebbing which are signs of apoptosis (Kang *et al*., 2007). The apoptotic and non-apoptotic cells can be differentiated by exposure to Hoechst 33342 for a brief period followed by fluorescence intensity comparison (Dive *et al*., 1992). In this experiment, the utilization of Hoechst/PI staining method revealed the cells treated with the 50 µM of swietenine acetate showing stronger blue fluorescence and also the presence of red fluorescence signals. This indicated that exposure to swietenine acetate caused the HCT116 cells to undergo apoptosis.

In order to check whether the observed growth inhibition was associated with oxidative stress, the treated cells were stained by DCFH-DA stain. During the incubation with normal cancer cells, DCFH-DA diffused into the cells and hydrolyzed to DCFH and was thereby trapped within the cells. This was followed by the oxidation by ROS such as H_2O_2 or oxygen derivatives eventually formation of highly fluorescence compound DCF (Bass *et al*., 1983). Figure 3.38 showed the histrogram of ROS detection after 4 h treatment with swietenine acetate which remarkably shifted towards the right hand side, indicating an increase in intracellular ROS or sign of oxidative stress.

Confirmation of induced oxidative stress by swietenine acetate was assessed through intracellular GSH level. GSH is a cysteine-containing tripeptide or commonly known as cellular antioxidant which acts by protecting the cells from damaging effects of free radicals or ROS. In certain cases, high level of GSH has been shown to protect cells from apoptotic cell death induction (Chiba *et al*., 1996; Hedley and Chow, 1994). In the current study, treatment with swietenine acetate eventually down regulated the total intracellular glutathione level in a time-dependent manner which further reflected the oxidative stress induction on HCT 116 cells complementary with high level of ROS detection.

The apoptotic inducing effect of swietenine acetate in colon cancer cells was further investigated by measuring the loss of $\Delta\psi m$, which is an apoptotic event (Zamzami *et al*., 2007). Hence, the change of $\Delta\psi m$ in treated cells was detected by using JC-1. In control untreated cells, JC-1 was in aggregate forms within the mitochondria resulting in higher level of red fluorescence, which corresponded to a polarized $\Delta\psi m$. In contrast, the treated cells, swietenine acetate dramatically reduced the formation of red fluorescent J-aggregates, indicating disruption of $\Delta\psi m$ in HCT 116 cells. The reduction of red/green fluorescence observed in the flow cytometry analysis proved that swietenine acetate evoked loss of $\Delta\psi m$ in HCT116 cells, one of the hallmarks for apoptosis.

The loss of MMP is normally associated with the release of cytochrome c. The released cytochrome c would bind with dATP to form apoptosome. The formation of apoptosome in turn binds and activates the procaspase -9 and subsequently activation of caspase -3/7 by caspase-9 (Jiang and Wang, 2004). In this study we examined the Bcl-2 family proteins, particularly Bax and its antagonist protein Bcl-2 which are involved in the regulatory process of mitochondrial membrane integrity during apoptosis (Miyashita

et al., 1994). This finding showed that the swietenine acetate caused alteration in expression in favor of apoptosis, as it upregulated Bax (pro-apoptotic) and downregulated Bcl-2 (anti-apoptotic) protein. This explained the observed disruption of MMP in our earlier study. Besides, increased level of SMAC was detected after swietenine acetate exposure would further promotes apoptosis event in cells as it is known to promote the activation of caspase -9 through binding to inhibitor of apoptosis proteins (IAPs) (Tews *et al*., 2008). Activation of caspase-9 would subsequently upregulating caspase -3/7 activities which is consistent with our earlier findings suggesting that apoptosis may occur through mitochondrial-mediated pathway.

Cell cycle analysis was performed as a mean to determine whether the apoptosis induction was associated with alteration of the cell cycle distribution. The rapid and accurate analysis using PI stain followed with flow cytometry analysis was performed (Riccardi and Nicoletti, 2006). After treatment with swietenine acetate, a conspicuous increase in G1-phase cell percentage was followed with sub-G1 percentage. These results seem to suggest that the cells were arrested in G1 phase and followed with the accumulation of fragmented cells with reduced DNA content. In order to evaluate the involvement of the cell regulatory proteins in cell cycle distribution, PCR array analysis revealed the cell regulatory proteins encoding genes were altered after treatment with swietenine acetate. The results showed that swietenine acetate exposure increased the expression of CDKN1A gene and its encoded p21 protein in HCT116 cells. Besides, numerous other genes including CDC25A, CDK2 and CDK4 that are important in regulating the progression of cell cycle were simultaneously downregulated. The ceased expression level of the CDC25A, CDK2 and CDK4 genes was shown to correlate with the arrest in the cell cycle (Ewen *et al*., 1995; Iavarone and Massagué, 1999; Neganova

et al., 2011; Wolter *et al*., 2001). These findings may explain the arrest of cells detected in cell cycle analysis.

The expression level of p53 and its encoding gene TP53 was upregulated following exposure to swietenine acetate. Besides, the level of p21 expression was confirmed using protein array which showed a marked increase throughout the treatment period. It has reported that the elevation of p21 protein can be induced by modulation of p53 protein which eventually contributed to the G1 phase arrest in cell cycle progression (Deiry *et al*., 1994). In our current study, p53 and p21 proteins were concurrently elevated suggesting that the arrest of the HCT116 cells by swietenine acetate might occur through p53-mediated upregulation of p21-induced cell cycle arrest pathway.

Naturally occurring compounds have been found to cause apoptosis through intrinsic and also extrinsic pathways, for an example curcumin derived from turmeric that is capable in inducing the apoptotic effect through both pathways (Reuter *et al*., 2008). The extrinsic pathway is normally initiated by the interaction between specific ligands and surface receptors (Klein *et al*., 2005), such as CD95/Fas/Apo1, Tumor necrosis factor (TNF) receptor 1 (TNFR1), TNF receptor 2 (TNFR2) and death receptor 3-6 (DR3-6) (Degterev *et al*., 2003). The interaction of signalling molecules with death receptors would result in translocation of a death signal from the extracellular microevironment to the inner cytoplasm. This subsequently caused the recruit of initiator caspases such as caspase-8 and -10 followed by effector caspases -3 and -7 (Klein *et al*., 2005).

The utilization of flow cytometry detection method in determining caspase-8 and-10 surprisingly showed an increase in both caspase enzyme activities. This provides clues

that the induction of apoptosis by swietenine acetate may also be associated to extrinsic apoptosis pathway. The involvement of the extrinsic pathway was further confirmed with the detection of high expression level of genes such as TNFRSF1A, TNFRSF10B and also TNFRSF25 which are encoding genes for TNF family receptors.

In normal cells, phosphatidylserine is normally confined to the inner leaflet of plasma membrane. However, it would be exported to the outer plasma membrane leaflet during apoptosis to serve as a trigger for recognition of apoptotic cells by phagocytes (Martin *et al*., 1996). Annexin V/PI stains utilized in this study demonstrated that treatment with swietenine acetate for 24 h caused an increase in the externalization of phosphatidylserine. Meanwhile, prolonged exposure to swietenine acetate did not significantly decrease the percentage of viable cancer cells but instead a significantly higher percentage of early apoptotic cells has entered the late apoptotic or dead stage. This phenomenon has raised question of the presence of any downstream signaling molecules that may have hampered the apoptotic activation pathway in HCT116 and thus an attempt was made in conducting further investigations.

SDS-PAGE was performed on the lysates obtained from the cells treated with swietenine acetate. The result showed the increase level of a protein band particularly at around ~70KDa. The band was then excised, digested with enzyme and with the help of LC-MS/MS analysis enables us to detect the presence of HSP 70 protein. HSP70 is a major heat shock protein and known as an effective inhibitor of apoptosis. In a common pathway, disruption of MMP, release of cytochrome c from mitochondria, activation of caspase-3 and particularly with low HSP70 will eventually lead cells to apoptosis. However, it is shown to be otherwise if the cells are expressing high level of HSP70 (Jäättelä *et al*., 1998; Mosser *et al*., 1997). Protein array analysis confirmed this finding

where the expression level of HSP70 increased throughout the treatment period. Thus, we postulated that the apoptotic pathway induced by swietenine acetate may have been halted to a certain extent by HSP70 protein.

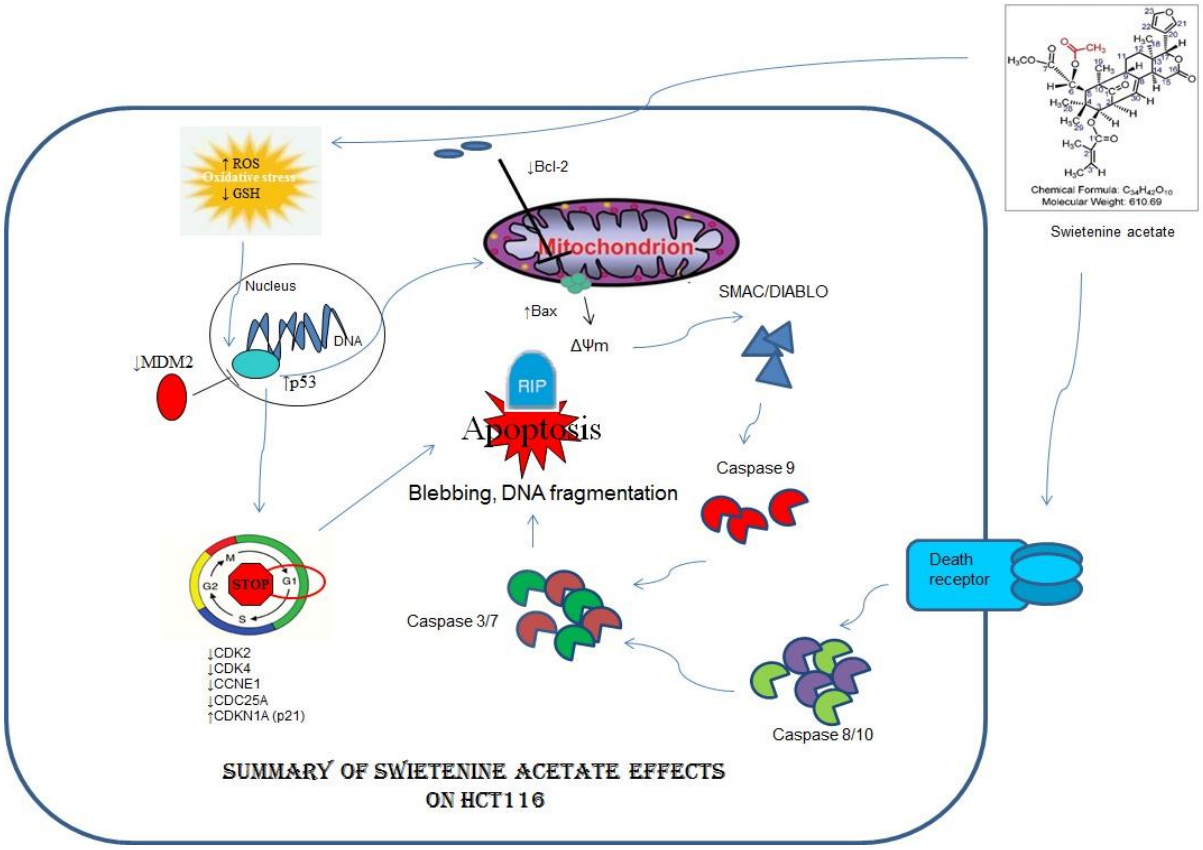

Figure 4.2 Summary of swietenine acetate apoptotic inducing effects on HCT116 cells.

Even though swietenine did not appear to be directly responsible for its bioactivities, the data generated in the present study may be applied towards the use of swietenine for the *in vivo* studies in the future. As studies have shown, diabetes is associated with a higher risk in developing cancer. Besides, reports have shown that individuals who suffer from both cancer and diabetes have a higher rate of mortality (Renehan *et al*., 2012; Yeh *et al*., 2012). Swietenine, a limonoid has been shown to be able to exert its hypoglycemic effects (Dewanjee *et al*., 2009a; Maiti *et al*., 2009) thus it would be very good if it can exert the growth inhibitory effect on colon cancer. In our current study we proved that

the acetylation of swietenine has resulted in a naturally occurring compound that is able to exert apoptotic inducing effect through intrinsic and extrinsic pathways. Thus, swietenine can be developed as a chemopreventive drug as acetylation is a very common metabolic reaction in human body. Acetylation can occur through the transfer of an acetyl group from acetyl-coenzyme A under catalysis of acetyltransferases enzyme (Gennaro, 2000). This explained the potential use of swietenine as chemopreventive drug, as it can exploited as a new lead compound for prodrug therapy.

CHAPTER 5

CONCLUSION

In summary, the findings from the present study provided an insight into the cytotoxic effect of *Swietenia macrophylla*. Cytotoxicity studies of *Swietenia macrophylla* on different cancer cell lines and subsequent chemical purification of bioactive SMEAF have led to the isolation of eight compounds which were mostly limonoids, namely, 3,6-*O*,*O*-diacetylswietenolide (1), swietenine (2), 3-*O*-tigloylswietenolide (3), swietenolide (4), hexadecanoic acid (5), proceranolide (6), khayasin T (7) and 6-O-acetylswietenolide (8). Compounds 3, 5, 6 and 7 were shown to possess cytotoxic effect against HCT116 cells. Acetylation of swietenine produced swietenine acetate which with an enhanced bioactivity as compared to its parent compound. The exposure to SMEAF and swietenine acetate eventually altered the oxidative balance of HCT 116 in favor of oxidative stress through the increased level of ROS and attenuation of intracellular GSH level. The simultaneous arrest of the G1 phase with an increase in p53 and p21 followed by a decrease in CDK2 and CDk4 may explain the inhibition of the cell cycle progression by SMEAF and swietenine acetate. Numerous apoptotic responses were identified, including cell shrinkage, chromatin condensation, DNA fragmentation, PS externalization, membrane blebbing and disruption of $\Delta\psi m$. The occurrence of mitochondrial-mediated apoptosis was further confirmed through the elevation of the Bax /Bcl-2 ratio and subsequent activation of caspase -3/7 and -9. In the mean time, exposure to swietenine acetate caused an upsurge in the expression level of HSP 70 protein which is a well-known anti-apoptotic protein associated with diminished efficiency of anticancer drugs. This finding may impact the future of cancer treatment by providing another avenue for the discovery of a combined anticancer drug treatment that targets the impeding effect of HSP70 and thus promotes induced apoptosis. This may pave the way for a possible intervention through the use of

limonoid(s) in combination with a HSP70 inhibitor for therapeutic and chemopreventive applications.

APPENDIX

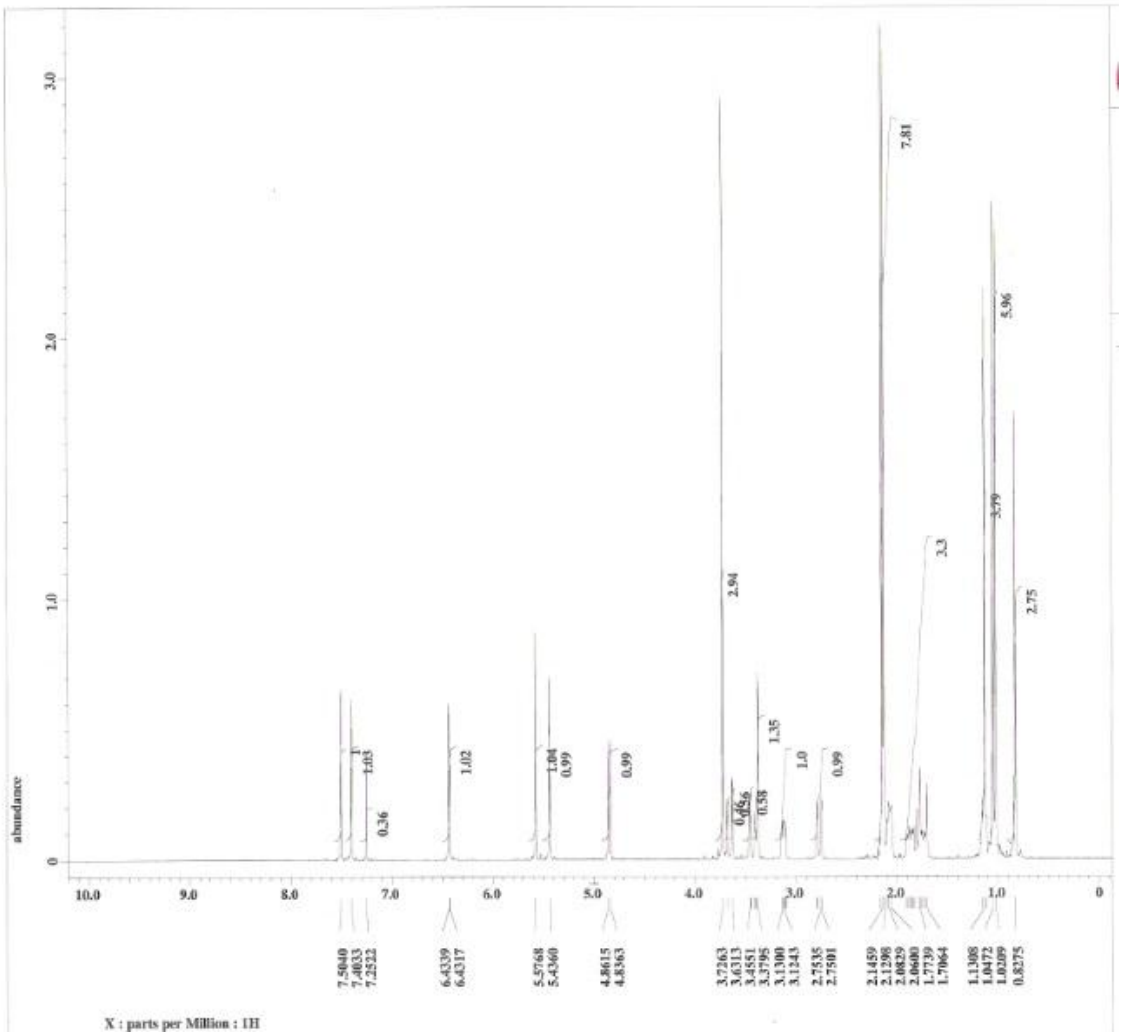

Appendix 1 ^{1}H NMR spectrum of diacetyl swietenolide (1).

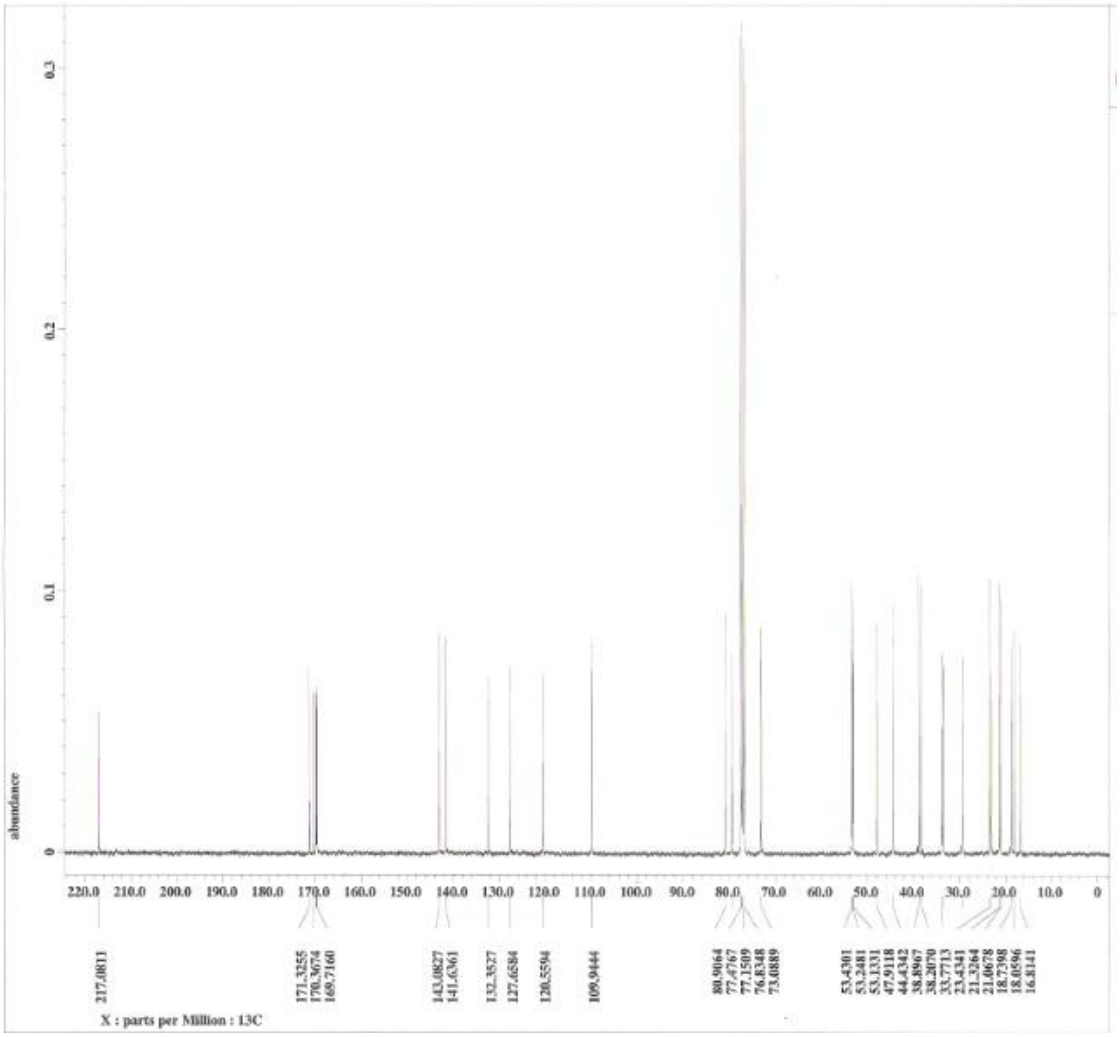

Appendix 2 ^{13}C NMR spectrum of diacetyl swietenolide (1).

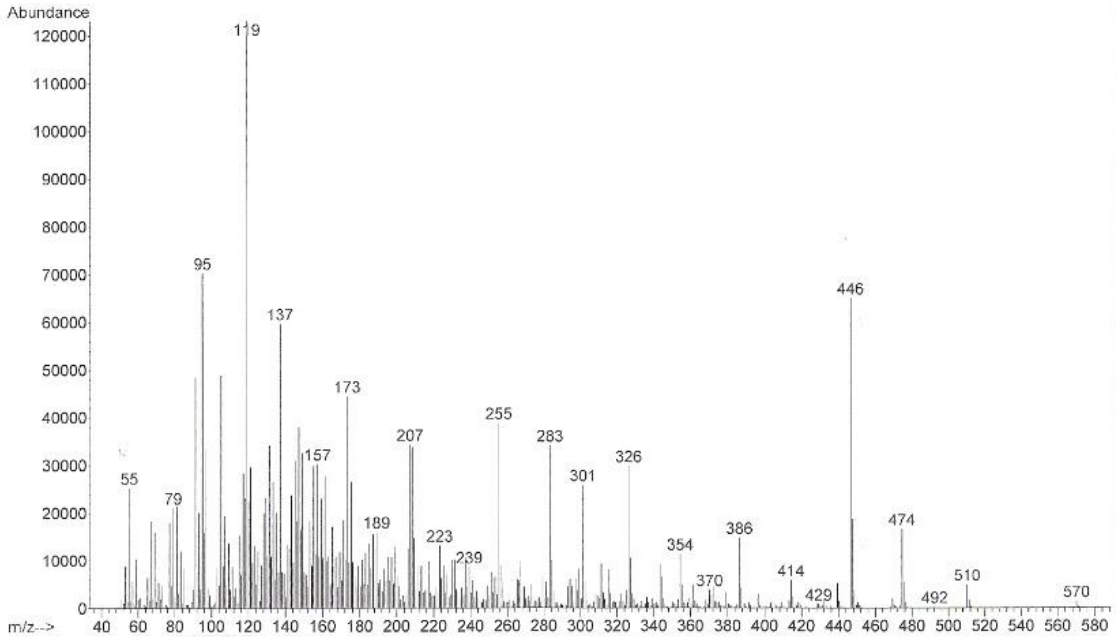

Appendix 3 Mass spectrum of diacetyl swietenolide (1).

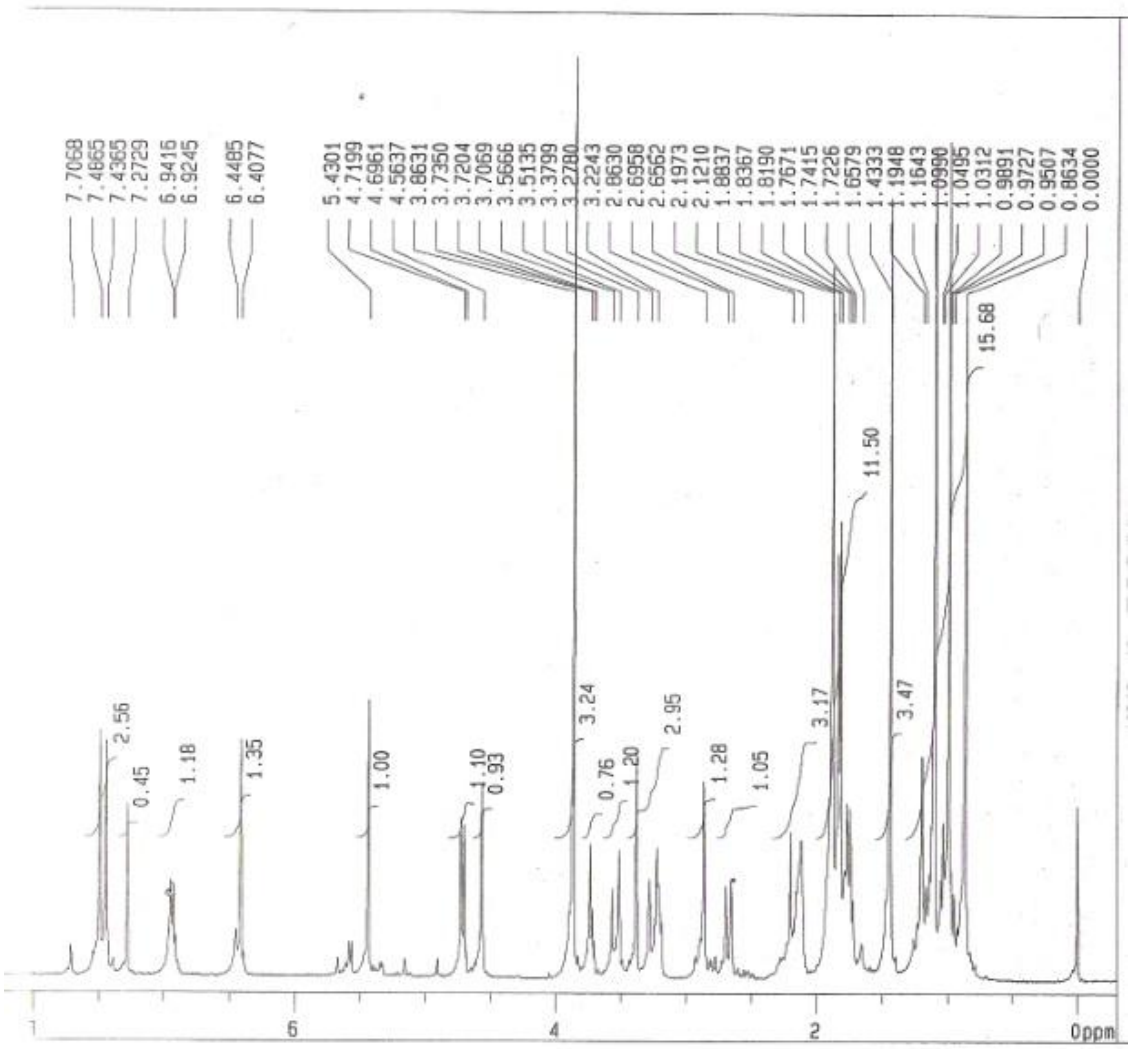

Appendix 4 ^{1}H NMR spectrum of diacetyl swietenine (2).

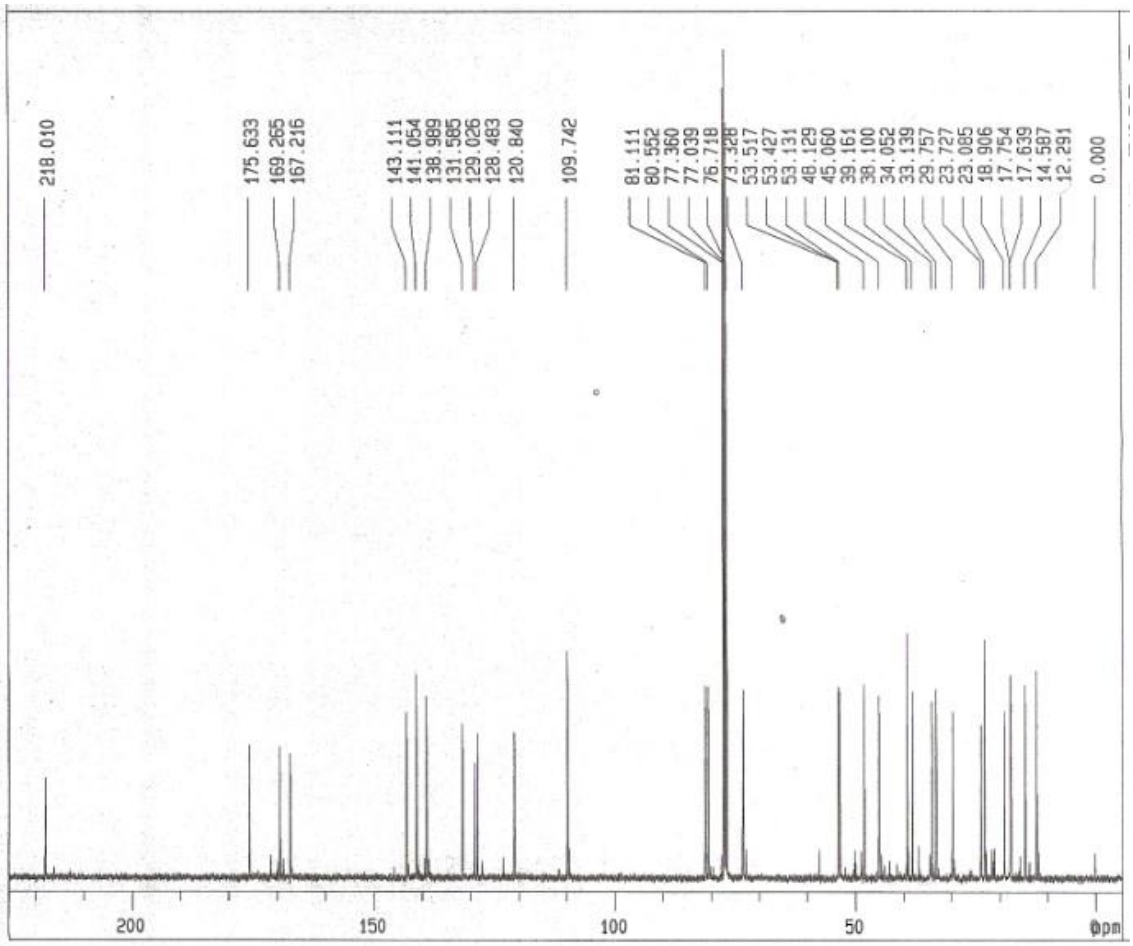

Appendix 5 ^{13}C NMR spectrum of swietenine (2).

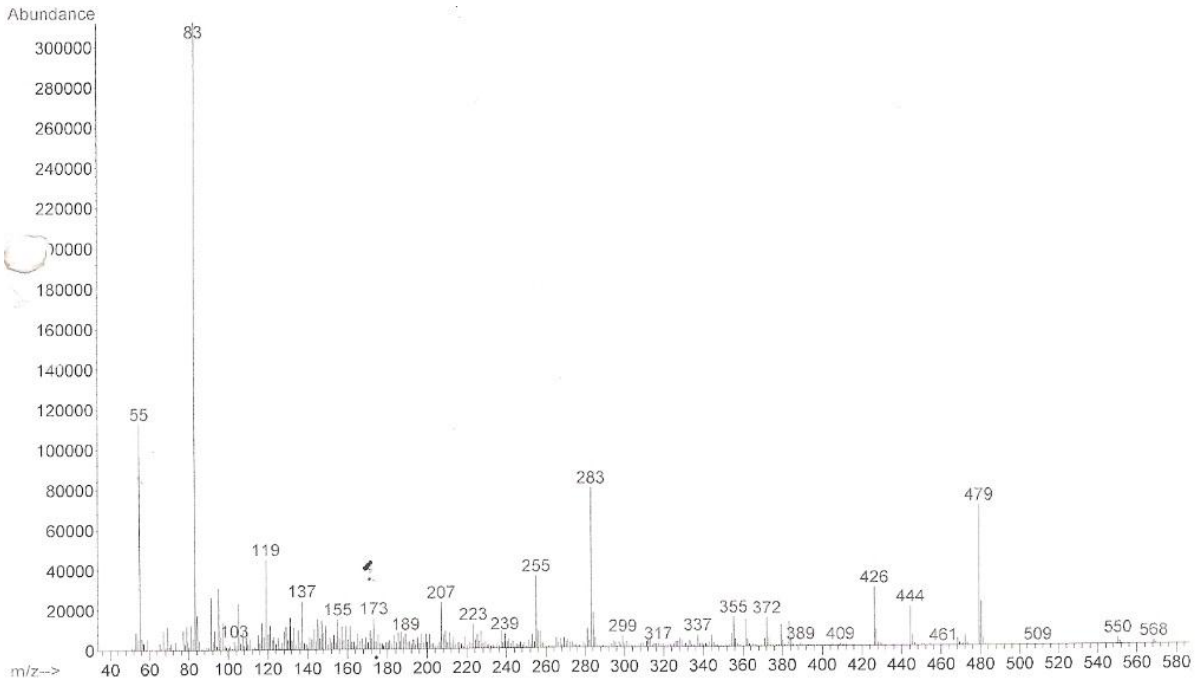

Appendix 6 Mass spectrum of swietenine (2).

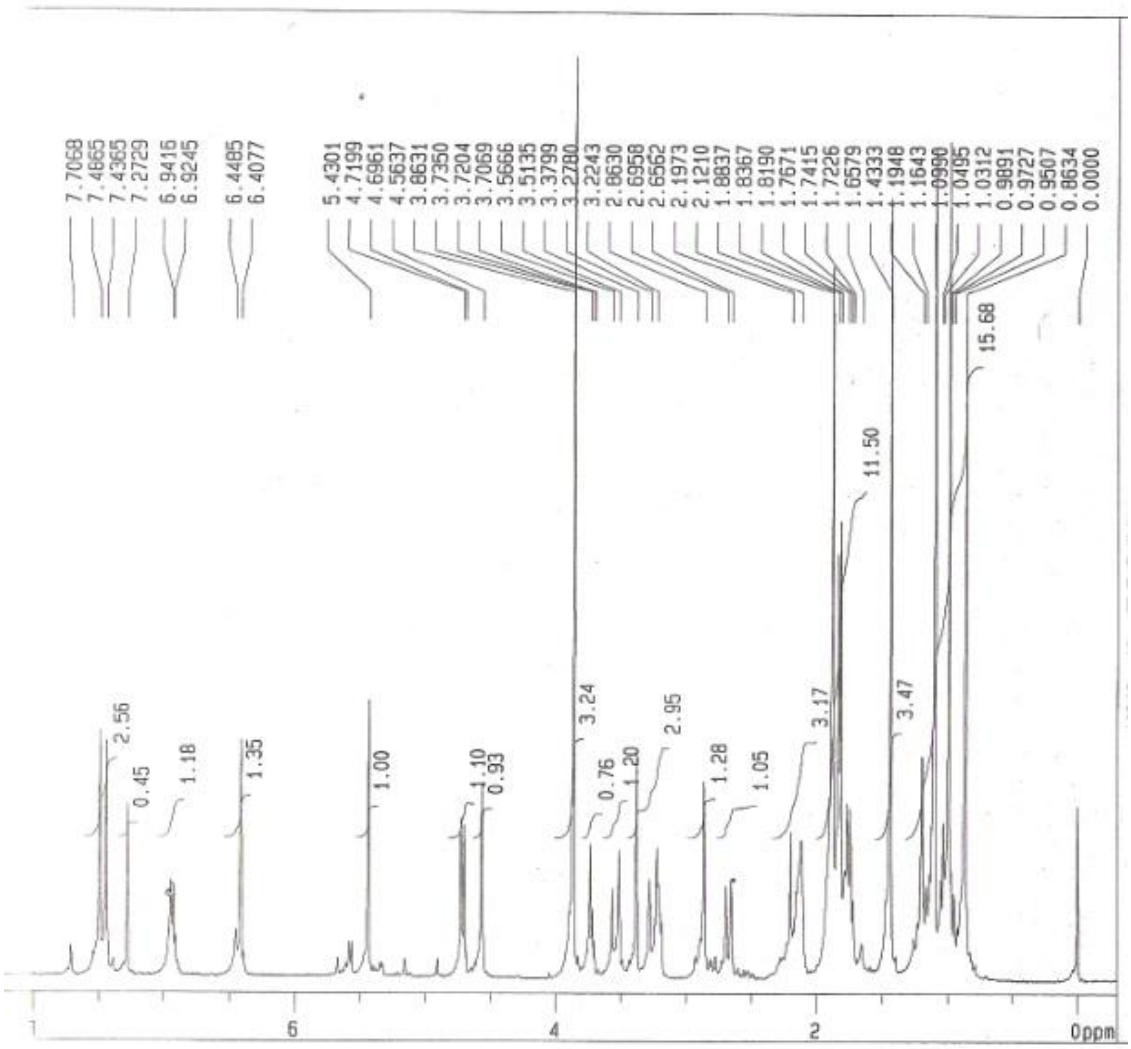

Appendix 7 ^{1}H NMR spectrum of 3-*O*-Tigloylswietenolide (3).

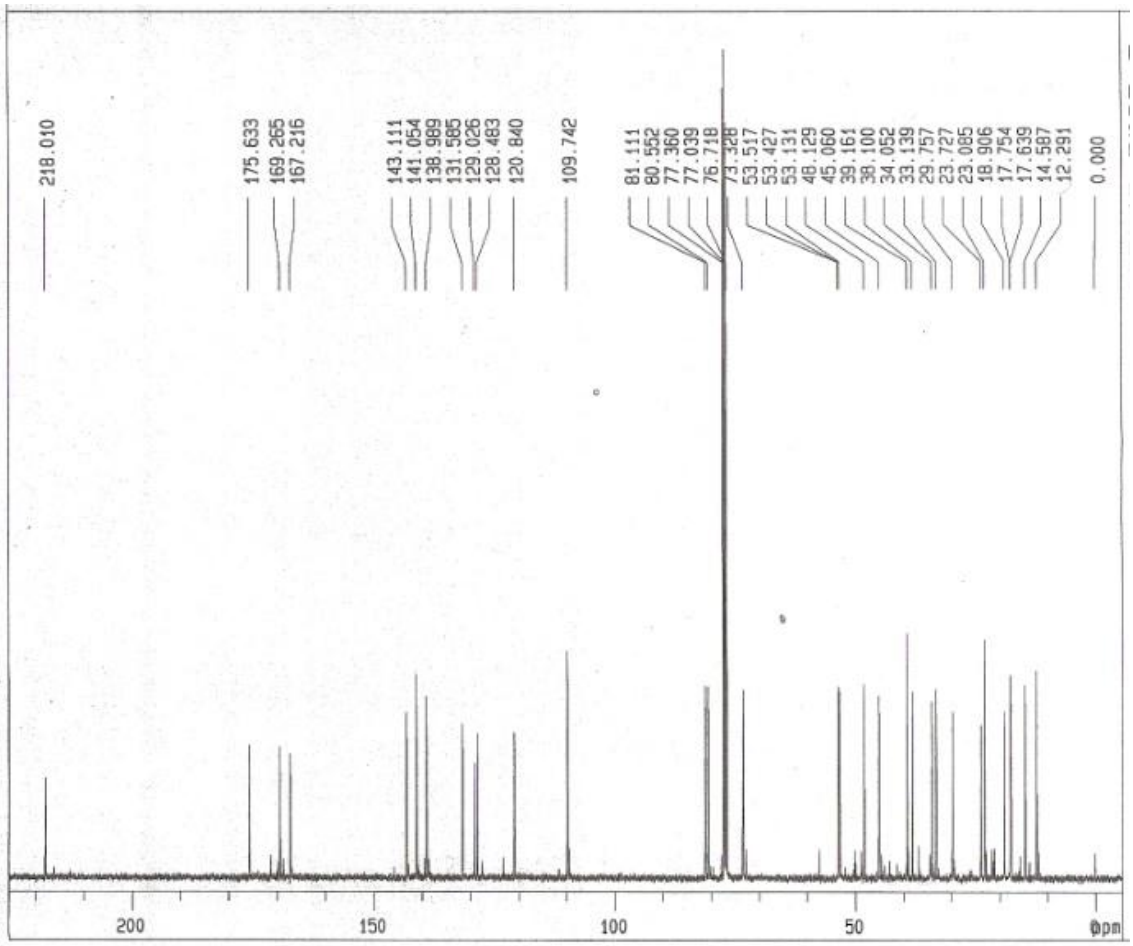

Appendix 8 ^{13}C NMR spectrum of 3-*O*-Tigloylswietenolide (3).

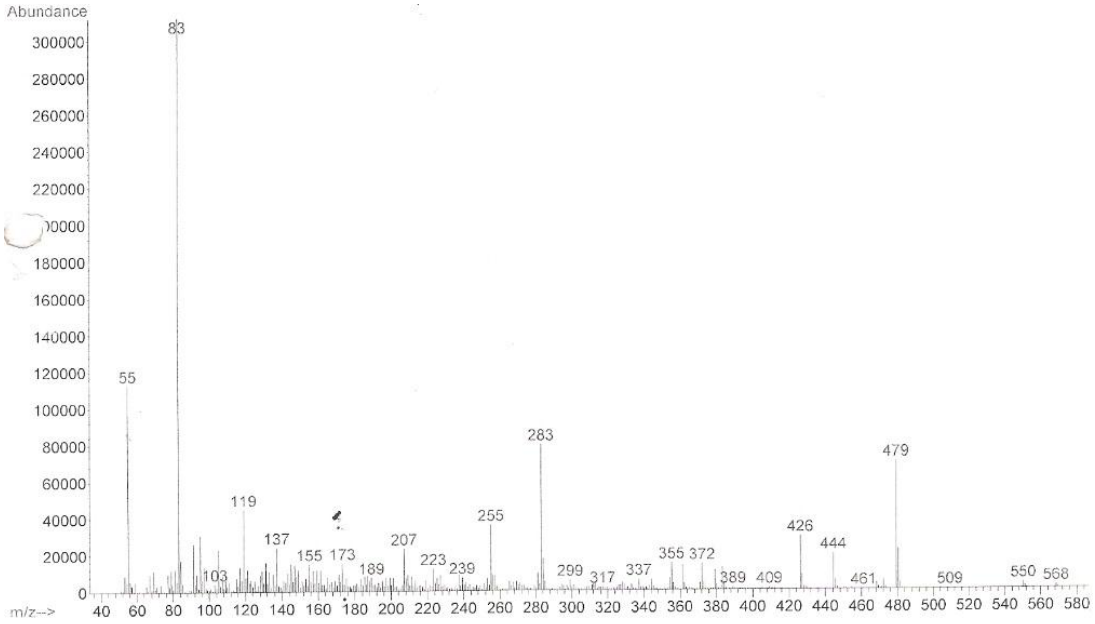

Appendix 9 Mass spectrum of 3-*O*-Tigloylswietenolide (3).

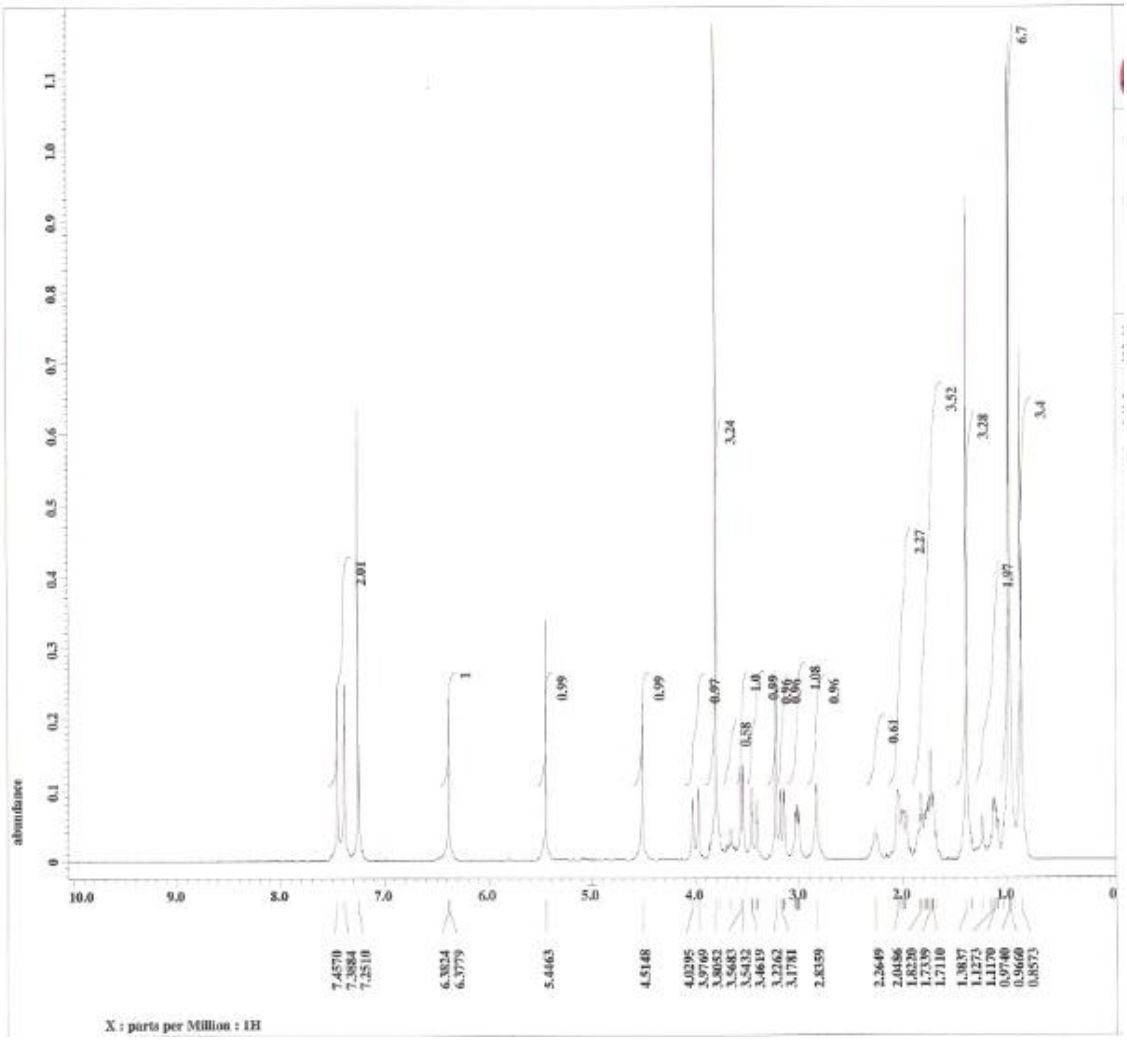

Appendix 10 ^{1}H NMR spectrum of swietenolide (4).

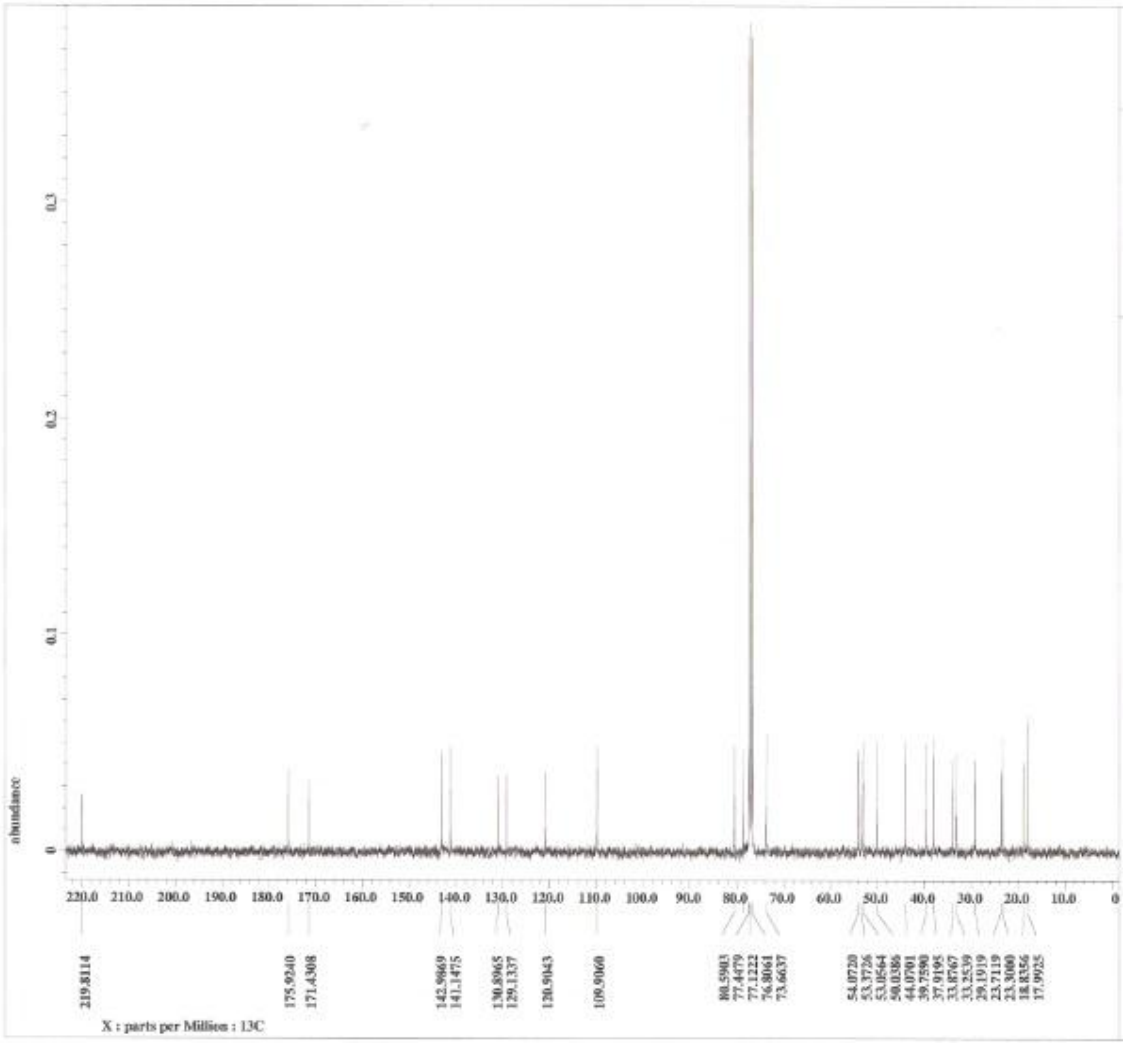

Appendix 11 ^{13}C NMR spectrum of swietenolide (4).

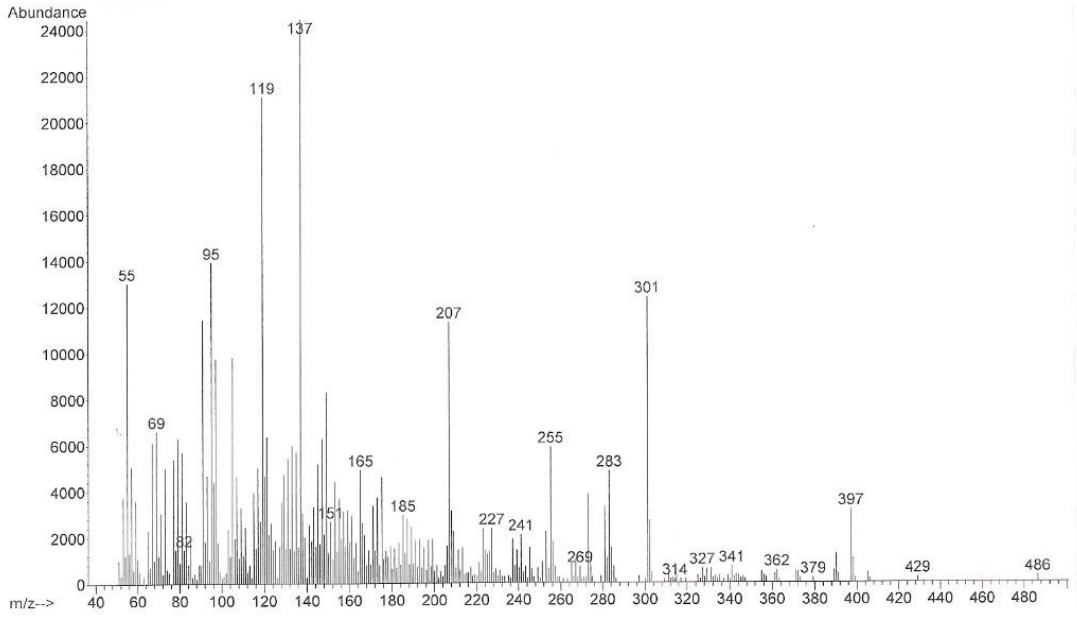

Appendix 12 Mass spectrum of swietenolide (4).

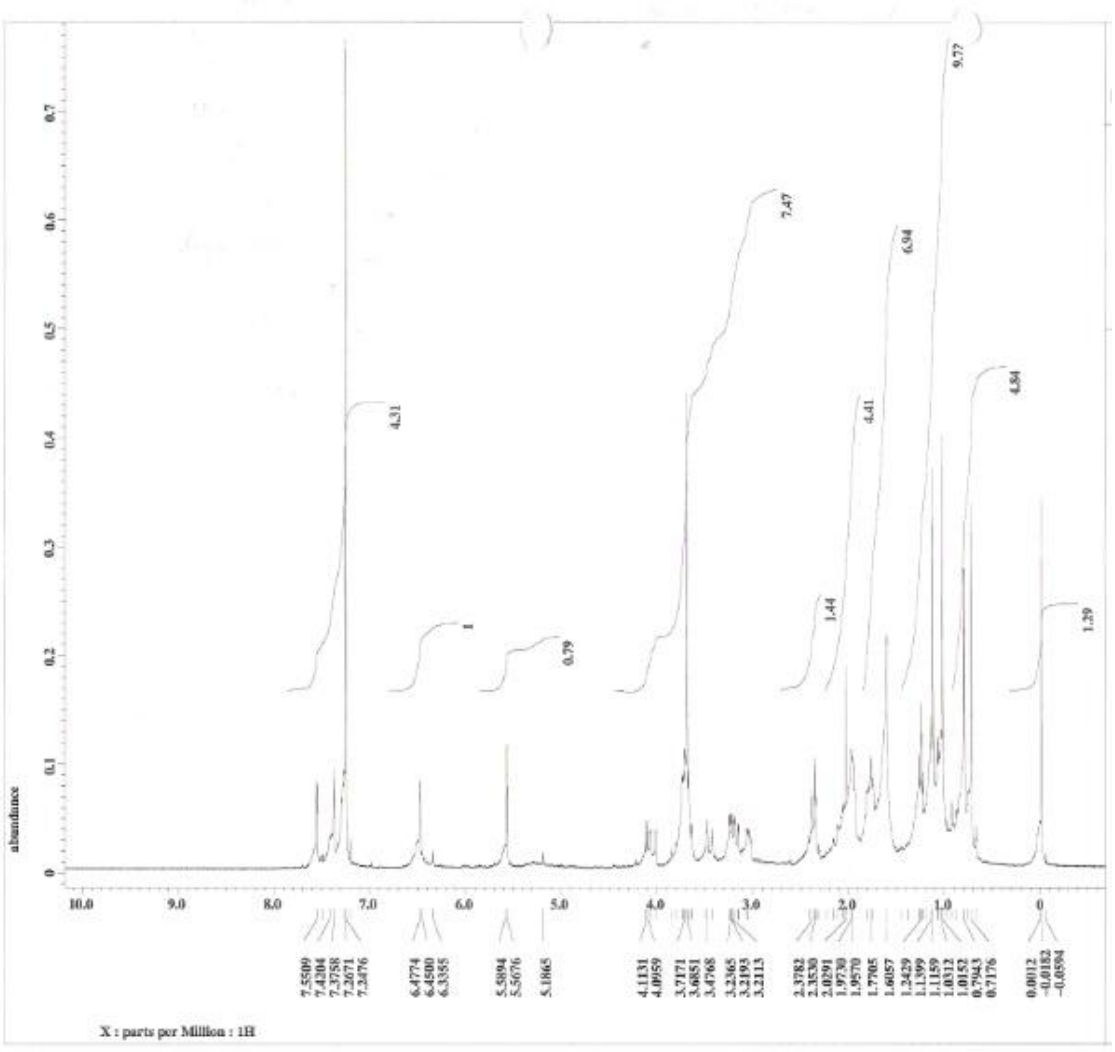

Appendix 13 ^{1}H NMR spectrum of proceranolide (6).

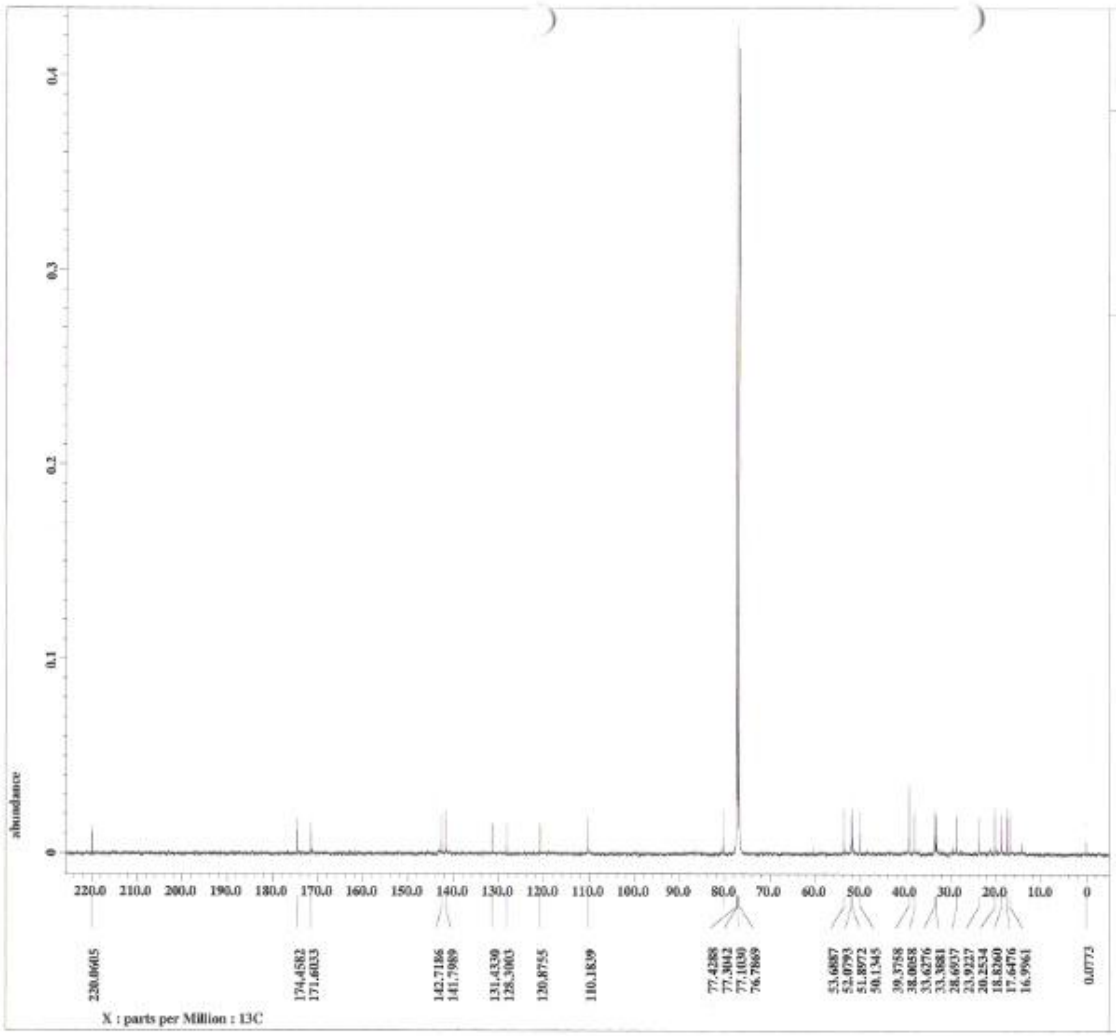

Appendix 14 ^{13}C NMR spectrum of proceranolide (6).

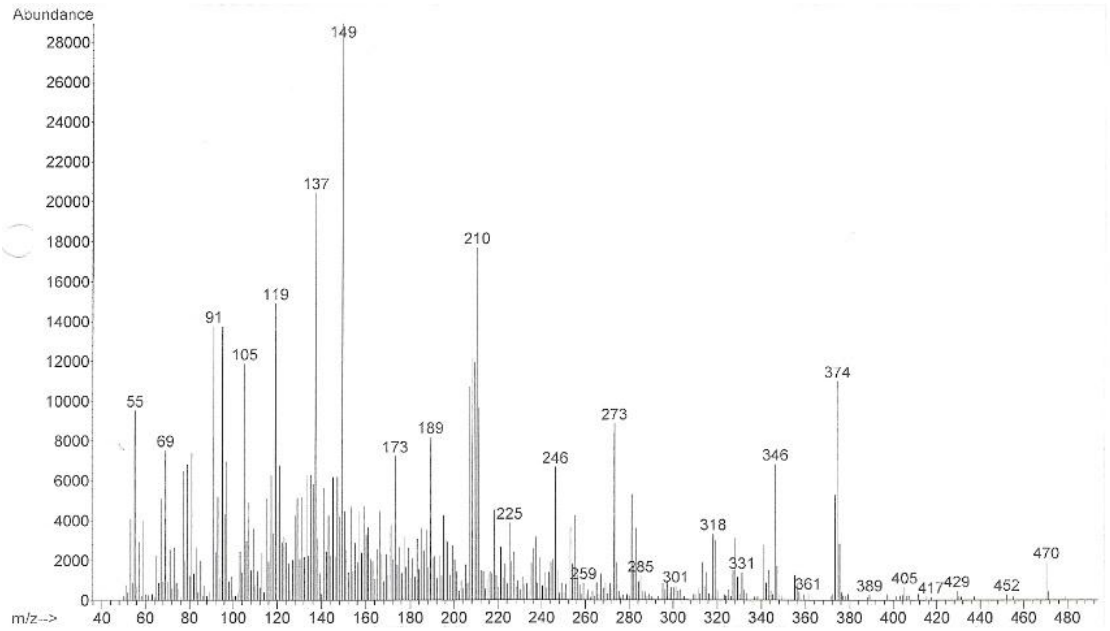

Appendix 15 Mass spectrum of proceranolide (6).

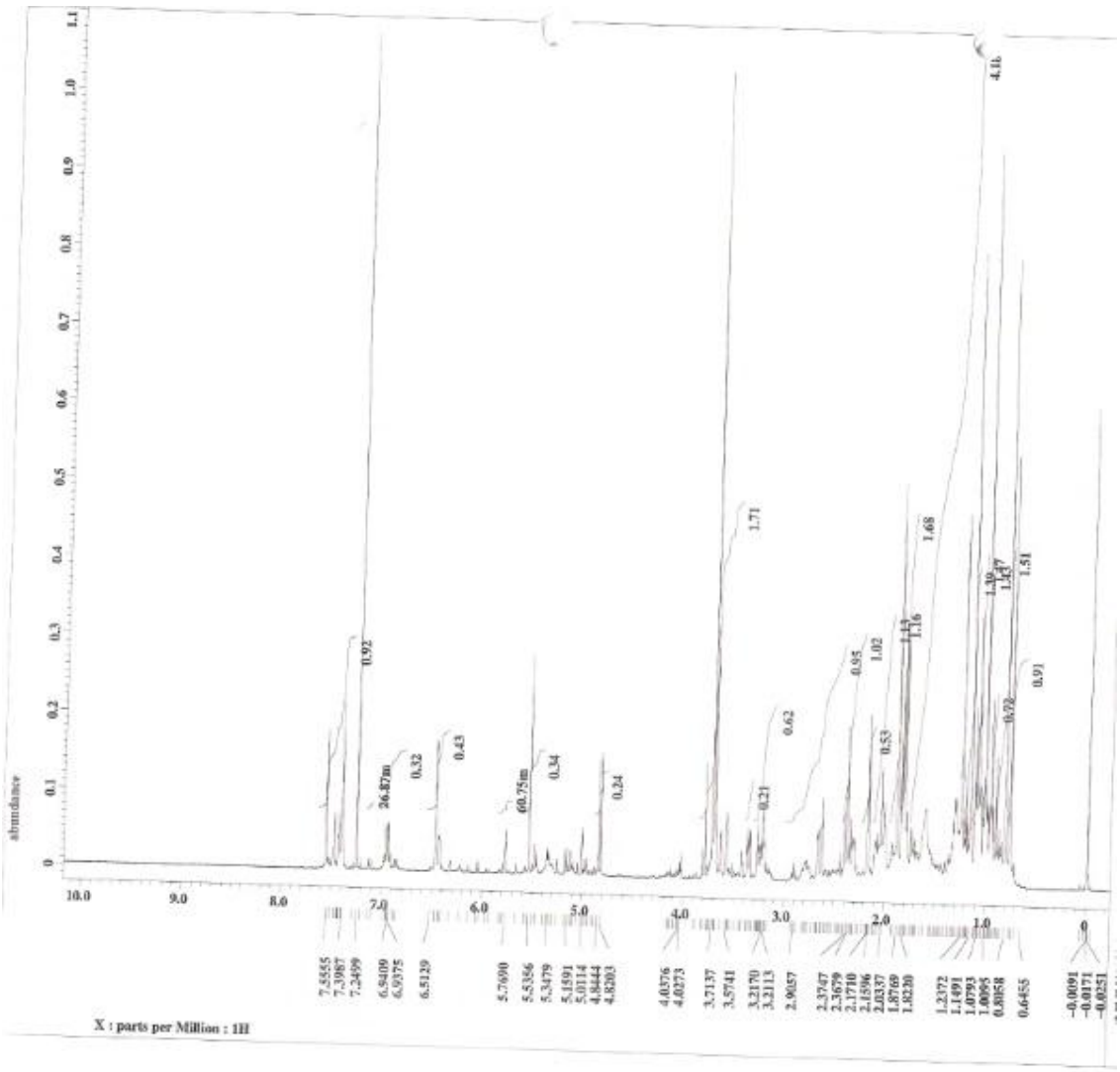

Appendix 16 ^{1}H NMR spectrum of Khayasin T (7).

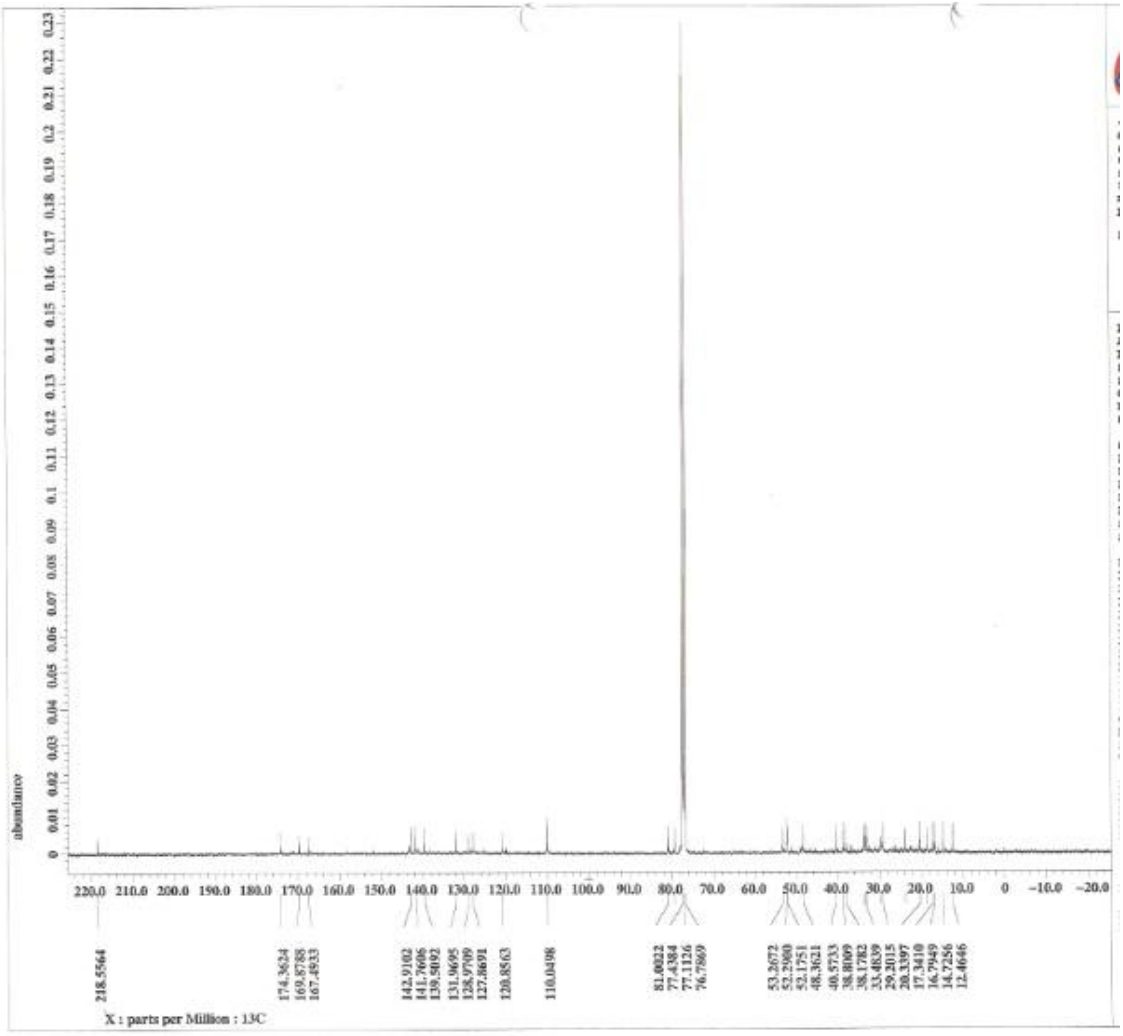

Appendix 17 ^{13}C NMR spectrum of Khayasin T (7).

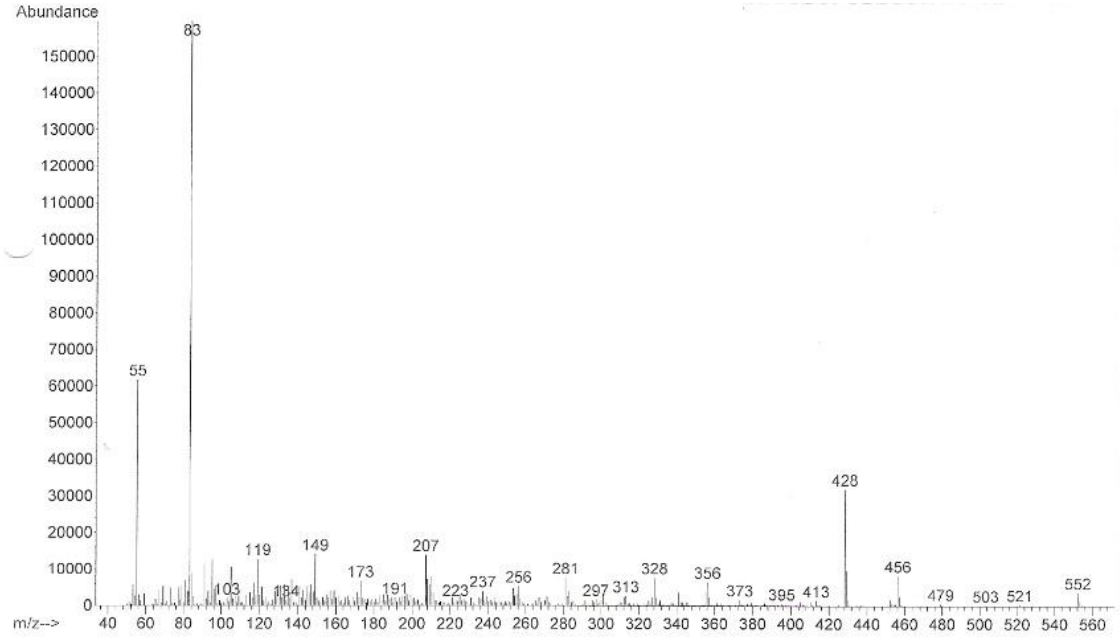

Appendix 18 Mass spectrum of Khayasin T (7).

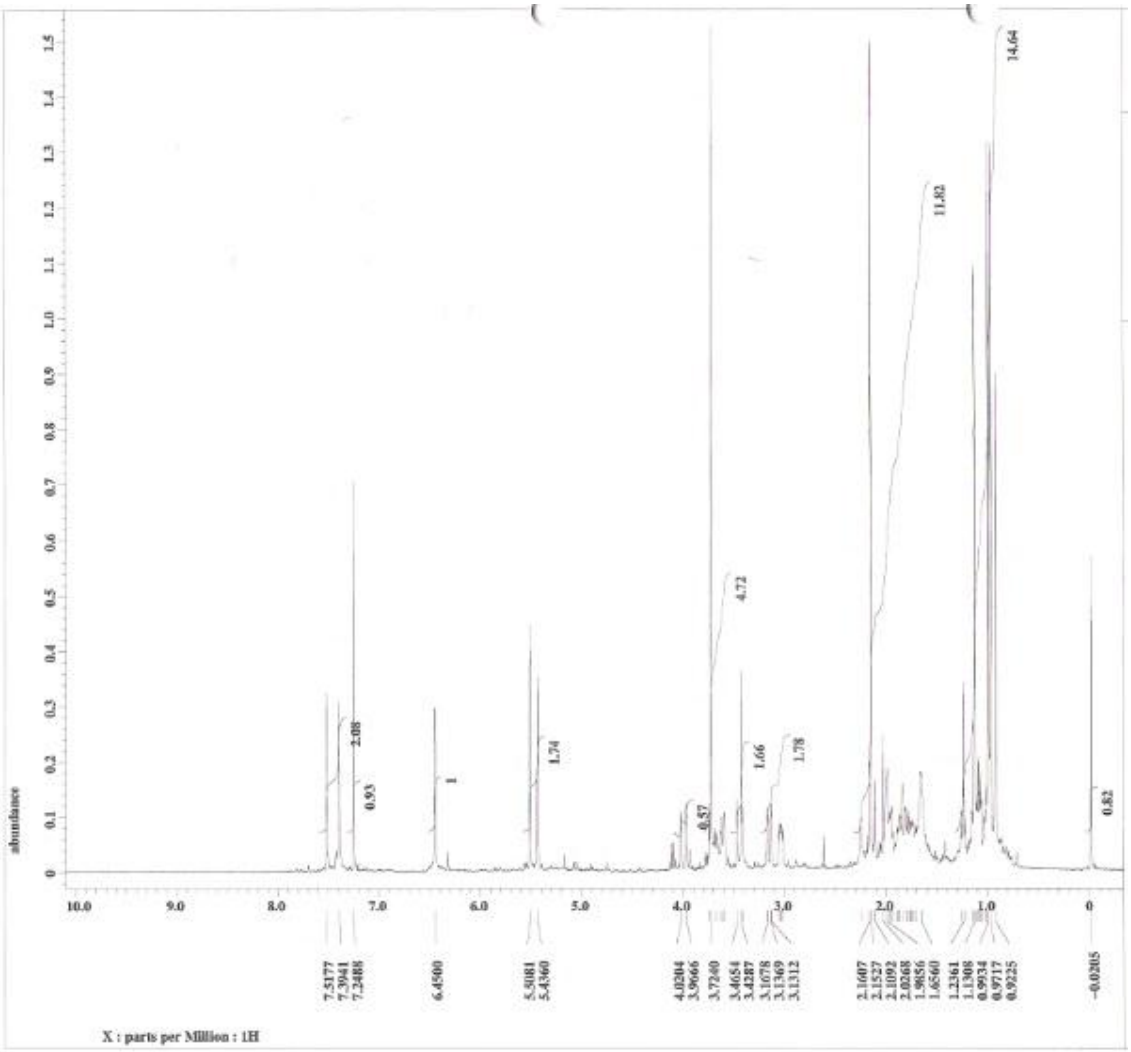

Appendix 19 ^{1}H NMR spectrum of 6-O-acetylswietenolide (8).

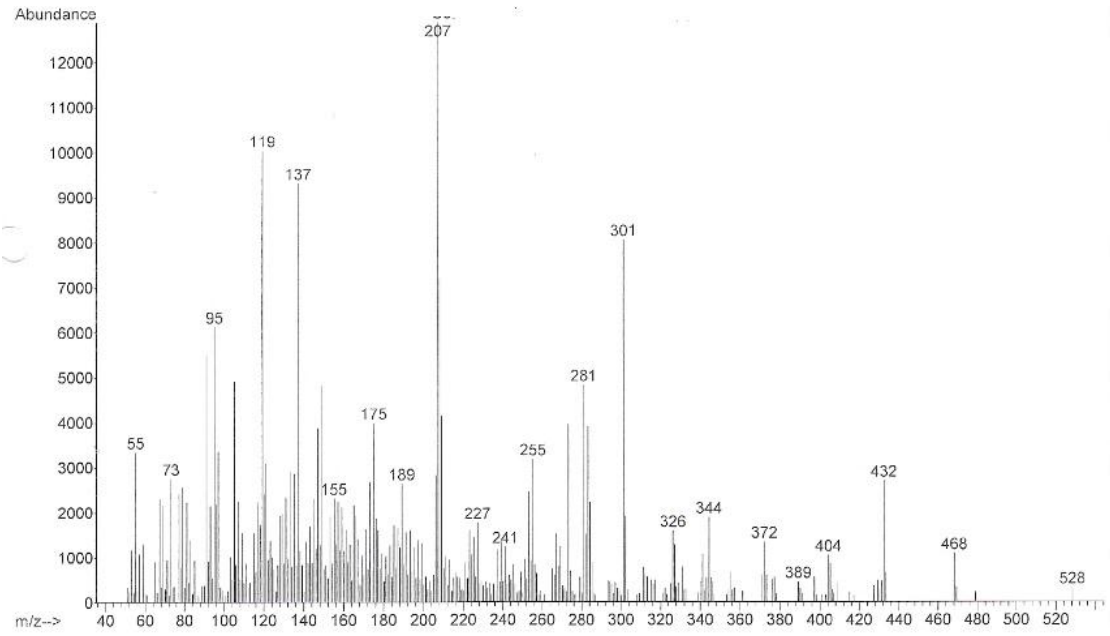

Appendix 20 Mass spectrum of 6-O-acetylswietenolide (8).

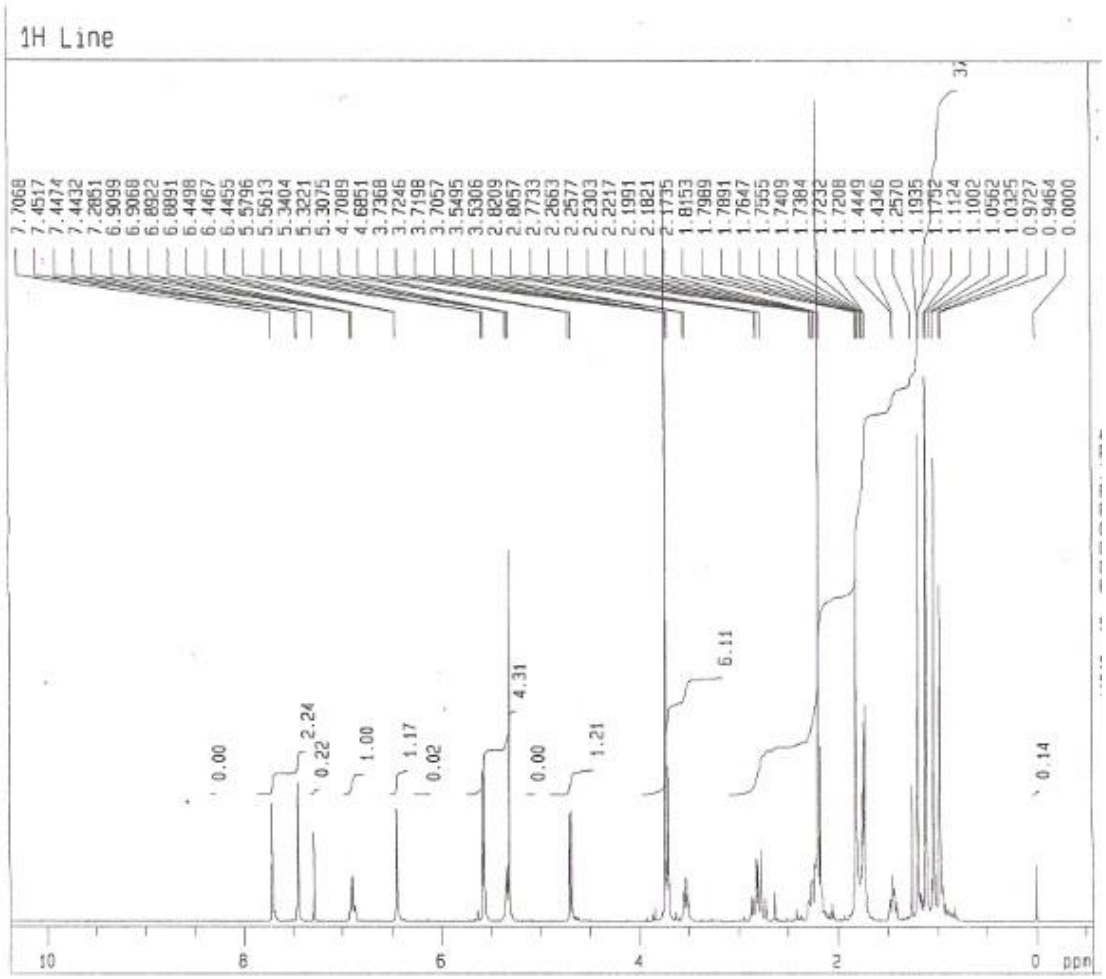

Appendix 21 ^{1}H NMR spectrum of swietenine acetate.

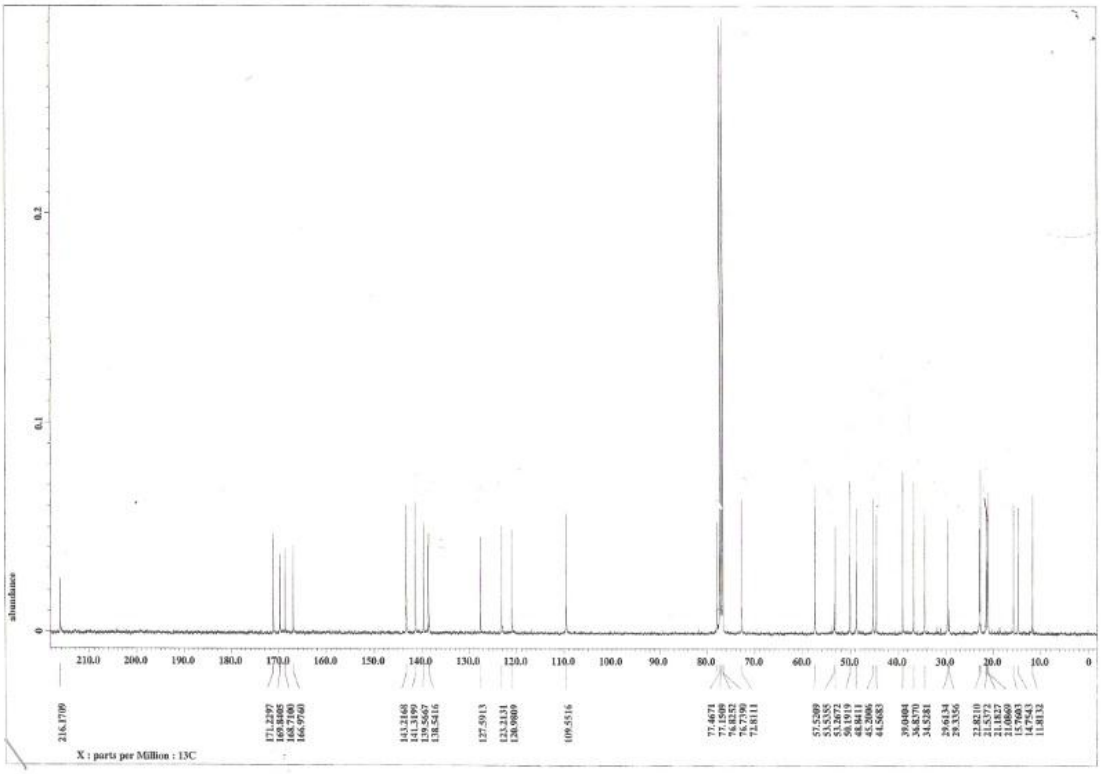

Appendix 22 ^{13}C NMR spectrum of swietenine acetate.

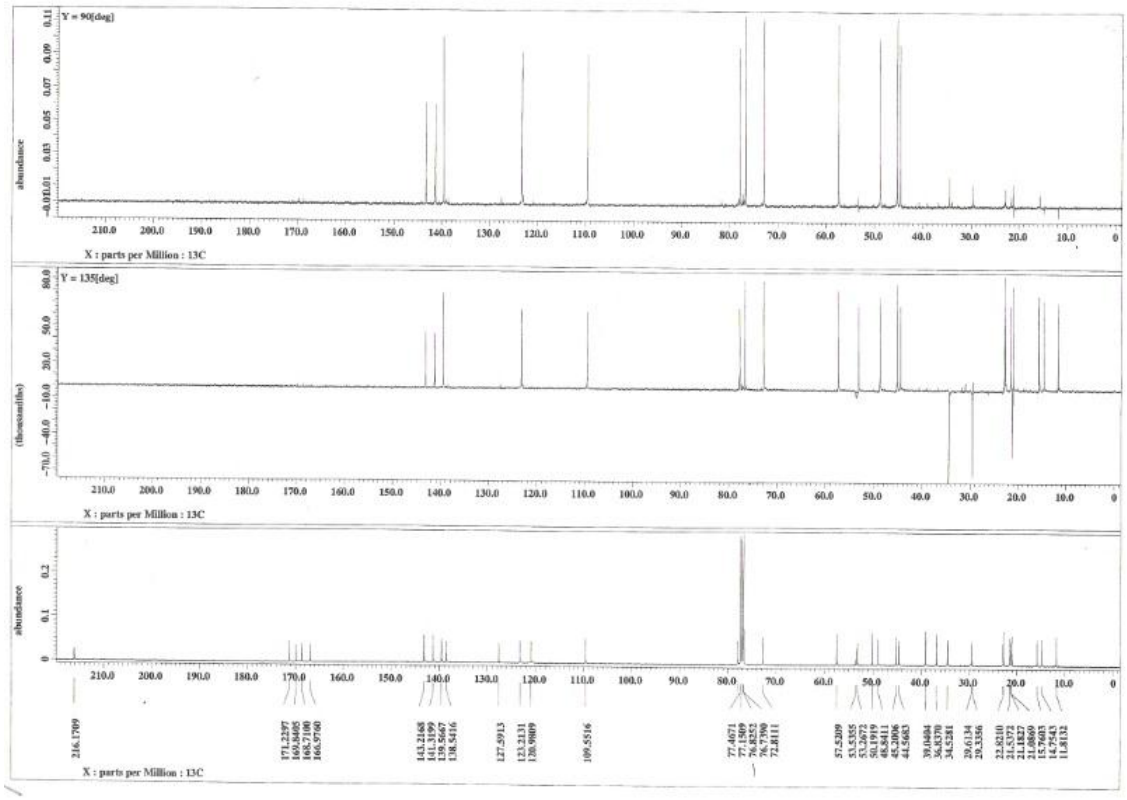

Appendix 23 DEPT NMR spectrum of swietenine acetate.

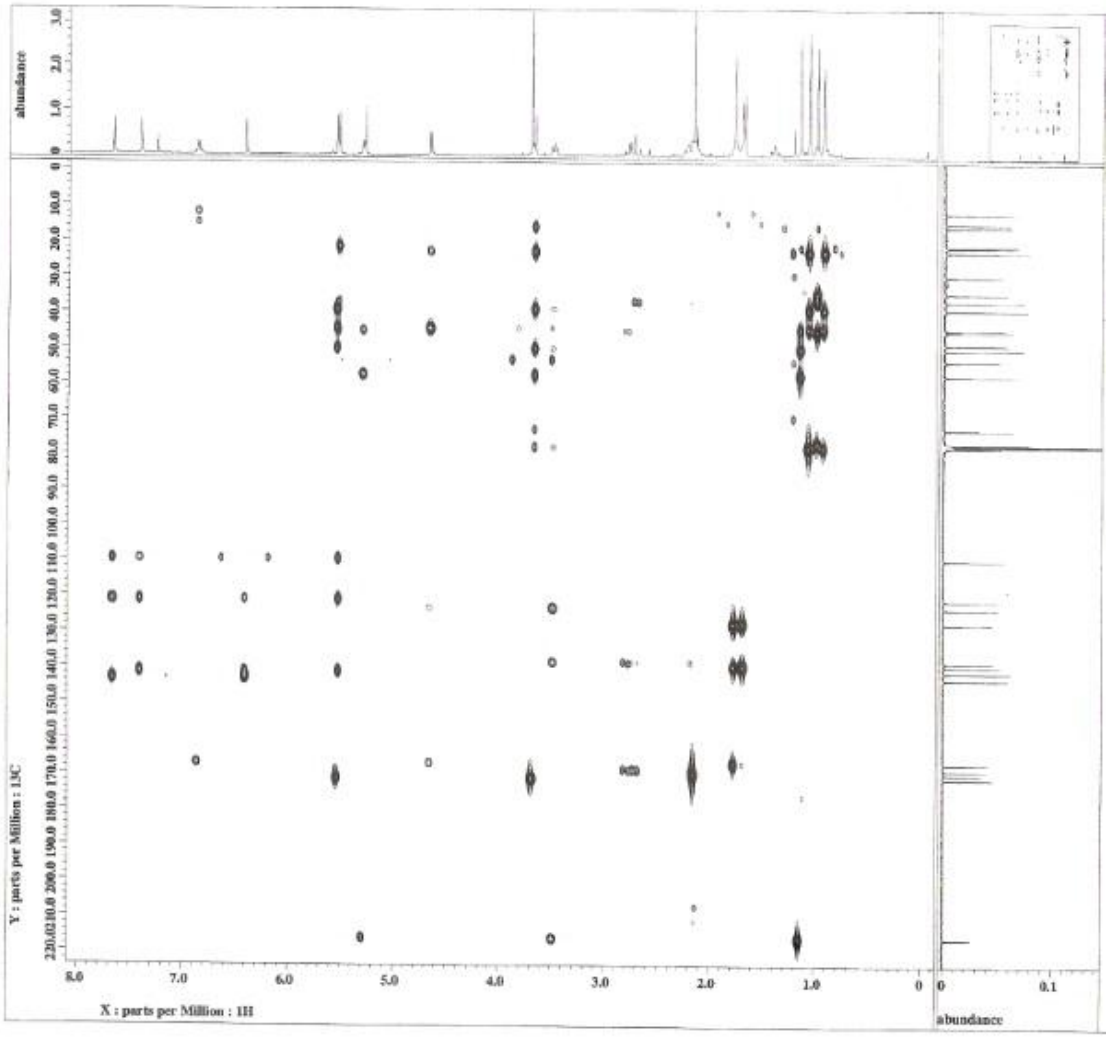

Appendix 24 HMBC NMR spectrum of swietenine acetate.

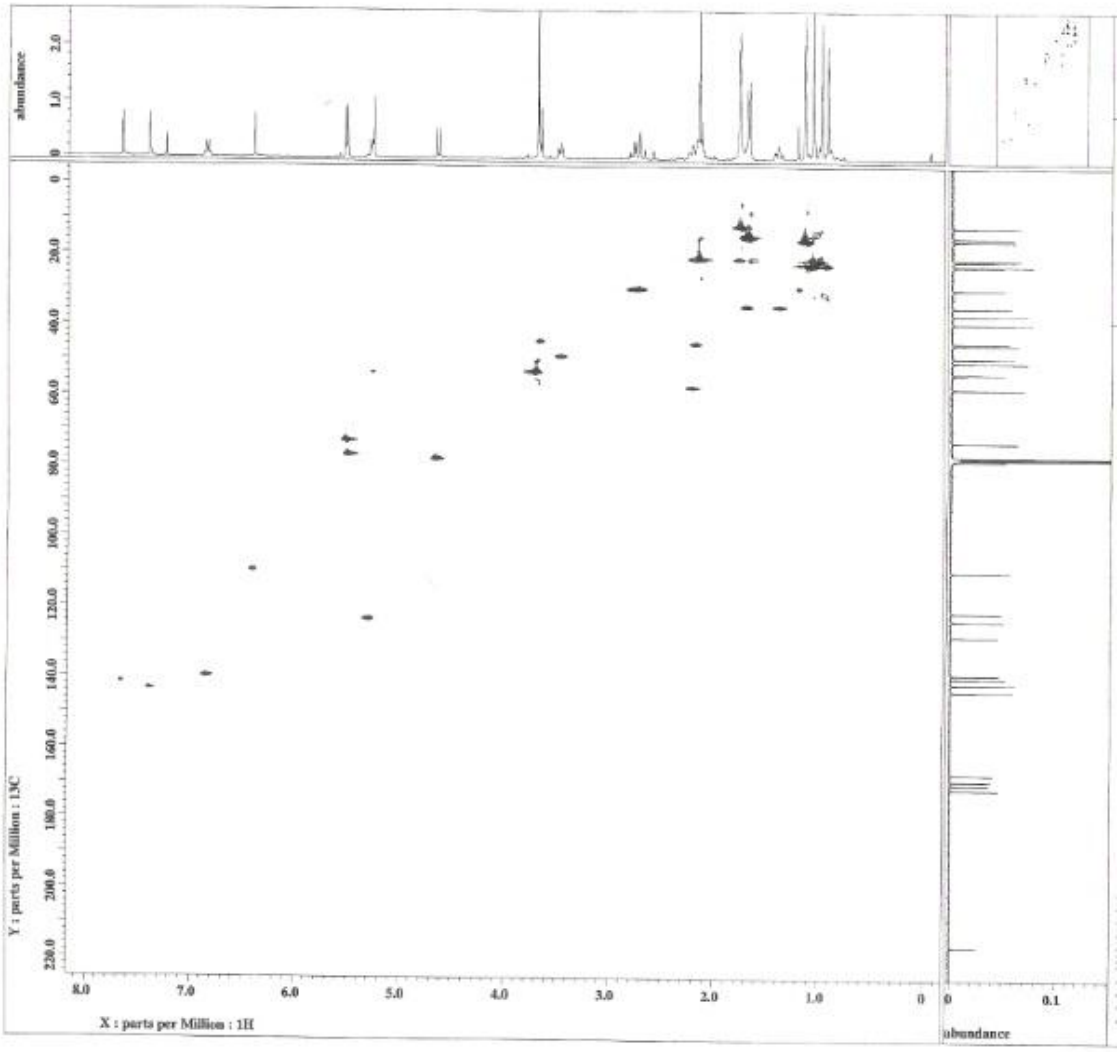

Appendix 25 HSQC NMR spectrum of swietenine acetate.

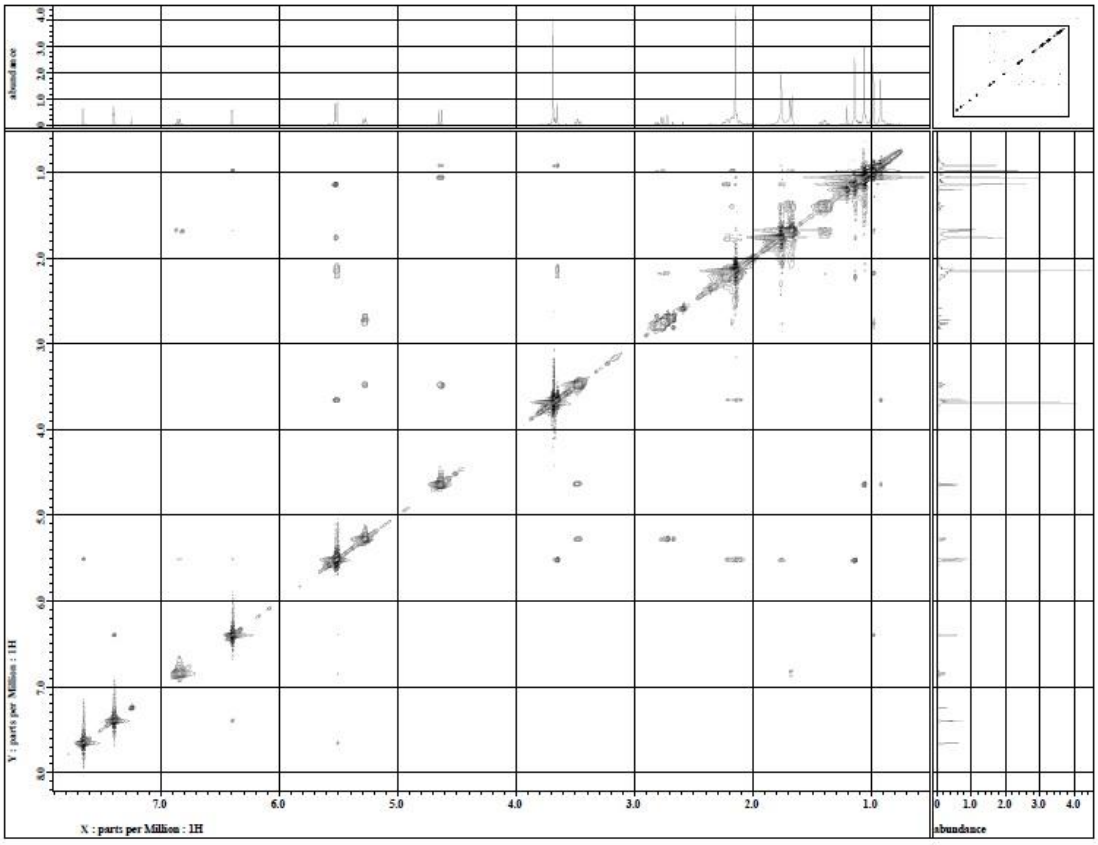

Appendix 26 NOESY NMR spectrum of swietenine acetate.

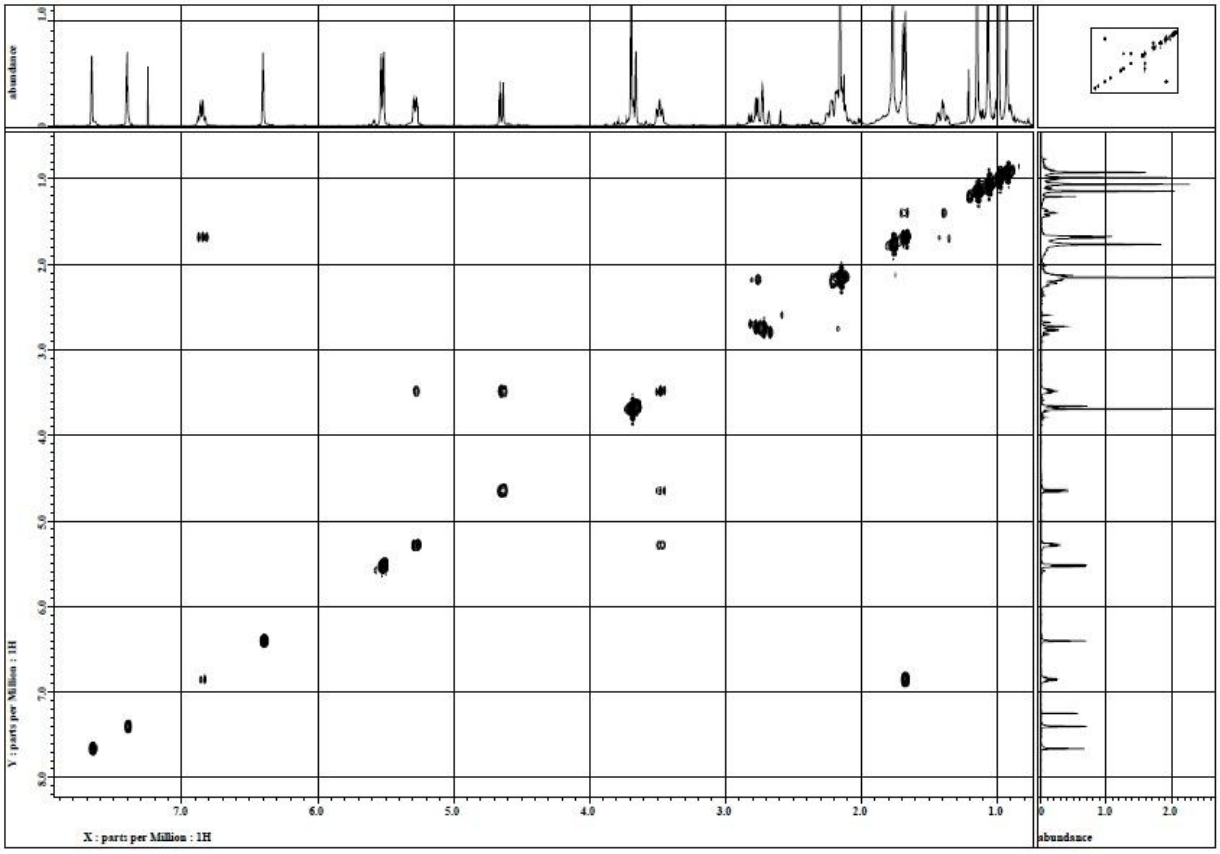

Appendix 27 COSY NMR spectrum of swietenine acetate.

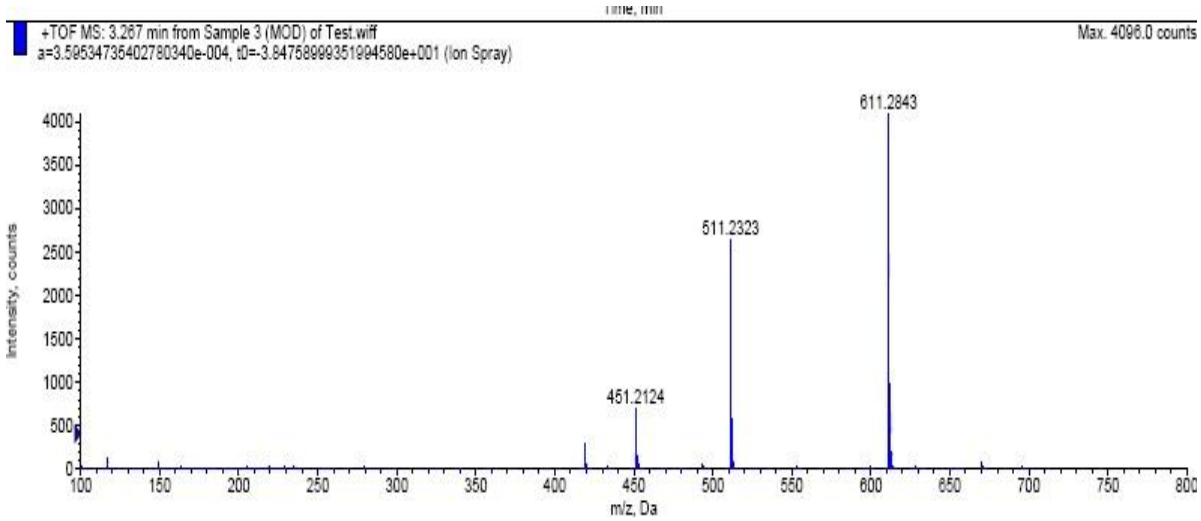

Appendix 28 HRMS of swietenine acetate.

BIBLIOGRAPHY

Adams, J. D., Flora, K., Goldspiel, B., Wilson, J., Arbuck, S., & Finley, R. (1993). Taxol: a history of pharmaceutical development and current pharmaceutical concerns. *Journal of the National Cancer Institute. Monographs, 15*, 141.

Adams, J. M., & Cory, S. (2007). Bcl-2-regulated apoptosis: mechanism and therapeutic potential. *Current Opinion in Immunoogyl, 19*(5), 488-496.

Albano, E., Bellomo, G., Parola, M., Carini, R., & Dianzani, M. U. (1991). Stimulation of lipid peroxidation increases the intracellular calcium content of isolated hepatocytes. *Biochimica et Biophysica Acta, 1091*(3), 310-316.

Alexandroff, A. B., Jackson, A. M., O'Donnell, M. A., & James, K. (1999). BCG immunotherapy of bladder cancer: 20 years on. *Lancet, 353*(9165), 1689-1694.

Alley, M. C., Scudiero, D. A., Monks, A., Hursey, M. L., Czerwinski, M. J., Fine, D. L., . . . Boyd, M. R. (1988). Feasibility of drug screening with panels of human tumor cell lines using a microculture tetrazolium assay. *Cancer Research, 48*(3), 589-601.

Alnemri, E. S., Livingston, D. J., Nicholson, D. W., Salvesen, G., Thornberry, N. A., Wong, W. W., & Yuan, J. (1996). Human ICE/CED-3 protease nomenclature. *Cell, 87*(2), 171.

Anderson, S., Bankier, A. T., Barrell, B. G., de Bruijn, M. H., Coulson, A. R., Drouin, J., . . . Young, I. G. (1981). Sequence and organization of the human mitochondrial genome. *Nature, 290*(5806), 457-465.

Anne, R. H. T. D., A.H. Taylor. (1983). Limonoid extractives from *Swietenia macrophylla*. *Phytochemistry, 22*(12), 2870-2871.

Apakama, I., Robinson, M. C., Walter, N. M., Charlton, R. G., Royds, J. A., Fuller, C. E., . . . Hamdy, F. C. (1996). bcl-2 overexpression combined with p53 protein accumulation correlates with hormone-refractory prostate cancer. *British Journal of Cancer, 74*(8), 1258-1262.

Arnoult, D., Gaume, B., Karbowski, M., Sharpe, J. C., Cecconi, F., & Youle, R. J. (2003). Mitochondrial release of AIF and EndoG requires caspase activation downstream of Bax/Bak-mediated permeabilization. *EMBO J, 22*(17), 4385-4399.

Arrick, B. A., & Nathan, C. F. (1984). Glutathione metabolism as a determinant of therapeutic efficacy: a review. *Cancer Research, 44*(10), 4224-4232.

Bacon, B. R., O'Neill, R., & Britton, R. S. (1993). Hepatic mitochondrial energy production in rats with chronic iron overload. *Gastroenterology, 105*(4), 1134-1140.

Baker, M. A., Cerniglia, G. J., & Zaman, A. (1990). Microtiter plate assay for the measurement of glutathione and glutathione disulfide in large numbers of biological samples. *Analytical Biochemistry, 190*(2), 360-365.

Baldwin, I. T., Halitschke, R., Kessler, A., & Schittko, U. (2001). Merging molecular and ecological approaches in plant–insect interactions. *Current Opinion in Plant Biology, 4*(4), 351-358.

Baretton, G. B., Diebold, J., Christoforis, G., Vogt, M., Muller, C., Dopfer, K., . . . Lohrs, U. (1996). Apoptosis and immunohistochemical bcl-2 expression in colorectal adenomas and carcinomas. Aspects of carcinogenesis and prognostic significance. *Cancer, 77*(2), 255-264.

Barry, M. A., Behnke, C. A., & Eastman, A. (1990). Activation of programmed cell death (apoptosis) by cisplatin, other anticancer drugs, toxins and hyperthermia. *Biochemical Pharmacology, 40*(10), 2353-2362.

Bartkova, J., Horejsi, Z., Koed, K., Kramer, A., Tort, F., Zieger, K., . . . Bartek, J. (2005). DNA damage response as a candidate anti-cancer barrier in early human tumorigenesis. *Nature, 434*(7035), 864-870.

Bass, D. A., Parce, J. W., Dechatelet, L. R., Szejda, P., Seeds, M. C., & Thomas, M. (1983). Flow cytometric studies of oxidative product formation by neutrophils: a graded response to membrane stimulation. *The Journal of Immunology, 130*(4), 1910-1917.

Becker, W. M. K., L. J.; Hardin, J. ; Bertoni, G. P. (2009). *The world of the cell* (7th ed.). San Francisco: Pearson.

Beere, H. M., Wolf, B. B., Cain, K., Mosser, D. D., Mahboubi, A., Kuwana, T., . . . Green, D. R. (2000). Heat-shock protein 70 inhibits apoptosis by preventing recruitment of procaspase-9 to the Apaf-1 apoptosome. *Nature Cell Biology, 2*(8), 469-475.

Bernardi, P., Krauskopf, A., Basso, E., Petronilli, V., Blachly-Dyson, E., Di Lisa, F., & Forte, M. A. (2006). The mitochondrial permeability transition from in vitro artifact to disease target. *FEBS J, 273*(10), 2077-2099.

Blum, R. H., Carter, S. K., & Agre, K. (1973). A clinical review of bleomycin--a new antineoplastic agent. *Cancer, 31*(4), 903-914.

Boehm, T., Folkman, J., Browder, T., & O'Reilly, M. S. (1997). Antiangiogenic therapy of experimental cancer does not induce acquired drug resistance. *Nature, 390*(6658), 404-407.

Born, T. L., Frost, J. A., Schonthal, A., Prendergast, G. C., & Feramisco, J. R. (1994). c-Myc cooperates with activated Ras to induce the cdc2 promoter. *Molecular Cell Biology, 14*(9), 5710-5718.

Bratton, D. L., Fadok, V. A., Richter, D. A., Kailey, J. M., Guthrie, L. A., & Henson, P. M. (1997). Appearance of phosphatidylserine on apoptotic cells requires calcium-mediated nonspecific flip-flop and is enhanced by loss of the aminophospholipid translocase. *The Journal of Biological Chemistry, 272*(42), 26159-26165.

Breinbauer, R., Vetter, I. R., & Waldmann, H. (2002). From protein domains to drug candidates-natural products as guiding principles in the design and synthesis of compound libraries. *Angewandte Chemie International Edition England, 41*(16), 2879-2890.

Bretscher, M. S. (1972). Asymmetrical lipid bilayer structure for biological membranes. *Nature New Biology, 236*(61), 11-12.

Briheim G., F. P., Sandstedt S.,. (1989). Relationship between intracellulary and extracellulary generated oxygen metabolites from primed polymorphonuclear leukocytes differs from that obtained from non-primed cells. *Inflammation, 13*, 455-464.

Bronner, M. P., Culin, C., Reed, J. C., & Furth, E. E. (1995). The bcl-2 proto-oncogene and the gastrointestinal epithelial tumor progression model. *American Journal of Pathology, 146*(1), 20-26.

Brown, N., Jennings, S., & Clements, T. (2003). The ecology, silviculture and biogeography of mahogany (*Swietenia macrophylla*): a critical review of the evidence. *Perspectives in Plant Ecology, Evolution and Systematics, 6*(1-2), 37-49.

Brunelle, J. K., & Letai, A. (2009). Control of mitochondrial apoptosis by the Bcl-2 family. *Journal of Cell Science, 122*(Pt 4), 437-441.

Bryan, T. M., & Cech, T. R. (1999). Telomerase and the maintenance of chromosome ends. *Current Opinion in Cell Biology, 11*(3), 318-324.

Bryan, T. M., Englezou, A., Gupta, J., Bacchetti, S., & Reddel, R. R. (1995). Telomere elongation in immortal human cells without detectable telomerase activity. *EMBO Journal, 14*(17), 4240-4248.

Bunz, F., Dutriaux, A., Lengauer, C., Waldman, T., Zhou, S., Brown, J., . . . Vogelstein, B. (1998). Requirement for p53 and p21 to sustain G2 arrest after DNA damage. *Science, 282*(5393), 1497-1501.

Butler, M. S. (2004). The Role of Natural Product Chemistry in Drug Discovery. *Journal of Natural Products, 67*.

Buzzard, K. A., Giaccia, A. J., Killender, M., & Anderson, R. L. (1998). Heat shock protein 72 modulates pathways of stress-induced apoptosis. *The Journal of Biolical Chemistry, 273*(27), 17147-17153.

Cai, J., Wang, M., Li, B., Wang, C., Chen, Y., & Zuo, Z. (2009). Apoptotic and necrotic action mechanisms of trimethyltin in human hepatoma G2 (HepG2) cells. *Chemical Research in Toxicology, 22*(9), 1582-1587.

Caldon, C. E., & Musgrove, E. A. (2010). Distinct and redundant functions of cyclin E1 and cyclin E2 in development and cancer. *Cell Division, 5*(1), 2.

Camacho, M., Phillipson, J., Croft, S., Solis, P., Marshall, S., & Ghazanfar, S. (2003). Screening of plant extracts for antiprotozoal and cytotoxic activities. *Journal of Ethnopharmacology, 89*(2), 185-191.

Capoulade, C., Bressac-de Paillerets, B., Lefrere, I., Ronsin, M., Feunteun, J., Tursz, T., & Wiels, J. (1998). Overexpression of MDM2, due to enhanced translation, results in inactivation of wild-type p53 in Burkitt's lymphoma cells. *Oncogene, 16*(12), 1603-1610.

Carlson, B. A., Dubay, M. M., Sausville, E. A., Brizuela, L., & Worland, P. J. (1996). Flavopiridol induces G1 arrest with inhibition of cyclin-dependent kinase (CDK) 2 and CDK4 in human breast carcinoma cells. *Cancer Research, 56*(13), 2973.

Castegna, A., Lauderback, C. M., Mohmmad-Abdul, H., & Butterfield, D. A. (2004). Modulation of phospholipid asymmetry in synaptosomal membranes by the lipid peroxidation products, 4-hydroxynonenal and acrolein: implications for Alzheimer's disease. *Brain Research, 1004*(1-2), 193-197.

Chai, J., Shiozaki, E., Srinivasula, S. M., Wu, Q., Datta, P., Alnemri, E. S., & Shi, Y. (2001). Structural basis of caspase-7 inhibition by XIAP. *Cell, 104*(5), 769-780.

Chai, J., Wu, Q., Shiozaki, E., Srinivasula, S. M., Alnemri, E. S., & Shi, Y. (2001). Crystal structure of a procaspase-7 zymogen: mechanisms of activation and substrate binding. *Cell, 107*(3), 399-407.

Chakravarty, T., & Chatterjee, A. . (1955). The constituent of swietenine: The non bitter principle of the seeds of Swietenia macrophylla. *Journal of Indian Chemical Society, 32*, 179-186.

Chakravarty, T., Chatterjee, A., & Krisnagar C. (1957). Constituent of swietenine, the non bitter bitter principle of the seeds of *Swietenia macrophylla*. *Journal of Indian Chemical Society, 34*, 117-120.

Chan, K. C., Tang, T.S. & Toh, H.T. (1976). Isolation of swietenolide diacetate from Swietenia macrophylla. *Phytochemistry, 15*(3), 429-430.

Chan, P. K., Frakes, R., Tan, E. M., Brattain, M. G., Smetana, K., & Busch, H. (1983). Indirect immunofluorescence studies of proliferating cell nuclear antigen in nucleoli of human tumor and normal tissues. *Cancer Research, 43*(8), 3770.

Cheah, P. L., & Looi, L. M. (2001). p53: an overview of over two decades of study. *Malaysia Journal of Pathology, 23*(1), 9-16.

Chen, J. J., Bertrand, H., & Yu, B. P. (1995). Inhibition of adenine nucleotide translocator by lipid peroxidation products. *Free Radical Biology & Medicine, 19*(5), 583-590.

Chen, J. J., Huang, S. S., Liao, C. H., Wei, D. C., Sung, P. J., Wang, T. C., & Cheng, M. J. (2010). A new phragmalin-type limonoid and anti-inflammatory constituents from the fruits of *Swietenia macrophylla*. *Food Chemistry, 120*(2), 379-384.

Chen, J. J., Huang, S.S., Liao, C.H., Wei, D.C., Sung, P.J., Wang, T.C., & Cheng, M.J. (2010). A new phragmalin-type limonoid and anti-inflammatory constituents from the fruits of *Swietenia macrophylla*. *Food Chemistry, 120*, 379-384.

Chen, T., Wong, Y. S., Zheng, W., & Liu, J. (2009). Caspase-and p53-dependent apoptosis in breast carcinoma cells induced by a synthetic selenadiazole derivative. *Chemico- Bioogical Interactions, 180*(1), 54-60.

Chen, X. J., Wang, X., Kaufman, B. A., & Butow, R. A. (2005). Aconitase couples metabolic regulation to mitochondrial DNA maintenance. *Science, 307*(5710), 714-717.

Cheng, A. L., Hsu, C. H., Lin, J. K., Hsu, M. M., Ho, Y. F., Shen, T. S., . . . Hsieh, C. Y. (2001). Phase I clinical trial of curcumin, a chemopreventive agent, in patients with high-risk or pre-malignant lesions. *Anticancer Research, 21*(4B), 2895-2900.

Chiba, T., Takahashi, S., Sato, N., Ishii, S., & Kikuchi, K. (1996). Fas-mediated apoptosis is modulated by intracellular glutathione in human T cells. *European Journal of Immunology, 26*(5), 1164-1169.

Chipuk, J. E., Moldoveanu, T., Llambi, F., Parsons, M. J., & Green, D. R. (2010). The BCL-2 family reunion. *Molecular Cell, 37*(3), 299-310.

Comis, R. L. (1994). Cisplatin: the future. *Seminars in Oncology, 21*, 109-113.

Conforti, F., Ioele, G., Statti, G., Marrelli, M., Ragno, G., & Menichini, F. (2008). Antiproliferative activity against human tumor cell lines and toxicity test on Mediterranean dietary plants. *Food and Chemical Toxicology, 46*(10), 3325-3332.

Connolly, J. D., Henderson, R., McCrindle, R., Overton, K.H., & Bhacca, N.S. . (1964). Constitution of swietenine, a novel tetranortriterpenoid. *Tetrahedron Letters, 37-38*, 2593-2597.

Cordell, G. A. (2002). Natural products in drug discovery – Creating a new vision. *Phytochemistry Reviews*, 261-273.

Cossarizza, A., Baccarani-Contri, M., Kalashnikova, G., & Franceschi, C. (1993). A new method for the cytofluorimetric analysis of mitochondrial membrane potential using the J-aggregate forming lipophilic cation 5,5',6,6'-tetrachloro-1,1',3,3'-tetraethylbenzimidazolcarbocyanine iodide (JC-1). *Biochemcal and Biophysical Research Communications, 197*(1), 40-45.

Cotter, T. G., Lennon, S. V., Glynn, J. M., & Green, D. R. (1992). Microfilament-disrupting agents prevent the formation of apoptotic bodies in tumor cells undergoing apoptosis. *Cancer Research, 52*(4), 997-1005.

Cragg, G. M., & Newman, D. J. (1999). Discovery and development of antineoplastic agents from natural sources. *Cancer Investigation, 17*(2), 153-163.

Cragg, G. M., & Newman, D. J. (2005). Plants as a source of anti-cancer agents. *Journal of Ethnopharmacology, 100*(1), 72-79.

Cragg, G. M., Newman, D. J., & Snader, K. M. (1997). Natural products in drug discovery and development. *Journal of Natural Products, 60*(1), 52-60.

Cross, S. M., Sanchez, C. A., Morgan, C. A., Schimke, M. K., Ramel, S., Idzerda, R. L., . . . Reid, B. J. (1995). A p53-dependent mouse spindle checkpoint. *Science, 267*(5202), 1353-1356.

Cryns, V. L., Bergeron, L., Zhu, H., Li, H., & Yuan, J. (1996). Specific cleavage of alpha-fodrin during Fas- and tumor necrosis factor-induced apoptosis is mediated by an interleukin-1beta-converting enzyme/Ced-3 protease distinct from the poly(ADP-ribose) polymerase protease. *The Journal of Biological Chemistry, 271*(49), 31277-31282.

Cuervo, A. M. (2004). Autophagy: many paths to the same end. *Molecular and Cellular Biochemistry, 263*(1-2), 55-72.

Cunningham, C. C. (1992). Actin structural proteins in cell motility. *Cancer Metastasis Review, 11*(1), 69-77.

Cunningham, C. C. (1995). Actin polymerization and intracellular solvent flow in cell surface blebbing. *The Journal of Cell Biology, 129*(6), 1589-1599.

Dameron, K. M., Volpert, O. V., Tainsky, M. A., & Bouck, N. (1994). The p53 tumor suppressor gene inhibits angiogenesis by stimulating the production of thrombospondin. *Cold Spring Harbor Symposia Quantitative Biology, 59*, 483-489.

Danial, N. N., & Korsmeyer, S. J. (2004). Cell death: critical control points. *Cell, 116*(2), 205-219.

Darzynkiewicz, Z., Galkowski, D., & Zhao, H. (2008a). Analysis of apoptosis by cytometry using TUNEL assay. *Methods, 44*(3), 250-254.

Darzynkiewicz, Z., Galkowski, D., & Zhao, H. (2008b). Analysis of apoptosis by cytometry using TUNEL assay. *Methods, 44*(3), 250-254.
Darzynkiewicz, Z., Huang, X., & Okafuji, M. (2006). Detection of DNA strand breaks by flow and laser scanning cytometry in studies of apoptosis and cell proliferation (DNA replication). *Methods in Molecular Biology, 314*, 81-93.

Das, A., Jeba Sunilson, J., Gopinath, R., Radhamani, S., & Nilugal, K. (2009). Anti-nociceptive activity of the fruits of *Swietenia macrophylla* King. *Journal of Pharmacy Research, 2*(9), 1367-1369.

DeGregori, J., Kowalik, T., & Nevins, J. R. (1995). Cellular targets for activation by the E2F1 transcription factor include DNA synthesis- and G1/S-regulatory genes. *Molecular and Cellular Biology, 15*(8), 4215-4224.

Degterev, A., Boyce, M., & Yuan, J. (2003). A decade of caspases. *Oncogene, 22*(53), 8543-8567.

Del Sal, G., Ruaro, E. M., Utrera, R., Cole, C. N., Levine, A. J., & Schneider, C. (1995). Gas1-induced growth suppression requires a transactivation-independent p53 function. *Molecular and Cellular Biology, 15*(12), 7152-7160.

DeLeo, A. B., Jay, G., Appella, E., Dubois, G. C., Law, L. W., & Old, L. J. (1979). Detection of a transformation-related antigen in chemically induced sarcomas and other transformed cells of the mouse. *Proceedings of the National Academy of Science U S A, 76*(5), 2420-2424.

Denault, J. B., Bekes, M., Scott, F. L., Sexton, K. M., Bogyo, M., & Salvesen, G. S. (2006). Engineered hybrid dimers: tracking the activation pathway of caspase-7. *Molecular Cell, 23*(4), 523-533.

Denecker, G., Vercammen, D., Steemans, M., Vanden Berghe, T., Brouckaert, G., Van Loo, G., . . . Vandenabeele, P. (2001). Death receptor-induced apoptotic and necrotic cell death: differential role of caspases and mitochondria. *Cell Death & Differerentiation, 8*(8), 829-840.

Denicourt, C., & Dowdy, S. F. (2004). Medicine. Targeting apoptotic pathways in cancer cells. *Science, 305*(5689), 1411-1413.

Desagher, S., & Martinou, J. C. (2000). Mitochondria as the central control point of apoptosis. *Trends in Cell Biology, 10*(9), 369.

Dewanjee, S., Maiti, A., Das, A. K., Mandal, S. C., & Dey, S. P. (2009a). Swietenine: a potential oral hypoglycemic from *Swietenia macrophylla* seed. *Fitoterapia, 80*(4), 249-251.
Dewanjee, S., Maiti, A., Das, A. K., Mandal, S. C., & Dey, S. P. (2009b). Swietenine: A potential oral hypoglycemic from *Swietenia macrophylla* seed. *Fitoterapia, 80*(4), 249-251.

Dive, C., Gregory, C. D., Phipps, D. J., Evans, D. L., Milner, A. E., & Wyllie, A. H. (1992). Analysis and discrimination of necrosis and apoptosis (programmed cell death) by multiparameter flow cytometry. *Biochimica et Biophysica Acta, 1133*(3), 275.

Dohlman, W., Caroti, M., Leflowitz, R., Nathans, J., Kubo, T., Bonner, T., . . . Julius, D. (1988). Bcl-2 gene promotes haemopoietic cell survival and cooperates with c-myc to immortalize pre-B cells. *Nature, 335*, 440-442.

Dong, J., Ma, X., Wei, Q., Peng, S., & Zhang, S. (2011). Effects of growing location on the contents of secondary metabolites in the leaves of four selected superior clones of Eucommia ulmoides. *Industrial Crops and Products*.

Droge, W. (2002). Free radicals in the physiological control of cell function. *Physiological Review, 82*(1), 47-95.

Duprez, L., Wirawan, E., Vanden Berghe, T., & Vandenabeele, P. (2009). Major cell death pathways at a glance. *Microbes and Infection, 11*(13), 1050-1062.

Dyson, N., Howley, P. M., Munger, K., & Harlow, E. (1989). The human papilloma virus-16 E7 oncoprotein is able to bind to the retinoblastoma gene product. *Science, 243*(4893), 934-937.

Edinger, A. L., & Thompson, C. B. (2004). Death by design: apoptosis, necrosis and autophagy. *Current Opinion in Cell Biology, 16*(6), 663-669.

El-Deiry, W. S., Harper, J. W., O'Connor, P. M., Velculescu, V. E., Canman, C. E., Jackman, J., . . . Wang, Y. (1994). WAF1/CIP1 is induced in p53-mediated G1 arrest and apoptosis. *Cancer Research, 54*(5), 1169.

el-Deiry, W. S., Tokino, T., Velculescu, V. E., Levy, D. B., Parsons, R., Trent, J. M., . . . Vogelstein, B. (1993). WAF1, a potential mediator of p53 tumor suppression. *Cell, 75*(4), 817-825.

Elmore, S. (2007). Apoptosis: a review of programmed cell death. *Toxicological Pathology, 35*(4), 495-516.

Enari, M., Sakahira, H., Yokoyama, H., Okawa, K., Iwamatsu, A., & Nagata, S. (1998). A caspase-activated DNase that degrades DNA during apoptosis, and its inhibitor ICAD. *Nature, 391*(6662), 43-50.

Essack, M., Bajic, V. B., & Archer, J. A. (2011). Recently confirmed apoptosis-inducing lead compounds isolated from marine sponge of potential relevance in cancer treatment. *Marine Drugs, 9*(9), 1580-1606.

Ewen, M. E., Oliver, C. J., Sluss, H. K., Miller, S. J., & Peeper, D. S. (1995). p53-dependent repression of CDK4 translation in TGF-beta-induced G1 cell-cycle arrest. *Genes & Development, 9*(2), 204-217.

Eyer, P., & Podhradsky, D. (1986). Evaluation of the micromethod for determination of glutathione using enzymatic cycling and Ellman's reagent. *Analytical Biochemistry, 153*(1), 57-66.

Fan, T. J., Han, L. H., Cong, R. S., & Liang, J. (2005). Caspase family proteases and apoptosis. *Acta Biochimica Biophysica Sinica, 37*(11), 719-727.

Fan, T. J., Xia, L., & Han, Y. R. (2001). Mitochondrion and Apoptosis. *Sheng Wu Hua Xue Yu Sheng Wu Wu Li Xue Bao (Shanghai), 33*(1), 7-12.

Fang, S., Jensen, J. P., Ludwig, R. L., Vousden, K. H., & Weissman, A. M. (2000). Mdm2 is a RING finger-dependent ubiquitin protein ligase for itself and p53. *Journal of Biological Chemistry, 275*(12), 8945.

Feher, M., & Schmidt, J. M. (2003). Property distributions: differences between drugs, natural products, and molecules from combinatorial chemistry. *Journal of Chemical Information and Modeling, 43*(1), 218-227.

Fernandes, R. S., & Cotter, T. G. (1994). Apoptosis or necrosis: intracellular levels of glutathione influence mode of cell death. *Biochem Pharmacol, 48*(4), 675-681.

Feron, O. (2009). Pyruvate into lactate and back: from the Warburg effect to symbiotic energy fuel exchange in cancer cells. *Radiotherapy Oncology, 92*(3), 329-333.

Festjens, N., Vanden Berghe, T., & Vandenabeele, P. (2006). Necrosis, a well-orchestrated form of cell demise: signalling cascades, important mediators and concomitant immune response. *Biochimica et Biophysica Acta, 1757*(9-10), 1371-1387.

Fischli A.E. (2002). Molecular basis of biodiversity, conservation, and sustained innovative utilization. *Pure and Applied Chemistry, 74*, 697 - 702.

Flohil, C. C., Janssen, P. A., & Bosman, F. T. (1996). Expression of Bcl-2 protein in hyperplastic polyps, adenomas, and carcinomas of the colon. *The Journal of Pathology, 178*(4), 393-397.

Folkman, J. (1998a). Angiogenic therapy of the human heart. *Circulation, 97*(7), 628-629.

Folkman, J. (1998b). Therapeutic angiogenesis in ischemic limbs. *Circulation, 97*(12), 1108-1110.

Foster, B. A., Coffey, H. A., Morin, M. J., & Rastinejad, F. (1999). Pharmacological rescue of mutant p53 conformation and function. *Science, 286*(5449), 2507-2510.

Fraenkel, G. S. (1959). The raison d'etre of secondary plant substances. *Science, 129*(3361), 1466.

Fridovich, I. (1997). Superoxide anion radical (O2-.), superoxide dismutases, and related matters. *The Journal of Biological Chemistry, 272*(30), 18515-18517.

Fuentes-Prior, P., & Salvesen, G. S. (2004). The protein structures that shape caspase activity, specificity, activation and inhibition. *Biochemcal Journal, 384*(Pt 2), 201-232.

Fynan, T. M., & Reiss, M. (1993). Resistance to inhibition of cell growth by transforming growth factor-beta and its role in oncogenesis. *Critical Review Oncogenesis, 4*(5), 493-540.

Galaktionov, K., Chen, X., & Beach, D. (1996). Cdc25 cell-cycle phosphatase as a target of c-myc. *Nature, 382*(6591), 511-517.

Galimard, N., Vassilev, K., Chevignard, M., Perrigot, M., & Mazevet, D. (2004). Spontaneous muscular haematomas in hemiplegic patients receiving anticoagulation therapy. *Revisa de Neurologia, 160*(6-7), 672-677.

Galluzzi, L., Morselli, E., Kepp, O., Vitale, I., Rigoni, A., Vacchelli, E., . . . Kroemer, G. (2010). Mitochondrial gateways to cancer. *Moecularl Aspects of Medicine, 31*(1), 1-20.

Gartel, A. L., & Radhakrishnan, S. K. (2005). Lost in transcription: p21 repression, mechanisms, and consequences. *Cancer Research, 65*(10), 3980.

Gately, D. P., & Howell, S. B. (1993). Cellular accumulation of the anticancer agent cisplatin: a review. *British Journal of Cancer, 67*(6), 1171-1176.

Gavathiotis, E., Suzuki, M., Davis, M. L., Pitter, K., Bird, G. H., Katz, S. G., . . . Tjandra, N. (2008). BAX activation is initiated at a novel interaction site. *Nature, 455*(7216), 1076-1081.

Gelderblom, H., Verweij, J., Nooter, K., & Sparreboom, A. (2001). Cremophor EL: the drawbacks and advantages of vehicle selection for drug formulation. *European Journal of Cancer, 37*(13), 1590-1598.

Gennaro, A. R. (2000). Remington: the science and practice of pharmacy. *Philadelphia, USA*.

Gerl, R., & Vaux, D. L. (2005). Apoptosis in the development and treatment of cancer. *Carcinogenesis, 26*(2), 263-270.

Gershell, L. J., & Atkins, J. H. (2003). A brief history of novel drug discovery technologies. *Nature Reviews Drug Discovery, 2*(4), 321-327.

Gidding, C. E., Kellie, S. J., Kamps, W. A., & de Graaf, S. S. (1999). Vincristine revisited. *Critical Reviews in Oncology/ Hematology, 29*(3), 267-287.

Goh, B. H., Abdul Kadir, H., Abdul Malek, S., & Ng, S. W. (2010a). (R, 4R, 4aR, 6aS, 7R, 8S, 10R, 11S)-Methyl-acetoxy-4-(3-furanyl)-10-hydroxy-4a, 7, 9, 9-tetramethyl-2, 13-dioxo-1, 4, 4a, 5, 6, 6a, 7, 8, 9, 10, 11, 12-dodecahydro-7, 11-methano-2H-cycloocta [f][2] benzopyran-8-acetate (6-O-acetylswietenolide) from the seeds of *Swietenia macrophylla*. *Acta Crystallographica Section E: Structure Reports Online, 66*(11), o2802-o2803.

Goh, B. H., Abdul Kadir, H., Abdul Malek, S., & Ng, S. W. (2010b). Swietenolide diacetate from the seeds of *Swietenia macrophylla*. *Acta Crystallographica Section E: Structure Reports Online, 66*(6), o1396-o1396.

Goh, B. H., & Kadir, A. (2011). In vitro cytotoxic potential of *Swietenia macrophylla* King seeds against human carcinoma cell lines. *Journal Medicinal Plants Research, 5*(8), 1395-1404.

Golstein, P., & Kroemer, G. (2007). Cell death by necrosis: towards a molecular definition. *Trends in Biochemical Sciences, 32*(1), 37-43.

Gonzales, G. F., & Valerio Jr, L. (2006). Medicinal plants from Peru: a review of plants as potential agents against cancer. *Anti-cancer Agents in Medicinal Chemistry, 6*(5), 429.

Govindachari, T., Suresh, G., Banumathy, B., Masilamani, S., Gopalakrishnan, G., & Krishna Kumari, G. (1999). Antifungal activity of some B, D-seco limonoids from two meliaceous plants. *Journal of Chemical Ecology, 25*(4), 923-933.

Govindachari T. R., S. G., Banumathy B., Masilamani S., Geetha Gopalakrishnan, Krishna Kumari G. N. (1999). Antifungal Activity of Some B-D-Seco Limonoids From Two Meliaceous Plants. *Journal of Chemical Ecology, 27*(4), 923-933.

Green, D. R., & Chipuk, J. E. (2008). Apoptosis: Stabbed in the BAX. *Nature, 455*(7216), 1047-1049.

Green, D. R., & Kroemer, G. (2004). The pathophysiology of mitochondrial cell death. *Science's STKE, 305*(5684), 626.

Green, D. R., & Reed, J. C. (1998). Mitochondria and apoptosis. *Science, 281*(5381), 1309-1312.

Griffith, O. W. (1980). Determination of glutathione and glutathione disulfide using glutathione reductase and 2-vinylpyridine. *Analytical Biochemistry, 106*(1), 207-212.
\

Gross, A., McDonnell, J. M., & Korsmeyer, S. J. (1999). BCL-2 family members and the mitochondria in apoptosis. *Genes & Development, 13*(15), 1899-1911.

Guevera, A., Apilado, A., Sakarai, H., Kozuka, M., & Tokunda, H. (1996). Anti-inflammatory, antimutagenecity and antitumor activity of mahagony seeds *Swietenia macrophylla* (Meliaceae). *Phillipine Journal of Science, 125*(4), 271-278.

Guha, S. S. S. G., & Chakraborty, T. (1951). Tetranortriterpenoid from *Swietenia macrophylla*. *Journal of Indian Chemical Society, 28*, 207-207.

Gupta, S., Kass, G. E., Szegezdi, E., & Joseph, B. (2009). The mitochondrial death pathway: a promising therapeutic target in diseases. *Journal of Cellular and Molecular Medicine, 13*(6), 1004-1033.

Gus'kova, R. A., Ivanov, II, Kol'tover, V. K., Akhobadze, V. V., & Rubin, A. B. (1984). Permeability of bilayer lipid membranes for superoxide (O2-.) radicals. *Biochimica et Biophysica Acta, 778*(3), 579-585.

Hall, D. G., Manku, S., & Wang, F. (2001). Solution- and solid-phase strategies for the design, synthesis, and screening of libraries based on natural product templates: a comprehensive survey. *Journal of Combinatorial Chemistry, 3*(2), 125-150.

Halliwell, B., & Gutteridge, J. (1989). Lipid peroxidation: a radical chain reaction. *Free Radicals in Biology and Medicine, 2*, 1989.1188-1276.

Hamada, M., Fujiwara, T., Hizuta, A., Gochi, A., Naomoto, Y., Takakura, N., . . . Orita, K. (1996). The p53 gene is a potent determinant of chemosensitivity and radiosensitivity in gastric and colorectal cancers. *Journal of Cancer Research and Clinal Oncology, 122*(6), 360-365.

Hamburger, M., & Hostettmann, K. (1991). 7. Bioactivity in plants: the link between phytochemistry and medicine. *Phytochemistry, 30*(12), 3864-3874.

Han, D., Antunes, F., Canali, R., Rettori, D., & Cadenas, E. (2003). Voltage-dependent anion channels control the release of the superoxide anion from mitochondria to cytosol. *The Journal of Bioogical Chemistry, 278*(8), 5557-5563.

Hanahan, D., & Weinberg, R. A. (2000). The hallmarks of cancer. *Cell, 100*(1), 57-70.

Hanahan, D., & Weinberg, R. A. (2011). Hallmarks of cancer: the next generation. *Cell, 144*(5), 646-674.

Hanif, R., Qiao, L., Shiff, S. J., & Rigas, B. (1997). Curcumin, a natural plant phenolic food additive, inhibits cell proliferation and induces cell cycle changes in colon adenocarcinoma cell lines by a prostaglandin-independent pathway. *Journal of Laboratory Clinical Medicine, 130*(6), 576-584.

Hansen, M. B., Nielsen, S. E., & Berg, K. (1989). Re-examination and further development of a precise and rapid dye method for measuring cell growth cell kill. *Journal of Immunological Methods, 119*(2), 203-210.

Harvey, A. L. (1999). Medicines from nature: are natural products still relevant to drug discovery? *Trends in Pharmacological Sciences, 20*(5), 196-198.

Hawk, E., Lubet, R., & Limburg, P. (1999). Chemoprevention in hereditary colorectal cancer syndromes. *Cancer, 86*, 2551-2563.

Heales, R., Davies, S., Bates, T., & Clark, J. (1995). Deoletion of brain glutathione is accompanied by impaired micochondrial function and decreased N-acetyl aspartate concentration. *Neurochemical Research, 20*(1), 31-38.

Hedley, D., & Chow, S. (1994). Glutathione and cellular resistance to anti-cancer drugs. *Methods Cell Biology, 42 Pt B*, 31-44.

Helmbrecht, K., Zeise, E., & Rensing, L. (2000). Chaperones in cell cycle regulation and mitogenic signal transduction: a review. *Cell Proliferation, 33*(6), 341-365.

Hennet, T., Bertoni, G., Richter, C., & Peterhans, E. (1993). Expression of BCL-2 protein enhances the survival of mouse fibrosarcoid cells in tumor necrosis factor-mediated cytotoxicity. *Cancer Research, 53*(6), 1456-1460.

Hernandez-Boussard, T., Montesano, R., & Hainaut, P. (1999). Sources of bias in the detection and reporting of p53 mutations in human cancer: analysis of the IARC p53 mutation database. *Genet Anal, 14*(5-6), 229-233.

Hoffmann, P. R., Kench, J. A., Vondracek, A., Kruk, E., Daleke, D. L., Jordan, M., . . . Fadok, V. A. (2005). Interaction between phosphatidylserine and the phosphatidylserine receptor inhibits immune responses in vivo. *The Journal of Immunology, 174*(3), 1393-1404.

Hollstein, M., Sidransky, D., Vogelstein, B., & Harris, C. C. (1991). p53 mutations in human cancers. *Science, 253*(5015), 49-53.

Honda N., & Santos-Magalhaesy ô, N. (2004). In vitro and in vivo properties of usnic acid encapsulated into PLGA-microspheres. *Journal of Microencapsulation, 21*(4), 371-384.

Horton, D. A., Bourne, G. T., & Smythe, M. L. (2003). The combinatorial synthesis of bicyclic privileged structures or privileged substructures. *Chemical Review, 103*(3), 893-930.

Hotchkiss, R. S., Strasser, A., McDunn, J. E., & Swanson, P. E. (2009). Cell death. *The New England Journal of Medicine, 361*(16), 1570-1583.

Hu, W. P., Yu, H. S., Sung, P. J., Tsai, F. Y., Shen, Y. K., Chang, L. S., & Wang, J. J. (2007). DC-81-Indole conjugate agent induces mitochondria mediated apoptosis in human melanoma A375 cells. *Chemical Research in Toxicology, 20*(6), 905-912.

Huang, M. T., Deschner, E. E., Newmark, H. L., Wang, Z. Y., Ferraro, T. A., & Conney, A. H. (1992). Effect of dietary curcumin and ascorbyl palmitate on azoxymethanol-induced colonic epithelial cell proliferation and focal areas of dysplasia. *Cancer Letter, 64*(2), 117-121.

Huang, M. T., Lou, Y. R., Ma, W., Newmark, H. L., Reuhl, K. R., & Conney, A. H. (1994). Inhibitory effects of dietary curcumin on forestomach, duodenal, and colon carcinogenesis in mice. *Cancer Research, 54*(22), 5841-5847.

Huang, M. T., Wang, Z. Y., Georgiadis, C. A., Laskin, J. D., & Conney, A. H. (1992). Inhibitory effects of curcumin on tumor initiation by benzo[a]pyrene and 7,12-dimethylbenz[a]anthracene. *Carcinogenesis, 13*(11), 2183-2186.

Iavarone, A., & Massagué, J. (1999). E2F and histone deacetylase mediate transforming growth factor β repression of cdc25A during keratinocyte cell cycle arrest. *Molecular and Cellular Biology, 19*(1), 916-922.

Isobe, M., Emanuel, B. S., Givol, D., Oren, M., & Croce, C. M. (1986). Localization of gene for human p53 tumour antigen to band 17p13. *Nature, 320*(6057), 84-85.

Jäättelä, M., Wissing, D., Kokholm, K., Kallunki, T., & Egeblad, M. (1998). Hsp70 exerts its anti-apoptotic function downstream of caspase-3-like proteases. *EMBO Journal, 17*(21), 6124-6134.

Jacobson, M. D., Weil, M., & Raff, M. C. (1997). Programmed cell death in animal development. *Cell, 88*(3), 347-354.

Jemal, A., Bray, F., Center, M. M., Ferlay, J., Ward, E., & Forman, D. (2011). Global cancer statistics. *A Cancer Journal for Clinicians, 61*(2), 69-90.

Jiang, B., Li, D. D., & Zhen, Y. S. (1995). Induction of apoptosis by enediyne antitumor antibiotic C1027 in HL-60 human promyelocytic leukemia cells. *Biochemical and Biophysical Research Communications, 208*(1), 238-244.

Jiang, X., & Wang, X. (2004). Cytochrome C-mediated apoptosis. *Annual Review of Biochemistry, 73*, 87-106.

Jin, Z., & El-Deiry, W. S. (2005). Review Overview of Cell Death Signaling Pathways. *Cancer Biology & Therapy, 4*(2), 139-163.

Jolly, C., & Morimoto, R. I. (2000). Role of the heat shock response and molecular chaperones in oncogenesis and cell death. *Journal of the National Cancer Institute, 92*(19), 1564-1572.

Joza, N., Susin, S. A., Daugas, E., Stanford, W. L., Cho, S. K., Li, C. Y., . . . Penninger, J. M. (2001). Essential role of the mitochondrial apoptosis-inducing factor in programmed cell death. *Nature, 410*(6828), 549-554.

Julka, S., & Regnier, F. E. (2004). Benzoyl derivatization as a method to improve retention of hydrophilic peptides in tryptic peptide mapping. *Analytical Chemistry, 76*(19), 5799-5806.

Kang, K., Lee, H. J., Kim, C. Y., Lee, S. B., Tunsag, J., Batsuren, D., & Nho, C. W. (2007). The chemopreventive effects of Saussurea salicifolia through induction of apoptosis and phase II detoxification enzyme. *Biological and Pharmaceutical Bulletin, 30*(12), 2352-2359.

Karoui, H., Hogg, N., Frejaville, C., Tordo, P., & Kalyanaraman, B. (1996). Characterization of sulfur-centered radical intermediates formed during the oxidation of thiols and sulfite by peroxynitrite. *Journal of Biological Chemistry, 271*(11), 6000-6009.

Kastan, M. B., & Bartek, J. (2004). Cell-cycle checkpoints and cancer. *Nature, 432*(7015), 316-323.

Kastan, M. B., Onyekwere, O., Sidransky, D., Vogelstein, B., & Craig, R. W. (1991). Participation of p53 protein in the cellular response to DNA damage. *Cancer Research, 51*(23 Pt 1), 6304-6311.

Kastan, M. B., Zhan, Q., el-Deiry, W. S., Carrier, F., Jacks, T., Walsh, W. V., . . . Fornace, A. J., Jr. (1992). A mammalian cell cycle checkpoint pathway utilizing p53 and GADD45 is defective in ataxia-telangiectasia. *Cell, 71*(4), 587-597.

Kawamori, T., Lubet, R., Steele, V. E., Kelloff, G. J., Kaskey, R. B., Rao, C. V., & Reddy, B. S. (1999). Chemopreventive effect of curcumin, a naturally occurring anti-inflammatory agent, during the promotion/progression stages of colon cancer. *Cancer Research, 59*(3), 597-601.

Kawamura, M., & Kasai, H. (2007). Delayed cell cycle progression and apoptosis induced by hemicellulase-treated Agaricus blazei. *Evidence Based Complementary and Alternative Medicine, 4*(1), 83-94.

Kayalar, C., Ord, T., Testa, M. P., Zhong, L. T., & Bredesen, D. E. (1996). Cleavage of actin by interleukin 1 beta-converting enzyme to reverse DNase I inhibition. *Proceedings National Academy of Science U S A, 93*(5), 2234-2238.

Kelman, Z. (1997). PCNA: structure, functions and interactions. *Oncogene, 14*(6), 629.

Kennedy, K. M., & Dewhirst, M. W. (2010). Tumor metabolism of lactate: the influence and therapeutic potential for MCT and CD147 regulation. *Future Oncology, 6*(1), 127-148.

Keston A.S., B. R. (1965). The fluorometric analysis of ultramicro quantities of hydrogen peroxide. *Analytical Biochemistry, 11*, 1-5.

Kidd, V. J. (1998). Proteolytic activities that mediate apoptosis. *Annual review of Physiology, 60*(1), 533-573.

Kim, J. A., Kang, Y. S., Jung, M. W., Kang, G. H., Lee, S. H., & Lee, Y. S. (2000). Ca2+ influx mediates apoptosis induced by 4-aminopyridine, a K+ channel blocker, in HepG2 human hepatoblastoma cells. *Pharmacology, 60*(2), 74-81.

Kim, R., Emi, M., & Tanabe, K. (2006). Role of mitochondria as the gardens of cell death. *Cancer Chemotherapy and Pharmacology, 57*(5), 545-553.

King, R. W., Deshaies, R. J., Peters, J. M., & Kirschner, M. W. (1996). How proteolysis drives the cell cycle. *Science, 274*(5293), 1652-1659.

King, R. W., Jackson, P. K., & Kirschner, M. W. (1994). Mitosis in transition. *Cell, 79*(4), 563-571.

Kingston, D. G., & Newman, D. J. (2002). Mother nature's combinatorial libraries; their influence on the synthesis of drugs. *Current Opinion in Drug Discovery & Development, 5*(2), 304-316.

Kinzler, K. W., & Vogelstein, B. (1996). Lessons from hereditary colorectal cancer. *Cell, 87*(2), 159-170.

Klein, S., McCormick, F., & Levitzki, A. (2005). Killing time for cancer cells. *Nature Reviews of Cancer, 5*(7), 573-580.

Klionsky, D. J. (2007). Autophagy: from phenomenology to molecular understanding in less than a decade. *Nature Reviews Molecular Cell Biology, 8*(11), 931-937.

Koopman, G., Reutelingsperger, C. P., Kuijten, G. A., Keehnen, R. M., Pals, S. T., & van Oers, M. H. (1994). Annexin V for flow cytometric detection of phosphatidylserine expression on B cells undergoing apoptosis. *Blood, 84*(5), 1415-1420.

Koornstra, J. J., de Jong, S., Hollema, H., de Vries, E. G., & Kleibeuker, J. H. (2003). Changes in apoptosis during the development of colorectal cancer: a systematic review of the literature. *Critical Reviews in Oncology/ Hematology, 45*(1), 37-53.

Krajewska, M., Moss, S. F., Krajewski, S., Song, K., Holt, P. R., & Reed, J. C. (1996). Elevated expression of Bcl-X and reduced Bak in primary colorectal adenocarcinomas. *Cancer Research, 56*(10), 2422-2427.

Kralovcova, D., Pejchalova, M., Rudolf, E., & Cervinka, M. (2008). Quantitative analysis of expression level of BCL2 and BAX genes in Hep-2 and HL-60 cells after treatment with etoposide. *Acta Medica, 51*(3), 191-195.

Kroemer, G., Dallaporta, B., and Resche-Rigon, M. (1998). The mitochondrial death/life regulator in apoptosis and necrosis. *Annual Reviews Physiology*.

Kroemer, G., El-Deiry, W. S., Golstein, P., Peter, M. E., Vaux, D., Vandenabeele, P., . . . Nomenclature Committee on Cell, D. (2005). Classification of cell death: recommendations of the Nomenclature Committee on Cell Death. *Cell Death & Differentiation, 12 Suppl 2*, 1463-1467.

Kroemer, G., & Jaattela, M. (2005). Lysosomes and autophagy in cell death control. *Nature Reviews of Cancer, 5*(11), 886-897.

Kroemer, G., & Reed, J. C. (2000). Mitochondrial control of cell death. *Nature Medicine, 6*(5), 513.

Ku, D. H., Wen, S. C., Engelhard, A., Nicolaides, N. C., Lipson, K. E., Marino, T. A., & Calabretta, B. (1993). c-myb transactivates cdc2 expression via Myb binding sites in the 5'-flanking region of the human cdc2 gene.*The Journal of Biological Chemistry, 268*(3), 2255-2259.

Kuma, A., Hatano, M., Matsui, M., Yamamoto, A., Nakaya, H., Yoshimori, T., . . . Mizushima, N. (2004). The role of autophagy during the early neonatal starvation period. *Nature, 432*(7020), 1032-1036.

Lamm, D. L., Thor, D. E., Winters, W. D., Stogdill, V. D., & Radwin, H. M. (1981). BCG immunotherapy of bladder cancer: inhibition of tumor recurrence and associated immune responses. *Cancer, 48*(1), 82-88.

Lane, D. P., & Crawford, L. V. (1979). T antigen is bound to a host protein in SV40-transformed cells. *Nature, 278*(5701), 261-263.

Lardeux, B. R., & Mortimore, G. E. (1987). Amino acid and hormonal control of macromolecular turnover in perfused rat liver. Evidence for selective autophagy. *The Journal of Biological Chemistry, 262*(30), 14514-14519.

LeBel, C. P., Ischiropoulos, H., & Bondy, S. C. (1992). Evaluation of the probe 2', 7'-dichlorofluorescin as an indicator of reactive oxygen species formation and oxidative stress. *Chemical Research in Toxicology, 5*(2), 227-231.

Lee, A., & Breitenbucher, J. G. (2003). The impact of combinatorial chemistry on drug discovery. *Current Opinion in Drug Discovery & Development, 6*(4), 494-508.

Lee, J., Shin, J., Kim, H., Heo, J., Kho, Y., Kang, H., & Park, S. (2012). Effect of combined treatment with progesterone and tamoxifen on the growth and apoptosis of human ovarian cancer cells. *Oncology Reports, 27*(1), 87.

Lee, K. H. (2000). Research and future trends in the pharmaceutical development of medicinal herbs from Chinese medicine. *Public Health Nutrition, 3*(4A), 515-522.

Levine, A. J. (1997). p53, the cellular gatekeeper for growth and division. *Cell, 88*(3), 323-331.

Levine, B., & Abrams, J. (2008). p53: The Janus of autophagy? *Nature Cell Biology, 10*(6), 637-639.

Levine, B., & Deretic, V. (2007). Unveiling the roles of autophagy in innate and adaptive immunity. *Nature Reviews Immunology, 7*(10), 767-777.

Levine, B., & Klionsky, D. J. (2004). Development by self-digestion: molecular mechanisms and biological functions of autophagy. *Developmental Cell, 6*(4), 463-477.

Li, L. Y., Luo, X., & Wang, X. (2001). Endonuclease G is an apoptotic DNase when released from mitochondria. *Nature, 412*(6842), 95-99.

Li, X., James, W. M., Traganos, F., & Darzynkiewicz, Z. (1995). Application of biotin, digoxigenin or fluorescein conjugated deoxynucleotides to label DNA strand breaks for analysis of cell proliferation and apoptosis using flow cytometry. *Biotechnics & Histochemistry, 70*(5), 234-242.

Lin, L. M., Li, B. X., Xiao, J. B., Lin, D. H., & Yang, B. F. (2005). Synergistic effect of all-trans-retinoic acid and arsenic trioxide on growth inhibition and apoptosis in human hepatoma, breast cancer, and lung cancer cells in vitro. *World Journal of Gastroenterology, 11*(36), 5633.

Lindquist, S. (1986). The heat-shock response. *Annual Review of Biochemistry, 55*, 1151-1191.

Linzer, D. I., & Levine, A. J. (1979). Characterization of a 54K dalton cellular SV40 tumor antigen present in SV40-transformed cells and uninfected embryonal carcinoma cells. *Cell, 17*(1), 43-52.

Liu, Y., Peterson, D. A., Kimura, H., & Schubert, D. (1997). Mechanism of cellular 3-(4,5-dimethylthiazol-2-yl)-2,5-diphenyltetrazolium bromide (MTT) reduction. *Journal of Neurochemistry, 69*(2), 581-593.

Livak, K. J., & Schmittgen, T. D. (2001). Analysis of relative gene expression data using real-time quantitative PCR and the 2(-Delta Delta C(T)) Method. *Methods, 25*(4), 402-408.

Lockshin, R. A., & Zakeri, Z. (2007). Cell death in health and disease. *Journal of Cellular and Molecular Medicine, 11*(6), 1214-1224.

Lowe, S. W., Schmitt, E. M., Smith, S. W., Osborne, B. A., & Jacks, T. (1993). p53 is required for radiation-induced apoptosis in mouse thymocytes. *Nature, 362*(6423), 847-849.

Lu, C. X., Fan, T. J., Hu, G. B., & Cong, R. S. (2003). Apoptosis-inducing factor and apoptosis. *Sheng Wu Hua Xue Yu Sheng Wu Wu Li Xue Bao (Shanghai), 35*(10), 881-885.

Lu, K. H., Lee, H. J., Huang, M. L., Lai, S. C., Ho, Y. L., Chang, Y. S., & Chi, C. W. (2011). Synergistic Apoptosis-Inducing Antileukemic Effects of Arsenic Trioxide and Mucuna macrocarpa Stem Extract in Human Leukemic Cells via a Reactive Oxygen Species-Dependent Mechanism. *Evidence-Based Complementary and Alternative Medicine, 2012*.

Macho, A., Hirsch, T., Marzo, I., Marchetti, P., Dallaporta, B., Susin, S. A., . . . Kroemer, G. (1997a). Glutathione depletion is an early and calcium elevation is a late event of thymocyte apoptosis. *The Journal of Immunology, 158*(10), 4612-4619.

Macho, A., Hirsch, T., Marzo, I., Marchetti, P., Dallaporta, B., Susin, S. A., . . . Kroemer, G. (1997b). Glutathione depletion is an early and calcium elevation is a late event of thymocyte apoptosis. *The Journal of Immunology, 158*(10), 4612-4619.

Madhusudan, S., & Middleton, M. R. (2005). The emerging role of DNA repair proteins as predictive, prognostic and therapeutic targets in cancer. *Cancer Treatment Reviews, 31*(8), 603-617.

Mailand, N., Falck, J., Lukas, C., Syljuåsen, R. G., Welcker, M., Bartek, J., & Lukas, J. (2000). Rapid destruction of human Cdc25A in response to DNA damage. *Science's STKE, 288*(5470), 1425.

Maiti, A., Dewanjee, S., & Mandal, S. C. (2007). In vivo evaluation of antidiarrhoeal activity of the seed of Swietenia macrophylla King (Meliaceae). *Tropical Journal of Pharmaceutical Research, 6*(2), 711-716.

Maiti, A., Dewanjee, S., Mandal, S. C., & Annadurai, S. (2007). Exploration of antimicrobial potential of methanol and water extract of seeds of Swietenia Macrophylla (Family: Meliaceae), to substantiate folklore claim. *Iranian Journal of Pharmacology & Therapeutics (IJPT), 6*(1).

Maiti, A., Dewanjee, S., & Sahu, R. (2009). Isolation of hypoglycemic phytoconstituent from Swietenia macrophylla seeds. *Phytotherapy Research, 23*(12), 1731-1733.

Maiti A., D. S., Mandal S.C. & Annadurai S. (2007). Exploration of antimicrobial potential of methanol and water extract of seeds of Switenia macrophylla to substantiate folklore claim. *Iranian Journal of Pharmacology & Therapeutic, 6*, 99-102.

Malkin, D., Li, F. P., Strong, L. C., Fraumeni, J. F., Jr., Nelson, C. E., Kim, D. H., . . . et al. (1990). Germ line p53 mutations in a familial syndrome of breast cancer, sarcomas, and other neoplasms. *Science, 250*(4985), 1233-1238.

Martin, S. J., Finucane, D. M., Amarante-Mendes, G. P., O'Brien, G. A., & Green, D. R. (1996). Phosphatidylserine externalization during CD95-induced apoptosis of cells and cytoplasts requires ICE/CED-3 protease activity. *The Journal of Biological Chemistry, 271*(46), 28753-28756.

Martin, S. J., Reutelingsperger, C. P., McGahon, A. J., Rader, J. A., van Schie, R. C., LaFace, D. M., & Green, D. R. (1995). Early redistribution of plasma membrane phosphatidylserine is a general feature of apoptosis regardless of the initiating stimulus: inhibition by overexpression of Bcl-2 and Abl. *The Journal of Experimental Medicine, 182*(5), 1545-1556.

Martinez-Velazquez, M., Melendez-Zajgla, J., & Maldonado, V. (2007). Apoptosis induced by cAMP requires Smac/DIABLO transcriptional upregulation. *Cell Signal, 19*(6), 1212-1220.

Mashima, T., Naito, M., Fujita, N., Noguchi, K., & Tsuruo, T. (1995). Identification of actin as a substrate of ICE and an ICE-like protease and involvement of an ICE-like protease but not ICE in VP-16-induced U937 apoptosis. *Biochemical and Biophysical Research Communications, 217*(3), 1185-1192.

McCarthy, N. J., Whyte, M. K., Gilbert, C. S., & Evan, G. I. (1997). Inhibition of Ced-3/ICE-related proteases does not prevent cell death induced by oncogenes, DNA damage, or the Bcl-2 homologue Bak. *The Journal of Cell Biol, 136*(1), 215-227.

Merritt, A. J., Potten, C. S., Watson, A. J., Loh, D. Y., Nakayama, K., Nakayama, K., & Hickman, J. A. (1995). Differential expression of bcl-2 in intestinal epithelia. Correlation with attenuation of apoptosis in colonic crypts and the incidence of colonic neoplasia. *Journal of Cell Science, 108*, 2261-2271.

Meulmeester, E., Frenk, R., Stad, R., de Graaf, P., Marine, J. C., Vousden, K. H., & Jochemsen, A. G. (2003). Critical role for a central part of Mdm2 in the ubiquitylation of p53. *Moecular andl Cellular Biology, 23*(14), 4929-4938.

Michiels, C., Raes, M., Toussaint, O., & Remacle, J. (1994). Importance of Se-glutathione peroxidase, catalase, and Cu/Zn-SOD for cell survival against oxidative stress. *Free Radical Biology & Medicine, 17*(3), 235-248.

Mills, J. C., Stone, N. L., Erhardt, J., & Pittman, R. N. (1998). Apoptotic membrane blebbing is regulated by myosin light chain phosphorylation. *The Journal of Cell Biology, 140*(3), 627-636.

Mirnikjoo, B., Balasubramanian, K., & Schroit, A. J. (2009). Suicidal membrane repair regulates phosphatidylserine externalization during apoptosis. *The Journal of Biological Chemistry, 284*(34), 22512-22516.

Mithöfer, K., Sandy, M. S., Smith, M. T., & Di Monte, D. (1992). Mitochondrial poisons cause depletion of reduced glutathione in isolated hepatocytes. *Archives of Biochemistry and Biophysics, 295*(1), 132.

Miyashita, T., Krajewski, S., Krajewska, M., Wang, H. G., Lin, H., Liebermann, D. A., . . . Reed, J. C. (1994). Tumor suppressor p53 is a regulator of bcl-2 and bax gene expression in vitro and in vivo. *Oncogene, 9*(6), 1799.

Miyoshi, H., Umeshita, K., Sakon, M., Imajoh-Ohmi, S., Fujitani, K., Gotoh, M., . . . Monden, M. (1996). Calpain activation in plasma membrane bleb formation during tert-butyl hydroperoxide-induced rat hepatocyte injury. *Gastroenterology, 110*(6), 1897-1904.

Mootoo, B. S., Ali, A., Motilal, R., Pingal, R., Ramlal, A., Khan, A., . . . McLean, S. (1999). Limonoids from *Swietenia macrophylla* and *S. aubrevilleana*. *Journal of Natural Products, 62*(11), 1514-1517.

Morimoto, R. I. (1993). Cells in stress: transcriptional activation of heat shock genes. *Science, 259*(5100), 1409-1410.

Moriyasu, Y., & Ohsumi, Y. (1996). Autophagy in Tobacco Suspension-Cultured Cells in Response to Sucrose Starvation. *Plant Physiology, 111*(4), 1233-1241.

Morris, R. G., Hargreaves, A. D., Duvall, E., & Wyllie, A. H. (1984). Hormone-induced cell death. 2. Surface changes in thymocytes undergoing apoptosis. *American Journal of Pathology, 115*(3), 426-436.

Mosmann, T. (1983). Rapid colorimetric assay for cellular growth and survival: application to proliferation and cytotoxicity assays. *Journal of Immunolgical Methods, 65*(1-2), 55-63.

Mosser, D. D., Caron, A. W., Bourget, L., Denis-Larose, C., & Massie, B. (1997). Role of the human heat shock protein hsp70 in protection against stress-induced apoptosis. *Molecular and Cellular Biology, 17*(9), 5317-5327.

Mosser, D. D., Caron, A. W., Bourget, L., Denis-Larose, C., & Massie, B. (1997). Role of the human heat shock protein hsp70 in protection against stress-induced apoptosis. *Molecular and Cellular Biology, 17*(9), 5317-5327.

Motterlini, R., Foresti, R., Bassi, R., & Green, C. J. (2000). Curcumin, an antioxidant and anti-inflammatory agent, induces heme oxygenase-1 and protects endothelial cells against oxidative stress. *Free Radic Biol Med, 28*(8), 1303-1312.

Munoz, V., Sauvain, M., Bourdy, G., Callapa, J., Rojas, I., Vargas, L., . . . Deharo, E. (2000). The search for natural bioactive compounds through a multidisciplinary approach in Bolivia. Part II. Antimalarial activity of some plants used by Mosetene indians. *Journal of Ethnopharmacol, 69*(2), 139-155.

Myung, J. K., Afjehi-Sadat, L., Felizardo-Cabatic, M., Slavc, I., & Lubec, G. (2004). Expressional patterns of chaperones in ten human tumor cell lines. *Proteome science, 2*(1), 8.

Nagata, S. (1997). Apoptosis by Death Factor Review. *Cell, 88*(355-365), 392.
Nakamura, T., Sakai, T., & Nariya, S. (1995). Cell death in colorectal polyps as evaluated by in situ 3'-tailing reaction and its relationship to BCL-2 expression. *Pathology International, 45*(10), 721-728.

Narender, T., Khaliq, T., & Shweta. (2008). 13C NMR spectroscopy of D and B, D-ring seco-limonoids of Meliaceae family. *Natural product research, 22*(9), 763-800.

Narita, M., Shimizu, S., Ito, T., Chittenden, T., Lutz, R. J., Matsuda, H., & Tsujimoto, Y. (1998). Bax interacts with the permeability transition pore to induce permeability transition and cytochrome c release in isolated mitochondria. *Proceedings of the National Academy of Sciences, 95*(25), 14681.

National Cancer Registry, M. o. H. M. (2006). Malaysian cancer statistics 2006. In Z. M. A. Zainal Ariffin Omar, Nor Saleha Ibrahim Tamin (Ed.), (pp. 112).

Neganova, I., Vilella, F., Atkinson, S. P., Lloret, M., Passos, J. F., Von Zglinicki, T., . . . Armstrong, L. (2011). An important role for CDK2 in G1 to S checkpoint activation and DNA damage response in human embryonic stem cells. *Stem Cells, 29*(4), 651-659.

Nesslany, F., Simar-Meintieres, S., Ficheux, H., & Marzin, D. (2009). Aloe-emodin-induced DNA fragmentation in the mouse in vivo comet assay. *Mutation Research, 678*(1), 13-19.

Newman, D. J., Cragg, G. M., & Snader, K. M. (2000). The influence of natural products upon drug discovery. *Natural Product Report, 17*(3), 215-234.

Nicotera, P., & Orrenius, S. (1998). The role of calcium in apoptosis. *Cell Calcium, 23*(2-3), 173-180.

Nsiama T.K., T. I., Hiroaki O., Matsumi D., Yoshiki M.,& Munehiro N. (2008). Limonoids from stem bark of Cedrela odorata. *Phytochemistry, 69*, 1782-1787.

O'Sullivan, S. M., Woods, J. A., & O'Brien, N. M. (2004). Use of Tween 40 and Tween 80 to deliver a mixture of phytochemicals to human colonic adenocarcinoma cell (CaCo-2) monolayers. *British Journal of Nutrition, 91*(5), 757-764.

Okouneva, T., Hill, B. T., Wilson, L., & Jordan, M. A. (2003). The effects of vinflunine, vinorelbine, and vinblastine on centromere dynamics. *Molecular Cancer Therapeutics, 2*(5), 427-436.

Olie, R. A., Boersma, A. W., Dekker, M. C., Nooter, K., Looijenga, L. H., & Oosterhuis, J. W. (1996). Apoptosis of human seminoma cells upon disruption of their microenvironment. *British Journal of Cancer, 73*(9), 1031-1036.

Oltval, Z. N., Milliman, C. L., & Korsmeyer, S. J. (1993). Bcl-2 heterodimerizes in vivo with a conserved homolog, Bax, that accelerates programed cell death. *Cell, 74*(4), 609-619.

Onodera, J., & Ohsumi, Y. (2005). Autophagy is required for maintenance of amino acid levels and protein synthesis under nitrogen starvation *The Journal of Biological Chemistry, 280*(36), 31582-31586.

Oren, M., & Rotter, V. (1999). Introduction: p53--the first twenty years. *Cellular and Molecular Life Sciences, 55*(1), 9-11.

Ott, M., Gogvadze, V., Orrenius, S., & Zhivotovsky, B. (2007). Mitochondria, oxidative stress and cell death. *Apoptosis, 12*(5), 913-922.

Pai, S. R., & Bird, R. C. (1994). c-fos expression is required during all phases of the cell cycle during exponential cell proliferation. *Anticancer Research, 14*(3A), 985-994.

Pan, G., O'Rourke, K., Chinnaiyan, A. M., Gentz, R., Ebner, R., Ni, J., & Dixit, V. M. (1997). The receptor for the cytotoxic ligand TRAIL. *Science, 276*(5309), 111-113.

Pardee, A. B. (1989). G1 events and regulation of cell proliferation. *Science, 246*(4930), 603-608.

Parsell, D. A., Taulien, J., & Lindquist, S. (1993). The role of heat-shock proteins in thermotolerance. *Philos Trans R Soc Lond B Biol Sci, 339*(1289), 279-285.

Pavlik, E. J., Kenady, D. E., Nagell, J. R., Keaton, K., Hanson, M. B., Donaldson, E. S., . . . Flanigan, R. C. (1983). Properties of anticancer agents relevant to in vitro determinations of human tumor cell sensitivity. *Cancer Chemotherapy and Pharmacology, 11*(1), 8-15.

Pereira, M. A., Grubbs, C. J., Barnes, L. H., Li, H., Olson, G. R., Eto, I., . . . Lubet, R. A. (1996). Effects of the phytochemicals, curcumin and quercetin, upon azoxymethane-induced colon cancer and 7,12-dimethylbenz[a]anthracene-induced mammary cancer in rats. [Research Support, U.S. Gov't, P.H.S.]. *Carcinogenesis, 17*(6), 1305-1311.

Peters, G. J., van der Wilt, C. L., van Moorsel, C. J., Kroep, J. R., Bergman, A. M., & Ackland, S. P. (2000). Basis for effective combination cancer chemotherapy with antimetabolites. [Review]. *Pharmacology & Therapeutics, 87*(2-3), 227-253.

Pezzuto, J. M. (1997). Plant-derived anticancer agents. *Biochemical Pharmacology, 53*(2), 121-133.

Plummer, S. M., Hill, K. A., Festing, M. F., Steward, W. P., Gescher, A. J., & Sharma, R. A. (2001). Clinical development of leukocyte cyclooxygenase 2 activity as a systemic biomarker for cancer chemopreventive agents. *Cancer Epidemiology, Biomarkers & Prevention, 10*(12), 1295-1299.

Pop, C., & Salvesen, G. S. (2009). Human caspases: activation, specificity, and regulation. *The Journal of Biological Chemistry, 284*(33), 21777-21781.

Ram, V. J., & Kumari, S. (2001). Natural products of plant origin as anticancer agents. *Drug News Perspect, 14*(8), 465.

Rao, C. V., Rivenson, A., Simi, B., & Reddy, B. S. (1995). Chemoprevention of colon carcinogenesis by dietary curcumin, a naturally occurring plant phenolic compound. *Cancer Research, 55*(2), 259-266.

Rao, C. V., Simi, B., & Reddy, B. S. (1993). Inhibition by dietary curcumin of azoxymethane-induced ornithine decarboxylase, tyrosine protein kinase, arachidonic acid metabolism and aberrant crypt foci formation in the rat colon. *Carcinogenesis, 14*(11), 2219-2225.

Raskin, I., Ribnicky, D. M., Komarnytsky, S., Ilic, N., Poulev, A., Borisjuk, N., . . . Fridlender, B. (2002). Plants and human health in the twenty-first century. *Trends in Biotechnology, 20*(12), 522-531.

Ratan, R. R., Murphy, T. H., & Baraban, J. M. (1994). Rapid Communication: Oxidative Stress Induces Apoptosis in Embryonic Cortical Neurons. *Journal of Neurochemistry, 62*(1), 376-379.

Raveh, T., Droguett, G., Horwitz, M. S., DePinho, R. A., & Kimchi, A. (2001). DAP kinase activates a p19ARF/p53-mediated apoptotic checkpoint to suppress oncogenic transformation. *Nature Cell Biology, 3*(1), 1-7.

Rawlins, M. D. (2004). Cutting the cost of drug development? *Nature Reviews Drug Discovery, 3*(4), 360-364.

Reers, M., Smiley, S. T., Mottola-Hartshorn, C., Chen, A., Lin, M., & Chen, L. B. (1995). Mitochondrial membrane potential monitored by JC-1 dye. *Methods Enzymology, 260*, 406-417.

Renehan, A., Yeh, H. C., Johnson, J., Wild, S., Gale, E. A. M., & Møller, H. (2012). Diabetes and cancer (2): evaluating the impact of diabetes on mortality in patients with cancer. *Diabetologia*, 1-14.

Renschler, M. F. (2004). The emerging role of reactive oxygen species in cancer therapy. *European Journal of Cancer, 40*(13), 1934-1940.

Rest, R. F. (1994). Measurement of human neutrophil respiratory burst activity during phagocytosis of bacteria. [In Vitro]. *Methods in Enzymology, 236*, 119-136.

Reuter, S., Eifes, S., Dicato, M., Aggarwal, B. B., & Diederich, M. (2008). Modulation of anti-apoptotic and survival pathways by curcumin as a strategy to induce apoptosis in cancer cells. *Biochemical Pharmacology, 76*(11), 1340-1351.

Riccardi, C., & Nicoletti, I. (2006). Analysis of apoptosis by propidium iodide staining and flow cytometry. *Nat Protocals, 1*(3), 1458-1461.

Richards, E. H., Hickey, E., Weber, L., & Master, J. R. (1996). Effect of overexpression of the small heat shock protein HSP27 on the heat and drug sensitivities of human testis tumor cells. *Cancer Research, 56*(10), 2446-2451.

Ritossa, P. (1962). Problems of prophylactic vaccinations of infants. *Riv Ist Sieroter Ital, 37*, 79-108.

Roberts, J. M., & Sherr, C. J. (2003). Bared essentials of CDK2 and cyclin E. *Nature Genetics, 35*(1), 8-9.

Roussi, S., Gosse, F., Aoude-Werner, D., Zhang, X., Marchioni, E., Geoffroy, P., . . . Raul, F. (2007). Mitochondrial perturbation, oxidative stress and lysosomal

destabilization are involved in 7beta-hydroxysitosterol and 7beta-hydroxycholesterol triggered apoptosis in human colon cancer cells. *Apoptosis, 12*(1), 87-96.

Roy, A., & Saraf, S. (2006). Limonoids: overview of significant bioactive triterpenes distributed in plants kingdom. *Biological & Pharmaceutical Bulletin, 29*(2), 191-201.

Rubinstein, L. V., Shoemaker, R. H., Paull, K. D., Simon, R. M., Tosini, S., Skehan, P., . . . Boyd, M. R. (1990). Comparison of in vitro anticancer-drug-screening data generated with a tetrazolium assay versus a protein assay against a diverse panel of human tumor cell lines. *Journal of the National Cancer Institute, 82*(13), 1113-1118.

Salvesen, G. S., & Riedl, S. J. (2008). Caspase mechanisms. *Advances in Experimental Medicine and Biology, 615*, 13-23.

Samali, A., Gorman, A. M., & Cotter, T. G. (1996). Apoptosis -- the story so far. *Experientia, 52*(10-11), 933-941.

Sanchez-Alcazar, J. A., Schneider, E., Hernandez-Munoz, I., Ruiz-Cabello, J., Siles-Rivas, E., de la Torre, P., . . . Navas, P. (2003). Reactive oxygen species mediate the down-regulation of mitochondrial transcripts and proteins by tumour necrosis factor-alpha in L929 cells. *Biochemical Journal, 370*(Pt 2), 609-619.

Saraf, A. R. S. (2006). Limonoids: Overview of Significant Bioactive Triterpenes Distributed in Plants Kingdom limonoids. *Biological and Pharmaceutical Bulletin, 29*(2).

Savill, J. (1997). Recognition and phagocytosis of cells undergoing apoptosis. *British Medical Bulletin, 53*(3), 491-508.

Schiff, P. B., Fant, J., & Horwitz, S. B. (1979). Promotion of microtubule assembly in vitro by taxol. *Nature, 277*(5698), 665-667.

Schiff, P. B., & Horwitz, S. B. (1980). Taxol stabilizes microtubules in mouse fibroblast cells. *Proceedings of National Academy of Science U S A, 77*(3), 1561-1565.

Schulze-Osthoff, K., Beyaert, R., Vandevoorde, V., Haegeman, G., & Fiers, W. (1993). Depletion of the mitochondrial electron transport abrogates the cytotoxic and gene-inductive effects of TNF. *EMBO Journal, 12*(8), 3095-3104.

Semenza, G. L. (2008). Hypoxia-inducible factor 1 and cancer pathogenesis. *IUBMB Life, 60*(9), 591-597.

Semenza, G. L. (2009). Regulation of cancer cell metabolism by hypoxia-inducible factor 1. *Seminars in Cancer Biology, 19*(1), 12-16.

Sharma, O. P. (1976). Antioxidant activity of curcumin and related compounds. *Biochemical Pharmacology, 25*(15), 1811-1812.

Sharma, R. A., Manson, M. M., Gescher, A., & Steward, W. P. (2001). Colorectal cancer chemoprevention: biochemical targets and clinical development of promising agents. *European Journal of Cancer, 37*(1), 12-22.

Shay, J. W., & Bacchetti, S. (1997). A survey of telomerase activity in human cancer. *European Journal of Cancer, 33*(5), 787-791.

Sheridan, J. P., Marsters, S. A., Pitti, R. M., Gurney, A., Skubatch, M., Baldwin, D., . . . Ashkenazi, A. (1997). Control of TRAIL-induced apoptosis by a family of signaling and decoy receptors. *Science, 277*(5327), 818-821.

Sherr, C. J. (1994). G1 phase progression: cycling on cue. *Cell, 79*(4), 551-555.

Sherr, C. J. (1998). Tumor surveillance via the ARF-p53 pathway. *Genes & Development, 12*(19), 2984-2991.

Sherr, C. J., & Roberts, J. M. (1995). Inhibitors of mammalian G1 cyclin-dependent kinases. *Genes Dev, 9*(10), 1149-1163.

Shintani, T., & Klionsky, D. J. (2004). Autophagy in health and disease: a double-edged sword. *Science, 306*(5698), 990-995.

Sies, H. (1999). Glutathione and its role in cellular functions. *Free Radical Biology & Medicine, 27*(9-10), 916-921.

Simon, H. U., Haj-Yehia, A., & Levi-Schaffer, F. (2000). Role of reactive oxygen species (ROS) in apoptosis induction. *Apoptosis, 5*(5), 415-418.

Skommer, J., Wlodkowic, D., & Pelkonen, J. (2007). Gene-expression profiling during curcumin-induced apoptosis reveals downregulation of CXCR4. *Experimental Hematology, 35*(1), 84-95.

Slamon, D. J. (1987). Proto-oncogenes and human cancers. *The New England Journal of Medicine, 317*(15), 955-957.

Smiley, S. T., Reers, M., Mottola-Hartshorn, C., Lin, M., Chen, A., Smith, T. W., . . . Chen, L. B. (1991). Intracellular heterogeneity in mitochondrial membrane potentials revealed by a J-aggregate-forming lipophilic cation JC-1. *Proceeings of National Academy of Science U S A, 88*(9), 3671-3675.

Smith, J. A., & Weidemann, M. J. (1993). Further characterization of the neutrophil oxidative burst by flow cytometry. *Journal of Immunological Methods, 162*(2), 261-268.

Soares G.M., F., M.F., & Lago, J.H. (2010). Interspecific variation in the composition of volatile oils from the leaves of *Swietenia macrophylla* King (Meliaceae). *Qu ímica Nova, 33*(5), 1141-1144.

Soares, M. G., Batista-Pereira, L. G., Fernandes, J. B., Corrêa, A. G., Da Silva, M. F. G. F., Vieira, P. C., . . . Ohashi, O. S. (2003). Electrophysiological responses of female and male *Hypsipyla grandella* (Zeller) to *Swietenia macrophylla* essential oils. *Journal of Chemical Ecology, 29*(9), 2143-2151.

Soediro, I., Padmawinata, K., Wattimena, J., & Rekita, S. (1990). Study of the active antimalarial methanolic extract of *Swietenia macrophylla* King (Meliaceae). *Acta Pharmaceutica Indonesia, 15*(1), 1-13.

Soediro, I., Padmawinata, K, Wattimena, J. R., & Rekita, S. (1990). Study of the active antimalarial methanolic extract of *Swietenia macrophylla* King *Acta Pharmaceutica Indonesia, 15*(1), 1-13.

Sovova, H. (2001). Solubility of ferulic acid in supercritical carbon dioxide with ethanol as cosolvent. *Journal of Chemical & Engineering Data, 46*(5), 1255-1257.

Srimal, R. C., & Dhawan, B. N. (1973). Pharmacology of diferuloyl methane (curcumin), a non-steroidal anti-inflammatory agent. *African Journal of Pharmacy and Pharmacology, 25(6), 447-452.*

Srivastava, S., Zou, Z. Q., Pirollo, K., Blattner, W., & Chang, E. H. (1990). Germ-line transmission of a mutated p53 gene in a cancer-prone family with Li-Fraumeni syndrome. *Nature, 348*(6303), 747-749.

Stadtman, E. R., & Berlett, B. S. (1998). Reactive oxygen-mediated protein oxidation in aging and disease. *Drug Metablism Reviews, 30*(2), 225-243.

Stahura, F. L., Godden, J. W., Xue, L., & Bajorath, J. (2000). Distinguishing between natural products and synthetic molecules by descriptor Shannon entropy analysis and binary QSAR calculations. *Journal of Chemical Information and Modeling, 40*(5), 1245-1252.

Stepp, J. R. (2004). The role of weeds as sources of pharmaceuticals. *Journal of Ethnopharmacology, 92*(2), 163-166.

Stillman, B. (1994). Smart machines at the DNA replication fork. *Cell, 78*(5), 725-728.

Stoklsa, T., & Golab, J. (2005). Prospects for p53-based cancer therapy. *Acta Biochimica Polonica, 52*(2), 321-328.

Strużyńska, L., Chalimoniuk, M., & Sulkowski, G. (2005). The role of astroglia in Pb-exposed adult rat brain with respect to glutamate toxicity. *Toxicology, 212*(2), 185-194.

Susin, S. A., Daugas, E., Ravagnan, L., Samejima, K., Zamzami, N., Loeffler, M., . . . Kroemer, G. (2000). Two distinct pathways leading to nuclear apoptosis. *The Journal of Experimental Medicine, 192*(4), 571-580.

Swisher, S. G., Roth, J. A., Komaki, R., Gu, J., Lee, J. J., Hicks, M., . . . Yin, M. (2003). Induction of p53-regulated genes and tumor regression in lung cancer patients after intratumoral delivery of adenoviral p53 (INGN 201) and radiation therapy. *Clinical Cancer Research, 9*(1), 93-101.

Takeshige, K., Baba, M., Tsuboi, S., Noda, T., & Ohsumi, Y. (1992). Autophagy in yeast demonstrated with proteinase-deficient mutants and conditions for its induction. *The Journal of Cell Biology, 119*(2), 301-311.

Tan, S.-K., Osman, H., Wong, K.-C., & Boey, P.-L. (2009). New phragmalin-type limonoids from *Swietenia macrophylla* King. *Food Chemistry, 115*(4), 1279-1285.

Taylor, A. R. H., & Taylor, D. A. H. (1983a). Limonoid extractives from *Swietenia macrophylla*. *Phytochemistry, 22*(12), 2870-2871.

Taylor, A. R. H., & Taylor, D. A. H. (1983b). Limonoid extractives *fromSwietenia macrophylla*. *Phytochemistry, 22*(12), 2870-2871.

Teng, M. W., Swann, J. B., Koebel, C. M., Schreiber, R. D., & Smyth, M. J. (2008). Immune-mediated dormancy: an equilibrium with cancer. *Journal of Leukocyte Biology, 84*(4), 988-993.

Tews, D., Behrhof, W., & Schindler, S. (2008). SMAC-expression in denervated human skeletal muscle as a potential inhibitor of coexpressed inhibitor-of-apoptosis proteins. *Applied immunohistochemistry & molecular morphology: AIMM/official publication of the Society for Applied Immunohistochemistry, 16*(1), 66.

Thomas Henkel, R. M. B., Hartwig Muller, Felix Reichel. (1999). Statistical investigation into the structural complementary of natural products and synthetic compounds. *Angewandte Chemie International Edition, 38*(5), 643-647.

Timmins, G. S. (2009). Drugs: From Discovery to Approval:Drugs: From Discovery to Approval. *Drug Development and Industrial Pharm*acy.

Toshiyuki, M., & Reed, J. C. (1995). Tumor suppressor p53 is a direct transcriptional activator of the human bax gene. *Cell, 80*(2), 293-299.

Trautinger, F., Kokesch, C., Herbacek, I., Knobler, R. M., & Kindas-Mugge, I. (1997). Overexpression of the small heat shock protein, hsp27, confers resistance to hyperthermia, but not to oxidative stress and UV-induced cell death, in a stably transfected squamous cell carcinoma cell line. *Journal of Photochemistry and Photobiology B, 39*(1), 90-95.

Travali, S., Reiss, K., Ferber, A., Petralia, S., Mercer, W. E., Calabretta, B., & Baserga, R. (1991). Constitutively expressed c-myb abrogates the requirement for insulinlike growth factor 1 in 3T3 fibroblasts. *Molecular and Cellular Biology, 11*(2), 731-736.

Truong, D. H., Mihajlovic, A., Gunness, P., Hindmarsh, W., & O'Brien, P. J. (2007). Prevention of hydrogen sulfide (H2S)-induced mouse lethality and cytotoxicity by hydroxocobalamin (vitamin B(12a)). *Toxicology, 242*(1-3), 16-22.

Umezawa, H., Ishizuka, M., Maeda, K., & Takeuchi, T. (1967). Studies on bleomycin. *Cancer, 20*(5), 891-895.

Vabulas, R. M., & Hartl, F. U. (2005). Protein synthesis upon acute nutrient restriction relies on proteasome function. *Science, 310*(5756), 1960-1963.

Vajdic, C. M., & van Leeuwen, M. T. (2009). Cancer incidence and risk factors after solid organ transplantation. *International Journal of Cancer, 125*(8), 1747-1754.

Van de Loosdrecht, A., Beelen, R., Ossenkoppele, G., Broekhoven, M., & Langenhuijsen, M. (1994). A tetrazolium-based colorimetric MTT assay to quantitate human monocyte mediated cytotoxicity against leukemic cells from cell lines and patients with acute myeloid leukemia. *Journal of Immunological Methods, 174*(1-2), 311-320.

Vanags, D. M., Porn-Ares, M. I., Coppola, S., Burgess, D. H., & Orrenius, S. (1996). Protease involvement in fodrin cleavage and phosphatidylserine exposure in apoptosis. *The Journal of Biological Chemistry, 271*(49), 31075-31085.

Vanderlaag, K., Samudio, I., Burghardt, R., Barhoumi, R., & Safe, S. (2006). Inhibition of breast cancer cell growth and induction of cell death by 1,1-bis(3'-indolyl)methane (DIM) and 5,5'-dibromoDIM. *Cancer Lett, 236*(2), 198-212.

Vanlangenakker, N., Vanden Berghe, T., Krysko, D. V., Festjens, N., & Vandenabeele, P. (2008). Molecular mechanisms and pathophysiology of necrotic cell death. *Current Moleular Medicine, 8*(3), 207-220.

Vermes, I., Haanen, C., Steffens-Nakken, H., & Reutelingsperger, C. (1995). A novel assay for apoptosis. Flow cytometric detection of phosphatidylserine expression on early apoptotic cells using fluorescein labelled Annexin V. *Journal of Immunological Methods, 184*(1), 39-51.

Vermes, I., Haanen, C., Steffens-Nakken, H., & Reutellingsperger, C. (1995). A novel assay for apoptosis flow cytometric detection of phosphatidylserine expression on early apoptotic cells using fluorescein labelled Annexin V. *Journal of Immunological Methods, 184*(1), 39-51.

Verpoorte, R. (1999). "Chemodiversity and the biological role of secondary metabolites, some thoughts for selecting plant material for drug development", in L.B. Bohlin, J.G. (eds) Bioassay Methods in Natural Product Research and Drug Development. Netherlands: Kluwer Academic Publishers.

Vogelstein, B., Lane, D., & Levine, A. J. (2000). Surfing the p53 network. *Nature, 408*(6810), 307-310.

Vousden, K. H., & Lu, X. (2002). Live or let die: the cell's response to p53. *Nature Reviews of Cancer, 2*(8), 594-604.

Vucic, D., Deshayes, K., Ackerly, H., Pisabarro, M. T., Kadkhodayan, S., Fairbrother, W. J., & Dixit, V. M. (2002). SMAC negatively regulates the anti-apoptotic activity of

melanoma inhibitor of apoptosis (ML-IAP). *The Journal of Biological Chemistry, 277*(14), 12275-12279.

Waga, S., Hannon, G. J., Beach, D., & Stillman, B. (1994). The p21 inhibitor of cyclin-dependent kinases controls DNA replication by interaction with PCNA. *Nature, 369*(6481), 574-578.

Waldman, T., Kinzler, K. W., & Vogelstein, B. (1995). p21 is necessary for the p53-mediated G1 arrest in human cancer cells. *Cancer Research, 55*(22), 5187.

Wang, H., & Joseph, J. A. (1999). Quantifying cellular oxidative stress by dichlorofluorescein assay using microplate reader1. *Free Radical Biology and Medicine, 27*(5-6), 612-616.

Wang, J., & Yi, J. (2008). Cancer cell killing via ROS. *Cancer Biology & Therapy, 7*(12), 1875-1884.

Wang J., C. H. J., Wong W., Spencer D.M. & Lenardo M.J. (2001). Caspase-10 is an initiator caspase in death receptor signaling. *Proceedings of National Academy of Sciences, United Stage of America, 98,* 13884-13888.

Wang, Z. B., Liu, Y. Q., & Cui, Y. F. (2005). Pathways to caspase activation. *Cell Biology International, 29*(7), 489-496.

Warburg, O. (1956). On respiratory impairment in cancer cells. *Science, 124*(3215), 269-270.

Warburg, O., Wind, F., & Negelein, E. (1927). The Metabolism of Tumors in the Body. *The Journal of General Physiology, 8*(6), 519-530.

Ward, T. H., Cummings, J., Dean, E., Greystoke, A., Hou, J. M., Backen, A., . . . Dive, C. (2008). Biomarkers of apoptosis. *British Journal of Cancer*. 99, 841-846.

Weinberg, R. A. (1995). The retinoblastoma protein and cell cycle control. *Cell, 81*(3), 323-330.

Wessjohann, L. A. (2000). Synthesis of natural-product-based compound libraries. *Current Opinion in Chemical Biology, 4*(3), 303-309.

Willis, S. N., Fletcher, J. I., Kaufmann, T., van Delft, M. F., Chen, L., Czabotar, P. E., . . . Huang, D. C. (2007). Apoptosis initiated when BH3 ligands engage multiple Bcl-2 homologs, not Bax or Bak. *Science, 315*(5813), 856-859.

Wiseman, H., Kaur, H., & Halliwell, B. (1995). DNA damage and cancer: measurement and mechanism. *Cancer Letter, 93*(1), 113-120.

Wolfe, L. S. (1993). *Molecular and Cellular Biology*. Belmont, California: Wadsworth Publishing Company.

Wolter, F., Akoglu, B., Clausnitzer, A., & Stein, J. (2001). Downregulation of the cyclin D1/Cdk4 complex occurs during resveratrol-induced cell cycle arrest in colon cancer cell lines. *The Journal of Nutrition, 131*(8), 2197-2203.

Wong, Y. H., Abdul Kadir, H., & Ling, S. K. (2011). Bioassay-guided isolation of cytotoxic cycloartane triterpenoid glycosides from the traditionally used medicinal plant Leea indica. *Evidence-Based Complementary and Alternative Medicine, 2012*.

Woo, J. H., Kim, Y. H., Choi, Y. J., Kim, D. G., Lee, K. S., Bae, J. H., . . . Kwon, T. K. (2003). Molecular mechanisms of curcumin-induced cytotoxicity: induction of apoptosis through generation of reactive oxygen species, down-regulation of Bcl-XL and IAP, the release of cytochrome c and inhibition of Akt. *Carcinogenesis, 24*(7), 1199-1208.

Wright, W. E., Pereira-Smith, O. M., & Shay, J. W. (1989). Reversible cellular senescence: implications for immortalization of normal human diploid fibroblasts. *Molecular and Cellular Biology, 9*(7), 3088-3092.

Wu, W., Liu, P., & Li, J. (2011). Necroptosis: An emerging form of programmed cell death. *Critical Reviews in Oncolgy/Hematology,* 82(3), 249-258.

Wyllie, A. H. (2010). "Where, O death, is thy sting?" A brief review of apoptosis biology. *Molecular Neurobiology, 42*(1), 4-9.

Xue, L., Fletcher, G. C., & Tolkovsky, A. M. (2001). Mitochondria are selectively eliminated from eukaryotic cells after blockade of caspases during apoptosis. *Current Biology, 11*(5), 361-365.

Yang, C. L., Ma, Y. G., Xue, Y. X., Liu, Y. Y., Xie, H., & Qiu, G. R. (2012). Curcumin induces small cell lung cancer NCI-H446 cell apoptosis via the reactive oxygen species-mediated mitochondrial pathway and not the cell death receptor pathway. *DNA and Cell Biology, 31*(2), 139-150.

Yang, C. W., Chang, C. L., Lee, H. C., Chi, C. W., Pan, J. P., & Yang, W. C. (2012). Curcumin induces the apoptosis of human monocytic leukemia THP-1 cells via the activation of JNK/ERK Pathways. *BMC Complementary and Alternative Medicines, 12*(1), 22.

Yarden, Y., & Ullrich, A. (1988). Molecular analysis of signal transduction by growth factors. *Biochemistry, 27*(9), 3113-3119.

Yee, K. W. H., Schittenhelm, M., O'Farrell, A. M., Town, A. R., McGreevey, L., Bainbridge, T., . . . Heinrich, M. C. (2004). Synergistic effect of SU11248 with cytarabine or daunorubicin on FLT3 ITD–positive leukemic cells. *Blood, 104*(13), 4202-4209.

Yeh, H. C., Platz, E. A., Wang, N. Y., Visvanathan, K., Helzlsouer, K. J., & Brancati, F. L. (2012). A Prospective Study of the Associations Between Treated Diabetes and Cancer Outcomes. *Diabetes Care, 35*(1), 113-118.

Yoshimoto, K., Hanaoka, H., Sato, S., Kato, T., Tabata, S., Noda, T., & Ohsumi, Y. (2004). Processing of ATG8s, ubiquitin-like proteins, and their deconjugation by ATG4s are essential for plant autophagy. *Plant Cell, 16*(11), 2967-2983.

Youle, R. J., & Strasser, A. (2008). The BCL-2 protein family: opposing activities that mediate cell death. *Nature Reviews of Molecular Cell Biology, 9*(1), 47-59.

Yuan, J. (2006). Divergence from a dedicated cellular suicide mechanism: exploring the evolution of cell death. *Molecular Cell, 23*(1), 1-12.

Zamzami, N., Maisse, C., Métivier, D., & Kroemer, G. (2007). Measurement of membrane permeability and the permeability transition of mitochondria. *Methods Cell Biology, 80*, 327-340.

Zhang, M., & James, S. P. (2005). Silylation of hyaluronan to improve hydrophobicity and reactivity for improved processing and derivatization. *Polymer, 46*(11), 3639-3648.

Zhang, Y., Marcillat, O., Giulivi, C., Ernster, L., & Davies, K. J. (1990). The oxidative inactivation of mitochondrial electron transport chain components and ATPase. *The Journal of Biological Chemistry, 265*(27), 16330-16336.

Zong, W. X., & Thompson, C. B. (2006). Necrotic death as a cell fate. *Genes & Development, 20*(1), 1-15.

Zusman, I. (1997). The role of p53 tumor-associated protein in colon cancer detection and prevention. *International Journal of Oncology, 10*(6), 1241-1249.